The Putative (1,3)-β-D-Glucan Synthase Gene Family in *Hordeum vulgare*

Submitted by

Michael Scott Schober

This thesis is submitted in fulfilment of the requirements
for the degree of Doctor of Philosophy

Discipline of Plant and Pest Science
School of Agriculture and Wine
Faculty of Sciences
University of Adelaide, Waite Campus
Glen Osmond, South Australia, 5064, Australia

January, 2006

Statement of Authorship

This thesis contains no material that has been accepted for the award of any other degree or diploma in any university and that, to the best of my knowledge and belief, this thesis contains no material previously published or written by another person, except where due reference being made in the text of the thesis.

I give consent to this copy of my thesis, when deposited in the University Libraries, being available for photocopying and loan.

Michael Scott Schober
January 2006

Table of Contents

Acknowledgements

I would like to thank my principal supervisor, Professor Geoff Fincher, for providing me with a scholarship and funding through an Australian Research Council grant. I would also like to thank him for providing guidance and direction throughout the duration of my project and also for his support and patience during difficult periods of my research. I also wish to thank my co-supervisors, Dr Rachel Burton and Dr Andrew Jacobs for their friendship, patience and guidance. Both Rachel and Andrew have taught me many molecular biological techniques and have provided useful discussions.

I would like to thank Dr Andreas Schreiber and Dr Andrew Harvey for their assistance with bioinformatics. I thank Dr Neil Shirley for providing his quantitative real-time PCR expertise. Thanks to Dr Paul Gooding for his molecular biology advice and friendship. I would like to thank Associate Professor Maria Hrmova for her intellectual conversation and for showing that good science can arise from determination and dedication. Thanks to Mrs Margaret Pallotta for providing assistance with gene mapping. I would also like to thank the many people that have contributed by interesting scientific discussions, advice and by making my research enjoyable. In particular, I thank Professor Bruce Stone, Dr David Gibeaut, Dr Jing Li, Dr Christina Lunde, Dr Qisen Zhang, Dr Brendon King, Mr Ahmad Wardak and Mrs Ursula Langridge and the current and past students in the Fincher laboratory including Mr Naser Farroki, Ms Jacinda Rethus, Ms Vanessa Richardson and Mr Damien Drew. I would also like to thank the past and present members of the Fincher laboratory.

I wish to thank both my family and the Rathjen family for their emotional and intellectual support. Finally and most importantly, I would like to thank my beautiful wife, Judy, for her love and patience.

Publications

Seminars

"The (1,3)-β-D-glucan synthase gene family in *Hordeum vulgare*"

17th September, 2003
University of Adelaide, Discipline of Plant and Pest Science
Postgraduate Symposium

"The (1,3)-β-D-glucan synthase gene family in *Hordeum vulgare*"

24th May, 2004
Functional Genomics Program
Collaboration with Department of Botany, Melbourne University

Conference Proceedings

Schober MS, Jacobs AK, Burton RA, Fincher GB. "The (1,3)-β-D-glucan synthase gene family in *Hordeum vulgare*" ComBio2004, Sept 26-30 2004, Burswood Resort Convention Centre, Perth, WA, Australia.

Jacobs AK, Lipka V, Burton RA, **Schober MS**, Panstruga R, Strizhov N, Schulze-Lefert P, Fincher GB. "The callose synthase gene family in Arabidopsis and barley" Plant and Animal Genome Conference 12, Jan 10-14 2004. Town and Country Convention Centre. San Diego, California USA

Abbreviations

3'RACE	.....3' rapid amplification of cDNA ends
3'UTR	.....3' untranslated region
A	.....Absorbance
aa	.....Amino acid(s)
ABF	.....Aniline blue fluorochrome
bp	.....Base pair(s)
CaMV	.....Cauliflower mosaic virus
CHAPS	.....3-[(cholamidopropyl)-dimethylammonio]-1-propane-sulphate
cDNA	.....Complementary DNA
Da	.....Dalton
dCTP	.....Deoxycytidine triphosphate
DNA	.....Deoxyribose nucleic acid
DNase	.....DNA hydrolase
dNTP	.....Deoxynucleotide triphosphate
DOP	.....Degree of polymerisation
DTT	.....Dithiothreitol
EDTA	.....Ethylene diamine tetra-acetic acid
EST	.....Expressed sequence tag
g	.....Unit of relative centrifugal force
GDP	.....Guanosine diphosphate
GFP	.....Green fluorescent protein
GSL	.....Glucan synthase-like
GTE	.....Glucose tris EDTA
GTP	.....Guanosine triphosphate
GUS	.....β-glucuronidase gene
hr	.....hour(s)
kb	.....Kilobase pairs
LB	.....Luria-Bertani
LBA	.....Luria-Bertani agar
M	.....Molar
MCS	.....Multiple cloning site
min	.....Minute(s)
mRNA	.....messenger RNA
MOPS	.....3-(N-morpholino)propanesulfonic acid
PCR	.....Polymerase chain reaction
PEG	.....Polyethylene glycol
QTL	.....Quantitative trait loci
RNA	.....Ribonucleic acid
RNase	.....RNA hydrolase
rpm	.....Revolutions per minute
RT	.....Room temperature
RT	.....Reverse transcriptase
SDS	.....Sodium dodecyl sulphate
SDS-PAGE	.....SDS-polyacyrlamide gel electrophoresis
sec	.....Second(s)
SSC	.....Standard saline citrate
TE	.....Tris EDTA
T_m	.....Melting temperature
tris	.....Tris[hydroxylmethyl] amino methane
UDP	.....Uridine diphosphate
UGT	.....UDP-glucose transferase
UV	.....Ultraviolet

Abstract

(1,3)-β-D-Glucan, which is often referred to as callose, is deposited in numerous locations and at various stages during normal growth and development in higher plants, as well as in response to abiotic and biotic stresses. For example, (1,3)-β-D-glucan is the main polysaccharide component of the forming cell plate during mitosis, and is deposited at various stages during the meiotic events of micro- and megasporogenesis. (1,3)-β-D-Glucan is also a structural component of plasmodesmatal canals, sieve plate pores and pollen tube walls, and is deposited during cellularisation of the developing endosperm. (1,3)-β-D-Glucan is deposited in response to mechanical wounding, metal toxicity, and in response to viral, bacterial, nematodal and fungal infection.

There are several lines of evidence that link **g**lucan **s**ynthase-**l**ike, or *GSL*, genes to the deposition of (1,3)-β-D-glucan in higher plants. In the work described in this thesis the role of individual barley (*Hordeum vulgare*) *GSL* genes in the deposition of (1,3)-β-D-glucan was investigated. There was an emphasis on the identification of the barley *HvGSL* gene involved in the deposition of (1,3)-β-D-glucan in the response to fungal infection, in the anticipation that disruption of the barley orthologue might lead to increased resistance to fungal diseases in an important cereal crop species.

In addition to the barley *HvGSL1* gene that had been characterised previously, an additional six (possibly seven) *HvGSL* genes were identified here from mRNA preparations of various barley tissues. The genes were placed on a high density barley genetic map, and are distributed across the genome. The deduced amino acid sequence of the *HvGSL8* gene, for which a near full-length cDNA was isolated, was predicted to have a large hydrophilic region located on the cytoplasmic side of the plasma membrane, flanked by six to eight transmembrane helices towards the COOH-terminus and five to seven transmembrane helices towards the NH_2-terminus. There were no obvious UDP-glucose binding motifs identified in the deduced amino acid sequences of any of the *HvGSL* genes. It was observed that the barley *HvGSL7* gene had the highest sequence identity to the Arabidopsis *AtGSL5* gene.

Potential *HvGSL* gene functions were investigated using quantitative real-time PCR and through the analysis of microarray data. It was assumed that genes that were up-regulated in particular tissues were candidates for the deposition of (1,3)-β-D-glucan specific for that tissue, and that co-transcribed genes might be involved in the overall process of (1,3)-β-D-glucan deposition. With this approach to *HvGSL* gene characterisation, it was concluded that the *HvGSL2* gene was potentially involved in the deposition of (1,3)-β-D-glucan during meiotic division. The analyses also suggested that *HvGSL3* might be involved in (1,3)-β-D-glucan deposition during endosperm cellularisation. The *HvGSL6* gene was also implicated in endosperm cellularisation, and in addition was also the most likely candidate for (1,3)-β-D-glucan deposition during cell plate formation in dividing cells. The barley *HvGSL4* gene might be required for deposition of (1,3)-β-D-glucan that is associated with closure of plasmodesmata. Finally, it was shown that *HvGSL7* was the only *HvGSL* gene that was up-regulated in epidermal tissue in response to *Blumeria graminis* infection.

To determine whether *HvGSL7* was required for (1,3)-β-D-glucan deposition in papillary structures that arise during fungal infection, an *HvGSL7* dsRNAi vector was generated and delivered into excised barley leaf blades by micro-projectile bombardment. Cells bombarded with the dsRNAi vector deposited less (1,3)-β-D-glucan in papillary structures resulting from *B. graminis* infection when compared with the experimental negative control. Based on sequence identity, transcription profile and post-transcriptional gene silencing, *HvGSL7* appears to be the barley orthologue of *AtGSL5* in Arabidopsis. It is uncertain at this stage if silencing *HvGSL7* results in increased resistance against virulent barley fungal pathogens. Transgenic *HvGSL7* dsRNAi barley lines were therefore generated, but are yet to be analysed.

Chapter 1

General Introduction

1.1 INTRODUCTION

The aim of the work described in this thesis was to isolate and characterise the genes encoding putative (1,3)-β-D-glucan synthases in barley (*Hordeum vulgare*). In plants, (1,3)-β-D-glucan is commonly referred to as callose and is a linear polymer of glucosyl residues covalently joined together by (1,3)-β-D-glucosidic linkages (*Figure 1.1*). In higher plants, (1,3)-β-D-glucan is deposited in specialised cells and associated structures and also in response to biotic and abiotic stresses. Given the range of locations and environmental cues that lead to (1,3)-β-D-glucan deposition, it is likely that a number of (1,3)-β-D-glucan synthases are responsible for (1,3)-β-D-glucan deposition.

Attempts to purify the proteins involved in the synthesis of (1,3)-β-D-glucan have been largely unsuccessful. There have been several reports of the enrichment of proteins that co-purify with (1,3)-β-D-glucan synthase activity, but there has been no conclusive evidence that these proteins are directly involved in (1,3)-β-D-glucan synthesis. Putative (1,3)-β-D-glucan synthases have been identified in fungi and plants by gene silencing followed by the observation of reduced (1,3)-β-D-glucan deposition (Douglas *et al.*, 1994; Jacobs *et al.*, 2003; Nishimura *et al.*, 2003). Throughout this thesis, individual putative (1,3)-β-D-glucan synthase genes will be referred to by the recommended nomenclature, which begins with the initials of the species-genus followed by *GSL* for **g**lucan **s**ynthase-**l**ike genes (http://cellwall.standford.edu/). For example, the nomenclature for a barley glucan synthase-like gene is *HvGSL*. In plants, putative (1,3)-β-D-glucan synthase genes exist as a family of 9 – 12 members. In the work described here, members of the putative (1,3)-β-D-glucan synthase gene family were analysed in an important cereal crop, barley, using various molecular techniques to determine gene transcription patterns and to assign possible functions to individual members of the gene family.

In this chapter the structure of (1,3)-β-D-glucans will be described, followed by a description of the cellular locations and associated functions of (1,3)-β-D-glucans in plants. An overview of biochemical techniques used to identify proteins that co-purify with (1,3)-β-D-glucan synthase activity is included to illustrate the limitations

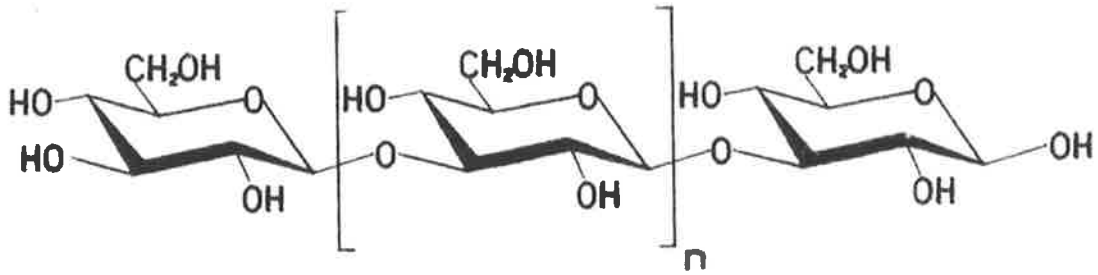

Figure 1.1: The chemical structure of (1,3)-β-D-glucan (Stone and Clarke, 1992).

of the procedures. The full length *GSLs* genes that have been identified so far in *Saccharomyces cerevisiae*, Arabidopsis, *Nicotiana alata*, barley and *Gossypium hirsutum* (cotton) and the molecular analysis of the putative (1,3)-β-D-glucan synthases are then described.

1.2 (1,3)-β-D-GLUCAN

1.2.1 Structural Properties

(1,3)-β-D-Glucan is a linear polymer of glucosyl residues covalently joined by (1,3)-β-D-glucosidic linkages (*Figure 1.1*). Variants of the polysaccharide may contain some (1,6)-linkages either within the backbone, as single residue substituents of the main chain, or as branch points where oligo- or polysaccharide chains are attached *via* carbon-6 of the glucosyl backbone (Stone and Clarke, 1992). Observation of (1,3)-β-D-glucan deposits *in vivo* is commonly achieved *via* specific staining with the aniline blue fluorochrome (ABF; *Figure 1.2*), which forms a complex with (1,3)-β-D-glucan (Nakanishi *et al.*, 1974; Stone *et al.*, 1984). When the (1,3)-β-D-glucan:ABF complex is irradiated with ultraviolet light a bright yellow fluorescence is induced (Evans *et al.*, 1984). The chemical basis for the specific binding of (1,3)-β-D-glucan with ABF is currently unknown.

The number of monosaccharides residues in a polysaccharide chain is referred to as the degree of polymerisation (DP). Studies of (1,3)-β-D-glucans from *Alcaligenes faecalis* show that chains with a DP of less than 25 are water-soluble and have a disordered conformation, whereas (1,3)-β-D-glucan chains with a DP greater than 25 are water-insoluble and have an ordered conformation (Ogawa and Tsurugi, 1973; Koreeda *et al.*, 1974). (1,3)-β-D-Glucan chains isolated from *A. faecalis*, which have a DP greater than 140 residues, form ordered microfibrils *in vitro* (Koreeda *et al.*, 1974). The *in vitro* samples of microfibrillar (1,3)-β-D-glucans isolated from *Lentinus elodes* have been shown to have triple helical structures (Bluhm and Sarko, 1977), as have those isolated from *Neurospora crassa* (Jabri *et al.*, 1989), *Saprolegnia monoica*, *Rubus fruiticosus* (Pelosi *et al.*, 2003) and Arabidopsis (Him *et al.*, 2001). It is yet to be determined if (1,3)-β-D-glucan *in vivo* also has a

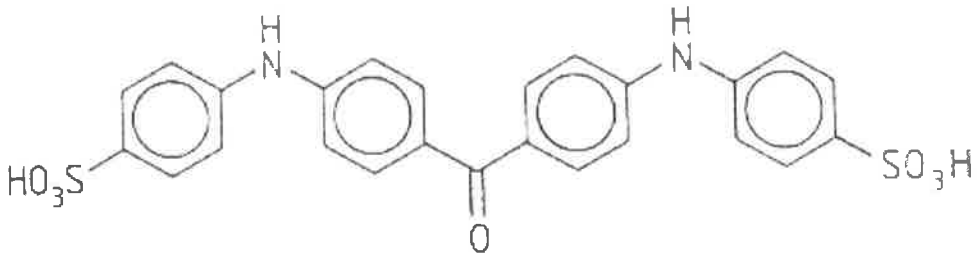

Figure 1.2: Aniline blue fluorochrome. The chemical structure of the specific staining dye for (1,3)-β-D-glucan (Evans *et al.*, 1984).

microfibrillar and helical nature. The ability of (1,3)-β-D-glucan to assume a highly ordered conformation has potential commercial application. The easily purified (1,3)-β-D-glucan from the bacterium *A. faecalis*, called curdlan, is produced as an extracellular polysaccharide (Stone and Clarke, 1992). Heating isolated (1,3)-β-D-glucan, which was insoluble in neutral solution, to 100°C for 3 min resulted in the formation of a resilient gel (Harada *et al.*, 1966) that increases in strength with increasing chain length (Nakanishi *et al.*, 1974). The gel-forming properties of (1,3)-β-D-glucans have made it a potential target in the food industry as a food texture modifier.

The functions of (1,3)-β-D-glucans are related to their structural properties, which vary depending on the organism and the location within the organism. In euglenoids and brown algae, (1,3)-β-glucans, referred to as paramylon and laminarin, are located in the cell wall as well as in the cytoplasm, where they serve as storage compounds (Kiss *et al.*, 1987; Bäumer *et al.*, 2001). In fungal species, (1,3)-β-D-glucans containing some (1,6)-linkages contribute between 30 – 60% of the polysaccharide component of the cell wall and function as major structural components (Stone and Clarke, 1992). In plants, (1,3)-β-D-glucans are deposited in specialised cells and associated structures as well as in response to abiotic and biotic stimuli (Stone and Clarke, 1992).

1.2.2 Cellular Locations and Associated Functions

1.2.2.1 Cell Plate Formation

Somatic cellular division in plants occurs in the apical meristem, at the leaf base and in the root tip. During plant mitosis, the forming cell wall that separates daughter cells along the plane of cell division is called the cell plate. The main polysaccharide component of the cell plate is (1,3)-β-D-glucan (Verma, 2001). During anaphase the two microtubule arrays responsible for the separation of replicated chromosomes form a loose cytoskeletal structure within the dividing cell. The ends of the microtubules of each array assemble and face each other, and the gap that forms between them is the region of cell plate formation (Verma, 2001). Large quantities of

Golgi-derived vesicles, containing components necessary for cell plate formation, are transported to the site *via* microtubules (Samuels *et al.*, 1995). It has been suggested that the Golgi-derived vesicles are attached to the microtubules by two molecules that resemble kinesin-like motor proteins, which propel them to the forming cell plate (Otegui *et al.*, 2001). Once at the cell plate, the Golgi derived vesicles fuse to form large tubulovesicular networks by a dynamin-like GTPase called phragmoplastin (Verma, 2001). Dynamins are a large family of proteins, of which 17 have been identified in Arabidopsis, and are involved in the endocytotic events at the plasma membrane, and also in the generation of trans-Golgi vesicles for exocytosis. Phragmoplastin has been observed at the forming cell plate by immuno-fluorescence (Gu and Verma, 1996), with an especially high concentration at the region of vesicle fusion (Gu and Verma, 1997). Protein-protein interaction studies have shown that phragmoplastin interacts with a putative (1,3)-β-D-glucan synthase, AtGSL6, in Arabidopsis (Hong *et al.*, 2001a). Following the formation of the tubulovesicular networks, the presence of (1,3)-β-D-glucan is observed at the forming cell plate (Fulcher *et al.*, 1976; Northcote *et al.*, 1989; Samuels *et al.*, 1995). Most enzymes responsible for the synthesis of (1,3)-β-D-glucan require the presence of Ca^{2+} for activity (discussed further in *Section 1.4.1.2*). It has been suggested that Ca^{2+} is probably released from cell plate associated endoplasmic reticulum (Cutler and Ehrhardt, 2002; Otegui and Staehelin, 2004). Kakimoto and Shibaoka (1992) observed that isolated phragmoplasts, but not isolated transport vesicles or Golgi apparatus, possessed the ability to synthesise (1,3)-β-D-glucan. These results suggest that the synthesis of (1,3)-β-D-glucan is an important step in cell plate formation and only occurs when all the necessary precursors are present.

1.2.2.2 Plasmodesmata and Sieve Plate Pores

Plasmodesmata

During the final stages of cell division, a portion of endoplasmic reticulum (ER) is positioned perpendicular to the plane of the forming cell plate and the newly deposited plasma membrane forces the ER into an appressed cylindrical form. It has been postulated that cytoskeletal elements are responsible for guiding the ER into position (Lucas *et al.*, 1993). The resulting cytoplasmic pores/bridges that connect

adjacent cells are called plasmodesmata. Plasmodesmata provide a means for cell-to-cell communication and for the transport of metabolites and macromolecules, as well as for the movement and prevention of movement of viral particles during infection (Lucas *et al.*, 1993; van Bel *et al.*, 2002). (1,3)-β-D-Glucans have been detected using specific antibodies at the plasmodesmata (Northcote *et al.*, 1989). A transient rise of cytosolic Ca^{2+}, triggered by many environmental responses (Reddy and Reddy, 2004), can lead to the deposition of (1,3)-β-D-glucan (Kauss, 1987). If this occurs in cells with plasmodesmata, a temporary reduction of the size exclusion limit, which is the maximum sized molecule that can pass through the pore, and reduced transport and signalling between cells occurs. The clearing of plasmodesmata requires the removal of (1,3)-β-D-glucan by the action of the hydrolysing enzyme (1,3)-β-D-glucanase (Lucas *et al.*, 1993). The process of plasmodesmatal closing by the deposition of (1,3)-β-D-glucan is many times more rapid than the re-opening of the pore (Lucas *et al.*, 1993).

Sieve Plate Pores

The evolution of land plants with photoautotrophic leaves and heterotrophic roots was reliant on the ability of the plant to develop a mechanism to allow the movement of photoassimilates from the leaves to the roots, and the movement of water and nutrients from the roots to the leaves (Lucas *et al.*, 1993). The phloem transport system contains large pores, called sieve plate pores, to facilitate this function. Sieve plate pores, derived from plasmodesmata, are formed by the initial deposition of large quantities of (1,3)-β-D-glucan around the plasma-membrane lining the plasmodesmata. The extent of (1,3)-β-D-glucan deposition appears to be under the influence of genetic and environmental factors, and it ultimately controls the size of the mature pore (Lucas *et al.*, 1993). Following the deposition of (1,3)-β-D-glucan, it is subsequently degraded by (1,3)-β-D-glucan hydrolase, resulting in the mature sieve plate pore (Esau and Thorsch, 1985).

In temperate regions, plants have adapted to decreased temperatures by developing a variety of mechanisms for tolerance to chilling. In regions where winters are harsh, plants respond to decreasing day length *via* regulation with phytochromes (Smith,

1995), which play a critical role in photomorphogenesis (Kircher *et al.*, 1999). Plants that become dormant in harsh a winter, which is usually accompanied by a rapid decrease in day length, have phloem that becomes obstructed by large amounts of (1,3)-β-D-glucan (Krabel *et al.*, 1993; Rinne and van der Schoot, 2003). Breaking the winter dormancy is achieved by hydrolysis of the (1,3)-β-D-glucan with (1,3)-β-D-glucan hydrolase (Krabel *et al.*, 1993). Thus, the deposition of (1,3)-β-D-glucan and the subsequent hydrolysis appear to be important processes during winter dormancy (Rinne and van der Schoot, 2003).

1.2.2.3 Reproductive Tissues

Microsporogenesis and Megasporogenesis

Male gametes of plants are found in the developing anthers of angiosperms and in the microsporangia of gymnosperms (Stone and Clarke, 1992). During first prophase of meiosis, (1,3)-β-D-glucan is deposited between the plasma membrane and the primary wall around the microsporocyte (pollen mother cell) and between the microspores following meiotic divisions, to form a microspore tetrad. The (1,3)-β-D-glucan pollen mother cell wall is degraded to release the microspore tetrad, followed by the degradation of the (1,3)-β-D-glucan walls separating the microspores within the tetrad, to release individual microspores. In angiosperms and gymnosperms, the megaspore is found within the nucellus, which is megasporangial tissue that eventually develops into the inner layer of the ovule wall (Stone and Clarke, 1992). (1,3)-β-D-Glucan is deposited around the megasporoctye and later between the megaspores of the linear array of the megaspore diad and tetrad. The (1,3)-β-D-glucan walls are subsequently degraded when the megaspores develop into the megagametophyte, or embryo sac.

Pollen Germination and Pollen Tubes

When a pollen grain comes into contact with the stigma it germinates to produce a pollen tube. The pollen tube grows down through the style to the embryo sac, where fertilisation occurs. Specific staining with aniline blue has detected plug-like deposits of (1,3)-β-D-glucan along the length of the pollen tube behind the nuclear zone, presumably to isolate the living tube tip from the empty, spent regions of the pollen

tube (Stone and Clarke, 1992). Unlike most plant tissues, pollen tube cell walls consist of approximately 75% (1,3)-β-D-glucan, which contains some (1,6)-linked branches (Rae *et al.*, 1985; Schlüpmann *et al.*, 1994). A Ca^{2+} concentration gradient that affects pollen tube growth and (1,3)-β-D-glucan deposition has been detected within the pollen tube. At the pollen tube tip there are high Ca^{2+} levels (490 nM) but these decrease to 170 nM approximately 50 μm from the tip (Steer and Steer, 1989; Miller *et al.*, 1992). It has been demonstrated that Ca^{2+} in the pollen tube tip is required for pollen germination, pollen tube growth and the specific direction of pollen tube growth (Steer and Steer, 1989). Specific staining with aniline blue fluorochrome indicates that (1,3)-β-D-glucan deposition occurs back from the pollen tube tip, in regions of the pollen tube that have a basal Ca^{2+} concentration (Rae *et al.*, 1985; Miller *et al.*, 1992). In pollen tubes membrane preparations, Ca^{2+} stimulation is not required for the *in vitro* synthesis of (1,3)-β-D-glucan (Schlüpmann *et al.*, 1993).

Developing Endosperm

Understanding the development of the endosperm in cereals such as barley, rice, wheat, rye and sorghum is of great commercial importance. After fertilisation the endosperm nucleus forms a syncytium by dividing repeatedly without the formation of cell walls, to become a characteristic coenocyte-stage endosperm (Olsen, 2004). In barley, the endosperm coenocyte stage is reached three days after pollination (Olsen, 2004). The process of cellularisation of the coenocyte involves the formation of radial microtubule systems (RMS) and alveolation. During cellularisation in barley it has been observed that each nucleus is enveloped by the RMS, marking the boundary of the nuclear cytoplasmic domain (Brown *et al.*, 1994). The adjacent nuclei/RMS structures extend until they meet, and (1,3)-β-D-glucan is deposited in the interzones. In cereals, membrane vesicles carrying components necessary for cell wall formation, including (1,3)-β-D-glucan synthases, migrate to the growing points of the cell wall (Becraft, 2001). (1,3)-β-D-Glucan is initially deposited in an aveolus-like structure toward the central vacuole in the developing endosperm of barley, detected by specific staining with aniline blue and by the binding of antibodies raised against (1,3)-β-D-glucan (Brown *et al.*, 1994). At the completion of aveolar wall formation, the nuclei divide in a periclinal fashion several times until the endosperm is

completely cellular. The completion of cellularisation in barley occurs between six to eight days post-fertilisation and in maize, wheat and rice approximately four days post-fertilisation (Olsen, 2004). The cells of the developing endosperm subsequently divide further in an apparent random fashion (Olsen, 2004), and (1,3)-β-D-glucan is replaced by cellulose, arabinoxylan and (1,3-1,4)-β-D-glucan (Stone and Clarke, 1992). (1,3-1,4)-β-D-Glucans are comprised of cellotriosyl and cellotetraosyl resides separated by single (1,3)-linkages and are the major component of endosperm walls of commercially important members of the Poaceae family including barley, wheat, rice, sorghum and rye (Stone and Clarke, 1992).

1.3 STRESS RELATED (1,3)-β-D-GLUCAN DEPOSITION

Plants are exposed to many forms of stress, ranging from those that are abiotic, such as mechanical, chemical and temperature induced wounding and metal toxicity to biotic stresses, which may be imposed by viral, bacterial, nematodal and fungal infections. Understanding the stress responses of commercially important plants is of great interest. A well documented plant response to abiotic and biotic stresses is the deposition of (1,3)-β-D-glucan.

1.3.1 Abiotic stress

1.3.1.1 Wounding

The deposition of (1,3)-β-D-glucan is one of many ways that a plant responds to wounding. Wound-induced (1,3)-β-D-glucan deposition can occur as a result of mechanical, chemical and heat shock treatment (Stone and Clarke, 1992), and as a result of fungal infection (Jacobs *et al.*, 2003; Nishimura *et al.*, 2003). At the wound site, the deposition of (1,3)-β-D-glucan may resemble infection papillae and is accompanied by cytoplasmic changes, including dilation of the rough ER and the appearance of deposits staining with aniline blue on cytoplasmic surfaces near the wound site (Stone and Clarke, 1992). (1,3)-β-D-Glucan is also observed in sieve tubes near wound sites and spatially resembles dormancy-type (1,3)-β-D-glucan deposition (Evert and Derr, 1964; Currier and Shih, 1968). The biochemical and physiological causes for the induction of (1,3)-β-D-glucan deposition are not known.

It has been suggested that deposition may be induced by hormonal signalling, or by an increase in Ca^{2+} or UDP-glucose resulting from membrane breakage, which leads to greater accessibility of the (1,3)-β-D-glucan synthase to its substrate (Stone and Clarke, 1992).

1.3.1.2 Metal toxicity

Plants have a stress response to metal ion toxicity that involves the deposition of (1,3)-β-D-glucan at a variety of locations. When epidermal cells of onion (*Allium cepa*) were exposed to a range of metal ions, copper was the most effective at inducing (1,3)-β-D-glucan deposition (Kartusch, 2003). It was concluded that metal ions may initiate a signal transduction pathway with subsequent disturbance of intracellular Ca^{2+} homeostasis that results in the deposition of (1,3)-β-D-glucan as a cellular defence reaction. Plants that are exposed to toxic levels of Al^{3+} have inhibited root elongation and high concentrations of (1,3)-β-D-glucan at the root tips (Schreiner *et al.*, 1994; Horst *et al.*, 1997; Massot *et al.*, 1999). Furthermore, leaf lesions resulting from Mn^{2+} toxicity show deposits of (1,3)-β-D-glucan, detected by specific staining with aniline blue (Wissemeier and Horst, 1987). Plants that are infected with mycorrhiza, which alleviate the symptoms of Mn^{2+} toxicity, show a decrease in (1,3)-β-D-glucan deposition in response to Mn^{2+} when compared with uninfected plants (Nogueira *et al.*, 2002). Following exposure to Pb^{2+}, cell wall thickenings containing (1,3)-β-D-glucan appear in the apical tip of moss (Krzeslowska and Wozny, 2000).

1.3.2 Biotic Stress

1.3.2.1 Viral infection

Plant viruses establish a systemic infection *via* passage between cells through the plasmodesmata (Hull, 1989). The normal size exclusion limit of plant plasmodesmata to small molecules is less than 1 kDa. As previously mentioned, the change in the size exclusion limit of plasmodesmata is primarily influenced by (1,3)-β-D-glucan deposition and removal (*Section 1.2.2.2*). The regulated deposition of (1,3)-β-D-glucan is therefore regarded as a general mechanism by which viral spread

is limited (Allison and Shalla, 1974). To overcome plant defences, some viruses have movement proteins that increase the plasmodesmatal size exclusion limit, allowing cell-to-cell movement of the viral particle (Lucas *et al.*, 1993). Studies using plant mutants deficient in (1,3)-β-D-glucanase have shown that viral particles are less able to establish a systemic infection due to the reduced plasmodesmatal size exclusion limit resulting from inefficient hydrolysis of (1,3)-β-D-glucan deposits (Beffa *et al.*, 1996; Iglesias and Meins, 2000).

1.3.2.2 Bacterial infection

The nodule-forming, nitrogen-fixing symbiont *Frankia* sp. penetrates the root-hair cell walls of *Alnus rubra*. In arrested infections, electron-dense papillae containing (1,3)-β-D-glucan are formed at the infection site, as detected by specific staining with the aniline blue fluorochrome (Berry and McCully, 1990). (1,3)-β-D-Glucan-containing papillae are only located in epidermal hair cells, and not the vascular tissue, and cells with arrested infections appear to have disintegrated and contained few or no recognisable organelles (Berry and McCully, 1990). In successful infections, no deposits of (1,3)-β-D-glucan were detected by staining with aniline blue fluorochrome (Berry and McCully, 1990).

1.3.2.3 Nematode infection

Plant nematodes are biotrophic. Migratory nematodes infect one cell at a time until immediately prior to the occurrence of plant cell death, and the nematode moves onto the next cell to infect. The degraded cell of root phloem in banana (*Musa* spp.) that had been infected by the migratory nematode, *Radopholus similis*, showed the presence of (1,3)-β-D-glucan (Valette *et al.*, 1997). It was suggested that the deposition of (1,3)-β-D-glucan may have been a wound response resulting from nematode invasion, and that the (1,3)-β-D-glucan may interfere with nematode migration or feeding (Valette *et al.*, 1997).

Cyst nematodes form elaborate feeding syncytia in infected plant tissues. The cyst nematodes breach the tissue surface with a stylet that penetrates into the initial plant

cell (Endo, 1991). An early plant response to cyst nematode infection is the accumulation of endoplasmic reticulum towards the site of stylet penetration, as observed in the infection of soybean by *Heterodera glycines* (Endo, 1991). A deposit of (1,3)-β-D-glucan is located around the stylet tip in a parasitized cell and is thought to reflect a wound response (Williamson and Hussey, 1996). At the beginning of syncytium induction, a callosic layer is deposited inside of the walls of the initial syncytial cell, followed by the widening of plasmodesmata to neighbouring cells (Gheysen and Fenoll, 2002). It is conceivable that the (1,3)-β-D-glucan depositions in the walls of the syncytium is a result of the opening of plasmodesmata, as described above (*Section 1.2.2.2*). This process is repeated *de novo* to incorporate hundreds of cells in the syncytial nematode feeding structure.

1.3.2.4 Fungal Infection

Plants may respond to pathogen infection in a number of ways, which include hypersensitive cell death, the sealing of vascular tissue with (1,3)-β-D-glucan and the formation of (1,3)-β-D-glucan-containing papillary structures at penetration sites. The pathogenic fungus *Stemphylium floridanum* penetrates leaves of *Solanum gilo via* stomatal apertures (Clerivet, 1993). Hyphal entrance may be inhibited through host induction of localised necrosis, where phenolic compounds and (1,3)-β-D-glucan are enriched (Clerivet, 1993). Plants commonly respond to vascular-infecting fungi by rapidly sealing attempted sites of penetration with large amounts of (1,3)-β-D-glucan in the sieve pores and plasmodesmata (*Section 1.2.2.2*). For example, in eggplant (*Solanum melongena* L. cv. Imperial Black Beauty) infected with *Verticillium albo-atrum*, (1,3)-β-D-glucan deposits were the main component of the sealing structures in the stem (Benhamou, 1995). Additionally, the vascular tissue of tomato (*Lycopersicon esculentum*) and cotton plants that were infected with *Fusarium oxysporum* showed immunocytochemically-detectable depositions of (1,3)-β-D-glucan (Mueller *et al.*, 1994). Specifically, the (1,3)-β-D-glucan was located in the apposition layers in the cells surrounding the initially infected vascular tissue (Mueller *et al.*, 1994). Thus, it appears that (1,3)-β-D-glucan is deposited to seal the vascular tissue and physically prevent the fungus from establishing infection in adjacent cells.

Another common plant response to fungal infection is the localised formation of papillary structures at the penetration site, between the plant cell wall and plasma membrane. Papillae consist of a localised deposit of (1,3)-β-D-glucan, inorganic elements including Ca^{2+}, Mn^{2+}, Mg^{2+} and silicon, phenolic compounds and active oxygen species, all of which are involved in the various processes of maturation and compaction of papillae (Zeyen *et al.*, 2002). The deposition of papillary (1,3)-β-D-glucan has been extensively studied in a wide variety of plants when triggered by many types of pathogens. To better understand the plant-fungal response, several research teams have compared (1,3)-β-D-glucan deposition in resistant and susceptible plant varieties. (1,3)-β-D-Glucan deposits are greater in size and accumulate faster in resistant *Zea mays* (maize) than in susceptible lines in response to *Helminthosporium maydis* infection (Angra-Sharma and Sharma, 1994), in *Glycine max* (soybean) in response to *Phytophthora megasperma* f.sp. glycinea (Bonhoff *et al.*, 1987), and in *Pennisetum glaucum* (pearl millet) seedlings in response to the downy mildew strain, *Sclerospora graminicola* (Kumudini and Shetty, 2002). However, large and rapid deposition of (1,3)-β-D-glucan is not always the basis of a plant's resistance to a fungal pathogen. It has been observed that when infected with *Sphaerotheca pannosa*, susceptible and partially resistant rose cultivars show no difference in the amount or timing of (1,3)-β-D-glucan or lignin deposition, but there is a large increase in the amounts of phenolics in the resistant cultivar (Conti *et al.*, 1986). Additionally, the appositions in cotton produced in response to *F. oxysporum* attack do not appear to stop fungal growth (Rodriguez-Galvez and Mendgen, 1995). Indeed, it has been suggested that the deposition of (1,3)-β-D-glucan triggered by fungal attack in a resistant host cultivar is not a typical wound or damage response (Skalamera and Heath, 1996).

Papillary (1,3)-β-D-glucan has also been detected in wheat in response to fungal attack by *Alternaria tenuis*, *Septoria apiicola*, *Botrytis allii*, and *Botrytis fabae* (Ride and Pearce, 1979). Following the silencing of the Arabidopsis gene, *AtGSL5*, there was a noticeable lack of (1,3)-β-D-glucan in response to wounding and a lack of (1,3)-β-D-glucan in papillary structures (Jacobs *et al.*, 2003; Nishimura *et al.*, 2003). It is therefore possible that the presence of (1,3)-β-D-glucan in papillae may be a plant response to wounding. It was subsequently observed that fungi were unable to

establish an infection when *AtGSL5* was silenced (Jacobs *et al.*, 2003). Therefore, it appears that although the (1,3)-β-D-glucan appears to be deposited in response to infection, it might actually be protecting the fungus from the plant defences (*Section 1.4.2.2*).

1.4 (1,3)-β-D-GLUCAN SYNTHASES

There have been many attempts to purify the proteins involved in the synthesis of (1,3)-β-D-glucan. The biochemical properties of (1,3)-β-D-glucan synthases have made purification attempts largely unsuccessful. (1,3)-β-D-Glucan synthases are closely associated with the membrane fraction of cell homogenates, which has resulted in the co-purification of many membrane associated proteins with (1,3)-β-D-glucan synthase activity. Following the enrichment of (1,3)-β-D-glucan synthase activity, six to nine major polypeptides with molecular sizes between 27-115 kDa are commonly co-purified (Slay *et al.*, 1992; Wasserman *et al.*, 1992; Pedersen *et al.*, 1993; Bulone *et al.*, 1995). It is thought that the proteins which commonly co-purify with (1,3)-β-D-glucan synthase activity may form an active complex. A protein complex enriched from *Euglena gracilis* with an apparent molecular weight of 670 kDa was shown to contain (1,3)-β-D-glucan activity (Bäumer *et al.*, 2001). There have also been many attempts to identify the proteins that make up the active protein complex.

1.4.1 The Biosynthesis of (1,3)-β-D-Glucan

1.4.1.1 The Requirement for UDP-Glucose

The monosaccharide donor for the synthesis of (1,3)-β-D-glucans by (1,3)-β-D-glucan synthases is UDP-glucose, as illustrated by the *in vitro* incorporation of radioactive glucose from either UDP-[^{14}C]-glucose or UDP-[^{3}H]-glucose into (1,3)-β-D-glucan (Stone and Clarke, 1992). The proteins involved in the synthesis of (1,3)-β-D-glucan catalyse the following reaction:

$$(Glu)_{DP} + UDP\text{-}Glu \rightarrow (Glu)_{DP+1} + UDP$$

Figure 1.3: The reaction of (1,3)-β-D-glucan synthesis. Glu: glucosyl residue. DP: degrees of polymerisation. UDP: uridine diphosphate.

UDP-Glucose binding proteins such as UDP-glucosyltransferase (UGT) have been identified in the analysis of the polypeptides that co-purify with (1,3)-β-D-glucan synthase activity. A novel UDP-glucose transferase (UGT1), which co-purified with a membrane bound (1,3)-β-D-glucan synthase complex, was shown to interact with phragmoplastin (Hong *et al.*, 2001b). It was suggested that UGT1 might transfer UDP-glucose to the (1,3)-β-D-glucan synthase, helping to form a substrate channel for (1,3)-β-D-glucan synthesis at the forming cell plate (Hong *et al.*, 2001b). In another attempt to identify UDP-glucose binding proteins that co-purify with (1,3)-β-D-glucan activity, solubilised membrane fractions with high (1,3)-β-D-glucan synthase activity were exposed to appropriate assay conditions and radiolabelled UDP-glucose analogues. Following irradiation with UV light, the radiolabelled UDP-glucose analogues 5-[^{125}I]ASA-UDP-glucose (365 nm), [α-^{32}P]UDP-glucose (254 nm) and 5-azido-[^{32}P]UDP-glucose (254 nm) irreversibly inactivated (1,3)-β-D-glucan synthase activity (Meikle *et al.*, 1991; Beauvais *et al.*, 1993; Dhugga and Ray, 1994; Bäumer *et al.*, 2001). The irradiated reaction samples were separated on an SDS-PAGE gel, transferred to a membrane and exposed to X-ray film. UDP-glucose binding proteins associated with (1,3)-β-D-glucan synthase activity were identified *via* this method in *Aspergillus fumigatus* with sizes of 31 kDa, 50 kDa and 115 kDa (Beauvais *et al.*, 1993), in *Lolium multiflorum* with a size of 31 kDa (Meikle *et al.*, 1991), in pea tissue with a size of 55 kDa (Dhugga and Ray, 1994) and in *E. gracilis* with sizes of 37 kDa and 54 kDa (Bäumer *et al.*, 2001). However, since this method non-specifically labels UDP-glucose binding proteins that co-purify with (1,3)-β-D-glucan synthase activity, it is uncertain if these proteins transfer glucose from UDP-glucose to the growing (1,3)-β-D-glucan chain or if they have another function.

1.4.1.2 The Requirement for Calcium

(1,3)-β-D-Glucan synthases can be categorised into two groups based on their requirements for Ca^{2+}. The first group contains (1,3)-β-D-glucan synthases that have Ca^{2+}-dependent activity at a Ca^{2+} concentration of 2 mM and are enriched in microsomal preparations derived from somatic tissue (Pedersen *et al.*, 1993; Schlüpmann *et al.*, 1993; Him *et al.*, 2001). A positive electrical transmembrane potential caused by a local increase in Ca^{2+} may facilitate the movement of the

negatively charged UDP-glucose into the cell, leading to the synthesis of (1,3)-β-D-glucan (Bacic and Delmer, 1981). It is interesting to note that Ca^{2+} precipitation has been used in the enrichment of (1,3)-β-D-glucan synthase activity. In this procedure, detergent-solubilised membranes are treated with 8 mM $CaCl_2$ and the pellet discarded after centrifugation at 13000 g for 15 min at 4°C. This step supposedly removes inhibitory proteins of (1,3)-β-D-glucan synthase (Bulone *et al.*, 1995) *via* a process called "salting out", which is one of the most widely used procedures for the precipitation of proteins. Generally this method involves solubilising proteins in salt concentrations of up to 3 M ammonium sulphate. Multiply charged anions such as SO_4^{2-} are more effective than singly charged anions (e.g. Cl^-), and multiply charged cations such as Mg^{2+}, Mn^{2+} and Ca^{2+} are generally avoided as they are likely to interact with the proteins (Scopes, 1982). Thus, a salt concentration of 8 mM Ca^{2+} is unlikely to precipitate inhibitory proteins, and instead may be affecting the folding of (1,3)-β-D-glucan synthase leading to the increased activity (Associate Professor Maria Hrmova, *personal communication*). The second group contains (1,3)-β-D-glucan synthases that show Ca^{2+}-independent activity, and these are enriched in microsomal preparations derived from pollen tubes (Schlüpmann *et al.*, 1993). In *Section 1.2.2.3* more information is provided on the deposition of (1,3)-β-D-glucan in relation to the distribution of Ca^{2+} in pollen tubes.

1.4.1.3 Regulation of (1,3)-β-D-Glucan Synthase Activity with GTPases

GTP hydrolases, or GTPases, are responsible for regulating the cycling of GTP to GDP and are important signal transducers involved in many cellular processes (Ridley, 2001). In a study that identified a *S. cerevisiae* GTP-binding protein (RhoIp), *RhoI* deletion mutants were used to show that the GTP-binding protein is required for (1,3)-β-D-glucan synthase activity (Drgonová *et al.*, 1996). The lack of (1,3)-β-D-glucan synthase activity was complemented by the addition of recombinant or purified RhoIp protein (Drgonová *et al.*, 1996). In Arabidopsis, a UDP-glucosyltransferase that co-purifies with (1,3)-β-D-glucan synthase activity was shown to bind to a Rho-like protein, but only in a GTP-bound conformation (Hong *et al.*, 2001b). Thus, it may be that GTPases regulate (1,3)-β-D-glucan synthase activity *via* an interaction with a UDP-glucosyltransferase. Several other studies in yeast

have shown that a GTP-binding protein regulates and co-purifies with (1,3)-β-D-glucan synthase activity (Mol *et al.*, 1994; Mazur and Baginsky, 1996). A GTP-insensitive (1,3)-β-D-glucan synthase from the oomycete *Phytophthora sojae* has been identified, suggesting that GTP-binding proteins may not always be required for (1,3)-β-D-glucan synthase activity (Antelo *et al.*, 1998). *S. cerevisiae* Rho1 homologues that co-purify with (1,3)-β-D-glucan synthase and are required for activity have been identified in *A. fumigatus* (Beauvais *et al.*, 2001), *Candida albicans* (Kondoh *et al.*, 1997) and *Schizosaccharomyces pombe* (Arellano *et al.*, 1996).

1.4.1.4 Membrane Location of (1,3)-β-D-Glucan Synthase Activity

Total cellular microsomal preparations have been used as a source of enriched (1,3)-β-D-glucan synthase activity in pollen tubes and cotyledon suspension cultures of *N. alata* Link et Otto (Schlüpmann *et al.*, 1993; Li *et al.*, 1997), *Phaseolus vulgaris* L. (McCormack *et al.*, 1997), Arabidopsis (Him *et al.*, 2001), and in the fungi *S. cerevisiae* (Inoue *et al.*, 1995), *S. pombe* (Ishiguro *et al.*, 1997) and *Aspergillus nidulans* (Beauvais *et al.*, 1993; Kelly *et al.*, 1996). It therefore appears likely that (1,3)-β-D-glucan synthases are closely associated with cellular membranes. It has been observed through many studies that (1,3)-β-D-glucan synthase activity is particularly enriched in plasma membrane preparations. Several methods have been used in the preparation of plasma membranes, and the first step is usually the extraction of a total cellular microsome fraction. Total microsomes may then be treated by overlaying a resuspended microsomal preparation on a discontinuous sucrose density gradient, as in the preparation of plasma membrane fractions from maize (Gibeaut and Carpita, 1990), *Beta vulgaris* L. (Wu *et al.*, 1991) and *N. alata* Link et Otto (Turner *et al.*, 1998). Plasma membranes may also be enriched by aqueous polymer two-phase partitioning of the microsomal fraction in a PEG-dextran system. The two-phase system has been used for the enrichment of (1,3)-β-D-glucan synthase activity from plasma membranes of pea tissue (Dhugga and Ray, 1994), *Apium graveolens* L. (Slay *et al.*, 1992), *Cucumis sativus* L. cv. Marvita (Schmele and Kauss, 1990) and barley (Pedersen *et al.*, 1993). An alternative method for the preparation of plasma membranes with enriched (1,3)-β-D-glucan synthase activity

involves coating intact protoplasts derived from *L. multiflorum* with the J539-myeloma protein, lysing the protoplasts, followed by pelleting the labelled plasma membranes with a short, low-speed centrifugation step (Henry *et al.*, 1983). The highest specific activity was observed in the plasma membrane fraction while 82% of the total activity was associated with the intracellular membrane fraction. In a similar experiment, intact protoplasts derived from *N. crassa* labelled with concanavalin A were lysed, and the pelleted plasma membrane fraction was shown to possess the highest (1,3)-β-D-glucan synthase activity (Jabri *et al.*, 1989). Thus, according to activity assays, (1,3)-β-D-glucan synthases seem to be associated with plant cellular membranes, and are possibly functional at the plasma membrane.

1.4.1.5 Detergent Activation of (1,3)-β-D-Glucan Synthases

Membrane preparations are commonly treated with amphipathic detergents to dissociate the (1,3)-β-D-glucan synthase from the membrane and to enhance *in vitro* (1,3)-β-D-glucan synthase activity. Zwitterionic detergents such as 3-[(cholamidopropyl)-dimethylammonio]-1-propane-sulphate (CHAPS: a derivative of cholic acid), Zwittergent 3-16 and 1-α-lysolecithin have been used to activate (1,3)-β-D-glucan synthase activity (Hrmova *et al.*, 1989; Wu *et al.*, 1991; Slay *et al.*, 1992; Beauvais *et al.*, 1993; Bulone *et al.*, 1995; Inoue *et al.*, 1995; Li *et al.*, 1997; Antelo *et al.*, 1998; Him *et al.*, 2001). Zwitterionic detergents cause membrane preparations to form vesicle-like structures, and just below the critical micellar concentration are able to increase (1,3)-β-D-glucan synthase activity 10 to 15-fold (Li *et al.*, 1997; Him *et al.*, 2001). Digitonin is a detergent extracted from the seeds of *Digitalis purpea* L. (foxglove), which forms a soapy suspension in water and is used extensively in the analysis of (1,3)-β-D-glucan synthases (Pedersen *et al.*, 1993; Dhugga and Ray, 1994; Li *et al.*, 1997; Turner *et al.*, 1998). The (1,3)-β-D-glucan synthase specific activity in membrane preparations is increased three to four-fold following digitonin treatment, presumably by increased membrane vesicle permeabilisation (Li *et al.*, 1997). Other detergents that have been used in the activation of (1,3)-β-D-glucan synthases in membrane preparations are *n*-octyl-β-D-glucopyranoside, which produces micelle-like structures as shown by cryo-transmission electron microscopy

(Him *et al.*, 2001), and the non-ionic detergent polyoxyethylene ether W1 (Kelly *et al.*, 1996).

1.4.1.6 Trypsin Activation of (1,3)-β-D-Glucan Synthases

Membrane preparations of pollen tubes from *N. alata* (Link et Otto) show a ten-fold increase in (1,3)-β-D-glucan synthase activity following treatment with trypsin, and the rate of reaction decreases rapidly with continued exposure to trypsin (Schlüpmann *et al.*, 1993). However, no trypsin activation of cotyledon suspension culture preparations has been observed (Schlüpmann *et al.*, 1993). It has been suggested that activation of pollen tube (1,3)-β-D-glucan synthase by trypsin resembles detergent activation (Li *et al.*, 1997). There are several potential reasons for the proteolytic activation of (1,3)-β-D-glucan synthase activity in pollen tubes including the removal of an inhibitory domain within the (1,3)-β-D-glucan synthase enzyme. Other possible explanations for the trypsin activation of (1,3)-β-D-glucan synthase activity include the proteolytic removal of a membrane associated inhibitor or the proteolytic activation of an inactive synthase zymogen (Schlüpmann *et al.*, 1993).

1.4.1.7 Product Entrapment of (1,3)-β-D-Glucan Synthase Activity

Another technique that has been used to enrich (1,3)-β-D-glucan synthase is product entrapment. This procedure requires the incubation of solubilised membrane preparations with UDP-glucose and Ca^{2+}, if required. Enzymes that remain bound to the newly synthesised polysaccharide are thereby "trapped" and can be pelleted along with the insoluble polysaccharide product of the synthase reaction (Wu *et al.*, 1991; Slay *et al.*, 1992; Pedersen *et al.*, 1993; Dhugga and Ray, 1994; Bulone *et al.*, 1995; Inoue *et al.*, 1995; Kelly *et al.*, 1996; Beauvais *et al.*, 2001). Following a single enrichment step, the protocol has resulted in a 300-fold increase in (1,3)-β-D-glucan synthase specific activity from *A. nidulans* (Kelly *et al.*, 1996), a 700-fold increase in specific activity from *S. cerevisiae* (Inoue *et al.*, 1995), a 400-fold increase in specific activity from membrane preparations and a 60-fold enrichment of CHAPS-extracted membranes from *L. multiflorum* (Bulone *et al.*, 1995). However,

even with modifications to the standard protocol such as the inclusion of iso-electric focusing (Dhugga and Ray, 1994), immunoprecipitation (Meikle *et al.*, 1991), native gel electrophoresis (Li *et al.*, 2003), anion exchange chromatography (Slay *et al.*, 1992; Antelo *et al.*, 1998), gel filtration chromatography and affinity chromatography (Slay *et al.*, 1992) many proteins are still co-purified with (1,3)-β-D-glucan synthase activity.

1.4.2 Putative (1,3)-β-D-Glucan Synthase Genes

1.4.2.1 Yeast *FKS* Genes

(1,3)-β-D-Glucan is a major component of the yeast cell wall. The putative catalytic subunit for the synthesis of (1,3)-β-D-glucan was first discovered in *S. cerevisiae* (Douglas *et al.*, 1994). The gene was identified in two different ways. In the first method, mutants were screened for resistance against a highly effective echinocandin, L-733,560, which is an anti-fungal compound that inhibits (1,3)-β-D-glucan synthase. The enzyme encoded by the disrupted gene was found to encode a membrane bound component, and was thought to be a subunit of (1,3)-β-D-glucan synthase. The gene was called *EGT1*. In the second method, the immunosuppressants FK506 and cyclosporin A, also possessing anti-fungal activity, were used. The FK506 and cyclosporin A bind to an intracellular receptor and inhibit the Ca^{2+}/calmodulin-dependent protein phosphatase calcineurin, thereby affecting the recovery from mating arrest. A yeast mutant was described that was hypersensitive to FK506 and cyclosporin A (Douglas *et al.*, 1994). The gene was called *FKS1*. Both *EGT1* and *FKS1* were cloned by complementation of the mutant phenotype and were found to be identical (Douglas *et al.*, 1994). The gene encodes a protein of 215 kDa with 16 predicted transmembrane helices (*Figure 1.4*). Disruption of the gene produces a slow growth phenotype, hypersensitivity to FK506 and cyclosporin A, a slight increase in echinocandin sensitivity, and a significant reduction in (1,3)-β-D-glucan synthase activity *in vitro*. It was observed that the *FKS1* mutants had residual (1,3)-β-D-glucan synthase activity and Southern hybridisation experiments suggested the existence of a second glucan synthase isoenzyme. A homologue to *FKS1* was soon cloned and sequenced in yeast and subsequently called *FKS2*

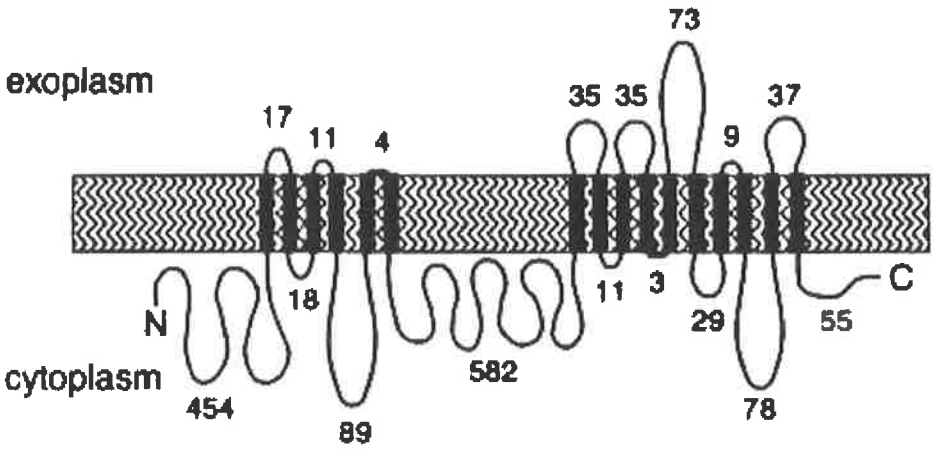

Figure 1.4: Membrane topology of the (1,3)-β-D-glucan synthase (FKS1) from *Saccharomyces cerevisiae* (Douglas *et al.*, 1994).

(Mazur *et al.*, 1995). The 217 kDa protein encoded by *FKS2* is 88% identical to *FKS1*, and it was found that the simultaneous disruption of *FKS1* and *FKS2* was lethal. These results suggested that *FKS1* and *FKS2* are genes with similar and overlapping functions.

The genes putatively encoding two *S. cerevisiae* (1,3)-β-D-glucan synthases were cloned by another research group, using amino acid sequence obtained from product entrapped proteins (Inoue *et al.*, 1995). By running product-entrapped proteins on an SDS-PAGE gel, it was observed that fractions with increased (1,3)-β-D-glucan synthase activity were enriched with a 200 kDa protein. Monoclonal antibodies were raised against the product entrapped proteins and used to immunoprecipitate the 200 kDa peptide, which was sequenced. Two genes were subsequently cloned from the amino-acid sequence obtained in this way, and encoded proteins that were 88% identical to each other and had 16 predicted transmembrane domains. These genes were the same as *FKS1* and *FKS2* (Douglas *et al.*, 1994; Inoue *et al.*, 1995; Mazur *et al.*, 1995).

Since the cloning of the putative (1,3)-β-D-glucan synthase genes in yeast, orthologues have been identified in *A. fumigatus* (Beauvais *et al.*, 2001), *A. nidulans* (Kelly *et al.*, 1996), *C. albicans* (Mio *et al.*, 1997), *Cryptococcus neoformans* (Thompson *et al.*, 1999), *Paracoccidioides brasiliensis* (Pereira *et al.*, 2000) and *S. pombe* (Ishiguro *et al.*, 1997).

1.4.2.2 Higher Plant *GSL* Genes

(1,3)-β-D-Glucan is a major component in the yeast cell wall, but in plants the deposition and removal of (1,3)-β-D-glucan is tightly regulated and is mainly located in specialised cells, at specific stages of development and in response to biotic and abiotic stresses (*Section 1.2*; *Section 1.3*). The putative (1,3)-β-D-glucan synthase gene family in *S. cerevisiae* consists of only two genes, *FKS1* and *FKS2*, whereas in Arabidopsis there are 12 *AtGSL*s and in rice (*Oryza sativa*) there are nine *OsGSL*s. The structure of plant *GSL* genes may be divided into two groups, the low intron and

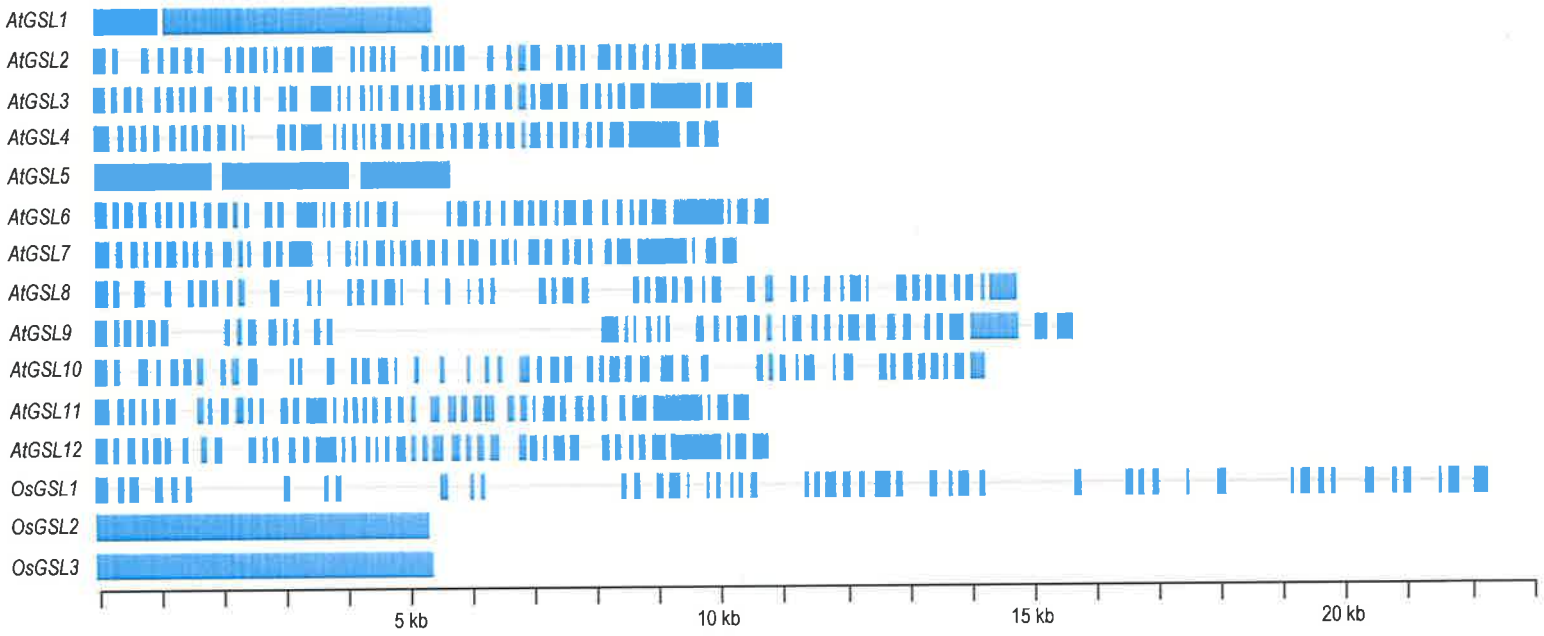

Figure 1.5: Schematic diagram of the gene structure of putative plant (1,3)-β-D-glucan synthases. Blue boxes represent exon sequence regions. Schematic downloaded from http://cellwall.stanford.edu/.

the high intron *GSL* genes (*Figure 1.5*). One group has relatively few introns, while the other consists of highly fragmented genes. The low intron *GSL* genes have zero, one or two introns, they span approximately 5.5 kb of genomic sequence and the group includes *AtGSL1*, *AtGSL5*, *OsGSL2* and *OsGSL3* (*Figure 1.5*). The high intron *GSL* genes have as many as 49 introns, they span as much as 22 kb of genomic sequence and include the remainder of the Arabidopsis and rice *GSL* genes (*Figure 1.5*). Several research groups have attempted to identify and characterise plant homologues of the yeast putative (1,3)-β-D-glucan synthases and to assign possible functions to these homologues (Cui *et al.*, 2001; Doblin *et al.*, 2001; Hong *et al.*, 2001a; Østergaard *et al.*, 2002; Jacobs *et al.*, 2003; Li *et al.*, 2003; Nishimura *et al.*, 2003).

In Arabidopsis, a gene showing homology to the *S. cerevisiae* putative (1,3)-β-D-glucan synthase was cloned (Hong *et al.*, 2001a). The gene had 41 introns, a transcript size of 6 kb and it encoded a 226 kDa protein with 16 putative transmembrane domains, with a 481 amino acid putative cytoplasmic NH_2-terminal region and a 779 amino acid putative hydrophilic loop that was predicted to face the cytoplasm (Hong *et al.*, 2001a). The gene was originally called *CalS1* but using the recommended nomenclature for glucan synthases (http://cellwall.stanford.edu/), it will be called *AtGSL6* throughout this thesis. An interaction between the AtGSL6 protein, phragmoplastin and a novel UDP-glucose transferase, which co-purified with the (1,3)-β-D-glucan synthase activity (Hong *et al.*, 2001a; Hong *et al.*, 2001b), was reported. Fusions between *AtGSL6* and the green fluorescent protein gene (*GFP*) were made and the fusion products were located at the growing cell plate (Hong *et al.*, 2001a). The over-expression of *AtGSL6* in transgenic tobacco plants under the control of the cauliflower mosaic virus (CaMV) promoter, showed an increase in (1,3)-β-D-glucan synthesis at the growing cell plate when compared with control lines (Hong *et al.*, 2001a). Thus, it is possible that AtGSL6 is involved in the deposition of (1,3)-β-D-glucan at the forming cell plate in dividing Arabidopsis cells.

Another *GSL* from Arabidopsis that has recently attracted much interest is *AtGSL5*. Three separate groups have identified the gene and reported on its potential function.

An analysis of *AtGSL5* transcript levels suggested that it is transcribed at its highest levels in floral tissues, and that the production of *AtGSL5* mRNA is induced when wild-type plants are treated with salicylic acid (Østergaard *et al.*, 2002). Similarly, in a second study using an *AtGSL5* mutant (*pmr4*), it was shown that silencing of *AtGSL5* resulted in an up-regulation of the salicylic acid pathway (Nishimura *et al.*, 2003). Additional effects of silencing *AtGSL5* were uncovered by the use of dsRNAi lines, where it was shown that *AtGSL5* was involved in the deposition of (1,3)-β-D-glucan in response to wounding (Jacobs *et al.*, 2003). There was an absence of papillary (1,3)-β-D-glucan in response to fungal infection in the Arabidopsis *AtGSL5*-silenced mutants, which were more resistant to *Peronospora parasitica* and to a number of virulent powdery mildew species than wild type plants (Jacobs *et al.*, 2003; Nishimura *et al.*, 2003). Fungal resistance in these lines might be a result of the fungus utilising the wound response to either mask the fungal wall from plant hydrolytic enzymes (Jacobs *et al.*, 2003). The relationship between the transcription of *AtGSL5* and the induction of the salicylic acid pathway is not yet known. Some insight has been obtained when susceptibility to powdery mildew infection was restored by the *pmr4-nahg* double mutant, suggesting the negative regulation of the salicylic acid pathway by *AtGSL5* (Nishimura *et al.*, 2003). The identification of *AtGSL5* orthologues in important cereal crop species, which are susceptible to fungal attack, could be of great economic importance if manipulation provided enhanced fungal resistance at a general level.

In addition to the function of *AtGSL5* in the deposition of (1,3)-β-D-glucan in response to wounding, this gene has recently been implicated in sporophytic development and in reproduction (Enns *et al.*, 2005). In this study, TILLING mutants with an inserted stop codon in the *AtGSL1* (*gsl1-1*) and *AtGSL5* (*gsl5-2*) genes were crossed with each other and with a T-DNA insertion *AtGSL5* (*gsl5-3*) mutant. Plants that were homozygous for *gsl1-1* were comparable to the wild-type, while plants that were homozygous for either of the two *gsl5* alleles had decreased leaf size (Enns *et al.*, 2005). Plants with a *gsl1-1*/+ *gsl5*/*gsl5* genotype had a more severe mutant phenotype than *gsl5*/*gsl5* mutants showing smaller leaves, extremely short lateral bolts, shorter roots and smaller floral organs (Enns *et al.*, 2005). Furthermore, the

seeds from *gsl1-1/+ gsl5/gsl5* plants had decreased viability when compared to seeds from wild-type plants (Enns *et al.*, 2005). When wild-type pollen was used to fertilise a *gsl1-1/+ gsl5/gsl5* plant, some of the offspring had both mutant alleles. However when pollen from a *gsl1-1/+ gsl5/gsl5* plant was used to fertilise a wild-type plant, none of the offspring inherited the two mutant alleles, suggesting that a chromosome with both mutations results in infertile pollen (Enns *et al.*, 2005). On closer analysis of pollen grain morphology it was observed that *gsl1-1/+ gsl5/gsl5* plants, as well as *gsl1-1/gsl1-1 gsl5/+* plants, produced pollen grains that were often collapsed and infertile. Furthermore, pollen grains from *gsl1-1/+ gsl5/gsl5* plants were sometimes abnormally large with unusual pore structures. In the *gsl1-1/+ gsl5/gsl5* genotype, the (1,3)-β-D-glucan-enriched wall was formed around the pollen mother cells as in the wild-type. However, in *gsl1-1/+ gsl5/gsl5* plants no (1,3)-β-D-glucan was present in the walls separating the tetrads (*Section 1.2.2.3*) This resulted in problems with tetrad dissociation (Enns *et al.*, 2005). It was concluded from this work that *AtGSL1* and *AtGSL5* play important and complementary roles in both sporophytic development and in the development of pollen (Enns *et al.*, 2005). In addition, it was suggested that *AtGSL1* and *AtGSL5* are responsible for the formation of the (1,3)-β-D-glucan wall that separates the microspores of the tetrad, and also play a gametophytic role later in pollen grain maturation (Enns *et al.*, 2005). The functional analyses of *AtGSL5* in response to wounding (Jacobs *et al.*, 2003; Nishimura *et al.*, 2003) and in sporophytic development and reproduction (Enns *et al.*, 2005), clearly show that individual *GSL* genes may have multiple and seemingly unrelated functions.

There have been relatively few reports of cloning and characterisation of putative (1,3)-β-D-glucan synthases from plant species other than Arabidopsis. Using primers based on the *FKS1* conserved region, a transcript was amplified from a cDNA population from *N. alata* pollen tubes (Doblin *et al.*, 2001). Reverse transcription PCR analysis showed that *NaGSL1* is transcribed predominantly in the developing and mature pollen, and in growing pollen tubes. A putative (1,3)-β-D-glucan synthase, *CFL1*, subsequently renamed *GhGSL1*, has also been cloned from cotton using EST data and 5'RACE methods (Cui *et al.*, 2001). The protein encoded by

*GhGSL1*is 219 kDa and has 13 putative transmembrane helices. Antibodies raised against an expressed soluble region of CFL1 bound to a protein of approximately 200 kDa that was located in a product entrapped fraction. *GhGSL1* is 21% identical and 41% similar over the entire length, and 31% identical and 52% similar over the cytoplasmic loop, when compared with *FKS1*. The transcription of *GhGSL1* was greatest in primary wall development in cotton fibres and young roots.

In barley there has been only one putative (1,3)-β-D-glucan synthase gene (*HvGSL1*) that has been cloned. A 6.1 kb cDNA was cloned and the transcript detected at high levels in the early developing grain, florets, coleoptiles and roots, but not in leaves infected with a fungal pathogen (Li *et al.*, 2003). A membrane fraction of barley suspension culture cells, subjected to CHAPS extraction, $CaCl_2$ treatment and sucrose density gradient centrifugation, had a 60-fold increase in (1,3)-β-D-glucan synthase activity (Li *et al.*, 2003). Proteins in the (1,3)-β-D-glucan synthase activity enriched fraction were separated on a non-denaturing polyacrylamide gel and in-gel (1,3)-β-D-glucan synthase activity assays showed that the active fraction barely entered the stacking gel (Li *et al.*, 2003). The suggested reason for the active fraction not readily entering the stacking gel was the poor migration of liposome associated (1,3)-β-D-glucan synthase proteins through the non-denaturing gel (Li *et al.*, 2003). Tryptic digestion of the active band from the non-denaturing gel and subsequent mass spectrometry showed that five tryptic fragments matched the deduced amino acid sequence of the *HvGSL1* cDNA (Li *et al.*, 2003). The (1,3)-β-D-glucan synthase active band in the non-denaturing gel was excised and separated on an SDS-PAGE gel and subsequently silver stained. A 220 kDa protein was the most abundant and was bound by antibodies that were raised against a 17 kDa protein generated by heterologous expression of an *HvGSL1* fragment (Li *et al.*, 2003). In addition to the 220 kDa protein, other smaller proteins were observed when the (1,3)-β-D-glucan synthase active fraction from the non-denaturing gel was separated by SDS-PAGE (Li *et al.*, 2003). These smaller proteins were similar in size to those previously reported co-purify with (1,3)-β-D-glucan synthase activity (Meikle *et al.*, 1991; Slay *et al.*, 1992; Dhugga and Ray, 1994; Gregory *et al.*, 2002). Although the HvGSL1 peptide appears to be abundant in the (1,3)-β-D-glucan synthase enriched fraction, it

remains possible, if unlikely, that the smaller proteins may be responsible for the synthesis of (1,3)-β-D-glucan (Li *et al.*, 2003). It was also suggested that these smaller proteins may form a larger, catalytically active protein complex or may simply be contaminants physically trapped in the CHAPS-generated micelles (Li *et al.*, 2003).

1.5 SUMMARY AND PROJECT AIMS

It is known that (1,3)-β-D-glucan is deposited in a variety of specialised plants tissues (*Section 1.2.2*) and in response to a number of biotic and abiotic stresses (*Section 1.3*). Various gene silencing techniques have clearly demonstrated that the *FKS* genes of yeast and the *GSL* genes of plants are essential for the synthesis and/or deposition of (1,3)-β-D-glucan (Douglas *et al.*, 1994; Jacobs *et al.*, 2003; Nishimura *et al.*, 2003). The proteins encoded by *GSL* genes are all approximately 200 kDa and have a large putative cytoplasmic hydrophilic domain flanked by two large hydrophobic domains, which are predicted to contain numerous transmembrane domains (*Figure 1.4*). The putative cytoplasmic domain contains a highly conserved region with an unknown function, and lacks similarity and key features, such as UDP-glucose binding motifs, with other proteins involved in polysaccharide synthesis (Li *et al.*, 2003). Although numerous biochemical studies have shown that the proteins encoded by the *GSL* genes co-purify with (1,3)-β-D-glucan synthase activity *in vitro* (*Section 1.4.1*), the exact role of GSL proteins in the synthesis of (1,3)-β-D-glucan is still unknown. Several small proteins, characterised as GTPases (*Section 1.4.1.3*) and UDP-glucose binding proteins (*Section 1.4.1.1*), also co-purify with (1,3)-β-D-glucan synthase activity and it has been suggested that they function in an active protein complex with the GSL proteins (Verma and Hong, 2001).

The overall aim of this project was to determine possible functions of individual members of the barley (1,3)-β-D-glucan synthase gene family. To date, only one plant *GSL* gene has been assigned a function. It was observed that when *AtGSL5* was silenced, Arabidopsis lines lacked wound-induced deposition of (1,3)-β-D-glucan, deposited no (1,3)-β-D-glucan in papillary structures in response to fungal attack, and exhibited an increase in fungal resistance (Jacobs *et al.*, 2003; Nishimura *et al.*,

2003). Since barley is a cereal crop subject to attack by numerous fungal pathogens, which frequently results in yield decreases, and because it is an important cereal in the food and brewing industries, the focus of the work was on determining potential barley orthologues to the Arabidopsis *AtGSL5* gene and assigning functions to these genes.

Within the overall objective, specific aims of the project were:

1) To clone cDNAs encoding putative (1,3)-β-D-glucan synthases from barley and to compare sequence data with other putative (1,3)-β-D-glucan synthases (*Chapter 2*).

2) To map the putative barley (1,3)-β-D-glucan synthases to a chromosomal location (*Chapter 2*).

3) To gain insights into barley (1,3)-β-D-glucan synthase functions through the analysis of transcription patterns in a variety of barley tissues, using EST data and quantitative real-time PCR (*Chapter 3*).

4) To determine which genes are co-ordinately transcribed with *HvGSL* genes, through the analysis of reference data from the barley microarray chip produced by Affymetrix (*Chapter 3*).

5) To determine the potential barley genes orthologous to *AtGSL5* in Arabidopsis, and to transiently alter transcript abundance of *AtGSL5* orthologues in barley through double-stranded RNA interference. These experiments were designed to determine if disruption of the *AtGSL5* orthologue in barley results in disruption of wound (1,3)-β-D-glucan deposition, as measured by a lack of (1,3)-β-D-glucan in papillary structures (*Chapter 4*).

6) In *Chapter 5* the results of the work are summarised and possible future directions for the project are discussed.

Chapter 2

Cloning, Mapping and Sequence Analysis of HvGSL *Genes from* Hordeum vulgare

2.1 INTRODUCTION

The main focus of this project was to characterise and to attempt to assign functions to ***Hordeum vulgare*** (barley) β-**g**lucan **s**ynthase-**l**ike genes (*HvGSL*), using molecular biological techniques. It was therefore necessary to clone DNA fragments of members of the *HvGSL* gene family to facilitate genetic mapping of the *HvGSL* genes, quantitative real-time PCR analysis of transcript levels (*Chapter 3*), the analysis of microarray experiments (*Chapter 3*) and the silencing of *HvGSL* genes with dsRNAi constructs (*Chapter 4*).

The identification of genes essential for the synthesis of (1,3)-β-D-glucan were first described in *Saccharomyces cerevisiae* (Douglas *et al.*, 1994; Inoue *et al.*, 1995). Since the discovery of the putative (1,3)-β-glucan synthases from *S. cerevisiae*, more have been uncovered in other fungal species, including *Yarrowia lipolytica* and *Aspergillus nidulans*, and also in higher plants. Genome sequencing projects have allowed the prediction of 12 *GSL* genes in Arabidopsis and nine *GSL* genes in *Oryza sativa* (rice). Full length cDNAs have been obtained for the *AtGSL5* and *AtGSL6* (*CalS1*) genes from Arabidopsis, the *NaGSL1* gene from *Nicotiana alata*, the *GhGSL1* (*CFL1*) gene from *Gossypium hirsutum* (cotton), the *HvGSL1* gene from *Hordeum vulgare* (barley), and the *LmGSL1* gene (accession: AY286332) from *Lolium multiflorum* (Cui *et al.*, 2001; Doblin *et al.*, 2001; Hong *et al.*, 2001a; Østergaard *et al.*, 2002; Jacobs *et al.*, 2003; Li *et al.*, 2003). Despite the rice genome sequence project, there have been no published reports of cloning *GSL* genes from rice.

The *FKS* genes from *S. cerevisiae* and the *GSL* genes from plants encode proteins that are predicted to be associated with the cellular membrane and to have a similar topology (Douglas *et al.*, 1994; Doblin *et al.*, 2001; Østergaard *et al.*, 2002; Li *et al.*, 2003). Li *et al.* (2003) have shown that a GSL protein in barley is associated with the synthesis of (1,3)-β-D-glucan, although the co-purification of other proteins with (1,3)-β-D-glucan synthase activity casts some uncertainty the exact role of GSL proteins in the synthesis of (1,3)-β-D-glucan (Meikle *et al.*, 1991; Slay *et al.*, 1992; Dhugga and Ray, 1994; Gregory *et al.*, 2002; Li *et al.*, 2003). In particular, no

obvious UDP-glucose binding site or catalytic amino acid residues can be identified, and it remains unclear as to whether the encoded protein would have any catalytic activity.

Gene silencing techniques have shown that the proteins encoded by *FKS* genes in *S. cerevisiae* and the *GSL* genes in Arabidopsis are essential for the synthesis of (1,3)-β-D-glucan (Douglas *et al.*, 1994; Jacobs *et al.*, 2003; Nishimura *et al.*, 2003). The *AtGSL5* gene from Arabidopsis was shown to be required for the formation of (1,3)-β-D-glucan in response to wounding (Jacobs *et al.*, 2003; Nishimura *et al.*, 2003). Arabidopsis lines with disrupted *AtGSL5* function lacked (1,3)-β-D-glucan in papillary structures in response to fungal attack and were more resistant to a range of fungal pathogens (Jacobs *et al.*, 2003; Nishimura *et al.*, 2003). Since barley is a cereal crop that is susceptible to a range of fungal pathogens, which could result in yield loss, the cloning effort described in this Chapter was particularly focused on the identification of the *AtGSL5* orthologue in barley.

The techniques used to obtain *GSL* gene sequences from barley are described in this Chapter. Initially, *HvGSL* EST sequences were downloaded from databases and contiguous sequences were constructed. These were used as a basis for cloning a number of *HvGSL* cDNAs from various barley cDNA populations, with an emphasis on the identification of the barley orthologue of *AtGSL5*. The sequence data of *HvGSL* genes were compared with *GSL* gene sequences already identified from other plant and fungal species, and the *HvGSL* genes were mapped to the chromosomal level. Sequences of the cloned *HvGSL* genes and the sequence analysis described in this Chapter were used in subsequent transcript profiling (*Chapter 3*) and gene silencing experiments (*Chapter 4*).

In setting out this chapter, general methods are first presented in the Materials and Methods (*Section 2.2*). The strategies used to generate the various cDNAs encoding individual *HvGSL* genes are subsequently described in the Results Section, because the isolation of the individual cDNA involved different cloning protocols.

2.2 MATERIALS and METHODS

2.2.1 Materials

The Elongase PCR reaction kit, 1 kb Plus DNA ladder, SSIII reverse transcriptase and buffers, RNaseOUT, RNaseH, Klenow and TRIZOL were purchased from Invitrogen Corporation (Carlsbad, CA, USA). Chloroform, propan-2-ol, calcium chloride, magnesium chloride, potassium chloride, sodium chloride, glucose, sodium hydroxide, dimethyl formamide and ethanol were purchased from Merck Pty. Ltd (Kilsyth, Vic, Australia). The DNA-free™ kit and nuclease-free distilled water was purchased from Ambion (Austin, TX, USA). Oligonucleotides used to amplify specific genes were purchased from Geneworks (Adelaide, SA, Australia). Ampicillin, EDTA, Tris, glycerol, MOPS, RNaseA, rubidium chloride, ethidium bromide, salmon sperm DNA and DTT were purchased from Sigma-Aldrich, Inc. (St. Louis, MO, USA). dNTPs, Taq DNA-polymerase, pGEM®-T Easy cloning vector, T4 DNA ligase and 2x T4 DNA ligation buffer were purchased from Promega (Madison, WI, USA). SDS was purchased from VWR International, Ltd. (Poole, England). Manganese chloride and Triton X-100 were purchased from BDH Chemical Australia Pty. Ltd. (Kilsyth, Vic, Australia). Agarose was from Scientifix (Cheltenham, Vic, Australia), and the Nucleospin Cleanup Kit was obtained from Macherey-Nagel (Düren, Germany). The QIAGEN PCR Purification Kit and the QIAGEN Gel Extraction Kit were from QIAGEN (Clifton Hill, Vic, Australia). Butan-1-ol was from APS Ajax Finechem (Auburn, NSW, Australia). The XL1-Blue and the DH5α *E. coli* strains were purchased from Stratagene (La Jolla, CA, USA). Bacto™tryptone and Bacto™yeast extract were purchased from Becton, Dickinson and Company (Sparks, MD, USA). The *E. coli* Gene Pulser® cuvettes were obtained from Bio-Rad (Hercules, CA, USA). Restriction endonucleases, the corresponding 10x digestion buffers and 100 bp DNA ladder were from New England Biolabs (Beverly, MA, USA). The [α-^{32}P]dCTP, Sepharose CL-6B and Sephadex G-100 was purchased from Amersham-Pharmacia (Castle Hill, NSW, Australia). The BigDye® Terminator v3.1 Cycle Sequencing Kit was purchased from Applied Biosystems (Foster City, CA, USA).

2.2.2 Bioinformatics

The nucleotide and deduced amino acid sequences of all publicly available full length *GSL* genes were obtained from the NCBI databases (http://www.ncbi.nlm.nih.gov/), using the nomenclature recommended in the Standford University cell wall web site (http://cellwall.standford.edu/). Barley EST sequences that showed sequence identity to known full length *GSL* genes were subsequently obtained either from the NCBI EST database (http://www.ncbi.nlm.nih.gov/ dbEST/index.html), or from the Standford University cell wall web site. The EST sequences were converted into contiguous sequences using the ContigExpress application of the VectorNTi computer program. Nucleotide and deduced amino acid sequence alignments of the full length *GSL* genes and the partial *HvGSL* sequences were performed with the ClustalW (http://www.ebi.ac.uk/clustalw/), ClustalX and Blast2 (http://www.ncbi.nlm.nih.gov/ blast/bl2seq/wblast2.cgi) computer programs. Translations were performed with the online program, "DNA to Protein Translation", located at http://bio.lundberg.gu.se/edu/translat.html. The phylogenetic tree was constructed using the ClustalX program, and subsequently viewed using the TreeView program. Membrane topology predictions were performed using PRED-TMR (http://biophysics.biol.uoa.gr/PRED-TMR/input.html), Phobius prediction (http://phobius.cgb.ki.se/) and HmmTop_v2 (http://www.enzim.hu/hmmtop/ html/submit.html).

2.2.3 Total RNA Extraction

A variety of barley tissues including nine day old dark grown whole seedlings, pre-anthesis whole flowers and *Blumeria graminis* infected barley epidermis were collected, frozen under liquid nitrogen and stored at -80°C. The frozen tissue (50 – 100 mg) was ground to a fine powder using two methods. The first method used a Teflon pestle in a 1.5 ml tube to grind 50 – 100 mg frozen tissue in 500 µl TRIZOL. An extra 500 µl TRIZOL was added when the tissue was ground to homogeneity. The second method used a 10 ml tube that contained 50 – 100 mg frozen tissue and four ball bearings (1x 9 mm diameter, 3x 4 mm diameter). The tissue was ground in

a "Gallenkamp Flask Shaker" at setting 6 – 7 a total of four times for 15 sec, returning the tubes to liquid nitrogen between shaking. The frozen tissue powder was resuspended in 1 ml TRIZOL, and transferred to a 1.5 ml tube. The insoluble cellular debris was pelleted by centrifugation at 12000 g for 15 min at 4°C. The supernatant was transferred to a new 1.5 ml tube, 200 µl chloroform was added and the sample was mixed by inversion several times and left at room temperature for 3 min. The mixture was centrifuged at 12000 g for 15 min at 4°C. The upper aqueous phase was removed and transferred to a clean 1.5 ml tube and 500 µl propan-2-ol was added to precipitate nucleic acids. The sample was mixed by inversion and allowed to stand at room temperature for 10 min. Nucleic acids were pelleted by centrifugation at 12000 g for 10 min at 4°C. The supernatant was discarded, and the pellet was washed by adding 1 ml 75% (v/v) ethanol and gently inverting the tube several times. The mixture was centrifuged at 7500 g for 5 min at 4°C and the supernatant discarded. The pelleted nucleic acid was left to air dry for 5 min, or until the pellet had become transparent. The dried pellet was resuspended in 26 µl sterile nuclease-free distilled water.

Removal of DNA from the total RNA extract was achieved using the DNA-*free*™ kit. The total RNA extract prepared as described above was added to 3 µl 10x DNase I buffer and 1 µl DNase I (2 units) in a total of 30 µl. The sample was mixed by gentle inversion and incubated at 37°C for 30 min. The DNase was inactivated by adding 5 µl DNase Inactivation Reagent to the sample. The sample was mixed by gently flicking the tube and was incubated at room temperature for 2 min. The resin in the DNase Inactivation Reagent was pelleted by centrifugation at 10000 g for 1 min. The DNA-free, total RNA preparation was stored at –80°C.

Total RNA samples were extracted from developing barley endosperm (two days post-pollination) and pooled embryo and scutellum tissue excised from grains that were imbibed for 24 hr and germinated for 8 hr (Dr Rachel Burton, *personal communication*).

2.2.4 First Strand cDNA Synthesis for PCR

Between 0.5 µg and 3 µg of total RNA (*Section 2.2.3*) was added to 1 µl 50 µM oligo(dT) primer and sterile distilled water in a total volume of 10 µl. The mixture was incubated at 65°C for 5 min and placed on ice. A 10 µl aliquot of Master RT mix (2 µl 10x RT Buffer, 1 µl 0.1 M DTT, 1 µl (40 units) RNase OUT Ribonuclease inhibitor, 2 µl 10 mM dNTP, 0.5 µl (7 units) RT and 1.5 µl sterile distilled water) was added to the mixture on ice. The reaction mixture was incubated at 52°C for 1 hr, followed by 85°C for 5 min. To cleave the RNA that was part of an RNA/DNA duplex, 1 unit RNaseH was added and incubated at 37°C for 20 min. The cDNA preparation was adjusted to a volume of 50 µl by adding 30 µl sterile distilled water. When making first strand cDNA for 3' **R**apid **A**mplification of **c**DNA **E**nds (3'RACE), the oligo(dT) primer was replaced with an equal amount of T-RACE primer (Frohman *et al.*, 1988).

2.2.5 PCR Amplification of Single Stranded cDNA

PCR

The polymerase chain reaction (PCR) was used to amplify DNA fragments with sizes in the range of 100 bp to about 2000 bp. Reactions were performed in a total volume of 25 µl and contained 1 µl cDNA (*Section 2.2.4*), 2 µl 10x PCR buffer (100 mM Tris-HCl buffer, pH 9.0, containing 500 mM KCl, 10% Triton X-100), 1.5 µl 25 mM $MgCl_2$, 1 µl 5mM dNTPs, 1 unit Taq DNA polymerase and 10 µM each of the forward and reverse gene-specific oligonucleotide primers. The PCR thermal cycling parameters for the amplification of DNA commonly started with a melt step of 95°C for 30 sec, followed by a primer annealing step with a temperature within 5°C of the primer T_m for 30 sec, and an extension step at 72°C for 1 min per 1000 bp of expected amplified product size. The PCR thermal cycling was repeated 35 times.

PCR using Elongase

When the expected PCR product was greater than 2000 bp, the Elongase enzyme mix was used. The reactions contained 1 µl synthesised cDNA (*Section 2.2.4*), 2.5 µl 10x Elongase buffer A and 2.5 µl 10x Elongase buffer B, 0.5 µl Elongase enzyme mix, 1

µl 5 mM dNTPs and 10 µM of each forward and reverse gene-specific oligonucleotide primers. The thermal cycling for the Elongase reaction was similar to that described above, except that the extension temperature was optimised for the Elongase enzyme mix (68°C).

Nested and Semi-Nested PCR

The fidelity of a PCR may be increased by the use of two reactions in succession. The first reaction was performed as described above. The primers that were used in the second reaction were nested with respect to the primers of the first reaction, and a dilution of the first reaction product was used as the template. This method was used in 3'RACE, genomic walking and when a degenerate primer was being used.

3'RACE

The amplification of the 3' untranslated region of transcripts (3'UTR) was achieved using the technique called 3'RACE (Frohman *et al.*, 1988). Two successive PCR reactions were performed in the 3'RACE method. The first PCR reaction was performed using the specifically designed cDNA that had a sequence adapted to the 3' end of the poly-T tail (*Section 2.2.4*) as the template. The PCR primers used in the first reaction were a forward gene specific primer and the reverse RACE-3' primer, which annealed to the 3' adaptor sequence of the cDNA template. A 1:100 dilution of the first PCR reaction was used as the template in the second PCR reaction. The PCR primers used in the second reaction were a nested forward gene specific primer and the reverse RACE-3' primer.

PCR Using Degenerate Primers

At times it was necessary to design primers in regions that have no sequence information available. In these cases, *GSL* gene sequences from Arabidopsis and rice were downloaded from either the Standford University cell wall web site (http://cellwall.stanford.edu/) or from the NCBI DNA database (http://www.ncbi.nlm.nih.gov/). The full length amino acid sequences were aligned using ClustalW and ClustalX (*Section 2.2.2*) along with the available sequence from barley. The corresponding nucleotide sequences of regions showing amino acid

sequence conservation were used for the design of degenerate primers. In cases where multiple nucleotide bases were used to code for the same amino acid, the alternative nucleotides were incorporated into the primer, hence creating primer degeneracy. Degenerate primers were commonly forward primers as they were designed to regions 5' of known sequence. When performing PCR with degenerate forward primers, two reverse nested gene-specific primers were used to increase the fidelity of the reaction.

Genomic Walking

The genomic walking protocol described by Siebert *et al.* (1995) is an effective way of obtaining unknown genomic sequence that is located 5' of know sequence data. A former member of the Fincher laboratory, Dr. Brendon King, prepared a genomic walking library by initially digesting barley genomic DNA with 17 combinations of blunt-end restriction endonuclease enzymes (*Dra*I, *Sma*I, *Stu*I, *Eco*RV, *Hin*dIII, *Sca*I, *Nru*I, *Pml*I, *Pvu*I, *Dra*I/*Eco*RI, *Sma*I/*Eco*RI, *Stu*I/*Eco*RI, *Hinc*II/*Eco*RI, *Sca*I/*Eco*RI, *Nru*I/*Eco*RI, *Pml*I/*Eco*RI, *Pvu*I/*Eco*RI). An adaptor sequence (5'-CTA ATA CGA CTC ACT ATA GGG CTC GAG CGG CCG CCC GGG CAG GT-3') was subsequently ligated to the blunt-ended genomic DNA fragments. The adaptor sequence contained the sequences of the AP1 and AP2 primers (*Appendix A*). The two adaptor specific primers were used with two nested gene-specific primers in a nested PCR to amplify genomic DNA sequence.

2.2.6 Cloning PCR Amplified Fragments into pGEM®-T Easy

PCR products were routinely checked prior to ligation by running a 5 µl aliquot of the reaction on a 1% agarose gel containing ethidium bromide. When one fragment size was observed on the agarose gel, the remainder of the PCR reaction was cleaned with either the NucleoSpin or the QIAGEN PCR Purification Kit. When two or more fragments were observed on the agarose gel, the remainder of the PCR reaction was separated on another 1% agarose gel, the band of expected size was excised, and DNA was cleaned with either the NucleoSpin or the QIAGEN Gel Extraction Kit. The final resuspension volume in both PCR purification methods was 25 µl, and the

volume was reduced to approximately 10 µl with a Speed-Vac (SC110, Savant) to further concentrate the PCR product.

Purified PCR products were commonly ligated into the pGEM®-T Easy cloning vector (*Figure 2.1*). The pGEM®-T Easy cloning vector is supplied as a linear fragment with T overhangs, which allow PCR products with A overhangs to be easily cloned. Purified PCR products and the pGEM®-T Easy vector were ligated together at an approximate ratio of 3:1, as determined by the brightness of bands on an agarose gel, with 2x T4 DNA ligation buffer and T4 DNA ligase. Ligation reactions were incubated at 14°C for 16 hr.

To successfully transform competent cells by electroporation, buffer salts must be removed from the ligation reaction. Salt removal was achieved by adding 40 µl sterile water to the ligation reaction along with 500 µl butan-1-ol. The mixture was vortexed and centrifuged at 16100 g for 15 min. The supernatant was removed, the pellet was dried using a SpeedVac® evaporator (SC110, Savant) and the DNA was resuspended in 10 µl sterile distilled water.

2.2.7 Transformation of *Escherichia coli*

Electroporation

The preparation of electrocompetent cells for transformation was as follows; a 500 ml culture of *E. coli* (strain XL1-Blue) in LB media (1% w/v bacto-tryptone, 0.5% w/v bacto-yeast extract, 1% w/v NaCl, pH 7) was grown at 37°C with 200 rpm shaking until an A_{600} of 0.6 was reached. Cells were centrifuged at 3220 g for 10 min and resuspended in 200 ml ice cold sterile water. The centrifugation was repeated and the cells were resuspended in 40 ml ice cold sterile water. The centrifugation was repeated again and the cells were resuspended in 10 ml ice cold sterile water. Centrifugation was repeated and the cells were resuspended in 10 ml ice cold sterile 10% glycerol. The cells were centrifuged once more and the final resuspension was in 3 ml ice cold sterile 10% glycerol. Forty microliter aliquots were snap frozen in liquid nitrogen and stored at -80°C.

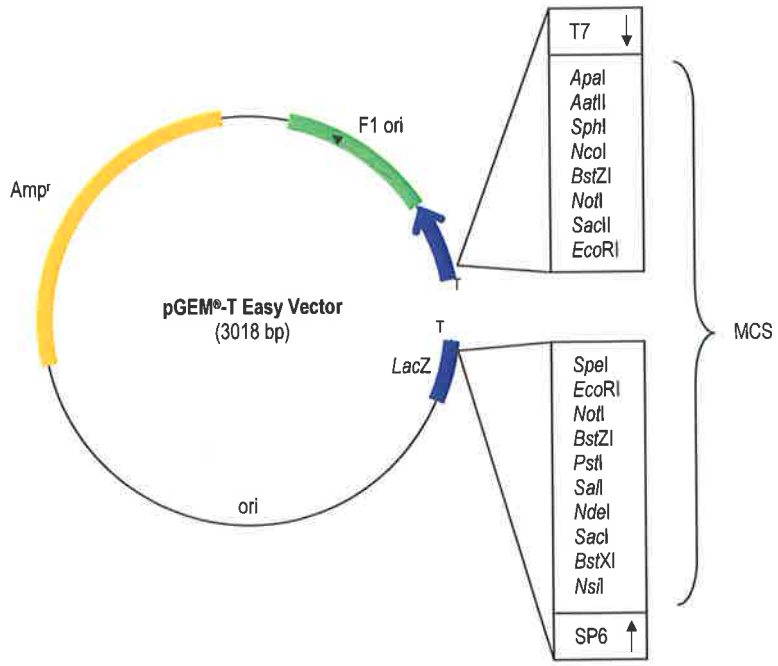

Figure 2.1: The pGEM®-T Easy PCR cloning vector that was used for cloning of the partial fragments of each of the *HvGSL*s. The pGEM®-T Easy vector is supplied as a linear DNA fragment with T-overhangs, which allow the ligation of PCR products with a single A-overhang. Ori: Origin of replication. Amp^r: Ampicillin resistance for antibiotic selection. *LacZ*: encodes β-galactosidase from the lac operon for blue-white selection of transformed colonies on agar plates containing X-gal. T7 and SP6: primers that were commonly used for sequencing the cloned insert (*Appendix A*). MCS: multiple cloning site. Image was adapted from the Promega website (www.promega.com).

E. coli Gene Pulser® Cuvettes along with butan-1-ol extracted ligations (*Section 2.2.6*) were placed on ice 2 hr prior to electroporation. Approximately 10 min prior to electroporation the prepared competent cells were thawed on ice. An aliquot of 5 µl of butan-1-ol extracted ligation was added to 40 µl electrocompetent cells and the mixture was placed immediately into the chilled cuvette, which was subsequently placed into the BIO-RAD Gene Pulser™ and subjected to electroporation at 1.8 V, 25 µFD and 200 Ω. The electroporated mixture was added to 300 µl LB and the cells were allowed to recover for 1 hr at 37°C. The cells were plated onto LB agar with 100 µg Ampicillin per 1 ml LBA and incubated for 16 hr at 37°C.

Heat Shock

Competent cells for transformation were prepared as follows. A 1 ml overnight culture of *E. coli* (strain DH5α) was used to inoculate 100 ml LB pre-warmed to 37°C. Cells were grown at 37°C with 200 rpm shaking until an A_{600} of 0.4 was reached, and were decanted into 25 ml Corex tubes. Cells were centrifuged at 6000 rpm at 4°C for 5 min, and each pellet was resuspended in 10 ml TfbI (30 mM potassium acetate buffer, pH 5.8, containing 100 mM rubidium chloride, 10 mM calcium chloride, 50 mM manganese chloride and 15% glycerol) and left on ice for 5 min. Cells were again centrifuged at 6000 rpm at 4°C for 5 min and each pellet was resuspended in 1 ml TfbII (10 mM MOPS buffer, pH 6.6, containing 75 mM calcium chloride, 10 mM rubidium chloride and 15% glycerol) and left on ice for 15 min. Aliquots of 100 µl were frozen in liquid nitrogen and stored at –80°C.

A 5 – 10 µl portion of the ligation was added to 50 µl heat shock competent DH5α cells. The sample was mixed by gentle inversion and placed on ice for 30 min. The cells were heat shocked in a 42°C water bath for 90 sec and allowed to recover by adding 250 µl LB and incubating for approximately 1 hr. The cells were spread on LB agar plates containing 0.1 $mg.ml^{-1}$ Ampicillin.

2.2.8 PCR Screening of Colonies

Since *E. coli* does not contain the putative (1,3)-β-D-glucan synthase genes, it was possible to screen colonies using a PCR-based method. Individual colonies from LBA plates transformed with ligated DNA (*Section 2.2.7*) were initially streaked on LBA plates containing the appropriate antibiotic for selection with a toothpick or pipette tip. Plates were incubated at 37°C for five to eight hours. The same toothpick or pipette tip was used to inoculate a PCR reaction containing gene-specific primers. PCR reaction conditions and thermal cycling parameters were as described above. A 5 µl aliquot of the PCR was run on a 1% agarose gel. Colonies having the expected sized inserts as determined by PCR were used to inoculate a 3 ml liquid LB culture containing the appropriate antibiotic, and the cells were grown overnight at 37°C with shaking at 200 rpm.

2.2.9 Plasmid DNA Mini-Preparations

E. coli transformed with plasmids containing cDNA and gene fragments of (1,3)-β-D-glucan synthases were grown in 2 ml LB with 100 $\mu g.ml^{-1}$ Ampicillin at 37°C for 16 hr with shaking at 200 rpm. Plasmid DNA was prepared using the alkaline lysis method. The 2 ml culture was centrifuged at 16100 g for 30 sec and the supernatant was discarded. Pelleted cells were resuspended in 100 µl GTE buffer (25 mM Tris-HCl buffer, pH 8.0, containing 10 mM EDTA and 50 mM glucose) and placed on ice for 1 min. To the resuspended cells, 200 µl freshly prepared NaOH/SDS solution (0.2 M NaOH, 1% SDS) was added and the sample was mixed by gentle inversion several times and placed on ice for 5 min. A solution of 150 µl 3 M potassium 5 M acetate (60 ml 5 M potassium acetate, 11.5 ml glacial acetic acid, 28.5 ml sterile water) was added and the sample was mixed by gentle inversion several more times and placed on ice for 5 min. The cellular debris was pelleted by centrifugation at 16100 g for 10 min. The supernatant was transferred to a clean 1.5 ml tube and 1 ml 100% ethanol was added to precipitate the plasmid DNA, the sample was mixed by inversion and allowed to stand at RT for 5 min. Plasmid DNA was pelleted by centrifugation at 16100 g for 10 min. The supernatant was removed and the pellet was gently washed with 70% (v/v) ethanol and dried using a SpeedVac® evaporator for 5 min. The dried

pellet was resuspended in 50 µl TE (10 mM Tris-HCl buffer, pH 7.5, containing 1 mM EDTA) and 1 µl 10 $mg.ml^{-1}$ RNase.

2.2.10 Restriction Endonuclease Digestion of DNA

Restriction endonuclease digests were performed using an aliquot of 2 – 5 µl of DNA with 1 unit restriction endonuclease and 2 µl of the appropriate 10x digestion buffer in a total volume of 20 µl. Reactions were commonly carried out at 37°C for 1 hr.

2.2.11 DNA Sequencing

Sepharose CL-6B Clean-up

To remove salts prior to sequencing, it was necessary to clean the DNA sample through a Sepharose CL-6B column. The column was made by punching a hole in the bottom of a 0.5 ml tube and placing it in a 1.5 ml tube. Between 5 and 10 small glass beads were placed in the bottom of the 0.5 ml tube and were overlaid with Sepharose CL-6B. The column was centrifuged twice at 2000 rpm for 3 min in a micro-centrifuge, discarding the flow-through after each spin. The 0.5 ml tube was placed in a clean 1.5 ml tube, the DNA sample to be sequenced was overlaid on the Sepharose column and centrifuged at 2000 rpm for 3 min in a micro-centrifuge.

BigDye PCR Sequencing Reaction

The BigDye® Terminator v3.1 Cycle Sequencing Kit was used to carry out the sequencing reaction. The sequencing reaction was performed in a total volume of 20 µl. The reaction contained 150 – 300 ng of double-stranded DNA template, 3.2 pmol of sequencing primer and 4 µl BigDye v3.1 sequencing buffer. The sequencing PCR thermal cycling parameters commonly started with an initial melt step of 96°C for 30 seconds, followed by 25 cycles of 96°C for 30 sec, 50°C for 30 sec and 60°C for 4 min with a final hold temperature of 4°C.

Propan-1-ol Cleanup of PCR Sequencing Reaction

Sequencing reactions were cleaned prior to submission to IMVS (Institute of Medical and Veterinary Science, Adelaide, Australia). The 20 µl sequencing reaction was

mixed with 80 µl freshly prepared 75% (v/v) propan-1-ol and incubated at room temperature for 15 min. The DNA was pelleted by centrifugation at 13200 rpm for 20 min in a table-top micro-centrifuge. The supernatant was discarded and the pellet was washed with 150 µl 75% (v/v) propan-1-ol. The DNA was pelleted by centrifugation at 13200 rpm for 5 min in a micro-centrifuge. The supernatant was discarded and the pellet was dried in a SpeedVac® evaporator for 10 min.

2.2.12 Genetic Mapping of *HvGSL* Genes

Mapping Populations

The wheat-barley addition lines were generated by Dr Rafiq Islam at the University of Adelaide (Islam and Shepherd, 1981). The Clipper-Sahara mapping population used in the gene mapping experiments was generated by Karakousis *et al.* (2003). Genomic DNA digests and the transfer of agarose gel-separated genomic fragments to membranes was performed by Margaret Pallotta (Australian Centre for Plant Functional Genomics, Adelaide, Australia). All solutions used in the Southern blots and hybridisation procedures were as described by Sambrook *et al.* (1987).

Preparation of HvGSL *Gene Specific Probes*

HvGSL gene-specific DNA probes were designed towards the poorly conserved 3' end of each gene. Gene-specific probes were PCR (*Section 2.2.5*) amplified from cloned *HvGSL* gene fragments and subsequently purified using the QIAGEN PCR cleanup kit.

A 3 µl aliquot of cleaned *HvGSL* gene-specific DNA was added to 0.3 µg of 9-mer random primers along with 3 µl water. The mixture was boiled for 5 min and subsequently chilled on ice for 5 min. To this DNA mixture, 13 µl 2x Oligo Buffer that contained all dNTPs with the exception of dCTP was added. A 1.5 µl volume of Klenow DNA polymerase and 3.5 µl [α-^{32}P]dCTP was added and mixed gently with a pipette tip. The sample was incubated at 37°C for 2 hr. To remove unincorporated [α-^{32}P]dCTP from the radiolabelled probe mixture, the sample was run through a Sephadex G-100 mini-column. The mini-column was constructed with a Pasteur

pipette plugged with a small amount of glass wool to prevent the gel passing through. To stop the Sephadex from drying, the top of the mini-column was sealed with parafilm. The radiolabelled mixture was added below the surface level of the Sephadex G-100 mini-column.

The tip of a 1ml plastic pipette tip was cut off and the remaining portion was fitted to the top of the mini-column, to act as a funnel and was filled with TE buffer. When the radioactivity of the eluate reached greater than 100 counts per second (cps) it was collected in a microcentrifuge tube. The level of radiation commonly reached greater than 2000 cps, and once the radiation levels returned to 500 cps, collection ceased. The labelled probe fraction was boiled for 5 min and subsequently chilled on ice.

Hybridisation of Membranes

The membranes were washed twice in 5x SSC and placed in hybridisation bottles. Excess 5x SSC solution was drained by inverting the bottles upside-down on tissue paper. A 30 ml aliquot of pre-hybridisation solution (150 ml 10x SSC solution, 30 ml Denhardt's III, 15 ml salmon sperm, 105 ml water) was placed in the bottles containing the membranes and left in a 65°C rotary incubator for 16 hr.

The pre-hybridisation solution was removed and replaced with 10 ml of 65°C hybridisation buffer (3 ml 5x HSB, 3 ml Denhardt's III, 3ml 25% (w/v) dextran sulphate, 500 µl sterile nanopure water) and the entire radiolabelled probe fraction prepared as described above. The hybridisation bottle was placed in the 65°C rotary incubator for 16 hr.

The hybridisation solution was discarded and the hybridisation bottles were quarter filled with wash buffer #1 (40ml 10% SDS and 400 ml 20x SSC made to 4 L with water) and incubated at 65°C for 25 min. The membranes were transferred to a container with wash buffer #2 (40ml 10% SDS and 200 ml 20x SSC made to 4 L with water) and incubated at 65°C for 25 min. The membranes were washed a final time in wash buffer #3 (40ml 10% SDS and 100 ml 20x SSC made to 4 L with water) at 65°C for approximately 2 hr.

The membranes were dried on tissue paper, covered with plastic and placed in a cassette with an RX X-ray film (Fuji Photo Film Co., Tokyo Japan). The X-ray film was exposed to the radiolabelled membranes for 5 days at -80°C and developed in an AGFA CP1000 X-ray processing/drying machine.

2.3 RESULTS

A total of 90 barley EST sequences that showed sequence homology to known *GSL* genes from Arabidopsis and rice were downloaded from either the NCBI database (http://www.ncbi.nlm.nih.gov/) or the Standford University cell wall web site (http://cellwall.standford.edu/). The ESTs were assembled into six contiguous sequences and six singletons were also identified using the Contig-Express application in the computer program VectorNTi (*Appendix B*).

2.3.1 Cloning of *HvGSL1*

The full sequence of an *HvGSL1* cDNA has already been determined by Dr Jing Li (Li *et al.*, 2003; *Appendix C*). There were 16 ESTs that aligned with the full open reading frame of *HvGSL1* (*Appendix B*).

2.3.2 Cloning of *HvGSL2* cDNA Fragments

Forty one ESTs formed a contiguous sequence that was designated *HvGSL2* (*Appendix B*). Gene-specific primers, *HvGSL2*_R2 and *HvGSL2*rev (*Appendix A*; *Figure 2.2*), were based on the contiguous EST sequence and were used to amplify a 1406 bp fragment of *HvGSL2*. PCR was performed with the *HvGSL2*_R2 and *HvGSL2*rev primers using cDNA derived from pooled embryo and scutellum tissue excised from 24 hr imbibed grain that had germinated for 8 hr. A portion of the PCR reaction was separated on an agarose gel and a 1406 bp fragment was observed (*Figure 2.3*). The remainder of the PCR reaction was cleaned using a QIAGEN PCR Purification Kit. A portion of the cleaned PCR was ligated into pGEM®-T Easy and used to transform competent *E. coli* cells. Plasmid DNA mini-preparations were made and the cloned insert was sequenced with the T7 and SP6 primers (*Appendix A*).

Gene-specific primers, *GSL2*_3RACE_F1 and *GSL2*_3RACE_F2 (*Appendix A*; *Figure 2.2*), were designed based on the 1406 bp *HvGSL2* nucleotide sequence described above. The *GSL2*_3RACE_F1/RACE3' primer pair was used in 3'RACE using cDNA derived from 2 day developing endosperm as the template. A second

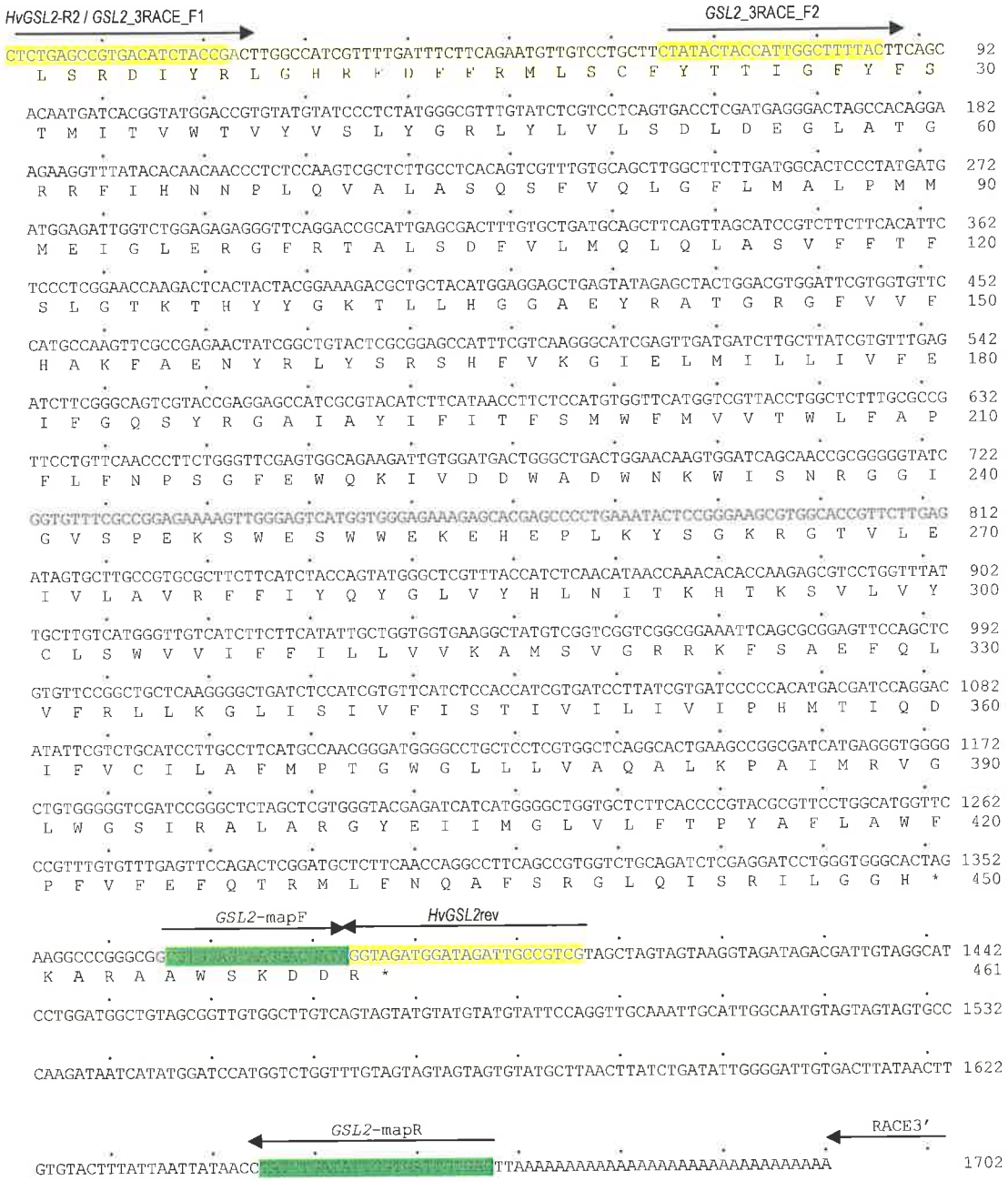

Figure 2.2: The nucleotide and deduced amino acid sequence of a cloned fragment of the *HvGSL2* cDNA. The primers used to amplify fragments of *HvGSL2* are highlighted and arrows indicate the orientation.

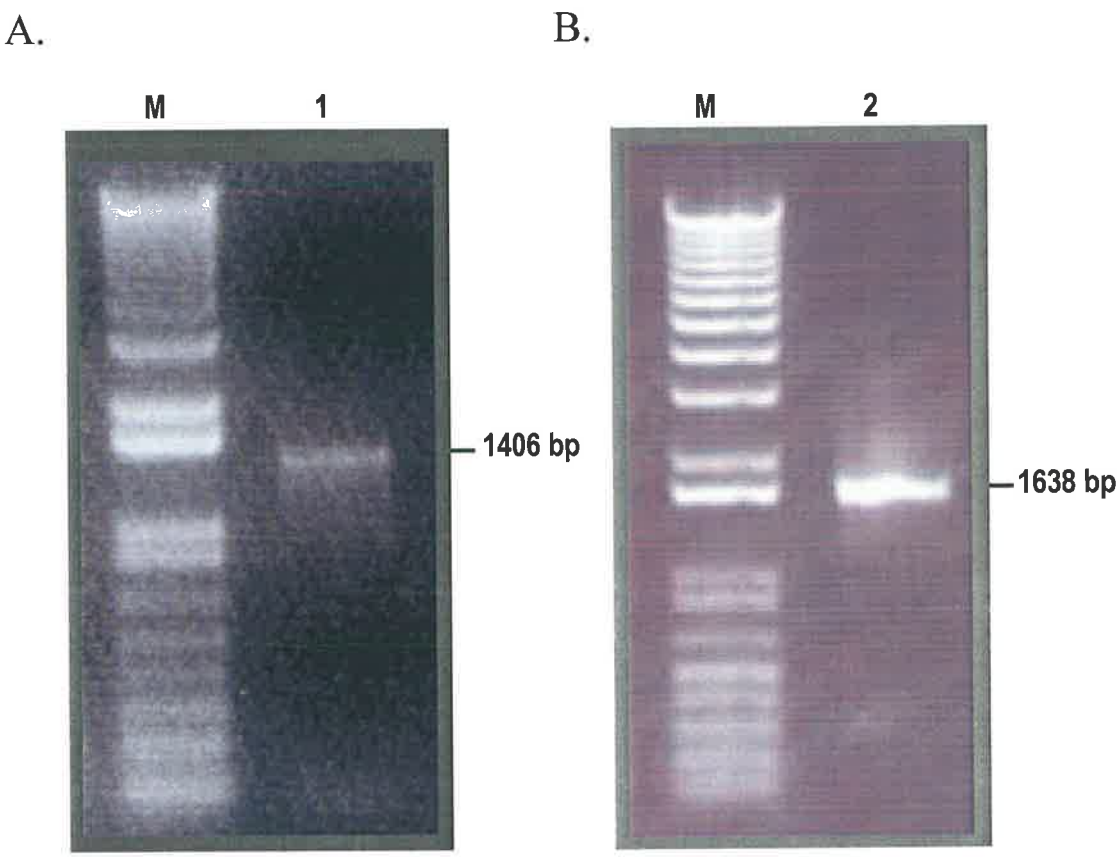

Figure 2.3: PCR amplified DNA fragments of *HvGSL2*. *Panel A.* M: 1 kb Plus DNA ladder; Lane 1: 1406 bp fragment amplified using the *HvGSL2*_R2 and *HvGSL2*rev primers derived from the EST contiguous sequence. *Panel B.* M: 1 kb Plus DNA ladder; Lane 2: 1638 bp fragment amplified using the *GSL2*_3RACE_F1 and *GSL2*_3RACE_F2 forward primers and the RACE3' reverse primer by 3'RACE PCR.

round of PCR was performed using the *GSL2*_3RACE_F2/RACE3' primer pair and a 1:100 dilution of the first round reaction product as the template. The 1638 bp fragment that was generated by 3'RACE was observed on an agarose gel (*Figure 2.3*), cleaned using a QIAGEN PCR Purification Kit, ligated into pGEM®-T Easy and used to transform competent *E. coli* cells. Plasmid DNA mini-preparations were sequenced with the T7 and SP6 primers.

The 1406 bp and the 1638 bp *HvGSL2* amplified fragments share a 1342 bp overlapping region (*Figure 2.2*; *Figure 2.3*). The resulting 1702 bp partial HvGSL2 cDNA sequence includes a 3' untranslated region of 317 bp that contains a poly-A^+ tail (*Figure 2.2*). The deduced 461 amino acid sequence is encoded by an open reading frame of 1385 bp (*Figure 2.2*).

2.3.3 Cloning of *HvGSL3* cDNA Fragments

Two ESTs formed a contiguous sequence, which was designated *HvGSL3* (*Appendix B*). Gene-specific primers, *HvGSL3*_F and *HvGSL3*_R (*Appendix A*; *Figure 2.4*), were based on the contiguous EST sequence and were designed to amplify a 126 bp fragment. PCR was performed with the *HvGSL3*_F and *HvGSL3*_R primers using cDNA derived from a 9 day old dark-grown seedling as the template. A portion of the PCR reaction was separated on a 1% agarose gel and a 126 bp fragment was observed (*Figure 2.5*). The remainder of the PCR reaction was cleaned using a Nucleospin Cleanup Kit and a portion was ligated in pGEM®-T Easy. The ligation was subsequently used to transform competent *E. coli* cells. The cloned PCR product was sequenced from a plasmid DNA mini-preparation with the T7 and SP6 primers.

The cloned 126 bp *HvGSL3* sequence was aligned with the rice *OsGSL* genes. The nucleotide sequences of *OsGSL7* and *OsGSL9*, which showed greatest identity to *HvGSL3*, had a 22 bp region that contained 18 conserved and four non-conserved nucleotides (*Figure 2.6*). The semi-conserved region between *OsGSL7* and *OsGSL9* was used to design a forward degenerate primer, *HvGSL236*_F3 (*Appendix A*; *Figure 2.4*; *Figure 2.6*). The first round of semi-nested PCR used the *HvGSL236*_F3

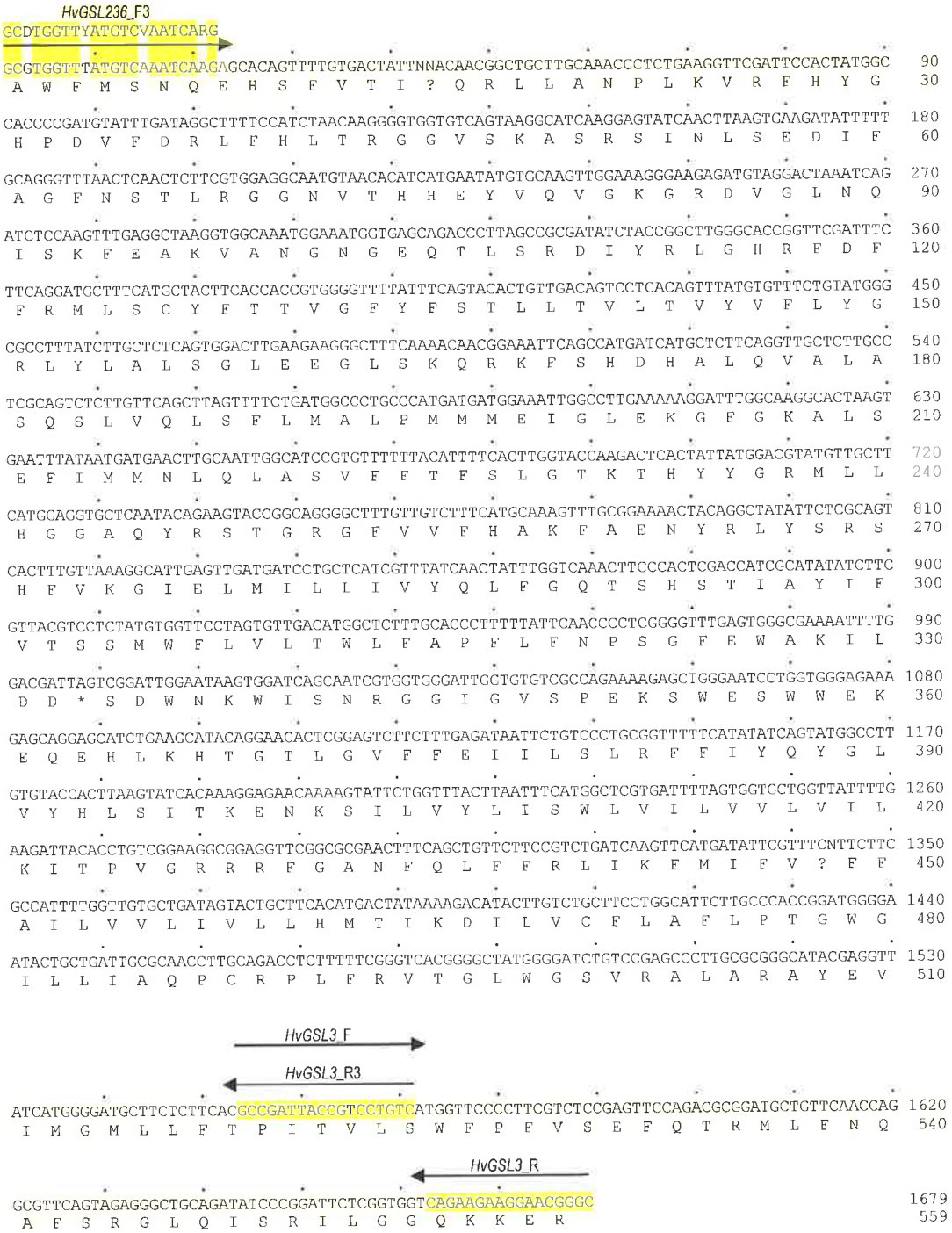

Figure 2.4: The nucleotide and deduced amino acid sequence of a fragment of the *HvGSL3* cDNA. The primers used to amplify fragments of *HvGSL3* are highlighted in yellow and arrows indicate the orientation. Single letter nucleotide degeneracy codes: D = A, G or T; Y = C or T; V = A, G or C; R = A or G.

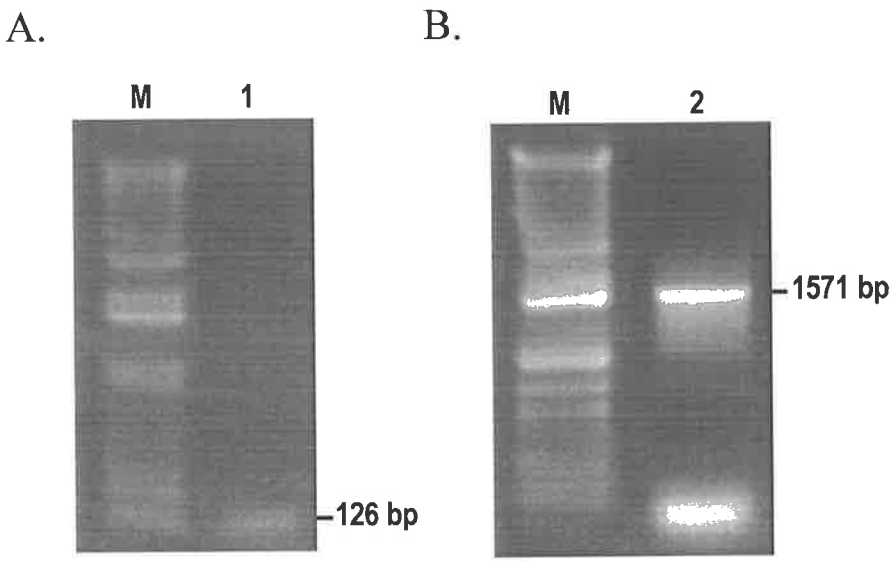

Figure 2.5: PCR amplified DNA fragments of *HvGSL3*. *Panel* A: M: 1 kb Plus DNA ladder; Lane 1: 126 bp fragment amplified using the *HvGSL3*_F and *HvGSL3*_R primers derived from the EST contiguous sequence. *Panel B*: M: 1 kb Plus DNA ladder; Lane 2: 1571 bp fragment amplified by semi-nested PCR using a forward degenerate primer *HvGSL236*_F3 and the nested reverse primers *HvGSL3*_R and *HvGSL3*_R3.

A.

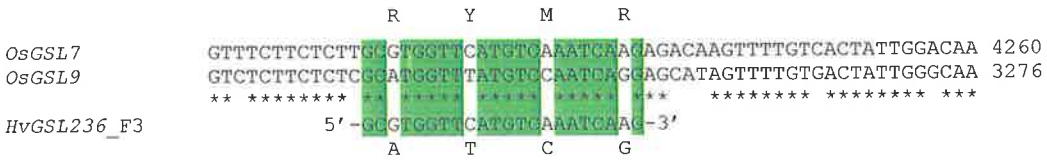

B.

Figure 2.6: The degenerate primers used in the PCR amplification of gene fragments of *HvGSL3* and *HvGSL8*. *Panel A*: The degenerate primer, *HvGSL236*_F3, used to amplify a fragment of *HvGSL3* cDNA and the conservation between *OsGSL7* and *OsGSL9*. *Panel B*: The degenerate primer, Group1-F3, used to amplify a fragment of *HvGSL8* and the conservation between *AtGSL5*, *AtGSL1*, *OsGSL2* and *OsGSL3*. The sequences highlighted in green are conserved.

degenerate forward primer with *HvGSL3*_R, using cDNA derived from 9 day old dark grown whole seedlings as the template. The second round of semi-nested PCR used the *HvGSL236*_F3 degenerate forward primer with the *HvGSL3*_R3 primer, using a 1:100 dilution of the first round reaction product as the template. A 1571 bp fragment (*Figure 2.5*) was excised from a 1% agarose gel, cleaned with a Nucleospin Cleanup Kit, ligated into pGEM®-T Easy and used to transform competent *E. coli* cells. The cloned PCR fragment was sequenced from a plasmid DNA mini-preparation with the T7 and SP6 primers.

The 126 bp and the 1571 bp PCR amplified *HvGSL3* fragments have an 18 bp overlapping region (*Figure 2.4*; *Figure 2.5*). The resultant 1679 bp partial *HvGSL3* sequence encodes a deduced 559 amino acids and does not include any 3' untranslated region (*Figure 2.4*).

2.3.4 Cloning of a *HvGSL4* cDNA Fragment

Eight barley ESTs formed a contiguous sequence that was designated *HvGSL4* (*Appendix B*). Two nested forward gene-specific primers, *HvGSL4*-1_F3 and *HvGSL4*-1_F1 (*Appendix A*; *Figure 2.7*), based on the contiguous sequence, were designed to amplify the 3' coding region of *HvGSL4* as well as the 3' untranslated region. The first round of 3'RACE was performed with the *HvGSL4*-1_F3 and RACE3'-adaptor (*Appendix A*) primers using 3'RACE cDNA derived from pre-anthesis whole flowers as the template. The second round of 3'RACE was performed with the *HvGSL4*-1_F1 and RACE3'-adaptor primers, using a 1:100 dilution of the first round reaction product as the template. An aliquot of the second round PCR product was separated on an agarose gel and an 895 bp fragment was observed (*Figure 2.8*). The PCR was cleaned and ligated into pGEM®-T Easy. The ligated PCR product was used to transform competent *E. coli* cells. Plasmid DNA mini-preparations were digested with *Eco*RI to determine the insert size. Plasmids with the correct sized insert were sequenced using T7 and SP6 primers.

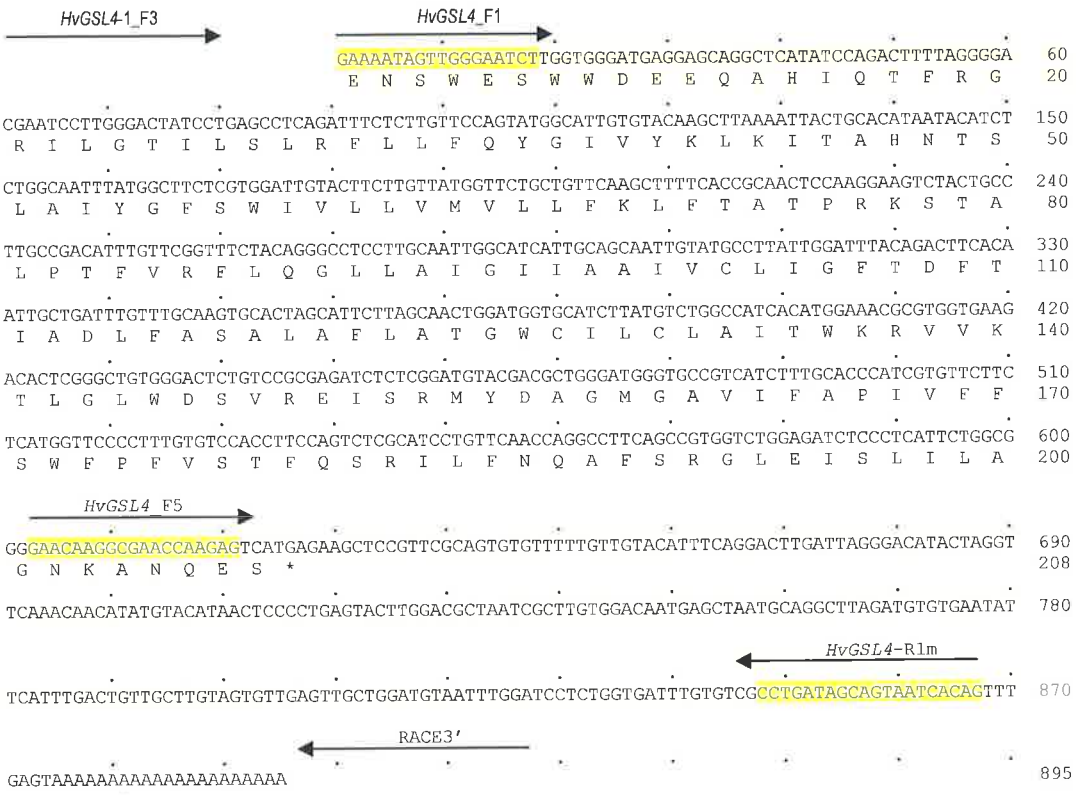

Figure 2.7: The nucleotide and deduced amino acid sequence of a fragment of the *HvGSL4* cDNA. The primers used to amplify fragments of *HvGSL4* are highlighted in yellow and arrows indicate the orientation.

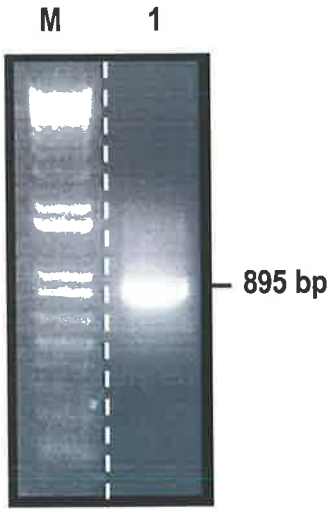

Figure 2.8: PCR amplified DNA fragment of *HvGSL4*. M: 1 kb Plus DNA ladder; Lane 1: 895 bp *HvGSL4* gene fragment amplified using the *HvGSL4*-1_F3 and *HvGSL4*_F1 forward nested primers and the RACE3' primer in 3'RACE PCR.

The sequence of the 895 bp PCR amplified *HvGSL4* fragment encodes a deduced peptide of 208 amino acids and includes a 3' untranslated region of 271 bp (*Figure 2.7*).

2.3.5 Cloning of a *HvGSL5* cDNA Fragment

Six barley ESTs formed a contiguous sequence, which was designated *HvGSL5* (*Appendix B*). Nested gene-specific primers were based on the contiguous EST sequence and were designed to amplify a 242 bp gene fragment of *HvGSL5*. The *HvGSL5*-F1 / *HvGSL5*-R1 primer pair was used in the first round of PCR and the *HvGSL5*-F2 / *HvGSL5*-R2 primer pair was used in the second round of PCR (*Appendix A*; *Figure 2.9*). The first round of PCR used the *HvGSL5*-F1 and *HvGSL5*-R1 primers, using cDNA derived from 9 day old dark grown whole seedlings as a template. The second round of PCR used the *HvGSL5*-F2 and *HvGSL5*-R2 primers, using a 1:100 dilution of the first round PCR product as the template. An aliquot of the second round PCR was separated on an agarose gel and a 242 bp PCR amplified fragment was observed (*Figure 2.10*). The remainder of the PCR amplified product was cleaned with a QIAGEN PCR cleanup kit, ligated into pGEM®-T Easy and used to transform competent *E. coli* cells. Cloned PCR products were sequenced from plasmid DNA preparations using T7 and SP6 primers.

The cloned 242 bp PCR amplified fragment of HvGSL5 encodes a deduced 80 amino acids (*Figure 2.9*).

2.3.6 Cloning of a *HvGSL6* cDNA Fragment

Two barley ESTs formed a contiguous sequence, which was designated *HvGSL6* (*Appendix B*). Two nested forward gene-specific primers, *HvGSL6*-1_F1 and *HvGSL6*-1_F2 (*Appendix A*; *Figure 2.11*), based on the contiguous sequence, were designed to amplify the 3' coding region of *HvGSL6* as well as the 3' untranslated region. The first round of 3'RACE was performed with the *HvGSL6*-1_F1 and RACE3'-adaptor (*Appendix A*) primers using cDNA derived from the total RNA of pre-anthesis whole flowers as the template. The second round of 3'RACE was

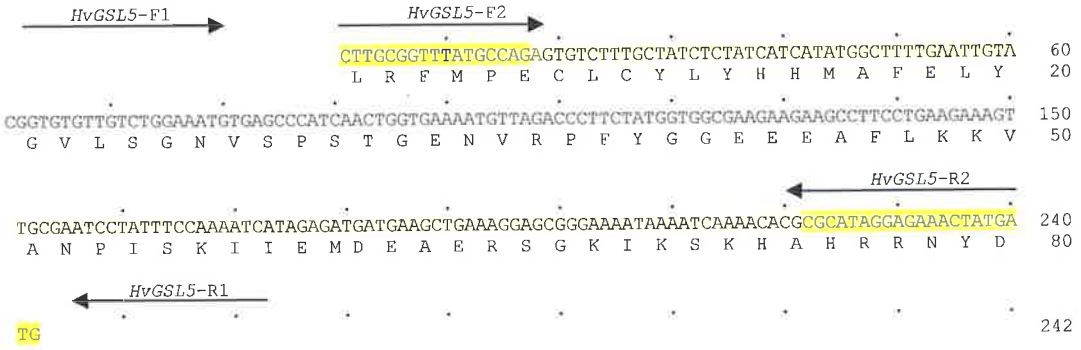

Figure 2.9: The nucleotide and deduced amino acid sequence of a fragment of the *HvGSL5* cDNA. The primers that were used to amplify fragments of *HvGSL5* are highlighted in yellow and arrows indicated the orientation.

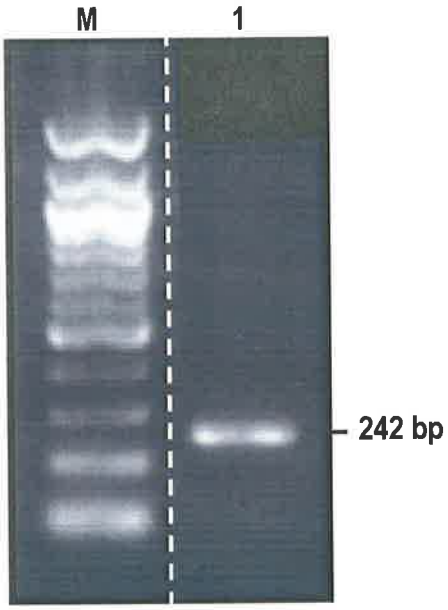

Figure 2.10: PCR amplified DNA fragment of *HvGSL5*. M: 100 bp DNA ladder; Lane 1: the 242 bp *HvGSL5* gene fragment amplified using nested PCR.

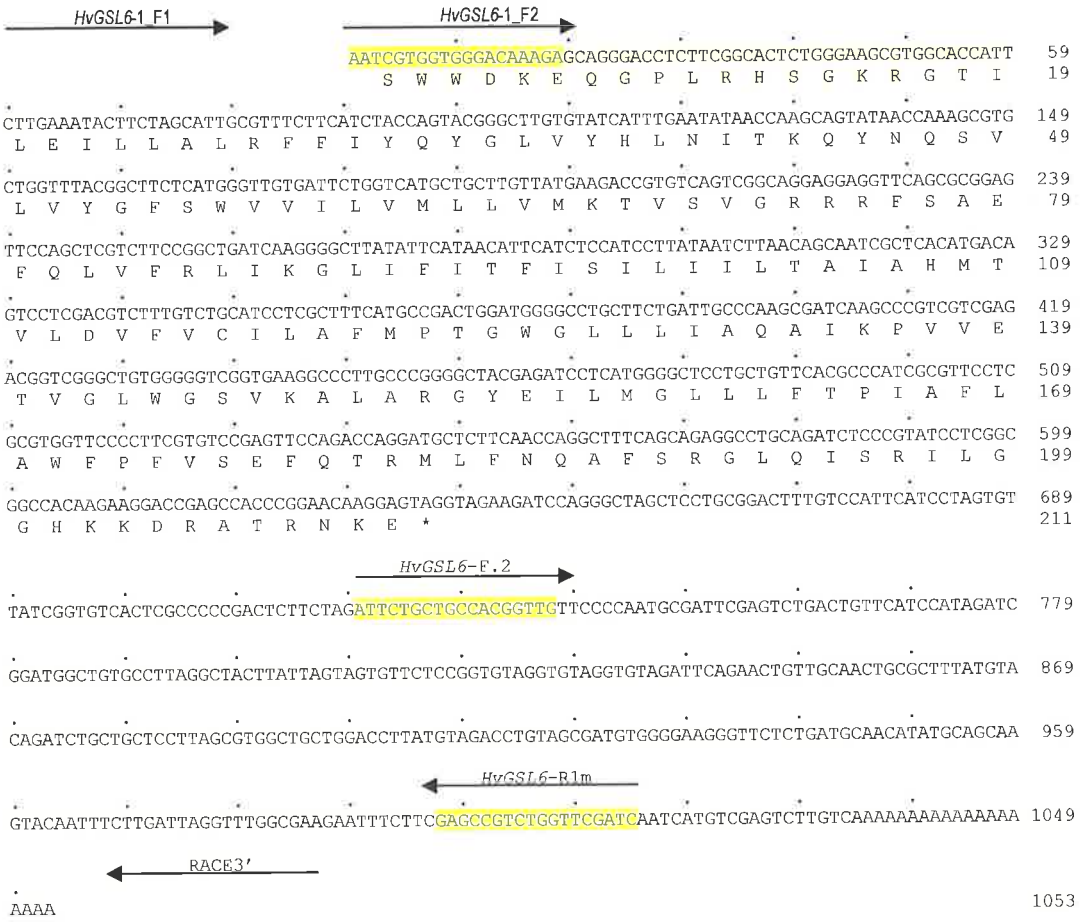

Figure 2.11: The nucleotide and deduced amino acid sequence of a fragment of the *HvGSL6* cDNA. The primers that were used to amplify fragments of *HvGSL6* are highlighted in yellow and arrows indicated the orientation.

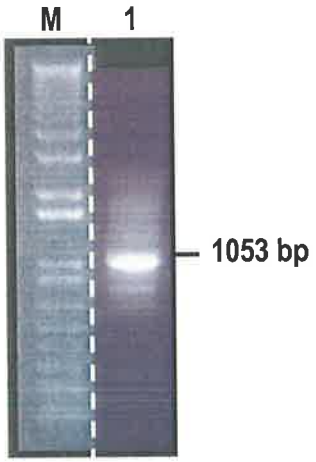

Figure 2.12: PCR amplified DNA fragment of *HvGSL6*. M: 1 kb Plus DNA ladder; Lane 1: the 1051 bp DNA *HvGSL6* gene fragment that was amplified by 3'RACE PCR.

performed with the *HvGSL6*-1_F2 and RACE3'-adaptor primers using a 1:100 dilution of the first round reaction as the template. An aliquot of the second round PCR was separated on an agarose gel and a product of 1053 bp was observed (*Figure 2.12*). The remainder of the PCR product was cleaned, ligated into pGEM®-T Easy and used to transform competent *E. coli* cells. Plasmid DNA mini-preparations were digested with *Eco*RI to determine the insert size. Plasmids showing an insert with the correct size were sequenced using the T7 and SP6 primers.

The sequence of the 1053 bp PCR amplified HvGSL6 gene fragment encodes a deduced 211 amino acids and has a 3' untranslated region of 418 bp (*Figure 2.11*).

2.3.7 Cloning of *HvGSL7* cDNA Fragments

There were six singleton barley EST sequences that were not included in any of the previously described constructed contiguous sequences for *HvGSL1*, *HvGSL2*, *HvGSL3*, *HvGSL4*, *HvGSL5* or *HvGSL6*. The deduced amino acid sequences of the EST singletons were aligned with the amino acid sequence of the 12 Arabidopsis GSL proteins and the nine rice GSL proteins (*data not shown*). The barley EST, accession number BJ462458, aligned with the low intron group of *GSL* genes from Arabidopsis and rice (*AtGSL1*, *AtGSL5*, *OsGSL2* and *OsGSL3*) and was designated *HvGSL7* (*Figure 1.5*).

Gene-specific primers, *HvGSL7*-F3 and *HvGSL7*-R2 (*Appendix A*; *Figure 2.13*), were based on the BJ462458 sequence and were designed to amplify a 473 bp fragment of *HvGSL7*. PCR was performed using cDNA derived from pooled embryo and scutellum tissue from grain imbibed for 24 hr and germinated for 8 hr as the template. A portion of the PCR was separated on an agarose gel and a product of 473 bp was observed (*Figure 2.14*). The remainder of the PCR was cleaned using a QIAGEN PCR Purification Kit, ligated into pGEM®-T Easy and electroporated into competent *E. coli* cells. Plasmid DNA mini-preparations were digested with the *Eco*RI restriction endonuclease and fragments were separated on an agarose gel and

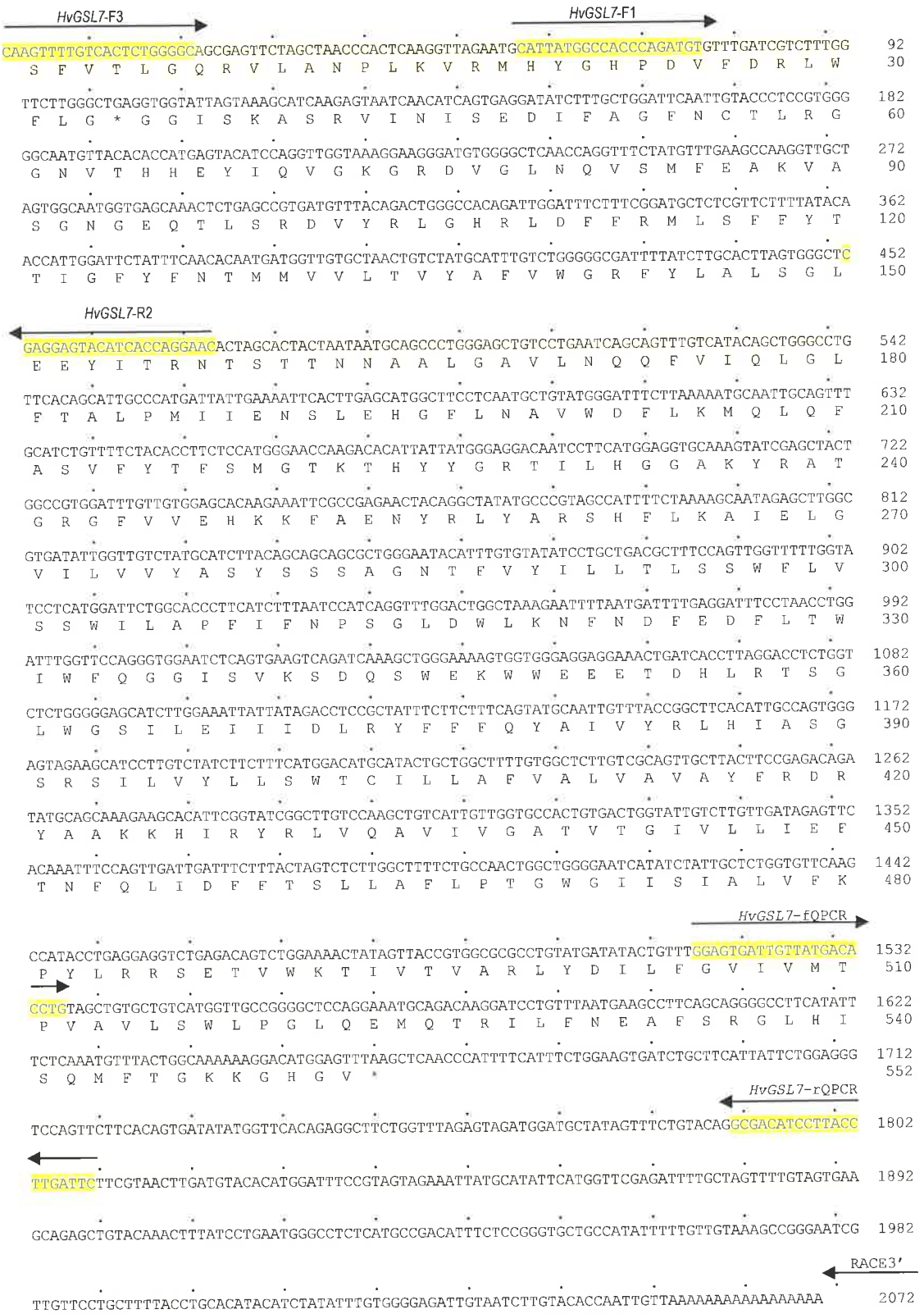

Figure 2.13: The nucleotide and deduced amino acid sequence of a fragment of the *HvGSL7* cDNA. The primers that were used to amplify fragments of *HvGSL7* are highlighted in yellow and arrows indicated the orientation.

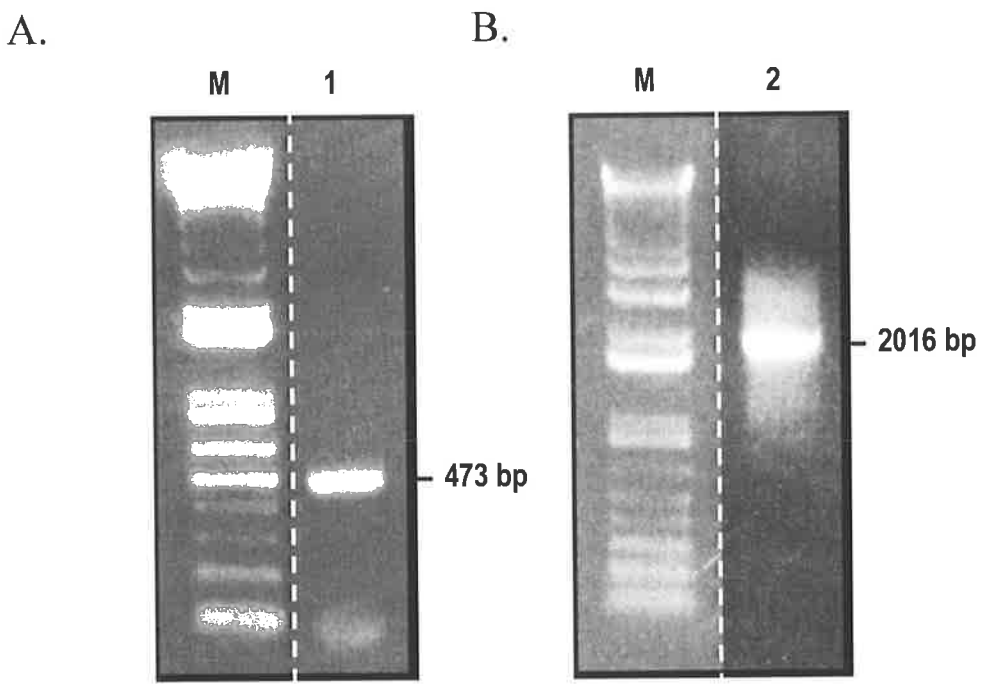

Figure 2.14: PCR amplified DNA fragments of *HvGSL7*. M: 1 kb Plus DNA ladder; *Panel A*, Lane 1: 473 bp *HvGSL7* gene fragment amplified using the *HvGSL7*-F3 and *HvGSL7*-R2 primers derived from the EST sequence; *Panel B*, Lane 2: 2016 bp *HvGSL7* gene fragment amplified by 3'RACE PCR using the *HvGSL7*-F3 and *HvGSL7*-F1 nested forward primers and the RACE3' reverse primer.

a 473 bp PCR insert was observed (*data not shown*). The insert was subsequently sequenced using the T7 and SP6 primers from a plasmid DNA mini-preparation.

Two nested forward gene-specific primers, *HvGSL7*-F3 and *HvGSL7*-F1 (*Appendix A*; *Figure 2.13*), were designed based on the previously described cloned 473 bp *HvGSL7* fragment. The first round of 3'RACE was performed with the *HvGSL7*-F3 and RACE3'-adaptor (*Appendix A*) primers using 3'RACE derived from pooled embryo and scutellum tissue (imbibed for 24 hr and germinated for 8 hr) as the template. The second round of 3'RACE was performed with the *HvGSL7*-F1 and RACE3'-adaptor primers using a 1:100 dilution of the first round reaction product as the template. A portion of the second round reaction was separated on an agarose gel and a PCR product of 2016 bp was observed. The remainder of the PCR was cleaned, ligated into pGEM®-T Easy and used to transform competent *E. coli* cells. Plasmid DNA mini-preparations were prepared from the transformed cells. PCR was used to screen for the presence of cloned fragments using a 1:100 dilution of the plasmid DNA mini-preparation as the template, the *HvGSL7*-F1 and RACE3' primers and the reaction conditions of the second round of PCR. The reaction mixture was separated on an agarose gel (*data not shown*). Plasmids with inserts of correct size were sequenced using T7 and SP6 primers.

The 473 bp and the 2016 bp PCR amplified *HvGSL7* fragments share an identical 417 bp overlapping region (*Figure 2.13*; *Figure 2.14*). The resultant 2072 bp partial *HvGSL7* cDNA sequence encodes a deduced 552 amino acids and a 410 bp 3' untranslated region containing the poly-A^+ tail (*Figure 2.13*).

2.3.8 Cloning of *HvGSL8* cDNA Fragments

Another singleton barley EST, accession number BU971000, also aligned with the low intron *GSL* genes of Arabidopsis and rice (*Figure 1.5*; *Section 2.3.7*). This EST was designated *HvGSL8*.

Gene-specific primers, *HvGSL8*-F3 and *HvGSL8*-R1 (*Figure 2.15*; *Appendix A*), were based on the BU971000 sequence and were designed to amplify a 329 bp fragment of *HvGSL8*. PCR was performed using cDNA derived from pre-anthesis whole flowers as the template. A portion of the PCR was separated on an agarose gel and a PCR product of 329 bp was observed (*Figure 2.16*). The remainder of the PCR product was cleaned with a QIAGEN PCR Purification Kit, ligated into pGEM®-T Easy and used to transform competent *E. coli* cells. Plasmid DNA mini-preparations were made from the transformed *E. coli*. A transformant containing a fragment of expected size as determined by *Eco*R1 digestion of the plasmid (*data not shown*), was selected. The sequence of the insert was determined using T7 and SP6 primers.

A large emphasis of the *HvGSL* cDNA cloning effort was to identify the barley orthologue of the Arabidopsis *AtGSL5* gene. When compared with all other *HvGSL* genes, the first cloned fragments of the *HvGSL8* cDNA shared the highest nucleotide sequence identity with the *AtGSL5* gene (*data not shown*). Therefore, attempts were made to obtain a near full-length sequence for the *HvGSL8* cDNA. To obtain the sequence located 5' to the 329 bp sequence of the *HvGSL* cDNA a forward degenerate primer, Group1-F3 (*Figure 2.6*; *Figure 2.15*; *Appendix A*), was designed to a semi-conserved region aligning to *OsGSL2* and *OsGSL3*. The 24 bp semi-conserved region contained 20 conserved nucleotides and 4 non-conserved nucleotides and was located in a region predicted to be 1000 bp in the 3' direction from the start codon (*Figure 2.6*). The Group1-F3 degenerate forward primer was used with two nested reverse primers, *HvGSL8*-R1 and *HvGSL8*-F3(r), which were based on the previously cloned 329 bp fragment (*Figure 2.15*; *Appendix A*). The first round of PCR was performed with the Group1-F3 and *HvGSL8*-R1 primers, using cDNA derived from pre-anthesis whole flowers as the template. The second round of PCR was performed with the Group1-F3 and *HvGSL8*-F3r primers, using a 1:10 dilution of the first round PCR product as the template. A portion of the second round reaction was separated on an agarose gel and a PCR product of 3365 bp was observed (*Figure 2.16*). The 3365 bp product was excised from the gel and cleaned using a QIAGEN PCR Purification Kit, ligated into pGEM®-T Easy and used to transform competent *E. coli* cells. The presence of the cloned 3365 bp insert was

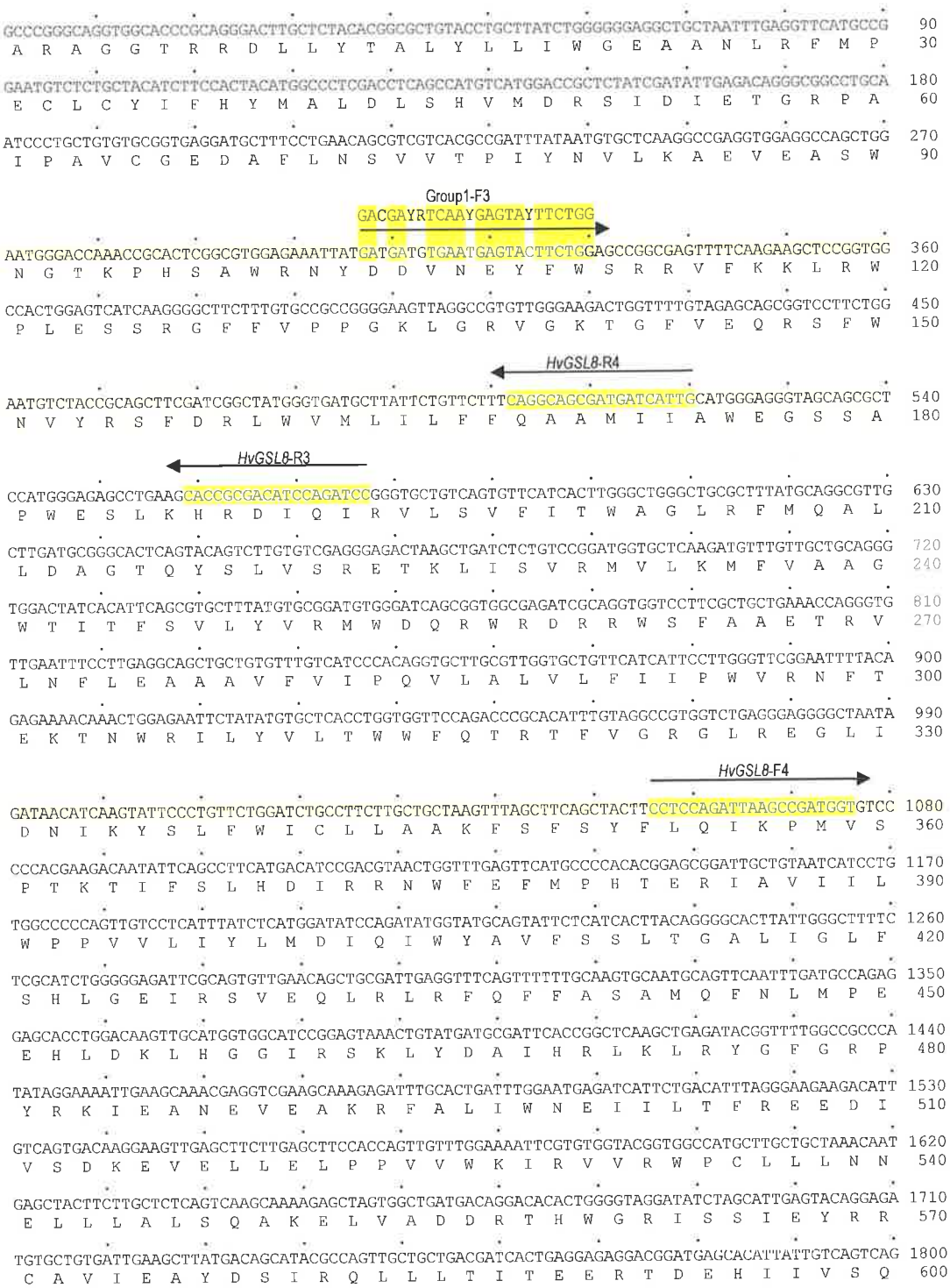
Group1-F3
GACGAYRTCAAYGAGTAYTTCTGG
HvGSL8-R4
HvGSL8-R3
HvGSL8-F4

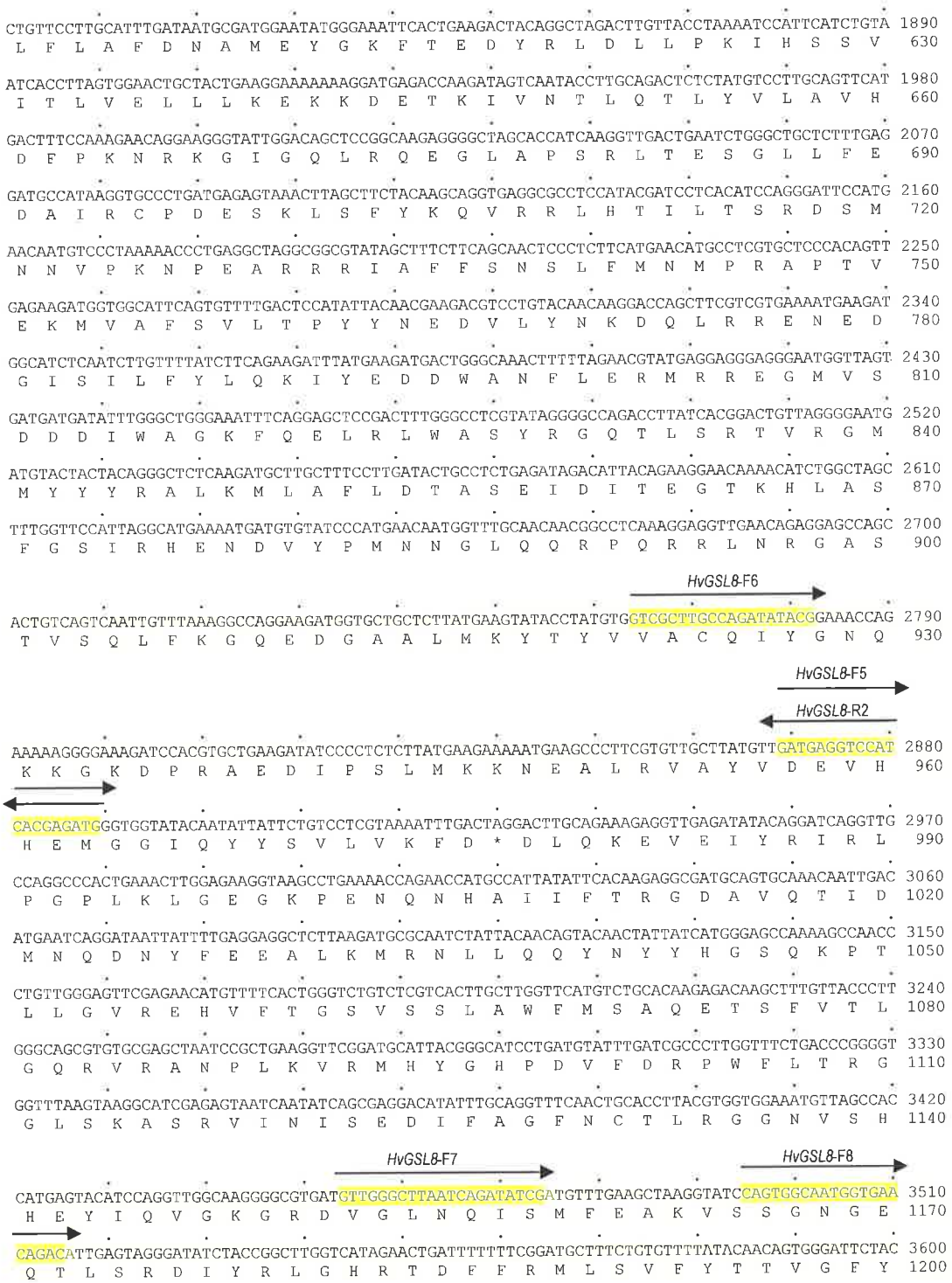
CTGTTCCTTGCATTTGATAATGCGATGGAATATGGGAAATTCACTGAAGACTACAGGCTAGACTTGTTACCTAAAATCCATTCATCTGTA 1890
L F L A F D N A M E Y G K F T E D Y R L D L L P K I H S S V 630
ATCACCTTAGTGGAACTGCTACTGAAGGAAAAAAAGGATGAGACCAAGATAGTCAATACCTTGCAGACTCTCTATGTCCTTGCAGTTCAT 1980
I T L V E L L L K E K K D E T K I V N T L Q T L Y V L A V H 660
GACTTTCCAAAGAACAGGAAGGGTATTGGACAGCTCCGGCAAGAGGGGCTAGCACCATCAAGGTTGACTGAATCTGGGCTGCTCTTTGAG 2070
D F P K N R K G I G Q L R Q E G L A P S R L T E S G L L F E 690
GATGCCATAAGGTGCCCTGATGAGAGTAAACTTAGCTTCTACAAGCAGGTGAGGCGCCTCCATACGATCCTCACATCCAGGGATTCCATG 2160
D A I R C P D E S K L S F Y K Q V R R L H T I L T S R D S M 720
AACAATGTCCCTAAAAACCCTGAGGCTAGGCGGCGTATAGCTTTCTTCAGCAACTCCCTCTTCATGAACATGCCTCGTGCTCCCACAGTT 2250
N N V P K N P E A R R R I A F F S N S L F M N M P R A P T V 750
GAGAAGATGGTGGCATTCAGTGTTTTGACTCCATATTACAACGAAGACGTCCTGTACAACAAGGACCAGCTTCGTCGTGAAAATGAAGAT 2340
E K M V A F S V L T P Y Y N E D V L Y N K D Q L R R E N E D 780
GGCATCTCAATCTTGTTTTATCTTCAGAAGATTTATGAAGATGACTGGGCAAACTTTTTAGAACGTATGAGGAGGGAGGGAATGGTTAGT 2430
G I S I L F Y L Q K I Y E D D W A N F L E R M R R E G M V S 810
GATGATGATATTTGGGCTGGGAAATTTCAGGAGCTCCGACTTTGGGCCTCGTATAGGGGCCAGACCTTATCACGGACTGTTAGGGGAATG 2520
D D D I W A G K F Q E L R L W A S Y R G Q T L S R T V R G M 840
ATGTACTACTACAGGGCTCTCAAGATGCTTGCTTTCCTTGATACTGCCTCTGAGATAGACATTACAGAAGGAACAAAACATCTGGCTAGC 2610
M Y Y Y R A L K M L A F L D T A S E I D I T E G T K H L A S 870
TTTGGTTCCATTAGGCATGAAAATGATGTGTATCCCATGAACAATGGTTTGCAACAACGGCCTCAAAGGAGGTTGAACAGAGGAGCCAGC 2700
F G S I R H E N D V Y P M N N G L Q Q R P Q R R L N R G A S 900
HvGSL8-F6
ACTGTCAGTCAATTGTTTAAAGGCCAGGAAGATGGTGCTGCTCTTATGAAGTATACCTATGTGGTCGCTTGCCAGATATACGGAAACCAG 2790
T V S Q L F K G Q E D G A A L M K Y T Y V V A C Q I Y G N Q 930
HvGSL8-F5
HvGSL8-R2
AAAAAGGGGAAAGATCCACGTGCTGAAGATATCCCCTCTCTTATGAAGAAAAATGAAGCCCTTCGTGTTGCTTATGTTGATGAGGTCCAT 2880
K K G K D P R A E D I P S L M K K N E A L R V A Y V D E V H 960
CACGAGATGGGTGGTATACAATATTATTCTGTCCTCGTAAAATTTGACTAGGACTTGCAGAAAGAGGTTGAGATATACAGGATCAGGTTG 2970
H E M G G I Q Y Y S V L V K F D * D L Q K E V E I Y R I R L 990
CCAGGCCCACTGAAACTTGGAGAAGGTAAGCCTGAAAACCAGAACCATGCCATTATATTCACAAGAGGCGATGCAGTGCAAACAATTGAC 3060
P G P L K L G E G K P E N Q N H A I I F T R G D A V Q T I D 1020
ATGAATCAGGATAATTATTTTGAGGAGGCTCTTAAGATGCGCAATCTATTACAACAGTACAACTATTATCATGGGAGCCAAAAGCCAACC 3150
M N Q D N Y F E E A L K M R N L L Q Q Y N Y Y H G S Q K P T 1050
CTGTTGGGAGTTCGAGAACATGTTTTCACTGGGTCTGTCTCGTCACTTGCTTGGTTCATGTCTGCACAAGAGACAAGCTTTGTTACCCTT 3240
L L G V R E H V F T G S V S S L A W F M S A Q E T S F V T L 1080
GGGCAGCGTGTGCGAGCTAATCCGCTGAAGGTTCGGATGCATTACGGGCATCCTGATGTATTTGATCGCCCTTGGTTTCTGACCCGGGGT 3330
G Q R V R A N P L K V R M H Y G H P D V F D R P W F L T R G 1110
GGTTTAAGTAAGGCATCGAGAGTAATCAATATCAGCGAGGACATATTTGCAGGTTTCAACTGCACCTTACGTGGTGGAAATGTTAGCCAC 3420
G L S K A S R V I N I S E D I F A G F N C T L R G G N V S H 1140
HvGSL8-F7
HvGSL8-F8
CATGAGTACATCCAGGTTGGCAAGGGGCGTGATGTTGGGCTTAATCAGATATCGATGTTTGAAGCTAAGGTATCCAGTGGCAATGGTGAA 3510
H E Y I Q V G K G R D V G L N Q I S M F E A K V S S G N G E 1170
CAGACATTGAGTAGGGATATCTACCGGCTTGGTCATAGAACTGATTTTTTTCGGATGCTTTCTGTGTTTTATACAACAGTGGGATTCTAC 3600
Q T L S R D I Y R L G H R T D F F R M L S V F Y T T V G F Y 1200

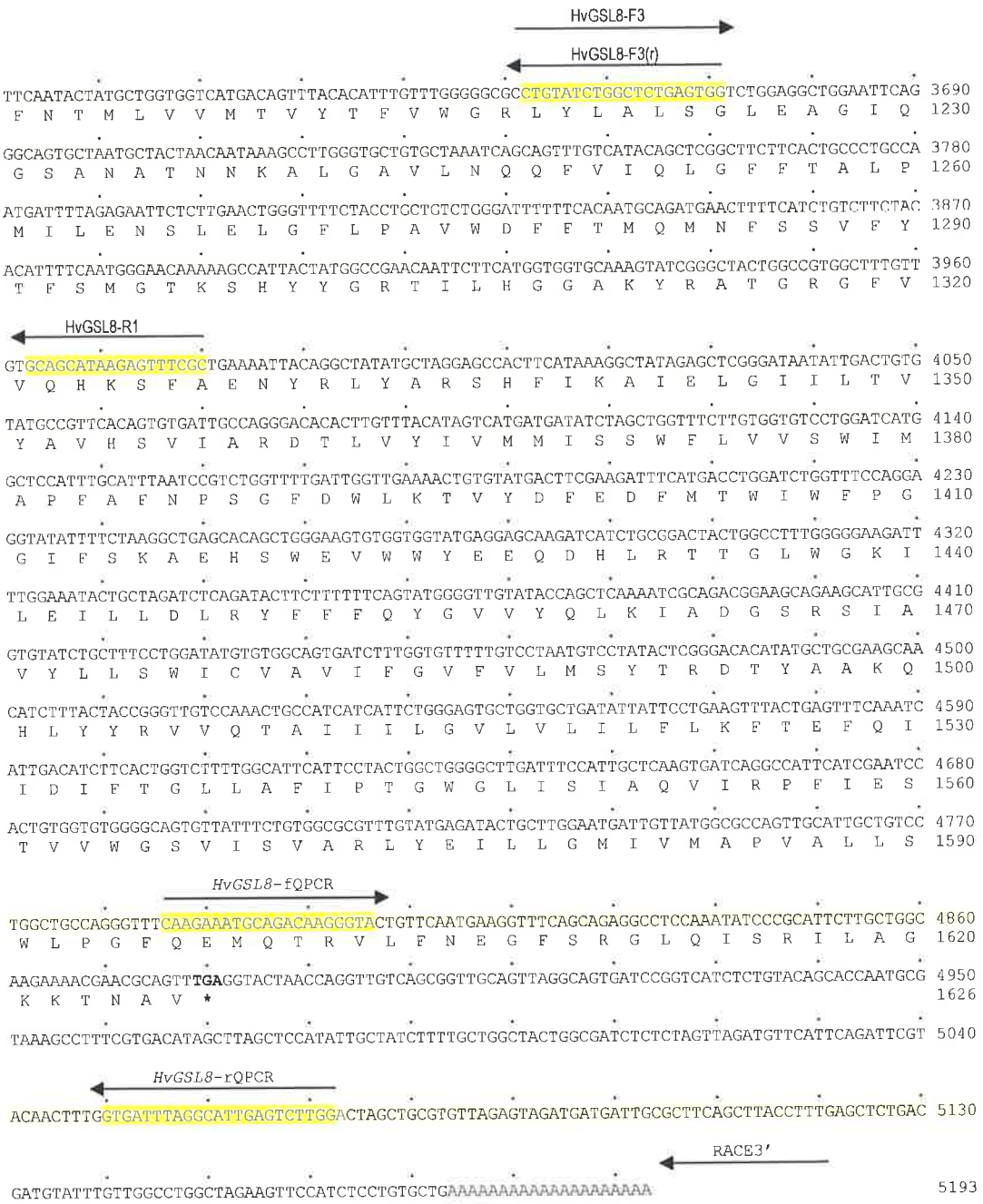

Figure 2.15: The nucleotide and deduced amino acid sequence of a fragment of the *HvGSL8* cDNA. The primers used to amplify fragments of *HvGSL8* are highlighted in yellow and arrows indicated the orientation. Single letter degeneracy codes Y = C or T, R = A or G.

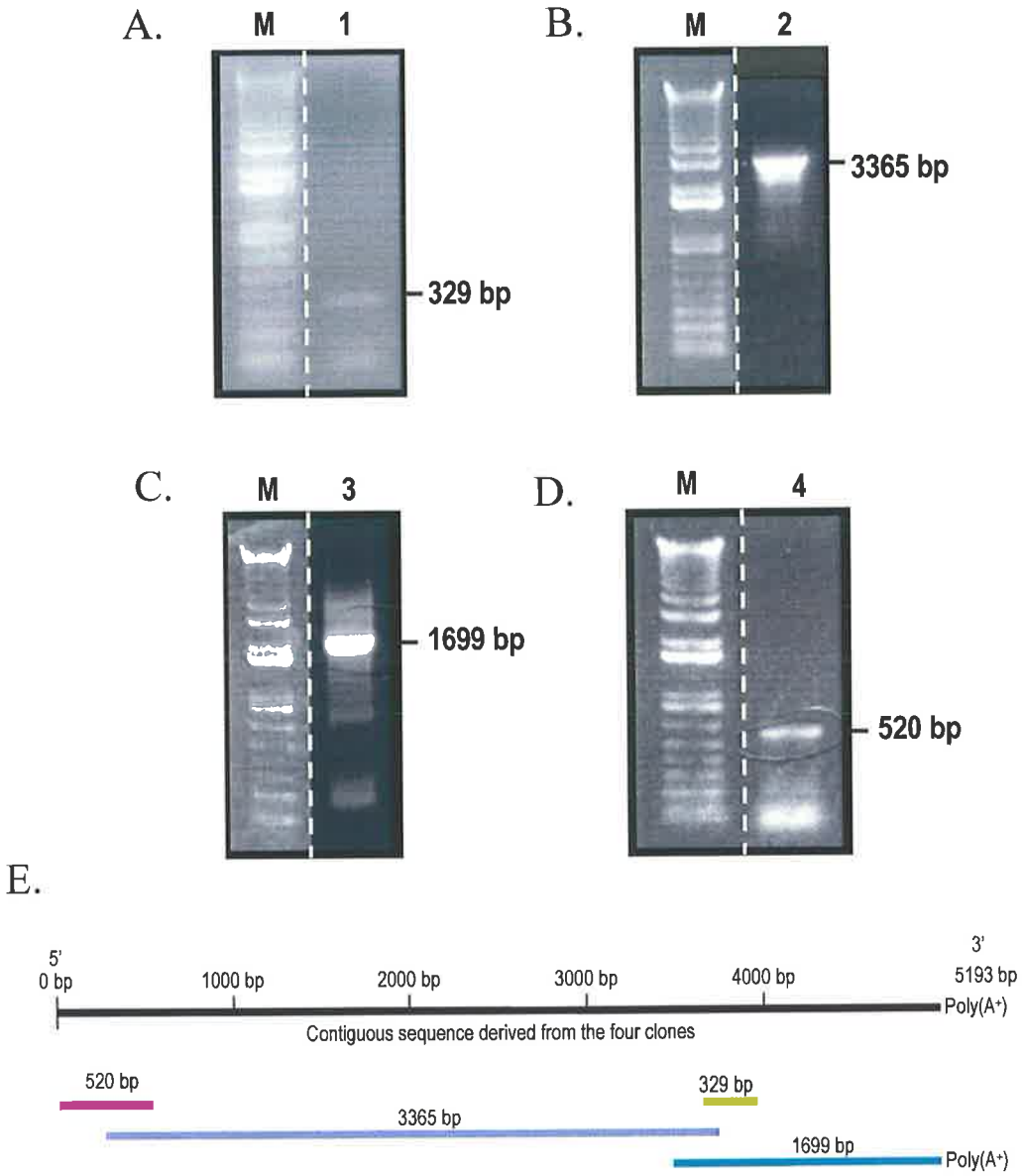

Figure 2.16: PCR amplified gene fragments of *HvGSL8*. M: 1kb+ DNA molecular ladder; *Panel A*, Lane 1: 329 bp fragment cloned from the EST; *Panel B*, Lane 2: 3365 bp fragment cloned using a degenerate primer (Group1-F3) in semi-nested PCR; *Panel C*, Lane 3: 1699 bp fragment amplified using 3'RACE PCR; *Panel D*, Lane 4: 520 bp fragment generated from the genomic walk; *Panel E*, A schematic diagram showing the overlapping nature of the four cloned fragments of *HvGSL8*.

confirmed by screening colonies with PCR using the Group1-F3 and *HvGSL8*-F3r primers. DNA plasmid mini-preparations were prepared from the PCR positive clones and the cloned fragment was sequenced with T7 and SP6 primers, as well as with the *HvGSL8*-F4, *HvGSL8*-F5, *HvGSL8*-F6 and *HvGSL8*-R2 primers (*Figure 2.15*; *Appendix A*).

The 329 bp and the 3365 bp fragment have an overlapping sequence of 20 bp (*Figure 2.15*; *Figure 2.16*).

To obtain the 3' sequence of *HvGSL8*, the following 3'RACE protocol was implemented. Two nested forward gene-specific primers, *HvGSL8*-F7 and *HvGSL8*-F8 (*Figure 2.15*; *Appendix A*), were designed to the previously described 3365 bp cloned fragment. The first round of 3'RACE was performed with the *HvGSL8*-F7 and RACE3'-adaptor primers (*Appendix A*), using cDNA derived from pooled embryo and scutellum tissue excised from 24 hr imbibed grain that had germinated for 8 hr as the template. The second round of 3'RACE was performed with the *HvGSL8*-F8 and RACE3'-adaptor primers, using a 1:100 dilution of the first round PCR product as the template. A portion of the PCR reaction was separated on an agarose gel and a product of 1699 bp was observed (*Figure 2.16*). The 1699 bp fragment was excised from the agarose gel, the DNA was cleaned, ligated into pGEM®-T Easy and used to transform competent *E. coli* cells. PCR was used to screen for colonies with the correctly sized insert and plasmid DNA mini-preparations were made from the positive colonies. The insert was subsequently sequenced using T7 and SP6 primers.

The 1699 bp fragment and the 3365 bp fragment have an overlapping region of 177 bp, while the 1699 bp fragment completely overlaps the 329 bp fragment (*Figure 2.15*; *Figure2.16*).

A genomic walk was performed to obtain *HvGSL8* gene sequence that was located 5' of the 3365 bp cloned fragment. The genomic walk involved two rounds of PCR using two *HvGSL8* gene-specific nested reverse primers, *HvGSL8*-R3 and *HvGSL8*-

R4 (*Figure 2.15*; *Appendix A*), which were based on the 5' end of the previously described 3365 bp cloned fragment. The first round of PCR was performed with the AP1 (*Appendix A*) and *HvGSL8*-R3 primers using the genomic walking library previously described as the template. The second round of PCR was performed with the AP2 (*Appendix A*) and *HvGSL8*-R4 primers using a 1:100 dilution of the first round PCR product. A portion of each PCR reaction was separated on an agarose gel and a product of 520 bp was observed (*Figure 2.16*). The fragment was excised from the gel and the DNA was cleaned, ligated into pGEM®-T Easy and used to transform competent *E. coli* cells. PCR was used to screen for colonies containing the correctly sized insert and plasmid DNA mini-preparations were made from the positive colonies. The insert was subsequently sequenced using the AP2 primer (*Figure 2.15*).

The 520 bp fragment from the genomic walk and the previously described 3365 bp fragment have an overlapping region of 214 bp (*Figure 2.15*; *Figure 2.16*)

2.3.9 Cloning Summary

The amino acid sequence of each *HvGSL* gene was deduced and subsequently aligned using the ClustalX program. *HvGSL1* has a full length open reading frame of 5745 bp encoding 1915 amino acids (Li *et al.*, 2003). During the work described here the longest sequence data was obtained for *HvGSL8* followed by *HvGSL7*, *HvGSL2*, *HvGSL3*, *HvGSL6*, *HvGSL4* and *HvGSL5* (*Figure 2.17*). The poly-A^+ tail was not obtained for *HvGSL3* or *HvGSL5* (*Figure 2.17*). The predicted amino acid sequence of *HvGSL5* is located approximately 500 amino acids from the start methionine and does not overlap with amino acid sequence of HvGSL2, HvGSL3, HvGSL4, HvGSL6 or HvGSL7 (*Figure 2.17*). Therefore eight *HvGSL*s have been identified to date, and their properties are summarised in *Figure 2.17*.

2.3.10 Genetic Mapping of *HvGSL*s

The *HvGSL1*, *HvGSL2*, *HvGSL4*, *HvGSL6*, *HvGSL7* and *HvGSL8* gene-specific mapping probes were generated by PCR (*Table 2.1*). The *HvGSL5* gene-specific

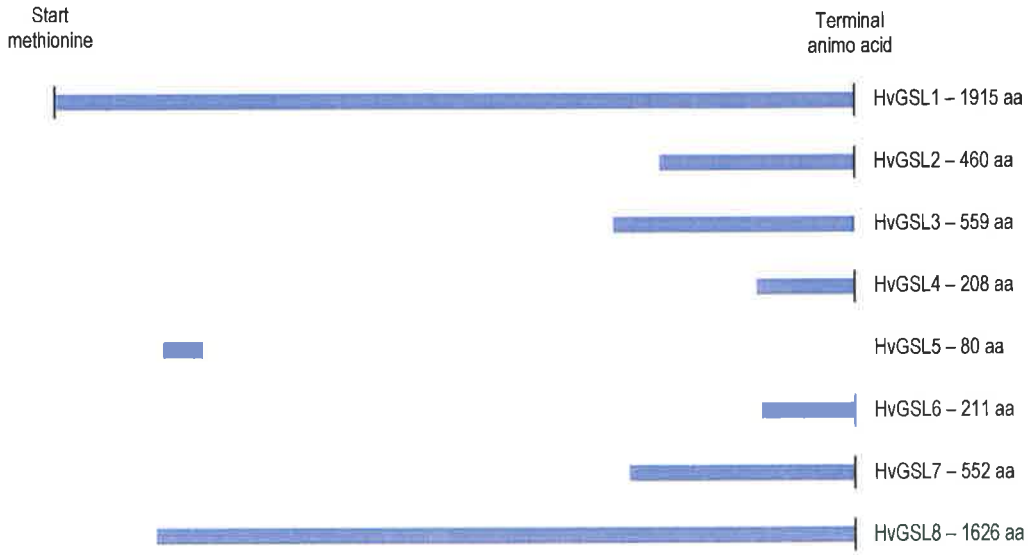

Gene	Nucleotide Sequence			Peptide Sequence
	Total	Protein encoding	3'UTR	
HvGSL1	6180 bp	5745 bp	435 bp	1915 aa
HvGSL2	1695 bp	1380 bp	315 bp	460 aa
HvGSL3	1679 bp	1677 bp	-	559 aa
HvGSL4	865 bp	624 bp	241 bp	208 aa
HvGSL5	242 bp	240 bp	-	80 aa
HvGSL6	1051 bp	663 bp	388 bp	221 aa
HvGSL7	2070 bp	1656 bp	414 bp	552 aa
HvGSL8	5193 bp	4878 bp	315 bp	1626 aa

Figure 2.17: Schematic diagram showing the relative positions of deduced amino acids of each *HvGSL* and a table summarising the properties of cloned *HvGSL* cDNA fragments. bp: nucleotide base pairs. aa: amino acid residues *HvGSL1* was identified by Dr. Jing Li (Li *et al.*, 2003).

Gene	Primers		Probe Size	Figure
	Forward	Reverse		
HvGSL1	*HvGSL1*-F	*HvGSL1*-R	266 bp	*Appendix C*
HvGSL2	*GSL2*-mapF	*GSL2*-mapR	302 bp	*Figure 2.2*
HvGSL3	-	-	-	-
HvGSL4	*HvGSL4*-F5	*HvGSL4*-R1m	265 bp	*Figure 2.7*
HvGSL5	-	-	242 bp	*Figure 2.9*
HvGSL6	*HvGSL6*-F.2	*HvGSL6*-R1m	295 bp	*Figure 2.11*
HvGSL7	*HvGSL7*-fQPCR	*HvGSL7*-rQPCR	295 bp	*Figure 2.13*
HvGSL8	*HvGSL8*-fQPCR	*HvGSL8*-rQPCR	287 bp	*Figure 2.15*

Table 2.1: Summary of the *HvGSL* gene mapping probes. PCR primers are given for mapping probes that were generated by PCR. The nucleotide sequence of PCR primers are shown in *Appendix A*. The *HvGSL5* mapping probe was generated by restriction digest of the cloned cDNA.

mapping probe was generated from a restriction digest of the 242 bp cloned fragment from pGEM®-T Easy (*Figure 2.9*; *Table 2.1*). No gene-specific mapping probe was generated for *HvGSL3*. Each *HvGSL* gene-specific probe was used to initially screen parental mapping populations to determine if a polymorphism between two parents was present (*Figure 2.18*). Polymorphisms were observed in the Clipper and Sahara parents for all *HvGSL* genes (*data not shown*). The *HvGSL* gene-specific probes were hybridised against the wheat-barley addition lines (Islam and Shepherd, 1981) to determine the chromosome that each *HvGSL* was located (*Figure 2.19*). Finally, each *HvGSL* gene-specific probe was used against the 150 double haploid individuals in the Clipper x Sahara mapping population (Karakousis *et al.*, 2003) to determine where the *HvGSL*s map in relation to previously described genetic markers (*Figure 2.20*). All the *HvGSL* genes were mapped as single copies distributed between chromosomes 3H, 4H, 6H and 7H (*Figure 2.21*). *HvGSL1* was mapped to a location on the long arm of chromosome 4H in the Clipper x Sahara mapping population (*Figure 2.21*). The chromosomal location of *HvGSL1* was also previously mapped to 4H in Clipper x Sahara and Galleon x Haruna Nijo populations (Li *et al.*, 2003). Both *HvGSL2* and *HvGSL5* map to exactly the same genetic position at the very end of the long arm of 6H (*Figure 2.21*). *HvGSL4* mapped to the end of the short arm of chromosome 4H while *HvGSL6* mapped near the end of the long arm of chromosome 4H (*Figure 2.21*). Both *HvGSL7* and *HvGSL8* were mapped to the long arm of chromosome 3H, very near the centromere (*Figure 2.21*).

Several Quantitative Trait Loci (QTLs) with agronomic importance, such as heading date, height, grain yield, head shattering, spike density, peduncle curve, lodging and ear grain number were located in the same chromosomal regions as the mapped *HvGSL* genes. There was also several grain quality QTLs, such as diastatic power, α-amylase and grain protein in the same chromosomal regions as the mapped *HvGSL* genes. Since the agronomic and grain quality QTLs have no obvious association with the synthesis of (1,3)-β-D-glucan the data is not presented in detail. However, since the *AtGSL5* gene has been associated with the deposition of (1,3)-β-D-glucan in response to wounding and fungal infection (Jacobs *et al.*, 2003; Nishimura *et al.*, 2003), the QTLs associated with biotic and abiotic stresses that are located in the same chromosomal region are listed in *Table 2.2*.

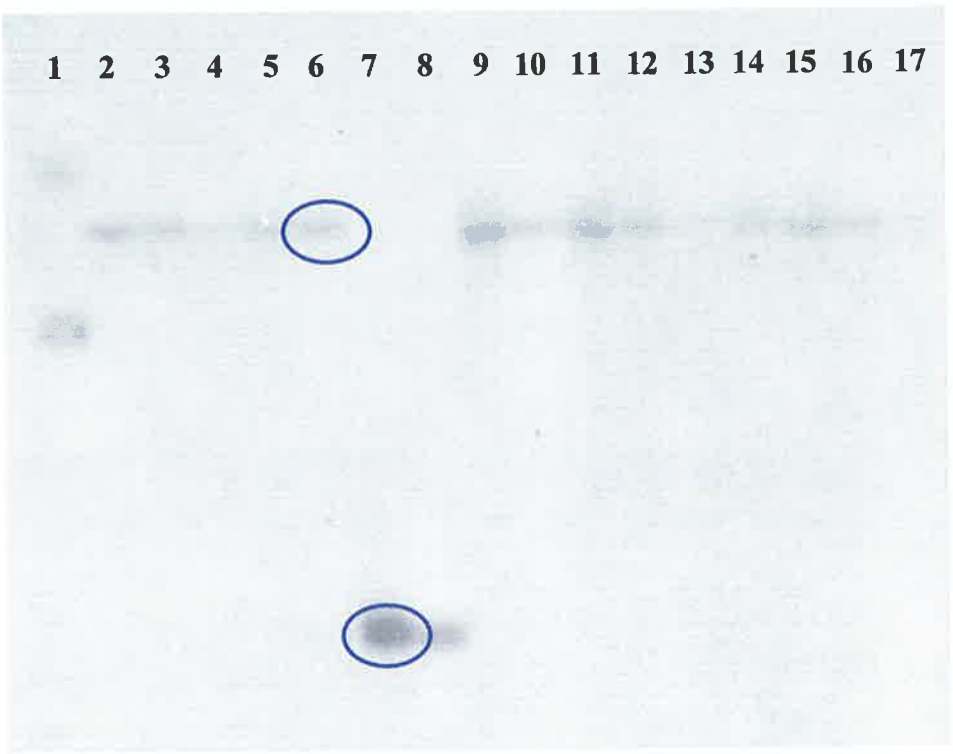

Figure 2.18: An autoradiograph of the parental population (digested with *Eco*RI) that was hybridised with the *HvGSL4* mapping probe. *Lane 1*: DNA ladder, *Lane 2*: Galleon, *Lane 3*: Haruna Nijo, *Lane 4*: Chebec, *Lane 5*: Harrington, *Lane 6*: Clipper, *Lane 7*: Sahara, *Lane 8*: Alexis, *Lane 9*: WI 2875-1, *Lane 10*: Sloop, *Lane 11*: Halcyon, *Lane 12*: Arapiles, *Lane 13*: Franklin, *Lane 14*: WI2585, *Lane 15*: Amagi Nijo, *Lane 16*: VB9524, *Lane 17*: ND11231-12. Since a good polymorphism was observed between Clipper and Sahara as indicated by the blue circles, the Clipper/Sahara mapping population (Karakousis *et al.*, 2003) was used to genetically map *HvGSL4*.

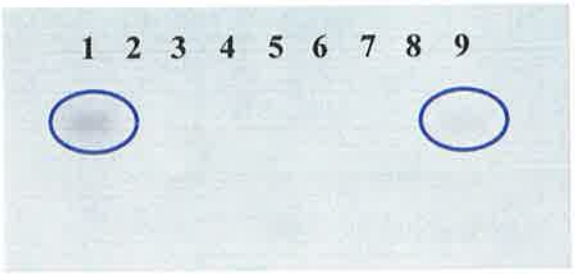

Figure 2.19: The wheat-barley addition line DNA digested with *Xba*I and hybridised with the *HvGSL4* mapping probe. *Lane 1*: Barley (cv. Betzes), *Lane 2*: Wheat (cv. Chinese spring; CS), *Lane 3*: CS + short arm of barley 1H, *Lane 4*: CS + barley 2H, *Lane 5*: CS + barley 3H, *Lane 6*: CS + barley 4H, *Lane 7*: CS + barley 5H, *Lane 8*: CS + barley 6H, *Lane 9*: CS + barley 7H. From the autoradiograph, it was determined that *HvGSL4* is located on the barley 7H chromosome.

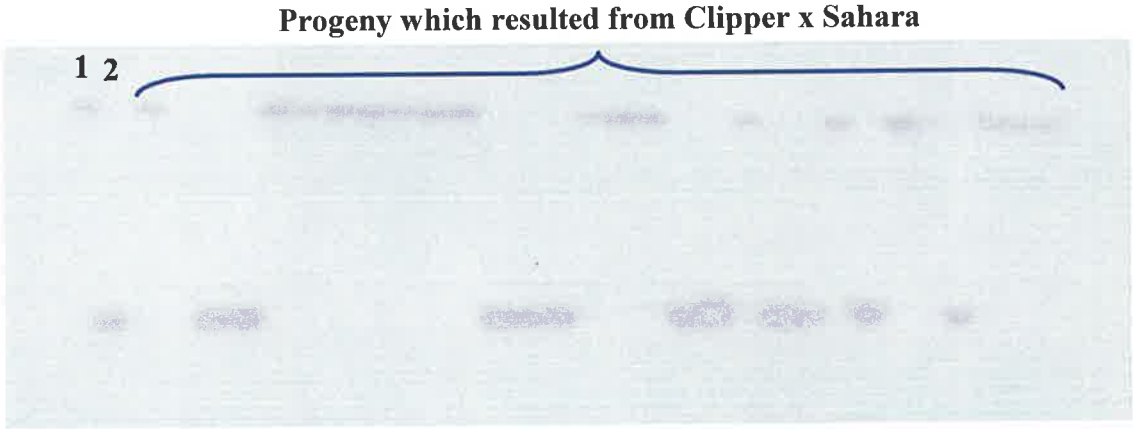

Figure 2.20: The Clipper x Sahara mapping population DNA digested with *Eco*RI probed with the *HvGSL4* mapping probe. Lane 1: Clipper, Lane 2: Sahara. Remaining lanes show individuals 61 to 90 (out of a total mapping population size of 150) that resulted from the Clipper x Sahara cross.

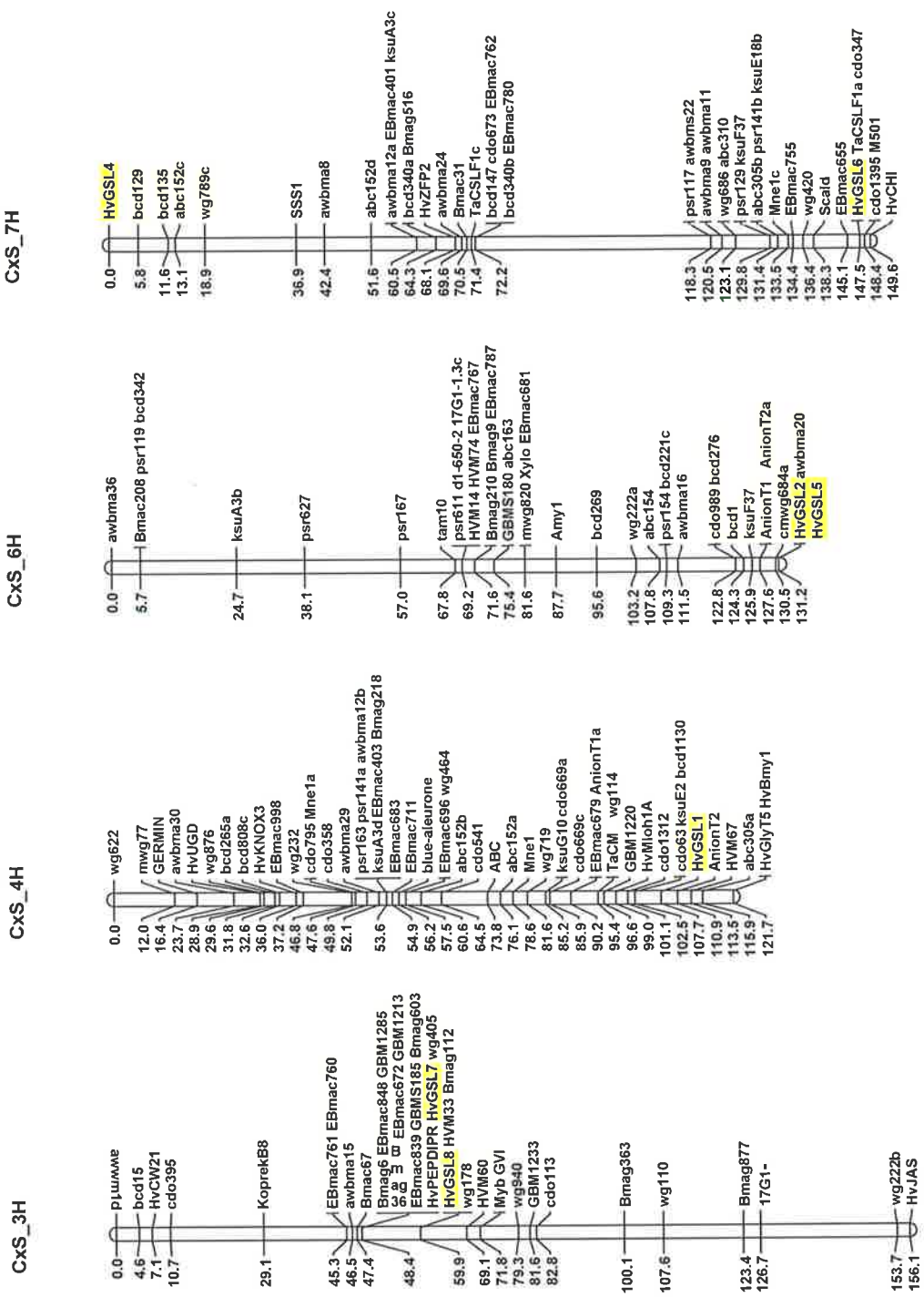

Figure 2.21: Genetic maps of chromosome 3H, 4H, 6H and 7H from the barley Clipper x Sahara mapping population (Karakousis *et al.*, 2003). *HvGSL7* and *HvGSL8* were genetically mapped to chromosome 3H. *HvGSL1* was mapped to chromosome 4H. *HvGSL2* and *HvGSL5* were mapped to the same genetic position at the very end of the long arm of chromosome 6H. *HvGSL4* was mapped to the short arm of chromosome 7H, while *HvGSL6* was mapped to the long arm of chromosome 7H.

2.3.11 Phylogenetic Tree

Following cloning of the *HvGSL* cDNA fragments and the acquisition of the corresponding nucleotide sequences, a phylogenetic tree was constructed for the barley GSL enzymes. The phylogenetic tree shows that the amino acid sequences deduced from the partial *HvGSL* gene sequences and the full length *HvGSL1* gene sequence may be placed into 3 main clades (*Figure 2.22*). Following the sequencing of the Arabidopsis and rice genomes, the genes encoding the AtGSL1, AtGSL5, OsGSL2 and OsGSL3 proteins have been identified as having 0, 1 or 2 introns and span approximately 5.5 kb of genomic sequence (*Figure 1.5*). Other *GSL* genes from Arabidopsis and rice have as many as 49 introns and may span as much as 22 kb of genomic sequence (*Figure 1.5*). Clade 1 in the phylogenetic tree contains the deduced amino acid sequence of *GSL* genes from Arabidopsis and rice that have a low number of introns, while Clade 2 and Clade 3 contains the deduced amino acid sequences of *GSL* genes that have a high number of introns (*Figure 1.5*; *Figure 2.22*). The deduced amino acid sequences of partial barley *GSL* genes that group with the deduced amino acid sequences of low intron *GSL* genes from Arabidopsis and rice are *HvGSL7* and *HvGSL8* (*Figure 2.22*). Clade 2 contains the deduced amino acid sequences of the previously described *HvGSL1* and *HvGSL4* cDNA sequences, while Clade 3 contains the deduced amino acid sequences of the partial *HvGSL2*, *HvGSL3*, *HvGSL5* and *HvGSL6* cDNAs (*Figure 2.22*).

2.3.12 Sequence Alignments

The deduced amino acid sequences encoded by the *HvGSL* gene fragments were aligned with respect to each other and also with respect to the amino acid sequence encoded by the known full length *GSL* genes from plants and fungi. Alignments were performed, and the percentage identity was recorded (*Table 2.3*). The highlighted percentages in the amino acid identity table (*Table 2.3*) represent GSL pairs that are located within the same clade of the phylogenetic tree (*Figure 2.22*). It is expected that the amino acid identity between barley GSL proteins and other plant GSL proteins will change with the acquisition of more sequence data.

Gene	Map Pos.	Possible Associated QTLs	Population	Reference
HvGSL1	4HL	Stripe rust resistance	Dicktoo/Morex	(Oziel *et al.*, 1996)
		Kernal discoloration	Gerbel/Heroit	(Hackett *et al.*, 1992)
			Steptoe/Morex	(Hayes *et al.*, 1993)
			Blenheim/Kym	(Bezant *et al.*, 1996)
				(Bezant *et al.*, 1997)
			Chevron/M69	(De la Pena *et al.*, 1999)
			Cali/Bowman	(Hayes *et al.*, 1996)
			Cali-sib/Bowman	(Chen *et al.*, 1994)
				(Hayes *et al.*, 1996)
HvGSL2	6HL	Scald resistance	Gobern/CMB	(Zhu *et al.*, 1999)
HvGSL5			Steptoe/Morex	(Kandemir *et al.*, 2000)
			Igri/Triumph	(Laurie *et al.*, 1995)
			Igri/Danilo	(Backes *et al.*, 1995)
HvGSL4	7HS	Net blotch resistance	Blenheim/Kym	(Bezant *et al.*, 1996)
		Fusarium HB resistance		(Bezant *et al.*, 1997)
			Harrington/TR306	(Tinker *et al.*, 1996)
			Steptoe/Morex	(Hayes *et al.*, 1993)
				(Steffenson *et al.*, 1996)
			Igri/Danilo	(Backes *et al.*, 1995)
			Chevron/M69	(De la Pena *et al.*, 1999)
			Gobern/CMB	(Zhu *et al.*, 1999)
HvGSL6	7HL	BYD virus resistance	Igri/Danilo	(Backes *et al.*, 1995)
		Fusarium HB resistance	Igri/Triumph	(Laurie *et al.*, 1995)
		# leaves-irrigated	Prisma/Apex	(Yin *et al.*, 1999)
		relative water content	Dicktoo/Morex	(Oziel *et al.*, 1996)
			Cali/Bowman	(Hayes *et al.*, 1996)
			Chevron/M69	(De la Pena *et al.*, 1999)
			Tadmor/Er-Apm	(Teulat *et al.*, 1998)
HvGSL7	3HL	*X. Campestris* resistance	Harrington/Morex	(Marquez-Cedillo *et al.*, 2000)
HvGSL8		Scald resistance	Steptoe/Morex	(Larson *et al.*, 1996)
		Fusarium HB resistance		(Larson *et al.*, 1997)
		Boron – relative root length		(Kandemir *et al.*, 2000)
				(Hayes *et al.*, 1993)
				(Mano *et al.*, 1996)
				(El Attari *et al.*, 1998)
			Blenheim/Kym	(Bezant *et al.*, 1997)
			Blenheim/E224/3	(Thomas *et al.*, 1995)
				(Powell *et al.*, 1997)
			Gobern/CMB	(Zhu *et al.*, 1999)
			Clipper/Sahara3771	(Jefferies *et al.*, 1999)

Table 2.2: The chromosomal map location and associated biotic and abiotic stress QTLs of the *HvGSL* genes. HB: head blight. BYD: barley yellow dwarf.

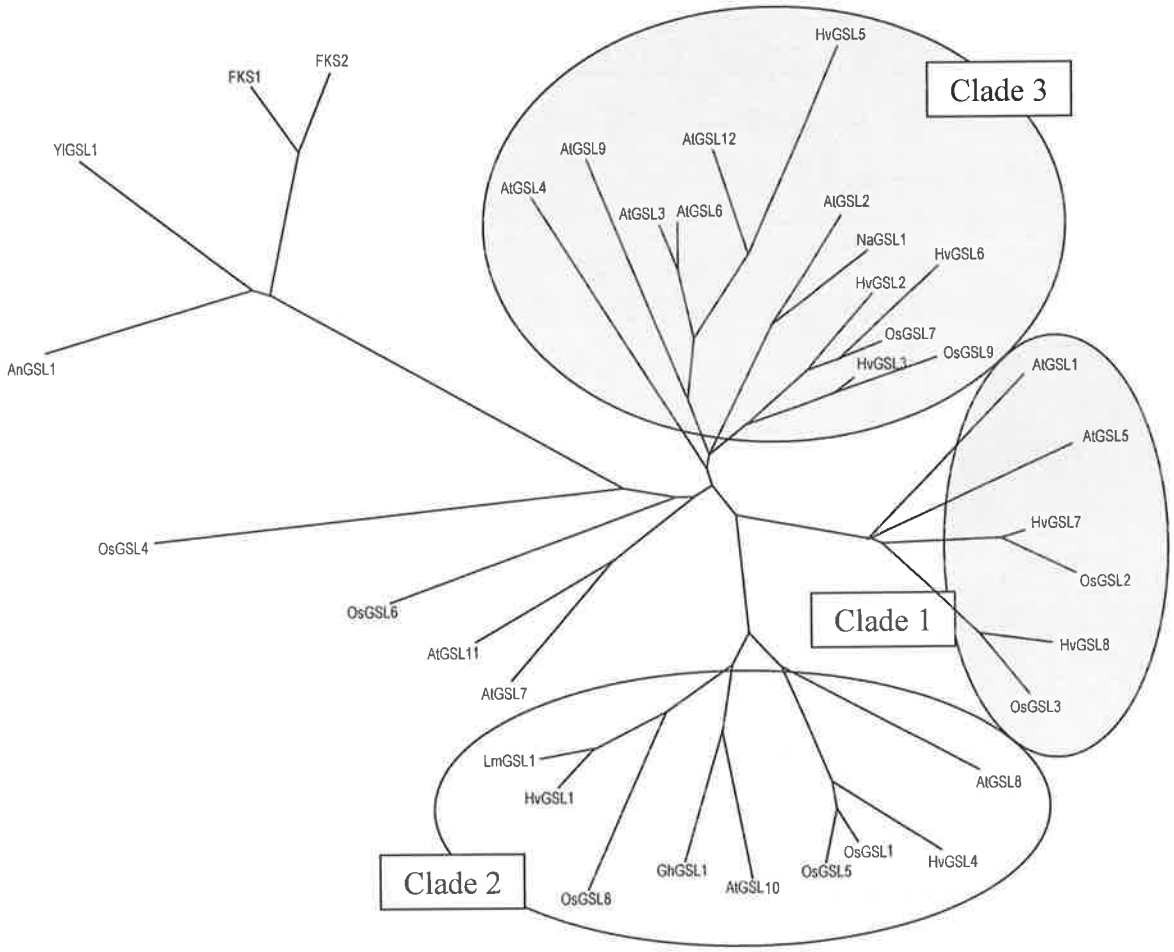

Figure 2.22: A phylogenetic tree, graphically representing amino acid sequence homology of all publicly available full length GSL sequences and the partially cloned fragments of HvGSL. Coloured regions represent the 3 clades that contain HvGSLs.

Following are the accession numbers of the GSLs in the above phylogenetic tree:

AtGSL1 (NM_116736), *AtGSL2* (NM_179622), *AtGSL3* (NM_179847), *AtGSL4* (NM_112317), *AtGSL5* (NM_116593), *AtGSL6* (AF237733), *AtGSL7* (NM_100528), *AtGSL8* (NM_179940), *AtGSL9* (NM_123045), *AtGSL10* (NM_111596), *AtGSL11* (NM_115772), *AtGSL12* (NM_121303), *OsGSL1* (XM_550490, *OsGSL2* (NM_191973), *OsGSL3* (NM_191270), *OsGSL4* (NM_193204), *OsGSL5* (NM_185408), *OsGSL6* (NM_193211), *OsGSL7* (XM_468556), *OsGSL8* (NM_187562), *OsGSL9* (NM_187591), GhGSL1 (AF085717), LmGSL1 (AY286332), NaGSL1 (AF304372), HvGSL1 (AY177665), YlGSL1 (AF198090), AnGSL1 (AACD01000061), FKS1 (SCU12893), FKS2 (SCU16783).

Amino Acid Sequence Identity

	HvGSL1	HvGSL2	HvGSL3	HvGSL4	HvGSL5	HvGSL6	HvGSL7	HvGSL8
HvGSL1								
HvGSL2	50.8%							
HvGSL3	58.2%	70.8%						
HvGSL4	50.7%	45.9%	40.2%					
HvGSL5	31.3%	-	-	-				
HvGSL6	43.1%	76.2%	58.3%	40.0%	-			
HvGSL7	54.8%	48.2%	50.7%	31.4%	-	40.2%		
HvGSL8	45.1%	49.4%	52.5%	36.1%	42.5%	44.3%	73.6%	
AtGSL1	44.7%	47.0%	52.3%	35.7%	48.8%	40.6%	71.9%	64.5%
AtGSL2	45.1%	61.1%	62.9%	37.8%	53.8%	55.5%	55.7%	46.8%
AtGSL3	44.0%	71.5%	68.0%	39.2%	68.8%	67.3%	56.0%	45.1%
AtGSL4	40.5%	57.3%	58.3%	34.0%	55.0%	51.2%	51.1%	42.5%
AtGSL5	45.1%	46.7%	51.2%	38.0%	43.9%	41.1%	72.1%	64.1%
AtGSL6	43.5%	72.1%	68.4%	38.2%	68.8%	66.8%	56.2%	45.4%
AtGSL7	43.9%	63.1%	61.9%	44.2%	46.3%	57.0%	54.2%	44.4%
AtGSL8	52.6%	48.4%	47.7%	54.8%	-	41.5%	49.2%	38.7%
AtGSL9	40.9%	60.2%	61.0%	33.0%	51.3%	53.1%	51.8%	41.9%
AtGSL10	65.0%	49.9%	53.3%	48.3%	31.7%	46.5%	56.4%	43.9%
AtGSL11	43.0%	61.3%	60.8%	42.2%	42.5%	56.5%	54.6%	44.1%
AtGSL12	43.6%	76.6%	74.1%	50.0%	73.8%	-	62.7%	45.1%
OsGSL1	56.6%	50.7%	53.1%	73.6%	37.0%	46.3%	55.8%	42.6%
OsGSL2	45.0%	48.9%	52.8%	34.0%	48.8%	40.6%	89.3%	66.1%
OsGSL3	43.0%	48.8%	52.3%	37.4%	42.5%	44.3%	74.1%	85.5%
OsGSL4	36.5%	-	-	-	34.1%	-	-	36.1%
OsGSL5	54.3%	49.3%	53.3%	69.7%	36.6%	40.5%	54.9%	46.9%
OsGSL6	42.9%	59.2%	59.6%	38.9%	43.3%	49.8%	54.0%	42.6%
OsGSL7	43.7%	87.6%	70.1%	38.3%	68.2%	79.6%	55.8%	45.2%
OsGSL8	84.1%	51.8%	52.9%	46.2%	-	44.8%	55.5%	47.0%
OsGSL9	45.9%	74.0%	79.1%	37.1%	62.1%	67.1%	56.6%	43.5%
NaGSL1	45.7%	61.7%	61.5%	41.5%	53.8%	57.6%	56.0%	48.0%
GhGSL1	69.2%	50.7%	54.6%	54.6%	31.3%	47.8%	55.1%	44.4%
LmGSL1	90.1%	51.0%	52.3%	47.3%	30.0%	43.6%	54.5%	44.0%
AnGSL1	32.3%	23.4%	27.5%	-	-	-	32.7%	30.1%
YlGSL1	31.3%	23.2%	27.6%	-	-	-	30.3%	30.0%
FKS1	31.6%	23.4%	30.3%	-	-	-	31.6%	28.1%
FKS2	31.5%	24.1%	30.8%	-	-	-	31.9%	28.4%

Table 2.3: The amino acid identities of the HvGSL partial sequence against the known full length GSL proteins. Highlighted regions indicate GSLs that located on the same branch of the phylogenetic tree (*Figure 2.22*). A dash (-) indicates an alignment that showed no significant identity. The table was constructed using the Blast-2 online computer program (http://www.ncbi.nlm.nih.gov/blast/bl2seq /wblast2.cgi).

Clade 1

The GSL proteins from Arabidopsis and rice, which are located in Clade 1 have a gene structure with low number of introns (*Figure 1.5*). *AtGSL5* is located in Clade 1 (*Figure 2.22*) and is transcribed in high quantities in floral tissue (Østergaard *et al.*, 2002), and has been demonstrated to be required for wound and papillary (1,3)-β-D-glucan formation (Jacobs *et al.*, 2003; Nishimura *et al.*, 2003). As presented in the amino acid identity table, HvGSL7 and HvGSL8 share 73.6% identity over 552 amino acids of overlapping sequence and are located in Clade 1 (*Figure 2.22*; *Table 2.3*). HvGSL7 has a high sequence identity to OsGSL2 (89.3%), AtGSL5 (72.1%) and AtGSL1 (71.9%; *Table 2.3*; *Table 2.4*; *Table 2.5*). HvGSL8 has a high sequence identity to OsGSL3 (85.5%), AtGSL1 (64.5%) and AtGSL5 (64.1%; *Table 2.3*; *Table 2.4*; *Table 2.5*).

Clade 2

The GSL proteins that were located in Clade 2 are encoded by genes with a high number of introns from *L. multiflorum*, rice, cotton, Arabidopsis and barley (*Figure 1.5*; *Figure 2.22*). The barley HvGSL1 and HvGSL4 deduced proteins, are both located in Clade 2 and share 50.7% identity over the 205 amino acids of overlapping sequence (*Figure 2.22*; *Table 2.3*). HvGSL1 has the highest sequence identity with LmGSL1 (90.1%; *Table 2.3*). The deduced protein of the *GhGSL1* gene from cotton is located in Clade 2 (*Figure 2.22*) and is transcribed during the development of the primary cell wall and in young roots and the orthologous barley gene is *HvGSL1* (*Table 2.4*). HvGSL4 was observed to have the highest sequence identity to OsGSL1 (73.6%) and OsGSL5 (69.7%; *Table 2.3*). Both OsGSL1 and OsGSL5 appear to be tightly grouped with HvGSL4 on the phylogenetic tree (*Figure 2.22*).

Clade 3

Clade 3 contains deduced GSL proteins encoded by genes with a high number of introns including those from Arabidopsis, barley, *N. alata*, and rice (*Figure 1.5*; *Figure 2.22*). HvGSL2 and HvGSL3 share 70.8% identity, while HvGSL2 and

Gene	Function/expression pattern	Reference	Barley Orthologue	
			Gene	aa Identity
AtGSL5	Flowers Wound response Fungal infection	(Østergaard *et al.*, 2002) (Enns *et al.*, 2005) (Nishimura *et al.*, 2003) (Jacobs *et al.*, 2003)	*HvGSL7* *HvGSL8*	72.1% 64.5%
AtGSL6 (*CalS1*)	Cell plate formation	(Hong *et al.*, 2001a)	*HvGSL2* *HvGSL6*	72.1% 66.8%
GhGSL1	Development of primary wall Young roots	(Cui *et al.*, 2001)	*HvGSL1*	69.2%
NaGSL1	Pollen tubes	(Doblin *et al.*, 2001)	*HvGSL2* *HvGSL3*	61.7% 61.5%

Table 2.4: The proposed function/transcription pattern and possible barley orthologues of non-barley plant *GSL* genes in the literature. The identification of orthologous genes in barley was based on the identity of the deduced amino acid sequence (*Table 2.3*). aa: amino acid. The inclusion of *HvGSL6* as a potential *AtGSL6* orthologue is based on results obtained in *Chapter 3*.

Possible Orthologues		
Barley	Arabidopsis	Rice
HvGSL1	*AtGSL10*	*OsGSL8*
HvGSL2	*AtGSL12*	*OsGSL7*
HvGSL3	*AtGSL12*	*OsGSL9*
HvGSL4	*AtGSL8*	*OsGSL1*
HvGSL5	*AtGSL12*	*OsGSL7*
HvGSL6	*AtGSL3*	*OsGSL7*
HvGSL7	*AtGSL5*	*OsGSL2*
HvGSL8	*AtGSL1*	*OsGSL3*

Table 2.5: The possible orthologues of barley HvGSL genes in Arabidopsis and rice. The identification of orthologous genes was based on the identity of the deduced amino acid sequence (*Table 2.3*).

HvGSL6 share 76.2% identity (*Table 2.3*). HvGSL3 and HvGSL6 share 58.3% amino acid sequence identity (*Table 2.3*). HvGSL5, due to the lack of overlapping sequence (*Figure 2.17*), does not share identity with any of the barley sequences within this clade (*Table 2.3*). HvGSL2 has the greatest amino acid sequence identity with a non-barley GSL, OsGSL7 (87.6%; *Table 2.3*). AtGSL6 (CalS1) is located in Clade 3 (*Figure 2.22*) and has been implicated in the formation of the cell plate during cellular division, the barley GSL with the highest amino acid identity to AtGSL6 is HvGSL2 at 72.1% (*Table 2.3*; *Table 2.4*). The gene encoding the NaGSL1 protein was observed to be transcribed in cultured *N. alata* pollen tubes and is also located in Clade 3 (*Figure 2.22*), the barley GSL proteins with the highest amino acid identity is HvGSL2 (61.7%) and HvGSL3 (61.5%; *Table 2.3*; *Table 2.4*). The GSL that HvGSL6 shares the highest amino acid sequence identity with was OsGSL7 with 79.6% identity (*Table 2.3*). It was also observed that HvGSL3 shared highest identity with OsGSL9 (79.1%) while HvGSL5 shared highest identity with AtGSL12 (73.8%; *Table 2.3*).

2.3.13 Membrane Topology Prediction of the HvGSL8 Protein

Since *HvGSL8* was initially considered the most likely barley orthologue of the Arabidopsis *AtGSL* gene, the cDNA sequence data was obtained for *HvGSL8* (*Section 2.3.8*). GSL proteins are believed to be associated with cellular membranes, and it was therefore of interest to predict the membrane topology of the amino acid sequence encoded by *HvGSL8*. The transmembrane prediction programs detected 11 – 15 putative transmembrane helices (*Figure 2.23*). The 11 transmembrane helices that were detected with PRED-TMR were also detected by Phobius and HmmTop_v2 (*Figure 2.23*). A hydrophilic domain of 766 – 789 amino acids was detected by all three prediction programs (*Figure 2.23*). The putative cytoplasmic loop is flanked by a COOH-terminal cluster of 6 – 8 putative transmembrane helices and an NH_2-terminal cluster of 5 – 7 putative transmembrane helices (*Figure 2.23*).

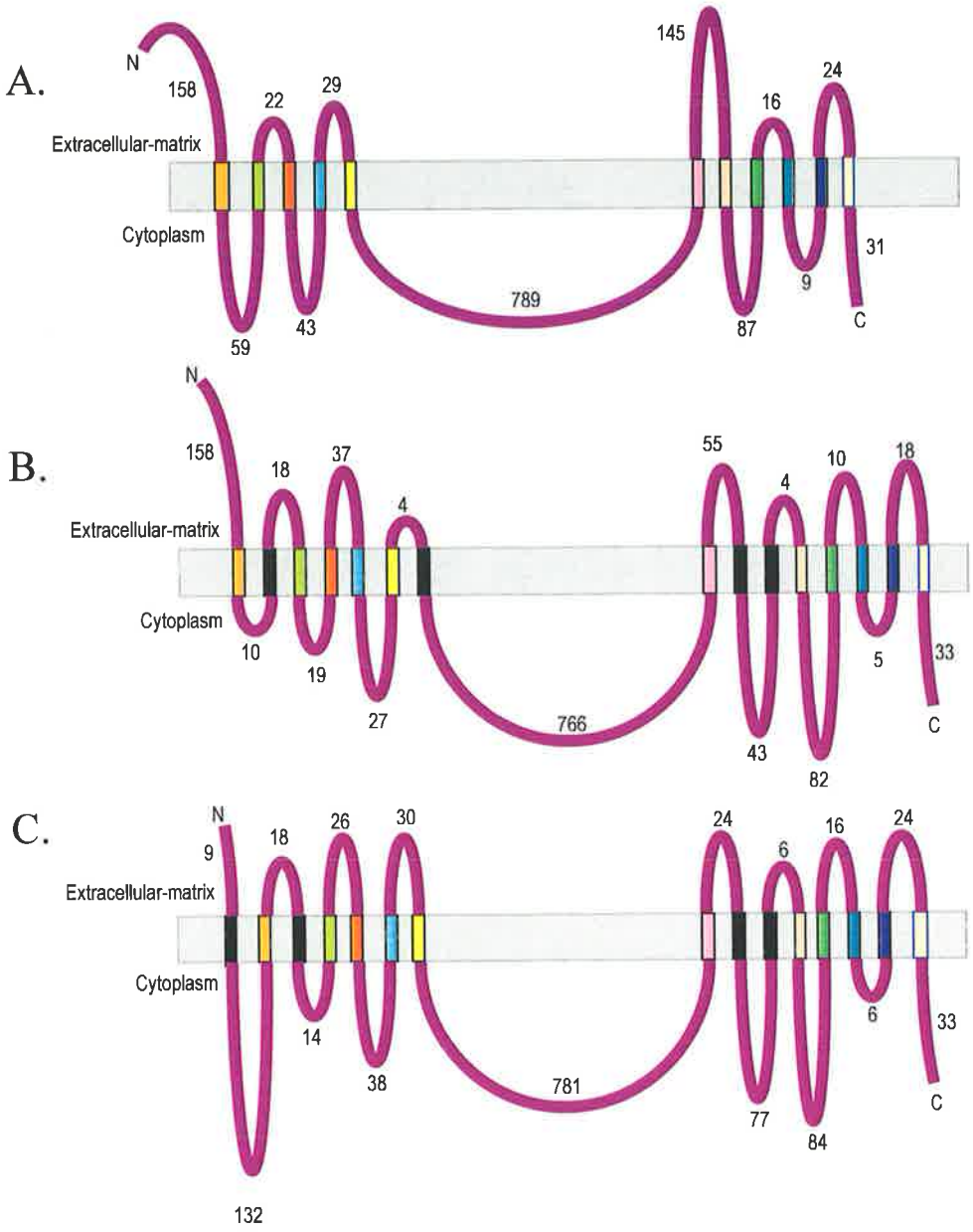

Figure 2.23: The membrane topology of HvGSL8 as predicted by three different transmembrane prediction programs. A: PRED-TMR (http://biophysics.biol.uoa.gr/PRED-TMR/input.html); **B:** Phobius prediction (http://phobius.cgb.ki.se/); **C:** HmmTop_v2 (http://www.enzim.hu/hmmtop/html/submit.html). The coloured transmembrane regions are predicted by all three programs, black transmembrane regions were not predicted by all three programs.

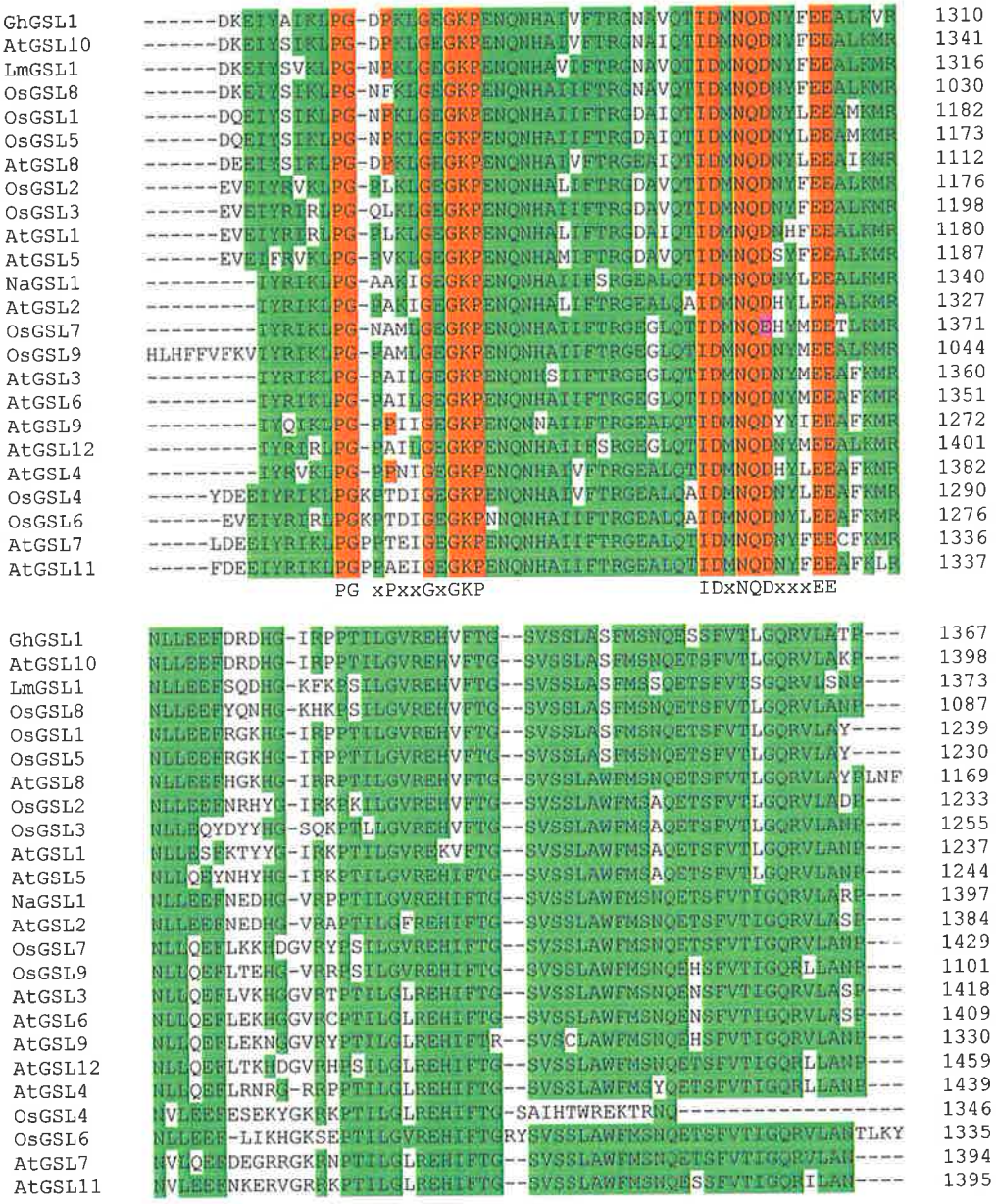

Figure 2.24: The conserved amino acid sequence region within the putative cytoplasmic loop of known full length GSL proteins from plants. The regions shaded in green are conserved in at least 50% of the available full length sequences. The regions shaded in red show conserved motifs located within this region.

2.3.14 Analysis of the Proposed Catalytic Site

All the full length GSL proteins were aligned using the ClustalW alignment program. The hydrophilic putative cytoplasmic region was the most highly conserved region of the sequence. The SET, PDEW, PGxPxxGxGKP, IDxNQDxxxEE and SED motifs have previously been proposed to be important in the reaction mechanism of the putative (1,3)-β-D-glucan synthases (Li *et al.*, 2003). It was observed that the SET motif was conserved across only 23% (6/26) of plant GSL proteins, and that in those six the central glutamate was absolutely conserved (*data not shown*). The PDEW motif was conserved in 77% (20/26) of the plant GSL proteins. In the six plant GSL proteins that had variations of the PDEW motif, the central aspartate and glutamate residues were replaced with ED, DD or EE residues. The tryptophan of the PDEW motif was conserved across all plant GSL proteins (*data not shown*). The PGxPxxGxGKP motif was conserved in 31% (8/26) of the available plant GSL proteins (*Figure 2.24*). The only variation of the PGxPxxGxGKP motif was the proline at the forth position (i.e. PGx**P**xxGxGKP), which was commonly replaced with a hydrophobic amino acid residue. It was observed that the IDxNQDxxxEE (*Figure 2.24*) and SED motifs were absolutely conserved across all 26 plant GSL amino acid sequences. The D,D,D35QxxRW motif, or the KAG or QTP motifs that have been identified in β-glycosyl transferases including the curdlan synthase of *Agrobacterium* sp. (Stasinopoulos *et al.*, 1999) were not found in any of the plant GSL proteins or putative fungal (1,3)-β-glucan synthases (*data not shown*). All the plant GSL proteins lack the putative D(WY)PX$_{3:6}$(IV)(WY)(ILV)(LV)DDG UDP-glucose binding motif (Stasinopoulos *et al.*, 1999). The putative RxTG UDP-glucose binding motif, proposed by Inoue *et al.* (1996) and Østergaard *et al.* (2002), was conserved in 85% (22 / 26) of plant GSL proteins.

2.4 DISCUSSION

At the commencement of this project, there were 12 full length *GSL* genes from Arabidopsis and nine full length *GSL* genes from rice in the NCBI database (http://www.ncbi.nlm.nih.gov/). There was also one each from cotton (Cui *et al.*, 2001), *N. alata* (Doblin *et al.*, 2001), barley (Li *et al.*, 2003), and *L. multiflorum* (accession: AY286332). It was expected that the number of (1,3)-β-D-glucan synthase genes in other monocot species, such as barley, would be comparable to the number found in rice. Based on data presented here, there are potentially eight *GSL* genes in barley (*Figure 2.17*). However, due to the lack of overlapping sequence between *HvGSL5* and the other barley *GSL* genes, it is possible that the *HvGSL5* sequence is located at the 5' end of *HvGSL2*, *HvGSL3*, *HvGSL4*, *HvGSL6* or *HvGSL7* (*Figure 2.17*). Since *HvGSL5* was mapped to the same position as *HvGSL2* (*Figure 2.21*), it is likely that they are fragments of the same gene. Unsuccessful attempts were made to clone the 3' region of *HvGSL5* (*data not shown*) to definitively link *HvGSL5* with *HvGSL2*. Thus, at least seven individual *HvGSL* genes have been identified so far and there is a possibility that at least one additional *HvGSL* gene will be identified in the barley genome. Since the Arabidopsis *AtGSL5* gene was the first, and only, plant *GSL* gene to be assigned a likely functional role to date (Jacobs *et al.*, 2003; Nishimura *et al.*, 2003) and because the first clones of *HvGSL8* had the highest identity to *AtGSL5*, particular effort was directed towards the cloning of *HvGSL8*. A total of 5193 bp of *HvGSL8* was cloned, which included a 315 bp 3' untranslated region and 4878 bp encoded 1626 amino acids of the protein (*Figure 2.17*). The cloning of additional *HvGSL* genes may be achieved by targeting the *HvGSL* EST singletons, as these may encode previously unidentified *HvGSL* genes. Additional unidentified *HvGSL* genes may be transcribed in tissues that are not represented in the EST databases, and PCR designed to conserved regions of Arabidopsis and rice *GSL* genes could uncover any additional barley genes.

In the barley genetic map, a single copy of each *HvGSL* gene was observed (*Figure 2.21*). The genomic regions near the *HvGSL* genes are associated with many agronomic, quality, biotic stress and abiotic stress QTLs (*Table 2.2*). The agronomic and grain quality QTLs cover many broad attributes such as grain size, grain weight,

heading date and diastatic power. It was impossible to determine the importance of (1,3)-β-D-glucan deposition in these traits. In addition to the agronomic and quality QTLs, there were several biotic and abiotic stress QTLs associated with the *HvGSL* gene chromosomal locations (*Table 2.2*). It appears likely that only one *GSL* in the gene family is associated with the (1,3)-β-D-glucan deposition in response to wounding and fungal attack (Jacobs *et al.*, 2003). Therefore, the stress QTLs in the region of the *AtGSL5* orthologue in barley were determined. The deduced HvGSL7 and HvGSL8 proteins have the highest amino acid sequence identities to the deduced AtGSL5 protein (*Table 2.3*; *Table 2.4*), and are therefore the most likely *AtGSL5* orthologues in barley. The QTLs in the region of the *HvGSL7* and *HvGSL8* chromosomal location were related to resistance to *Xanthomonas campestris*, *Rhynchosporium secalis* and *Fusarium* head blight, as well as boron tolerance (*Table 2.2*). At this stage, it is uncertain which role, if any, the *HvGSL7* and the *HvGSL8* genes have in these traits.

The only full length barley *GSL* cDNA cloned to date is *HvGSL1*, which encodes a deduced protein of 1915 amino acid residues with a calculated molecular mass of about 218 kDa (Li *et al.*, 2003). The protein encoded by the *HvGSL1* gene was associated with a cellular membrane fraction that also contains (1,3)-β-D-glucan synthase activity (Li *et al.*, 2003). Further evidence that *GSL* genes encode membrane proteins is given by the predicted membrane topology of the proteins. The deduced amino acid sequence of the full length plant *GSL* genes and the yeast *FKS* genes are predicted to contain 13 – 16 putative transmembrane helices and a large putative, hydrophilic, cytoplasmic domain (Douglas *et al.*, 1994; Cui *et al.*, 2001; Doblin *et al.*, 2001; Østergaard *et al.*, 2002; Li *et al.*, 2003). Since most sequence data was obtained for *HvGSL8*, the predicted membrane topology of the deduced amino acid sequence was determined and compared to that of previously described GSL proteins. Using three membrane topology prediction programs, it was predicted that a large, central, hydrophilic loop of 766 – 789 amino acids was flanked by 6 – 8 putative transmembrane helices at the COOH-terminus and 5 – 7 putative transmembrane helices at the NH_2-terminus (*Figure 2.23*). The amino acid alignment of HvGSL8 against the full length GSL proteins from Clade 1 showed that HvGSL8

was truncated at the N-terminal end by approximately 170 amino acids (*data not shown*) and it is possible that more transmembrane helices may be present in this region. The predicted membrane topology of the protein encoded by the partial *HvGSL8* cDNA, shown in *Figure 2.23*, bears a strong resemblance to the membrane topology predicted for the FKS1 protein (Douglas *et al.*, 1994), NaGSL1 (Doblin *et al.*, 2001), GhGSL1 (Cui *et al.*, 2001), AtGSL5 (Østergaard *et al.*, 2002) and HvGSL1 (Li *et al.*, 2003).

Within the large putative cytoplasmic hydrophilic domain a conserved region was observed, which was thought to contain the catalytic site for enzymatic activity (Li *et al.*, 2003). The activity of the putative (1,3)-β-D-glucan synthases, like other glycosyltransferases, involves the transfer of a sugar group from an activated donor sugar, such as UDP-glucose, to an acceptor. (1,3)-β-D-Glucan synthases require Ca^{2+} for activity, except in pollen tubes (Schlüpmann *et al.*, 1993), while most glycosyltransferases require the involvement of a metal ion, commonly Mg^{2+} or Mn^{2+}, to act as a Lewis acid to assist in the removal of the nucleoside diphosphate (Williams and Davies, 2001). Since the mechanism of sugar attachment to the growing chain requires the acceptor sugar to be deprotonated, probable amino acid candidates are those with an acid/base functional group (Williams and Davies, 2001; Lairson and Withers, 2004), such as aspartate (D), glutamate (E) and histidine (H). The 350 amino acid region between residue-1056 and residue-1406 of the HvGSL1 large putative cytoplasmic hydrophilic domain was previously considered likely to contain the active site, and includes conserved motifs with aspartate, glutamate and histidine amino acid residues (Li *et al.*, 2003). However, unlike other proteins involved in the addition of glucose, from UDP-glucose, to a growing polysaccharide chain, there are no characteristic amino acid sequences such as UDP-glucose binding motifs anywhere in the GSL amino acid sequences. This includes the putative UDP-glucose binding motif, D(WY)P$X_{3:6}$(IV)(WY)(ILV)(LV)DDG, which is encoded in curdlan synthase genes of glycosyl transferase family GT2 of *Agrobacterium* sp. (Stasinopoulos *et al.*, 1999). The D(WY)P$X_{3:6}$(IV)(WY)(ILV)(LV)DDG motif is also located in other glycosyltransferases such as the cellulose synthases from

Acetobacter xylinum, *Escherichia coli*, *Paramecium bursaria*, Arabidopsis, rice, barley, *Streptococcus pyogenes* and *Rhyzobium meliloti* (Stasinopoulos *et al.*, 1999).

Another putative UDP-glucose binding motif of glycogen synthases in yeast and rabbits, RxGG (Mahreholz *et al.*, 1989; Farkas *et al.*, 1990), is not found in the peptide sequence of plant GSL proteins, although a similar motif, RxTG, has been identified in *S. cerevisiae* (FKS1 and FKS2) and Arabidopsis (AtGSL5) on the putative cytosolic face of a small loop between two transmembrane domains at the COOH-terminal end (Inoue *et al.*, 1996; Østergaard *et al.*, 2002). Due to the putative RxTG UDP-glucose binding motif not being absolutely conserved (*Section 2.3.14*) and the lack of direct evidence that the motif aids in the binding of UDP-glucose, it is not clear if the RxTG motif is involved in the binding of UDP-glucose.

Other motifs located within the putative cytoplasmic domain of plant GSL proteins have been identified, such as the SET, PDEW, PGxPxxGxGKP, IDxNQDxxxEE and SED motifs, which were previously thought to be absolutely conserved in all plant GSL proteins (Li *et al.*, 2003). However, since the acquisition of more plant GSL amino acid sequence data, it is possible to exclude some of these motifs as potential catalytic sites. Only the IDxNQDxxxEE (*Figure 2.24*) and SED motifs are absolutely conserved across all the 26 plant GSL amino acid sequences that span this region, and these are therefore potential candidates as functional components in the activity of plant GSL proteins. Motifs such as the D,D,D35QxxRW, KAG and QTP that have been identified in curdlan synthase and cellulose synthases from a variety of organisms (Stasinopoulos *et al.*, 1999), were not identified in any of the full length GSL proteins. It appears that GSL proteins have no amino acid similarity to other proteins involved in the transfer of UDP-glucose to a growing polysaccharide chain. Based on this lack of amino acid sequence conservation with any other glycosyltransferases, there is no evidence that plant GSL proteins directly catalyse the synthesis of (1,3)-β-D-glucan. However, it remains possible that a previously unidentified UDP-glucose binding motif may be present, allowing GSL proteins to be directly involved in the synthesis of (1,3)-β-D-glucan. In addition, the lack of a UDP-glucose binding motif supports the theory that (1,3)-β-D-glucan may be

synthesised by a multi-protein complex, comprising of a GSL protein and a UDP-glucose binding protein (*Section 1.4.1.1*).

In plants, (1,3)-β-D-glucan is deposited in many types of specialised tissues at many stages of development and under various biotic and abiotic stresses (*Chapter 1*). It is conceivable that individual members of the putative (1,3)-β-D-glucan synthase gene family may be essential for (1,3)-β-D-glucan deposition under different conditions. In addition, it is possible that orthologous *GSL* genes in different species may have similar functions. Therefore, the deduced amino acid sequence of identified *HvGSL* genes were compared to the amino acid sequences of other plant GSL proteins that have been functionally analysed. The most convincing functional characterisation of a plant *GSL* gene has been done on the Arabidopsis *AtGSL5* gene. *AtGSL5* has been demonstrated to be essential for the deposition of (1,3)-β-D-glucan in response to wounding and in the formation of papillary structures in response to fungal attack (Jacobs *et al.*, 2003; Nishimura *et al.*, 2003). It has also been observed that the level of *AtGSL5* transcription is highest in flowers (Østergaard *et al.*, 2002). Arabidopsis plants with a disrupted AtGSL5 gene have been observed to be more resistant to a variety of pathogenic fungi (Jacobs *et al.*, 2003; Nishimura *et al.*, 2003). Since barley is a crop species that is subjected to a variety of yield reducing, virulent fungal pathogens, a special effort was made to identify the orthologous gene of *AtGSL5* in barley. The first clones encoding fragments of the HvGSL8 protein initially had the highest identity to AtGSL5 (*data not shown*), but as more sequence data was acquired a lower amino acid identity was observed over the near full length HvGSL8 sequence (64.1%) than HvGSL7 (72.1%) to AtGSL5 (*Table 2.3*; *Table 2.4*). Based on the identities of encoded amino acid sequences, *HvGSL7* is the most likely barley orthologue to *AtGSL5* in Arabidopsis (*Table 2.4*).

Other plant *GSL* genes that have been functionally analysed include the *NaGSL1* gene from *N. alata*, which may be essential for the deposition of (1,3)-β-D-glucan in pollen tubes (Doblin *et al.*, 2001). The barley GSL proteins that had the greatest amino acid sequence identity to NaGSL1 are HvGSL2 (61.7%) and HvGSL3 (61.5%; *Table 2.3*; *Table 2.4*). The *GhGSL1* gene from cotton, cloned from cotton

fibres, was shown to be transcribed at highest levels during primary wall development, and in young roots (Cui *et al.*, 2001). The barley GSL protein that has the highest amino acid identity to GhGSL1 is HvGSL1 (69.2%; *Table 2.3*; *Table 2.4*), which has also been shown to be transcribed in roots as well as in the early developing grain, florets and coleoptiles (Li *et al.*, 2003). The *AtGSL6* gene from Arabidopsis has been suggested to be involved in the formation of the cell plate during cellular division (Hong *et al.*, 2001a). It appears that the HvGSL2 protein has the highest sequence identity to AtGSL6 (72.1%; *Table 2.3*; *Table 2.4*) despite the apparent distance observed in the phylogenetic tree (*Figure 2.22*).

It is important to note that most of the barley *HvGSL* clones are not full length, and that the identification of orthologous genes in other plants might be subject to change with the acquisition of more sequence data. These sequence comparisons and possible *GSL* orthologues between plant species are summarised in *Table 2.3* and *Table 2.4*. The possibility that plant *GSL* orthologues perform similar functions in different species is explored by *HvGSL* gene transcription analysis experiments (*Chapter 3*) and gene silencing experiments (*Chapter 4*).

Chapter 3

Transcript Profiling of HvGSL *Genes*

3.1 INTRODUCTION

In higher plants, (1,3)-β-D-glucan is deposited in a variety of specialised cellular structures, as well as in response to biotic and abiotic stresses (*Chapter 1*). Genome sequencing projects have identified *GSL* gene families of 12 *AtGSL*s in Arabidopsis and nine *OsGSL*s in rice. At least seven barley *HvGSL* genes were identified in this project (*Chapter 2*), and it is probable that individual members of the *GSL* gene family will be responsible for the specialised deposition of (1,3)-β-D-glucan in precise spatial and temporal patterns. Regulation of the synthesis and deposition of (1,3)-β-D-glucan may occur through the control of transcriptional activity of individual (1,3)-β-D-glucan synthase genes. Alternatively, (1,3)-β-D-glucan synthesis may be controlled through the activation or deactivation of (1,3)-β-D-glucan synthase enzymes by the presence or absence of Ca^{2+}, or by the presence or absence of other precursors required for enzyme activation.

The aim of experiments described in this Chapter was to define the transcriptional activities of individual *HvGSL* genes through the analysis of *HvGSL* mRNA abundance in a range of barley tissues. The level of transcription in particular tissues was determined using three methods. In the first method, the tissue sources of *HvGSL* expressed sequence tags (EST) were recorded and analysed. In the second method, quantitative real-time PCR (Q-PCR) was used to measure the level of *HvGSL* mRNA transcripts in vegetative tissues, floral tissues, *Blumeria graminis* infected epidermal tissue as well as in different tissues at various stages of normal growth and development (Fink *et al.*, 1998). The third method involved the determination of genes that are co-ordinately transcribed with *HvGSL* genes, through the analysis of data generated from the Affymetrix Barley1 microarray chip. These co-ordinately transcribed genes were subsequently analysed to determine if they were tissue specific, developmentally specific or if the encoded proteins were potentially part of a (1,3)-β-D-glucan synthase protein complex.

3.2 MATERIALS and METHODS

3.2.1 Materials

The materials, and the source companies, which were used in standard molecular biological protocols covered here are listed in *Chapter 2*. The 2x QuantiTect SYBR green PCR reagent and the 10x SYBR green reagent were purchased from QIAGEN (Valencia, CA, USA). The *Hpa*II digest of pUC19 was obtained from Geneworks (Adelaide, SA, Australia).

3.2.2 Bio-Informatics

The tissue source was recorded for each barley *HvGSL* EST (*Appendix B*). Pearson correlations were performed using the Data Analysis application in Microsoft Excel, and the Euclidean correlation of microarray data (Dr Andreas Schreiber, *personal communication*).

3.2.3 Microarray Analysis

The Barley1 Chip (Affymetrix, Inc., Santa Clara, CA) oligonucleotide array was based on contiguous sequences that were constructed by aligning all publicly available barley sequences and EST sequences (Close *et al.*, 2004). The reference data for the Barley1 Chip were generously made available by Dr Robbie Waugh (Scottish Crop Research Institute, Invergowrie, Scotland). A total of 22840 contigs, including singletons, were generated and 11 pairs of 25mer oligonucleotides, one of which had a perfect match to the contig while the other had a mismatch at the 13th nucleotide, were designed on the basis of the last 600 bp at the 3' end of each sequence, and subsequently synthesised directly on the chip (http://www.barleybase.org/ index.php).

The normalised results of 21 microarray hybridisation experiments using cDNA from various barley tissues, 15 from the Morex cultivar (Mx) and six from the Golden Promise cultivar (GP), were publicly available (Close *et al.*, 2004). The corresponding code for each tissue type, listed in *Table 3.1*, is used throughout the Chapter. A Blast alignment of cloned *HvGSL* gene sequences (*Chapter 2*)

Tissue	Tissue Code	
	Golden Promise	Morex
Hypocotyl (2 d germinating seed)	GEM_GP	GEM_Mx
Seminal root (2 d germinating seed)	RAD_GP	RAD_Mx
Coleoptile (2 d germinating seed)	COL_GP	COL_Mx
Stem (10 cm seedlings)	CRO_GP	CRO_Mx
Root (10 cm seedlings)	ROO_GP	ROO_Mx
Leaf (10 cm seedlings)	LEA_GP	LEA_Mx
Developing caryopsis 3-5 DAP	-	CAR5_Mx
Developing caryopsis 8-10 DAP	-	CAR10_Mx
Developing caryopsis 14-16 DAP	-	CAR16_Mx
22 DAP developing endosperm	-	END_Mx
22 DAP developing embryo	-	DEM_Mx
6-10 cm immature inflorescence	-	INF_Mx
Bracts (1-2 d before anthesis)	-	BRC_Mx
Anthers (1-2 d before anthesis)	-	ANT_Mx
Pistils (1-2 d before anthesis)	-	PST_Mx

Table 3.1: The cDNA tissue sources that were used in the 21 hybridisation experiments on the Affymetrix Barley1 Chip. Tissues were collected from the Golden Promise and Morex barley cultivars. DAP: days after pollination. Experimental data was downloaded from http://www.barleybase.org/index.php (Close *et al.*, 2004).

against the contig sequences found on the microarray chip was performed at the BarleyBase website (http://www.barleybase.org/ blastbarley.php). The contigs that had a similar transcription profile to *HvGSL* genes that were represented on the microarray chip across the 15 experiments were determined by Euclidean and Correlation clustering methods (Kaminski and Friedman, 2002). The transcription patterns of *HvGSL1*, *HvGSL2*, *HvGSL3* and *HvGSL4* were compared to each other in a correlation matrix (Dr Andreas Schreiber, *personal communication*).

3.2.4 Quantitative Real-Time PCR

General Molecular Techniques

Several standard molecular biology protocols described in *Section 2.2* were also used in the experiments described in this Chapter. These protocols include total RNA extraction (*Section 2.2.3*), first strand cDNA synthesis for PCR (*Section 2.2.4*), PCR amplification of single stranded cDNA (*Section 2.2.5*), cloning PCR amplified fragments into pGEM®-T Easy (*Section 2.2.6*), transformation of *Escherichia coli* (*Section 2.2.7*), plasmid DNA mini-preparations (*Section 2.2.9*) and DNA sequencing (*Section 2.2.11*).

Tissue Collection, RNA Extraction and cDNA Synthesis

Total RNA was extracted and first-strand cDNA was synthesised from a variety of tissues, making the "tissue series", "leaf series", "root series" and the "developing endosperm series" (*Table 3.2*; Dr Rachel Burton, *personal communication*). These series were subsequently used for transcript analysis through Q-PCR.

The genes involved in the deposition of (1,3)-β-D-glucan in papillae in response to fungal infection are considered to be the same as in the response to wounding (Jacobs *et al.*, 2003). To analyse the regulation of barley putative (1,3)-β-D-glucan synthase genes in response to *B. graminis* infection, an infection tissue series was prepared. Since *B. graminis* only infects the epidermal layer of barley, efforts were made to isolate only epidermal cells for transcript analysis. It was possible to peel

Series	Tissue description
Tissue Series	First leaf tip First leaf base Root tip Root, mature zone Floral, early Floral, anthesis Developing grain, early Developing grain, mid Coleoptile, 3 day Stem
Leaf Series (Total leaf length: 133mm)	Leaf E, 0 - 3mm (base) Leaf D, 46 - 56mm Leaf C, 86 - 97mm Leaf B, 107 - 117mm Leaf A, 128 - 133mm (tip)
Root Series (Total root length: 106mm)	Root 4, 35 - 45mm (mature zone) Root 3, 63 - 73 mm Root 2, 80 - 90 mm Root 1, 97 - 106 mm (tip)
Developing Endosperm Series	2 days after pollination 3 days after pollination 4 days after pollination 5 days after pollination 6 days after pollination 7 days after pollination 8 days after pollination 9 days after pollination 10 days after pollination 11 days after pollination

Table 3.2: The tissues that comprise each series analysed by Q-PCR. All synthesised cDNA samples for each series were kindly donated by Dr Rachel Burton. The "tissue series", "leaf series" and "root series" were those as described by Burton *et al.* (2004).

away the epidermal layer from the mesophyll layer of young barley seedling leaves with relative ease. A very shallow incision was made across the ventral leaf surface with a scalpel and the epidermal layer was peeled away with a pair of forceps. Collected epidermal tissues were immediately frozen under liquid nitrogen to minimise the accumulation of transcript that may result from wounding, because the deposition of (1,3)-β-D-glucan in response to wounding is observable within minutes of mechanical damage (Stone and Clarke, 1992). This precaution ensured that the transcript levels that were observed were a result of fungal infection, not mechanical wounding. The first sample (T_0 hr), was prepared by collecting the epidermis from 10 uninfected first leaves of six to eight day old barley seedlings, snap freezing them immediately in liquid N_2 and storing the collected samples at -80°C. Following T_0 hr tissue collection, half of the barley seedlings were infected with *B. graminis* by spores from an infected donor barley plant. At 4, 8, 12, 16, 20 and 24 hr epidermal tissues from 10 infected seedling leaves and 10 uninfected seedling leaves were snap frozen in liquid N_2. Total RNA was extracted using the ball-bearing method (*Section 2.2.3*) and cDNA was synthesised for Q-PCR analysis (*Section 2.2.4*). At the completion of cDNA synthesis, the cDNA preparation was usually diluted 1:10, which was the working concentration for Q-PCR.

Primer Design

The control genes used in the Q-PCR experiments were heat shock protein 70 [HSP70], cyclophilin, glyceraldehyde-3-phosphate dehydrogenase [GAPDH], *HvCesA1* and α-tubulin, and the Q-PCR primers used are those described in *Table 3.3* (Burton *et al.*, 2004). The primer pairs for specific *HvGSL* genes were designed to the poorly conserved 3' gene regions. The *HvGSL* gene specific primers were compared to entries in the NCBI non-redundant nucleotide database (http://www.ncbi.nlm.nih.gov/) to ensure no cross reacting genes were likely to be amplified in the Q-PCR reactions. *HvGSL* gene specific primers were analysed with the NetPrimer applet program (http://www.premierbiosoft.com/netprimer/netprlaunch/netprlaunch.html) and primers that formed hairpins with a ΔG lower than -0.5 kcal.mol^{-1} or a cross-dimer with a ΔG lower than -8 kcal.mol^{-1} with the other primer in the pair were avoided.

Gene	Forward Primer	Reverse Primer	PCR Product	Acquisition Temperature
GAPDH	GTGAGGCTGGTGCTGATTACG	TGGTGCAGCTAGCATTTGAGAC	198 bp	80°C
HSP70	CGACCAGGGCAACCGCACCAC	ACGGTGTTGATGGGGTTCATG	108 bp	83°C
α-Tubulin	AGTGTCCTGTCCACCCACTC	AGCATGAAGTGGATCCTTGG	248 bp	80°C
Cyclophilin	CCTGTCGTCTCGTCGGTCTAAA	ACGCAGATCCAGCAGCCTAAAG	122 bp	79°C
HvCesA1	TGTGGCATCAACTGCTAGGAAA	CGTACAAAGTGCCTCATAGGAAA	267 bp	75°C

Table 3.3: Q-PCR primers and PCR amplified product sizes together with the optimal acquisition temperatures for the control genes. Primer sequences are written 5' to 3'. This table is adapted from *Table IV*, Burton *et al.* (2004).

Determination of the Optimal Temperature for Data Acquisition

A melt curve for each *HvGSL* Q-PCR reaction product was obtained by heating the product from 70°C to 99°C. The optimal temperature for data acquisition, at which maximum fluorescence was observed, was determined from the melt curve generated by the Rotor Gene 2000 Real-Time Cycler (Burton *et al.*, 2004). The optimal temperature for data acquisition for each of control gene is listed in *Table 3.3*. The optimal temperature for data acquisition for each *HvGSL* gene is presented in *Figure 3.7*.

HPLC Purification of the PCR Products

The gene specific PCR products from several reactions were pooled, purified using reverse phase HPLC and quantified (Dr Neil Shirley, *personal communication*). Between four and six replicate PCR reactions for each *HvGSL* were combined and purified by HPLC (Wong *et al.*, 2000) on Varian Helix DNA column 50 x 3 mm. At a flow rate of 0.45 mL/min and at a temperature of 50°C, the eluants (*Buffer A* was comprised of 0.1 M TEAA, 0.1 mM EDTA in water, while *Buffer B* was comprised of 0.1 M TEAA, 0.1 mM EDTA in methyl cyanide) were passed through the column at a gradient of 70% *Buffer A*, 30% *Buffer B* to 32% *Buffer A*, 68% *Buffer B* and subsequently held at 32% *Buffer A*, 68% *Buffer B* for 1 minute.

The DNA was detected by measuring the absorbance at 260 nm (A_{260}). The HPLC purified PCR products from each *HvGSL* were quantified by comparison of peak area with the peak areas of fragments of known length and mass, which resulted from an *Hpa*II digest of pUC19. In 2 µl of a 500 ng.µl^{-1} digest, the peaks used for reference were 147 bp, representing 55 ng, 190 bp (71 ng) and 242 bp (90 ng). The quantified HPLC purified PCR product of each gene was dried in a SpeedVac® (SC110, Savant) and redissolved in water to a final concentration of 20 ng.µl^{-1}.

Preparation of the Standard Dilution Series

An aliquot of the 20 ng.µl^{-1} HPLC purified PCR product from each *HvGSL* was further diluted to contain 10^9 copies.µl^{-1} of water. The 10^9 copies.µl^{-1} stock solution

was used to create a logarithmic dilution series covering seven orders of magnitude from 10^7 to 10^1 copies.μl^{-1}. Every Q-PCR experiment included three replicates of each of the seven standard concentrations along with two "no template" controls.

Q-PCR

A 1:10 dilution of each cDNA template was sufficient to obtain mRNA abundance data with an acceptable standard deviation for each *HvGSL*. Four replicate Q-PCR reactions were performed for each cDNA population. Q-PCR reactions were performed in a 20 µl volume and contained 1 µl cDNA solution, 3 µl of each forward and reverse primer at 4 µM, 10 µl 2x QuantiTect SYBR green PCR reagent, 0.6 µl 10x SYBR green in water, freshly diluted 1:10000 in dimethyl sulfoxide, and 2.4 µl water (Burton *et al.*, 2004). PCR thermal cycling and fluorescence detection was performed in a Rotorgene 2000 Real-Time cycler, RG2072: 15 min at 95°C followed by 45 cycles of 20 seconds at 95°C, 30 seconds at 55°C, 30 seconds at 72°C and 15 seconds at the optimal acquisition temperature (*Table 3.3*; *Figure 3.7*). At the end of the Q-PCR amplification a melt curve was obtained by heating the product from 70°C to 99°C. The Q-PCR data were analysed using the DNA Sample Analysis System v4.2 software from Corbett Research (Mortlake, NSW, Australia; Dr Neil Shirley, *personal communication*). The transcription levels of *HvGSL*s in Q-PCR reactions were determined by comparison with the standard dilution series and a mean and standard deviation were calculated from the four replicates of each cDNA.

3.3 RESULTS

3.3.1 EST Data Analysis

The EST data that were collected from the NCBI database and the Standford University cell wall web site (http://cellwall.standford.edu/) were analysed to determine the tissue source. The tissues were broadly categorised into seven groups; leaf, root, seed, male inflorescence, female inflorescence, embryo and other. Overall, ESTs corresponding to *HvGSL2* were the most abundant, particularly in leaf tissue (*Figure 3.1*). The number of ESTs for *HvGSL1*, *HvGSL4* and *HvGSL5* were lower, while very few ESTs corresponding to *HvGSL3*, *HvGSL6*, *HvGSL7* and *HvGSL8* were detected (*Figure 3.1*).

3.3.2 Microarray Analysis

The DNA sequence of each *HvGSL* was aligned against contigs represented on the Affymetrix Barley1 chip. Contigs on the microarray chip corresponded to *HvGSL1* (Contig8428_at), *HvGSL2* (Contig4949_at), *HvGSL3* (Contig19065_at) and *HvGSL4* (Contig13152_at). No contigs were found on the Barley1 chip that represented *HvGSL5*, *HvGSL6*, *HvGSL7* or *HvGSL8*. The transcription patterns of *HvGSL1*, *HvGSL2*, *HvGSL3* and *HvGSL4* in the 21 barley tissues were compared using the Pearson correlation coefficient. It was observed that transcript levels for *HvGSL3* only weakly correlated with those for other *HvGSL* genes (*Figure 3.2*). The highest correlation between mRNA levels was observed between *HvGSL1* and *HvGSL4* (0.80; *Figure 3.2*).

Possible correlations between *HvGSL* transcription patterns and of those genes represented on the Barley1 microarray chip were identified using Pearson correlation and Euclidean clustering analysis. The Pearson correlation shows the strength and direction of a linear relationship between two sets of variables. A Pearson correlation coefficient of 1.00 shows a perfect corrclation pattern of gene transcription, where a value of 0 shows no linear relationship between transcription patterns (Freund, 2004). The Euclidean clustering determines the linear distance, or "transcript pattern distance", between two sets of variables. A Euclidean transcript pattern distance of

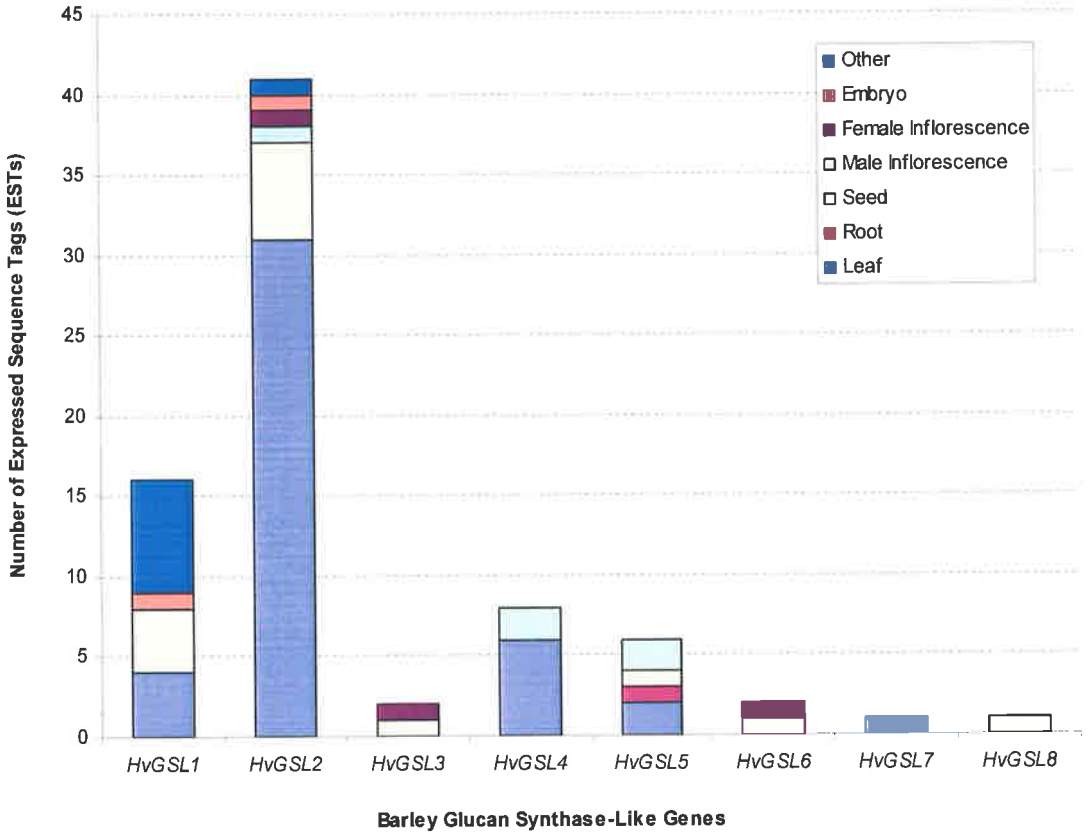

Figure 3.1: The tissue source of ESTs that were aligned to form the *HvGSL* contigs. The tissue source of each EST was broadly categorised into seven groups. The ESTs used in this analysis were those used to clone *HvGSL* cDNAs (*Chapter 2*). The total number of *HvGSL* ESTs detected in the databases was 90.

A.

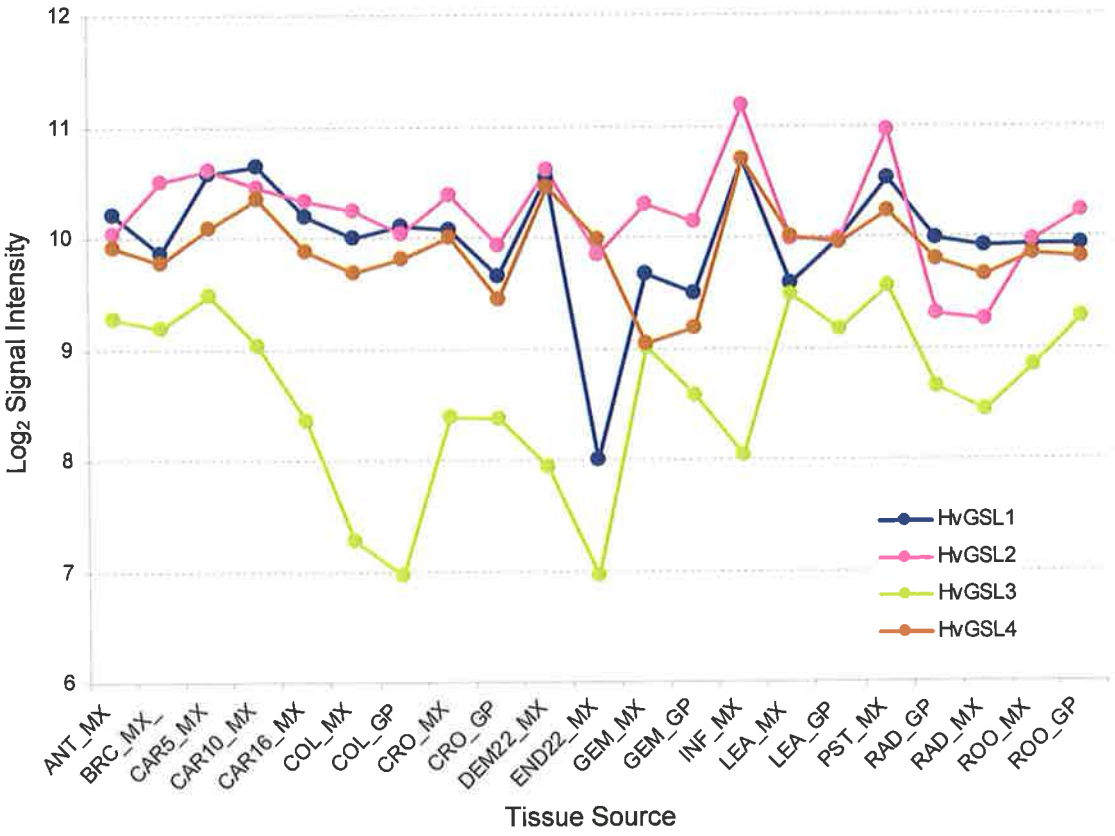

B.

	HvGSL1	*HvGSL2*	*HvGSL3*	*HvGSL4*
HvGSL1	1.00			
HvGSL2	0.65	1.00		
HvGSL3	-0.10	-0.03	1.00	
HvGSL4	0.80	0.58	-0.10	1.00

Figure 3.2: The normalised transcription patterns of contigs corresponding to *HvGSL1*, *HvGSL2*, *HvGSL3* and *HvGSL4* in 21 barley tissues. A: The graphed normalised Barley1 transcription data. The tissue codes on the x-axis are explained in *Table 3.1*. B: The Pearson correlation of transcription patterns of the *HvGSL* genes represented on the Barley1 chip across the 21 barley tissues.

zero between two genes indicates perfect co-ordinate expression (Quackenbush, 2001).

The 14 genes represented on the Barley1 chip with transcription profiles closest to *HvGSL1*, *HvGSL2*, *HvGSL3* and *HvGSL4* as determined by Pearson correlation and Euclidean clustering were determined (*Table 3.4*; *Table 3.5*; *Table 3.6*; *Table 3.7*). The two analytical methods frequently gave rise to different co-ordinately transcribing genes, although the methods did reveal correlations with the same genes. The nucleotide sequence of each contig was blasted against the NCBI protein database to establish the identities of genes co-ordinately transcribed with the *HvGSL* genes. The accession number, E-value, organism and description of the closest match were recorded for each contig that was apparently co-ordinately transcribed with *HvGSL1* (*Table 3.4*), *HvGSL2* (*Table 3.5*), *HvGSL3* (*Table 3.6*) and *HvGSL4* (*Table 3.7*).

The top 14 *HvGSL* co-ordinately transcribing genes, as determined by either the Pearson correlation or the Euclidean clustering, were assessed for their possible participation in the synthesis of (1,3)-β-D-glucan. Of the genes that had a similar transcription pattern with *HvGSL1*, none had obvious biochemical or cell biological links with (1,3)-β-D-glucan synthesis, at least within the limits or our current understanding of the process (*Table 3.4*). For example, ATPases and ATPase-inhibitor proteins are known to be transcribed throughout the cell, but it is not clear if the apparent correlation of transcription profiles of *HvGSL1* and the ATPase inhibitor has any biological significance (*Figure 3.3*). Similarly, the analysis indicated that *HvGSL2* had a comparable transcription pattern with a contig that had a high sequence identity to a barley gene encoding the DMC1 protein, which is a meiotic specific protein required for recombination (Leipe *et al.*, 2000). There have been no reports that (1,3)-β-D-glucan or (1,3)-β-D-glucan synthases are involved in DNA recombination during meiosis. One contig on the Affymetrix Barley1 Chip for which transcript patterns were similar to *HvGSL3* was identified as a putative glycosyltransferase, but details of its substrate specificity and function are not known (*Figure 3.5*). *HvGSL4* had transcription patterns that were similar to

HvGSL1 (Contig8428_at)

Pearson Correlation		BLASTX of Microarray Contigs Against the NCBI database			
Contig	Corr.	Accession	E-value	Organism	Description
Contig8428_at	*1.00000*	AAO46087	0	Barley	putative callose synthase
HA06g08r_s_at	0.93211	XP_483762	3.00E-16	Rice	F1F0-ATPase inhibitor protein
Contig15904_s_at	0.92187	CAH86939	2.1	*Plasmodium chabaudi*	Pc-fam-2 protein, putative
HVSME10022I23r2_at	0.92222	BAD73039	7.00E-16	Rice	putative Not4-Np
EBpi01_SQ003_M12_at	0.92152	-	-	-	*No significant similarity found*
Contig8888_at	0.91939	XP_550278	2.00E-61	Rice	putative brassinosteroid insensitive 1-associated receptor kinase 1
		XP_462817		Rice	putative receptor-like kinase
EBpi01_SQ002_B23_at	0.91906	AAO60423	7.1	*Ictalurus punctatus*	sodium channel 4
Contig16628_at	0.91790	XP_465130	2.00E-90	Rice	reticulon-like
Contig20404_at	0.91625	EAA66866		*Aspergillus nidulans*	hypothetical protein AN8301.2
HU10A18u_s_at	0.91218	XP_550278	2.00E-61	Rice	putative brassinosteroid insensitive 1-associated receptor kinase 1
		XP_462817		Rice	putative receptor-like kinase
Contig11423_at	0.91217	BAD82327	e-153	Rice	putative Endoribonuclease Dicer homolog
Contig13662_at	0.90806	AAT42170	2.3	*Sorghum bicolor*	putative actin depolymerizing factor
Contig25991_at	0.90675	NP_006250	8.8	*Homo sapiens*	protein kinase, cGMP-dependent, type II
Contig23005_at	0.90140	DAA01740	3.1	*Homo sapiens*	TPA: LRRC15
Contig12105_at	0.90108	XP_467673	0	Rice	putative nicastrin

Euclidean Cluster		BLASTX of Microarray Contigs Against the NCBI database			
Contig	Dist.	Accession	E-value	Organism	Description
Contig8428_at	*0.00000*	AAO46087	0	Barley	putative callose synthase
HA06g08r_s_at	0.49421	XP_483762	3.00E-16	Rice	F1F0-ATPase inhibitor protein
Contig15904_s_at	0.54309	CAH86939	2.1	*Plasmodium chabaudi*	Pc-fam-2 protein, putative
Contig16628_at	0.57129	XP_465130	2.00E-90	Rice	reticulon-like
Contig13662_at	0.57808	AAT42170	2.3	*Sorghum bicolor*	putative actin depolymerizing factor
Contig21220_at	0.60905	BAD36680	e-132	Rice	unknown protein
Contig9977_at	0.61201	XP_464412	4.00E-52	Rice	phytoene dehydrogenase-like protein
HW09B15u_at	0.61473	XP_547917	3.1	*Canis familiaris*	PREDICTED: similar to Feline leukemia virus subgroup C receptor-related protein 2
Contig2846_at	0.63911	XP_472610	1.00E-47	Rice	OJ000114_01.13
HX03D08u_s_at	0.67102	AAD54904	4	*Nephroselmis olivacea*	putative plastid division protein
Contig16517_at	0.67359	AAS79607	1.00E-35	*Ipomoea trifida*	hypothetical protein
Contig15885_at	0.67612	BAD53492	e-130	Rice	WD-40 repeat protein-like
HD04E24u_at	0.67966	XP_463888	7.00E-30	Rice	APG5 (autophagy 5)-like protein
Contig14116_at	0.69049	BAC42918	5.00E-74	Arabidopsis	putative acetyl-CoA synthetase
Contig25811_at	0.69507	-	-	-	*No significant similarity found*

Table 3.4: Genes represented on the Barley1 microarray that exhibit a similar transcription pattern to *HvGSL1* as determined by Pearson Correlation and Euclidean clustering. The contig sequences identified were compared to the proteins in the NCBI database. The best BLASTX matches for each contig are presented with the accession number, E-value, the organism the gene was identified in, as well as the description of each gene.

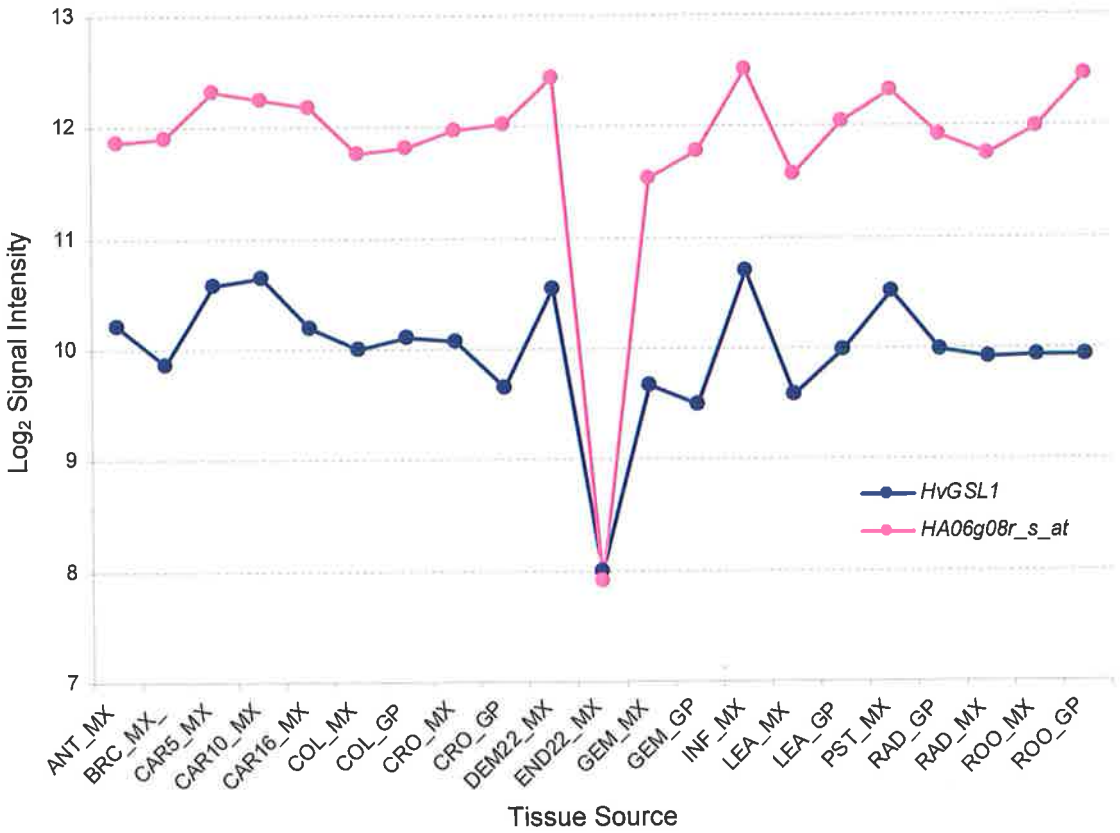

Figure 3.3: The normalised co-ordinate transcription of *HvGSL1* with the HA06g08r_s_at contig in 21 barley tissues. The HA06g08r_s_at nucleotide sequence was compared to the NCBI sequence database and is high sequence identity to a gene that encodes a F1F0-ATPase inhibitor protein in rice. The tissue codes on the x-axis are explained in *Table 3.1*.

HvGSL2 (Contig4949_at)

Pearson Correlation		BLASTX of Microarray Contigs Against the NCBI database			
Contig	Corr.	Accession	E-value	Organism	Description
Contig4949_at	*1.00000*	AAP84973	0	Rice	Callose synthase-like protein
HK03H05r_s_at	0.91728	XP_470099	2.00E-29	Rice	unknown protein
Contig19614_at	0.90788	BAD30894	2.00E-13	Rice	unknown protein
Contig14634_at	0.90617	AAN05323	e-152	Rice	Hypothetical protein
Contig7191_at	0.89336	XP_465255	e-126	Rice	putative N7 protein
HM03L14u_at	0.88882	NP_915049	4.00E-22	Rice	putative pectin methylesterase
HVSMEf0017F17r2_at	0.88807	XP_474428	0.8	Rice	OSJNBa0070M12.6
Contig12720_at	0.88465	YP_064646	0.005	*Desulfotalea psychrophila*	probable ribonuclease H
rbah44m17_s_at	0.87759	AAM93675	2.00E-21	Rice	putative glycine-rich protein
Contig8695_at	0.86902	BAD68869	4.00E-45	Rice	unknown protein
Contig191_s_at	0.86816	AAK11228	2.00E-49	Arabidopsis	Copper-binding protein CUTA
Contig24208_at	0.86717	S52020	1.00E-49	*Nicotiana tabacum*	translation initiation factor eIF-4A 15
Contig10078_at	0.86653	AAP53614	e-136	Rice	putative Transcription initiation factor IIE, beta subunit
Contig1030_s_at	0.86609	BAD38105	7.00E-80	Rice	polyubiquitin 2
Contig9753_at	0.86490	AAF42940	0	Barley	DMC1 protein
Contig18874_at	0.86240	BAD30766	3.00E-82	Rice	putative HEN1
Contig12136_at	0.86231	XP_475606	5.00E-81	Rice	putative RNA polymerase II fifth largest subunit

Euclidean Cluster		BLASTX of Microarray Contigs Against the NCBI database			
Contig	Dist.	Accession	E-value	Organism	Description
Contig4949_at	*0.00000*	AAP84973	0	Rice	Callose synthase-like protein
Contig14634_at	0.72886	AAN05323	e-152	Rice	Hypothetical protein
Contig19614_at	0.84507	BAD30894	2.00E-13	Rice	unknown protein
Contig1030_s_at	0.86221	BAD38105	7.00E-80	Rice	polyubiquitin 2
HVSMEf0017F17r2_at	0.87172	XP_474428	0.8	Rice	OSJNBa0070M12.6
rbah44m17_s_at	0.87971	AAM93675	2.00E-21	Rice	putative glycine-rich protein
Contig8695_at	0.88037	BAD68869	4.00E-45	Rice	unknown protein
baak1h04_s_at	0.91522	ZP_00282372	0.61	*Burkholderia fungorum*	Flavodoxin reductases (ferredoxin-NADPH reductases) family 1
Contig12482_at	0.92168	XP_479192	1.00E-48	Rice	putative anther ethylene-upregulated protein ER1
Contig4788_at	0.93366	AAM89289	0	*Zea mays*	SET domain-containing protein SET102
Contig12720_at	0.93769	YP_064646	0.005	*Desulfotalea psychrophila*	probable ribonuclease H
Contig13495_at	0.95336	BAD36394	e-103	Rice	unknown protein
Contig10078_at	0.95801	AAP53614	e-136	Rice	putative Transcription initiation factor IIE, beta subunit
Conitg17507_at	0.95947	AAL73486	7.00E-33	*Triticum aestivum*	repressor protein
Contig21639_at	0.96026	XP_541520	6.00E-04	*Canis familiaris*	PREDICTED: similar to N-methyl-D-aspartate receptor subunit
Conitg18874	0.96094	BAD30766	3.00E-82	Rice	putative HEN1
Contig9243_at	0.96400	XP_469289	e-106	Rice	unknown protein

Table 3.5: Genes represented on the Barley1 microarray that exhibit a similar transcription pattern to *HvGSL2* as determined by Pearson Correlation and Euclidean clustering. The contig sequences identified were compared to the proteins in the NCBI database. The best BLASTX matches for each contig are presented with the accession number, E-value, the organism the gene was identified in, as well as the description of each gene.

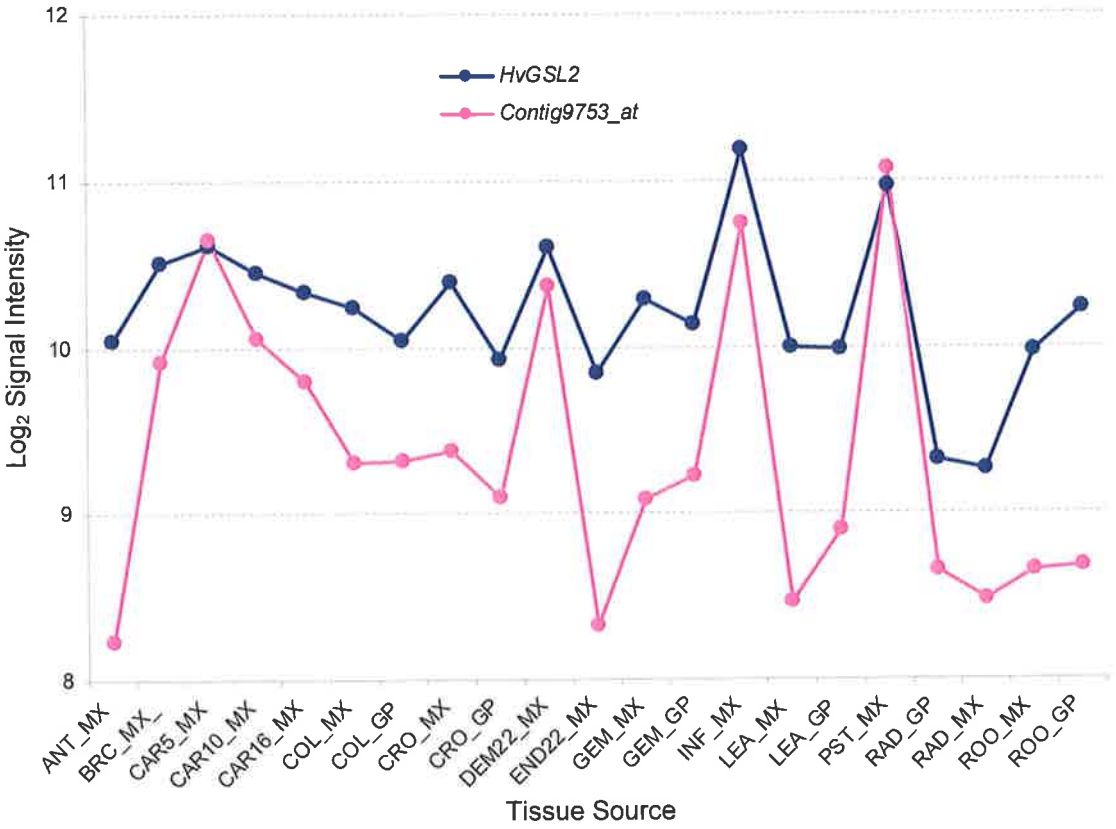

Figure 3.4: The normalised co-ordinate transcription of *HvGSL2* with Contig9753_at in 21 barley tissues. The Contig9753_at nucleotide sequence was compared to the NCBI sequence database and has high sequence identity to a gene encoding a DMC1 protein in barley. The tissue codes on the x-axis are explained in *Table 3.1*.

HvGSL3 (Contig19065_at)

Pearson Correlation		BLASTX of Microarray Contigs Against the NCBI database			
Contig	Corr.	Accession	E-value	Organism	Description
Contig19065_at	*1.00000*	NP_912480	6.00E-46	Rice	Putative glucan synthase
Contig14742_at	0.88806	AAP53972	5.00E-45	Rice	putative glucosyltransferase
Contig8596_at	0.86536	AAB86682	9.00E-03	*Takifugu rubripes*	unknown
Contig5731_at	0.86139	NP_912546	E-106	Rice	unknown protein
Contig10358_at	0.85980	NP_917454	E-116	Rice	putative telomere repeat binding factor
Contig6283_s_at	0.85757	XP_480370	E-107	Rice	unknown protein
Contig6587_s_at	0.85622	BAD27922	3.00E-57	Rice	harpin-induced protein-like
Contig5329_at	0.84426	XP_474420	6.00E-06	Rice	OSJNBa0088H09.16
Contig9030_at	0.83919	AAQ73746	1.30E+00	*Psittacid herpesvirus 1*	unknown
Contig10651_s_at	0.83537	AAP50957	e-109	Rice	Hypothetical protein
Contig5740_at	0.83266	NP_912844	E-155	Rice	unnamed protein product
Contig14345_at	0.83093	XP_463469	2.00E-61	Rice	secretory carrier membrane protein
Contig4804_at	0.82992	NP_912417	6.00E-48	Rice	Hypothetical protein
Contig3800_s_at	0.82135	AAN17457	E-155	Barley	hypersensitive-induced reaction protein 1
Contig6394_at	0.82068	AAP54864	0	Rice	protein kinase-like protein
Euclidean Cluster		**BLASTX of Microarray Contigs Against the NCBI database**			
Contig	Dist.	Accession	E-value	Organism	Description
Contig19065_at	*0.00000*	NP_912480	6.00E-46	Rice	Putative glucan synthase
Contig8596_at	1.28219	AAB86682	9.00E-03	*Takifugu rubripes*	unknown
Contig6283_s_at	1.28492	XP_480370	E-107	Rice	unknown protein
Contig9030_at	1.39384	AAQ73746	1.30E+00	*Psittacid herpesvirus 1*	unknown
Contig10651_s_at	1.39411	AAP50957	e-109	Rice	Hypothetical protein
Contig4804_at	1.39504	NP_912417	6.00E-48	Rice	Hypothetical protein
Contig14345_at	1.39961	XP_463469	2.00E-61	Rice	secretory carrier membrane protein
Contig4088_s_at	1.43980	AAP80854	2.00E-61	*Triticum aestivum*	autophagy
HF08O15r_at	1.45549	AAM64166	8.80E+00	Arabidopsis	cleavage stimulation factor 77
Contig6394_at	1.45980	AAP54864	0	Rice	protein kinase-like protein
Contig7289_at	1.48991	XP_483595	0.00E+00	Rice	ankyrin-like protein
Contig11098_at	1.49254	NP_912420	2.00E-24	Rice	Putative NAM (no apical meristem) protein
EBro03_SQ005_C24_s_at	1.50957	XP_477708	2.00E-14	Rice	unknown protein
EBro04_SQ002_K10_at	1.51224	XP_506991	1.00E-03	Rice	PREDICTED P0539D10.38 gene product
Contig10650_at	1.51651	AAP50957	4.00E-53	Rice	hypothetical protein
Contig5331_at	1.53354	XP_474420	e-102	Rice	OSJNBa0088H09.16
Contig21080_at	1.53426	AAS90676	2.00E-72	Rice	putative senescence-associated protein
Contig3801_at	1.53461	AAN17457	1.00E-71	Barley	hypersensitive-induced reaction protein 1
Contig7864_at	1.54310	XP_477708	6.00E-90	Rice	unknown protein
Contig26527_at	1.54693	XP_549745	3.9	*Canis familiaris*	PREDICTED: hypothetical protein XP_549745

Table 3.6: Genes represented on the Barley1 microarray that exhibit a similar transcription pattern to *HvGSL3* as determined by Pearson Correlation and Euclidean clustering. The contig sequences identified were compared to the proteins in the NCBI database. The best BLASTX matches for each contig are presented with the accession number, E-value, the organism the gene was identified in, as well as the description of each gene.

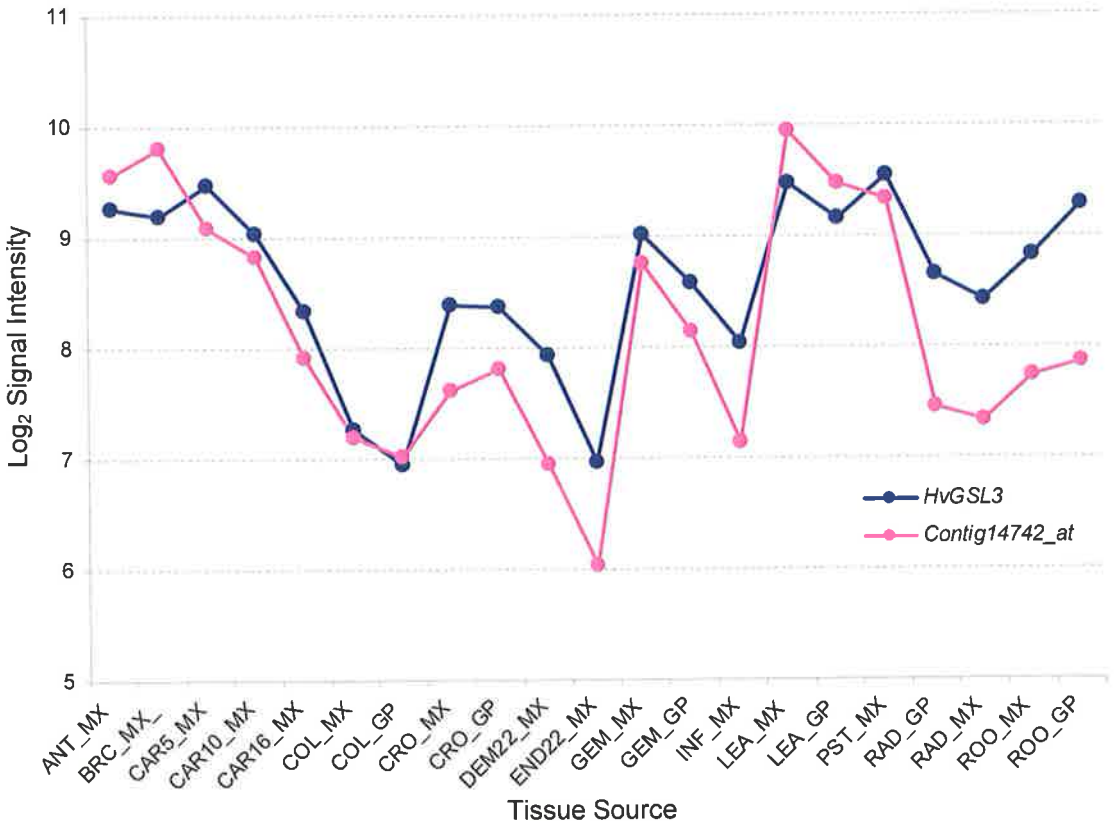

Figure 3.5: The normalised co-ordinate transcription of *HvGSL3* with Contig14742_at in 21 barley tissues. The Contig14742_at nucleotide sequence was compared to the NCBI sequence database and has a high sequence identity to a gene encoding a putative glucosyltransferase in barley. The tissue codes on the x-axis are explained in *Table 3.1*.

HvGSL4 (Contig13152_at)

Pearson Correlation		BLASTX of Microarray Contigs Against the NCBI database			
Contig	Corr.	Accession	E-value	Organism	Description
Conti13152_at	*1.00000*	XP_550490	0	Rice	putative beta 1,3 glucan synthase
Contig12671_at	0.91797	XP_473416	e-125	Rice	OSJNBb0034G17.7
Contig13757_at	0.90331	XP_479060	e-111	Rice	putative histone deacetylase
HD04E24u_at	0.90023	XP_463888	7.00E-30	Rice	APG5 (autophagy 5)-like protein
Contig11527_at	0.89935	EAL43212	3.00E-21	*Entamoeba histolytica*	hypothetical protein
Contig20812_at	0.89799	BAD52708	8.00E-44	Rice	zinc finger-like
Contig15918_at	0.89016	AAN18074	3.00E-20	Arabidopsis	At2g30580/T6B20.7
Contig8444_at	0.88469	XP_493852	2.00E-87	Rice	putative protein kinase
Contig22689_at	0.87585	AAC49734	6.00E-57	Arabidopsis	SABRE
Contig982_at	0.87542	XP_479104	e-168	Rice	Putative membrane protein
EBem08_SQ003_O18_at	0.87254	AAG51195	0.009	Arabidopsis	unknown protein
Contig12806_at	0.87164	AAW78347	e-142	*Zea mays*	target of rapamycin
Contig19550_at	0.87133	XP_480755	6.00E-54	Rice	putative sno protein
Contig11528_s_at	0.86896	AAA29616	9.00E-14	*Plasmodium lophurae*	histidine-rich protein
Contig18288_s_at	0.86531	XP_482865	3.00E-35	Rice	putative Hec1 protein
Contig23781_at	0.86460	AAB48193	2.00E-06	*Mus musculus*	ORFB
HB26D17r_x_at	0.86433	ZP_00318393	3.00E-04	*Microbulbifer degradans*	COG0328: Ribonuclease HI
Contig14270_s_at	0.86028				*No significant similarity found*

Euclidean Cluster		BLASTX of Microarray Contigs Against the NCBI database			
Contig	Dist.	Accession	E-value	Organism	Description
Conti13152_at	*0.00000*	XP_550490	0	Rice	putative beta 1,3 glucan synthase
Contig20812_at	0.63638	BAD52708	8.00E-44	Rice	zinc finger-like
HD04E24u_at	0.64153	XP_463888	7.00E-30	Rice	APG5 (autophagy 5)-like protein
Contig11528_s_at	0.71577	AAA29616	9.00E-14	*Plasmodium lophurae*	histidine-rich protein
Contig12671_at	0.73299	XP_473416	e-125	Rice	OSJNBb0034G17.7
Contig15918_at	0.74624	AAN18074	3.00E-20	Arabidopsis	At2g30580/T6B20.7
Contig9336_at	0.76462	AAN15388	6.00E-04	Arabidopsis	26S proteasome ATPase subunit
Contig22689_at	0.76892	AAC49734	6.00E-57	Arabidopsis	SABRE
Contig19550_at	0.77131	XP_480755	6.00E-54	Rice	putative sno protein
Contig11527_at	0.78481	EAL43212	3.00E-21	*Entamoeba histolytica*	hypothetical protein
Contig3066_at	0.78649	XP_481944	8.00E-54	Rice	putative CRS1
Contig847_at	0.79032	BAD33131	4.00E-14	Rice	hypothetical protein
Contig23781_at	0.79450	AAB48193	2.00E-06	*Mus musculus*	ORFB
HA06g08r_s_at	0.79829	XP_483762	3.00E-16	Rice	putative F1F0-ATPase inhibitor protein
Contig15885_at	0.80909	BAD53492	e-130	Rice	WD-40 repeat protein-like
HVSMEi0006J13r2_at	0.81197	BAD27978	0.47	Rice	putative calcium-transporting ATPase
Contig10352_at	0.82333	XP_470217	0.00E+00	Rice	Hypothetical protein
HVSMEb0004D21r2_at	0.82836	AAO60427	3.00E-10	*Gossypium hirsutum*	FPh1
		AAM29178	5.00E-08	*Triticum aestivum*	biostress-resistance-related protein
EBpi03_SQ001_N19_at	0.84525	ZP_00353474	6.00E-07	*Kineococcus radiotolerans*	hypothetical protein Krad07003195
Contig19657_at	0.84870	XP_466958	6.00E-14	Rice	ALG2-interacting protein X-like

Table 3.7: Genes represented on the Barley1 microarray that exhibit a similar transcription pattern to *HvGSL4* as determined by Pearson Correlation and Euclidean clustering. The contig sequences identified were compared to the proteins in the NCBI database. The best BLASTX matches for each contig are presented with the accession number, E-value, the organism the gene was identified in, as well as the description of each gene.

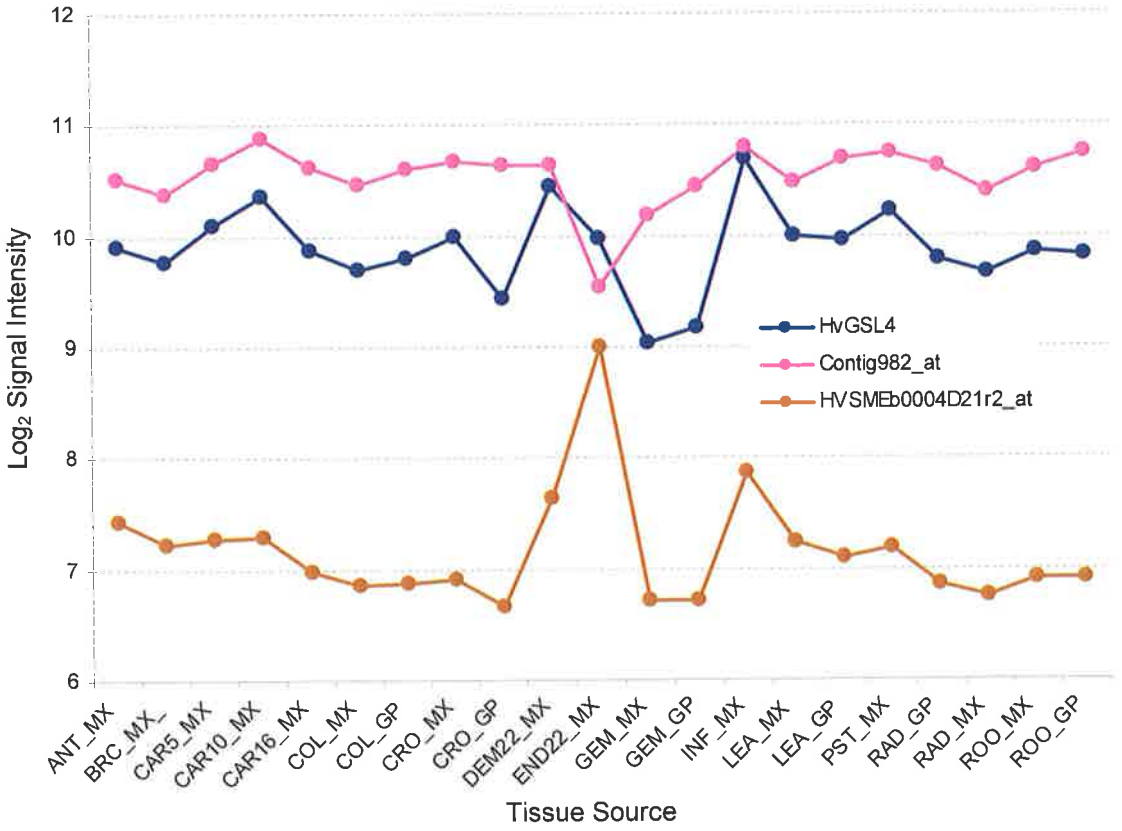

Figure 3.6: The normalised co-ordinate transcription of *HvGSL4* with Contig982_at and HVSMEb00004D21r2_at in 21 barley tissues. The nucleotide sequence of the co-ordinately transcribing genes were compared to the NCBI sequence database and Contig982_at was found to have a sequence similar to a gene encoding a putative membrane protein in barley, while HvSMEb0004D21r2_at had a similar sequence to a gene encoding a wheat bio-stress related protein. The tissue codes on the x-axis are explained in *Table 3.1*.

contigs that had high sequence identity to genes that encode putative membrane proteins and a biostress-resistance-related protein (*Figure 3.6*).

3.3.3 Q-PCR Analysis

HvGSL *Q-PCR Product Analysis*

The specificity of the primers was assessed prior to running the Q-PCR experiments, to ensure they only amplified the desired *HvGSL*. The *HvGSL* gene specific Q-PCR primer pairs (*Appendix A*) were used in RT-PCR to amplify a fragment from a cDNA population derived from a variety of barley plant tissues (*HvGSL1, HvGSL3*: pre-anthesis whole flower; *HvGSL2, HvGSL4, HvGSL6*: pooled embryo and scutellum tissue excised from grains that were imbibed for 24 hr and germinated for 8 hr; *HvGSL7, HvGSL8*: all ten tissues in the tissue series). An aliquot of the PCR product was separated on an agarose gel and only one band for each primer pair was observed. The remainder of the amplified product was cleaned, ligated into pGEM®-T Easy and transformed into competent *E. coli* cells. The fragment was sequenced from a plasmid DNA mini-preparation using the T7 and SP6 primers (*Appendix A*). The *HvGSL* gene-specific primers (*Appendix A*) and Q-PCR product sequences are presented in *Figure 3.7*. In every case, the gene specific primers amplified the correct product.

Normalisation of Q-PCR Data

To enable comparisons of *HvGSL* mRNA abundance levels in cDNA samples derived from different tissues, it was necessary to normalise the data using the genNorm program (Vandesompele *et al.*, 2002). The gene transcription data generated for each *HvGSL* gene was normalised with respect to stably transcribed control genes. The control genes were heat shock protein 70 (*HSP70*), cyclophilin, glyceraldehyde-3-phosphate dehydrogenase (*GAPDH*), cellulose synthase (*HvCesA1*) and α-tubulin, which are transcribed at relatively stable levels in a range of barley tissues (Bustin, 2000; Ozturk *et al.*, 2002; Burton *et al.*, 2004). An M-value, which is a measure of average transcription stability, was assigned to individual genes. A low M-value indicates good transcription stability and suitability as a control gene (Vandesompele *et al.*, 2002; Burton *et al.*, 2004).

HvGSL1

Q-PCR product size: 266 bp
Acquisition temperature: 78°C

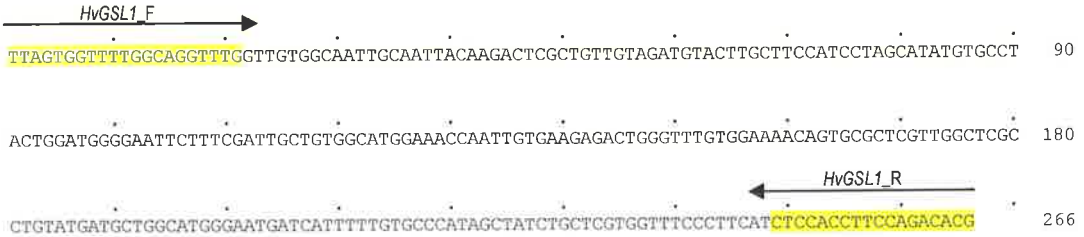

HvGSL2

Q-PCR product size: 188 bp
Acquisition temperature: 82°C

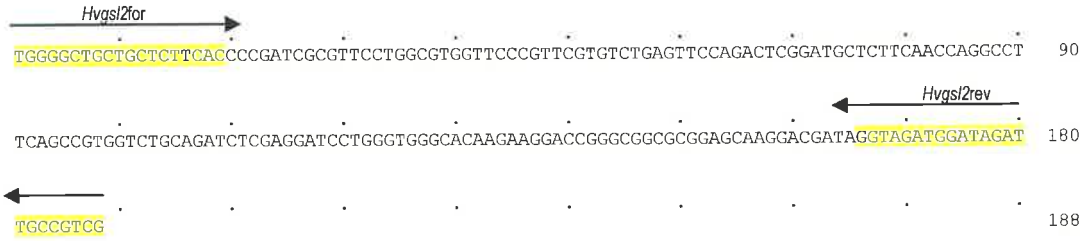

HvGSL3

Q-PCR product size: 125 bp
Acquisition temperature: 79°C

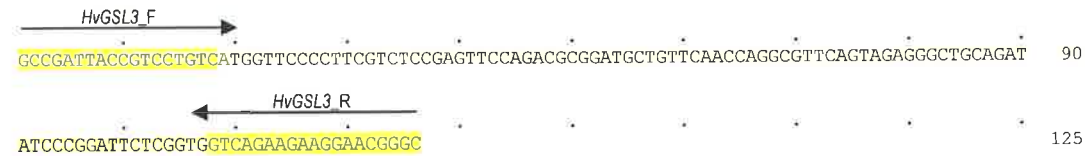

HvGSL4

Q-PCR product size: 140 bp
Acquisition temperature: 75°C

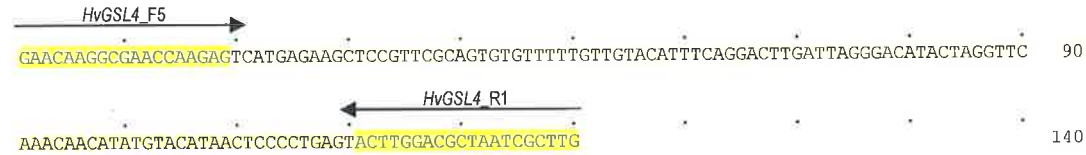

HvGSL6

Q-PCR product size: 208 bp
Acquisition temperature: 78°C

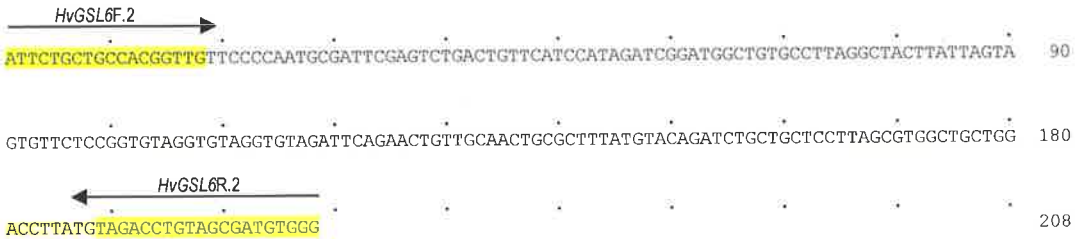

HvGSL7

Q-PCR product size: 295 bp
Acquisition temperature: 76°C

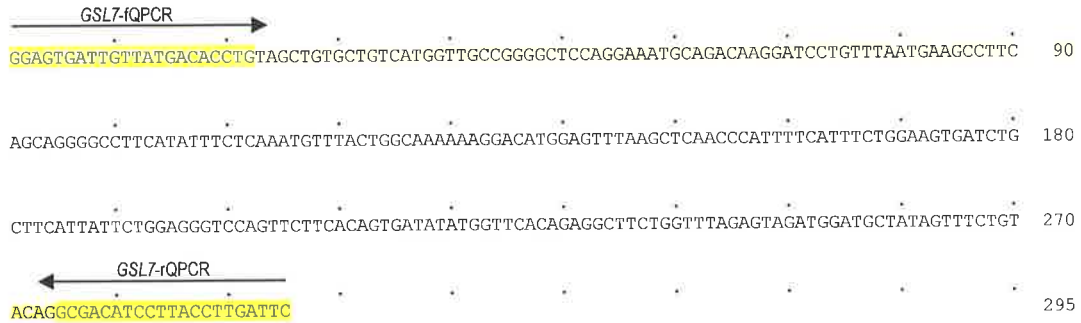

HvGSL8

Q-PCR product size: 287 bp
Acquisition temperature: 77°C

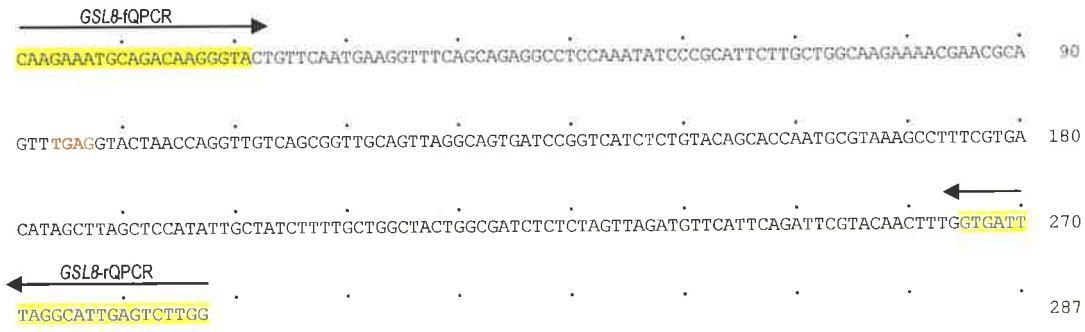

Figure 3.7: The gene-specific Q-PCR primers of *HvGSL*s, Q-PCR amplified products and the optimal temperature for data acquisition. Highlighted sequences indicate primer position, arrows indicate primer orientation. The sequence of each primer pair is given in *Appendix A*.

The normalisation factor (NF) was subsequently calculated for each cDNA population from the geometric mean of the most stably transcribed control genes (*Table 3.8*). The normalised transcription data for each *HvGSL* gene was calculated by dividing the raw transcription data by the normalisation factor. The most highly active metabolic tissues within the tissue series were frequently observed to have higher normalisation factors (*Table 3.8*). These highly active metabolic tissues were the root tip, the leaf base, floral tissue at anthesis and the three day stage of the developing grain (*Table 3.8*).

Transcript Profiling of HvGSL *Genes in a Range of Tissues*

To obtain information on the general transcription patterns of *HvGSL* genes throughout the plant, the mRNA abundance of each gene was determined in a wide variety of plant tissues. Furthermore, to identify the tissues that individual *HvGSL* genes had a maximum abundance of transcript, the normalised data (*Figure 3.8.A*) were presented as a percent of the maximum of normalised transcription (*Figure 3.8.B*). It was observed that the individual *HvGSL* genes were frequently transcribed at levels that were at least 20% of the maximum transcript level (*Figure 3.8.B*). Overall, *HvGSL* transcript levels were highest in early floral tissues (*HvGSL4*, *HvGSL6* and *HvGSL7*), the first leaf tip (*HvGSL1*, *HvGSL3* and *HvGSL8*) and the first leaf base (*HvGSL2*; *Figure 3.8.B*).

Transcript Profiling of HvGSL *Genes in Leaf Tissue*

The mRNA transcript levels of *HvGSL* genes in various segments along the first leaf of a seven day old barley seedling (*Table 3.2*) were analysed using Q-PCR (*Figure 3.9*). Leaf-E was the region of cellular division (Sharman, 1942), Leaf-D was the region of cell elongation, where Leaf-C, Leaf-B and Leaf-A are regions of cell maturation (Burton *et al.*, 2004).

There were three obvious patterns of *HvGSL* gene transcription in the leaf regions analysed by Q-PCR (*Figure 3.9.B*; *Figure 3.9.C*; *Figure 3.9.D*). The gene transcription pattern of *HvGSL1* and *HvGSL4* were highly comparable, with a

Tissue	Control Genes	NF
First leaf tip	Cyclophilin, GAPDH, a-tubulin	0.24
First leaf base	Cyclophilin, GAPDH, a-tubulin	1.55
Root tip	Cyclophilin, GAPDH, a-tubulin	2.66
Root m/zone	Cyclophilin, GAPDH, a-tubulin	0.49
Floral early	Cyclophilin, GAPDH, a-tubulin	1.79
Floral anthesis	Cyclophilin, GAPDH, a-tubulin	2.57
Developing grain (3 days)	Cyclophilin, GAPDH, a-tubulin	3.18
Developing grain (13 days)	Cyclophilin, GAPDH, a-tubulin	0.12
Coleoptile (3 days)	Cyclophilin, GAPDH, a-tubulin	1.40
Stem	Cyclophilin, GAPDH, a-tubulin	0.84
Leaf E (base)	Cyclophilin, GAPDH, HSP70	3.15
Leaf D	Cyclophilin, GAPDH, HSP70	0.92
Leaf C	Cyclophilin, GAPDH, HSP70	0.72
Leaf B	Cyclophilin, GAPDH, HSP70	0.54
Leaf A (tip)	Cyclophilin, GAPDH, HSP70	0.89
Root 4 (m/zone)	Cyclophilin, CesA1, a-tubulin	0.32
Root 3	Cyclophilin, CesA1, a-tubulin	0.91
Root 2	Cyclophilin, CesA1, a-tubulin	0.76
Root 1 (tip)	Cyclophilin, CesA1, a-tubulin	4.56
Developing Endosperm (2 days)	Cyclophilin, a-tubulin, ELF1	0.49
Developing Endosperm (3 days)	Cyclophilin, a-tubulin, ELF1	1.25
Developing Endosperm (4 days)	Cyclophilin, a-tubulin, ELF1	1.88
Developing Endosperm (5 days)	Cyclophilin, a-tubulin, ELF1	0.57
Developing Endosperm (6 days)	Cyclophilin, a-tubulin, ELF1	5.11
Developing Endosperm (7 days)	Cyclophilin, a-tubulin, ELF1	3.34
Developing Endosperm (8 days)	Cyclophilin, a-tubulin, ELF1	0.28
Developing Endosperm (9 days)	Cyclophilin, a-tubulin, ELF1	0.65
Developing Endosperm (10 days)	Cyclophilin, a-tubulin, ELF1	0.95
Developing Endosperm (11 days)	Cyclophilin, a-tubulin, ELF1	0.53
Uninfected epidermis (0 hr)	Cyclophilin, GAPDH, a-tubulin	0.67
Uninfected epidermis (4 hr)	Cyclophilin, GAPDH, a-tubulin	0.86
Uninfected epidermis (8 hr)	Cyclophilin, GAPDH, a-tubulin	0.80
Uninfected epidermis (12 hr)	Cyclophilin, GAPDH, a-tubulin	1.32
Uninfected epidermis (16 hr)	Cyclophilin, GAPDH, a-tubulin	0.53
Uninfected epidermis (20 hr)	Cyclophilin, GAPDH, a-tubulin	0.96
Uninfected epidermis (24 hr)	Cyclophilin, GAPDH, a-tubulin	0.64
Infected epidermis (4 hr)	Cyclophilin, GAPDH, a-tubulin	2.18
Infected epidermis (8 hr)	Cyclophilin, GAPDH, a-tubulin	1.04
Infected epidermis (12 hr)	Cyclophilin, GAPDH, a-tubulin	1.60
Infected epidermis (16 hr)	Cyclophilin, GAPDH, a-tubulin	1.27
Infected epidermis (20 hr)	Cyclophilin, GAPDH, a-tubulin	0.74
Infected epidermis (24 hr)	Cyclophilin, GAPDH, a-tubulin	1.47

Table 3.8: Normalisation factors calculated by geNorm for each cDNA based on the combination of the three best control genes.

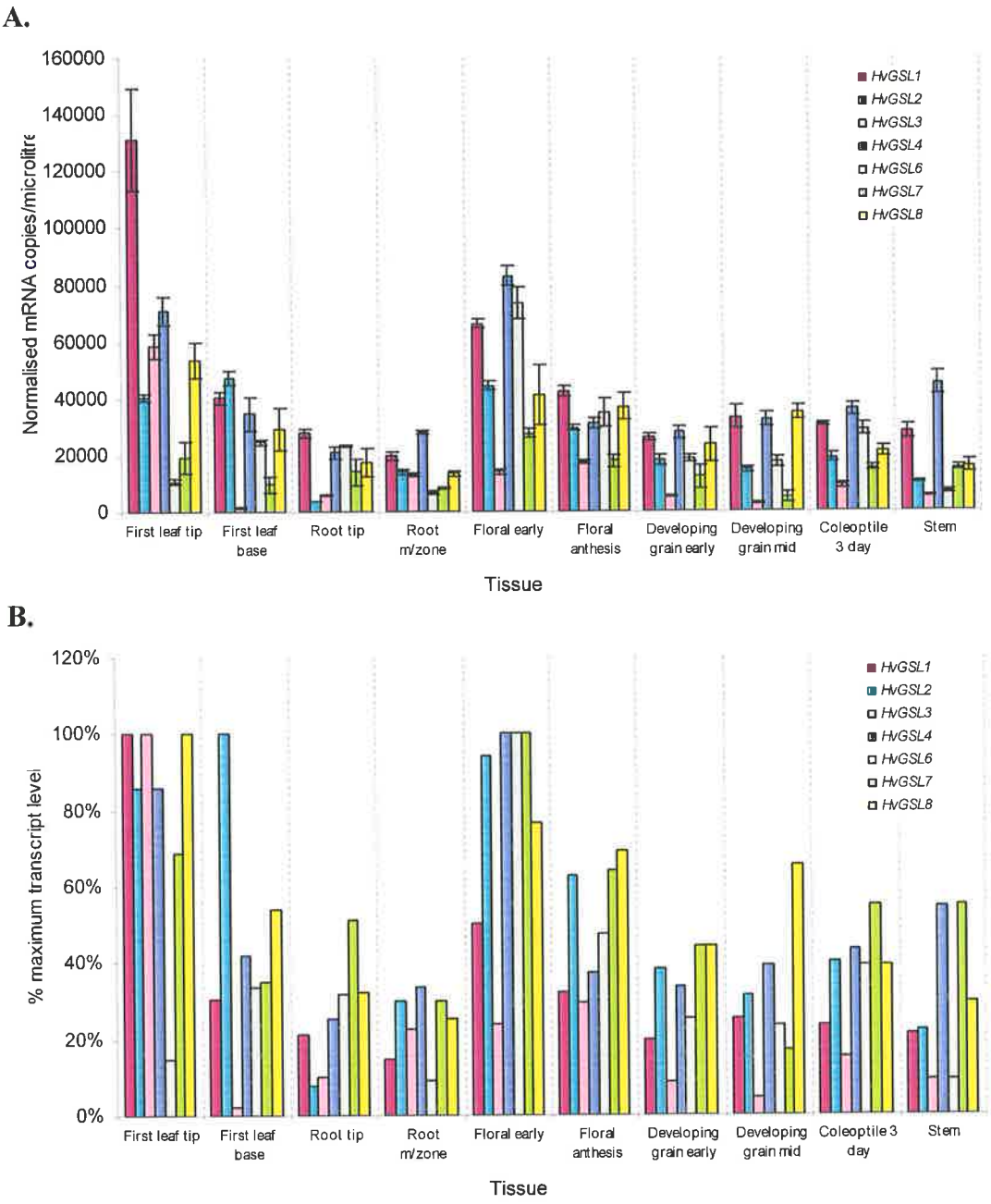

Figure 3.8: Normalised transcription levels of *HvGSL* genes in a variety of tissues. A: Normalised transcription levels of *HvGSL* genes are presented as number of copies per microliter of cDNA. B: Normalised transcription of *HvGSL* genes in a variety of tissues, displayed as the percent maximum of normalised transcription.

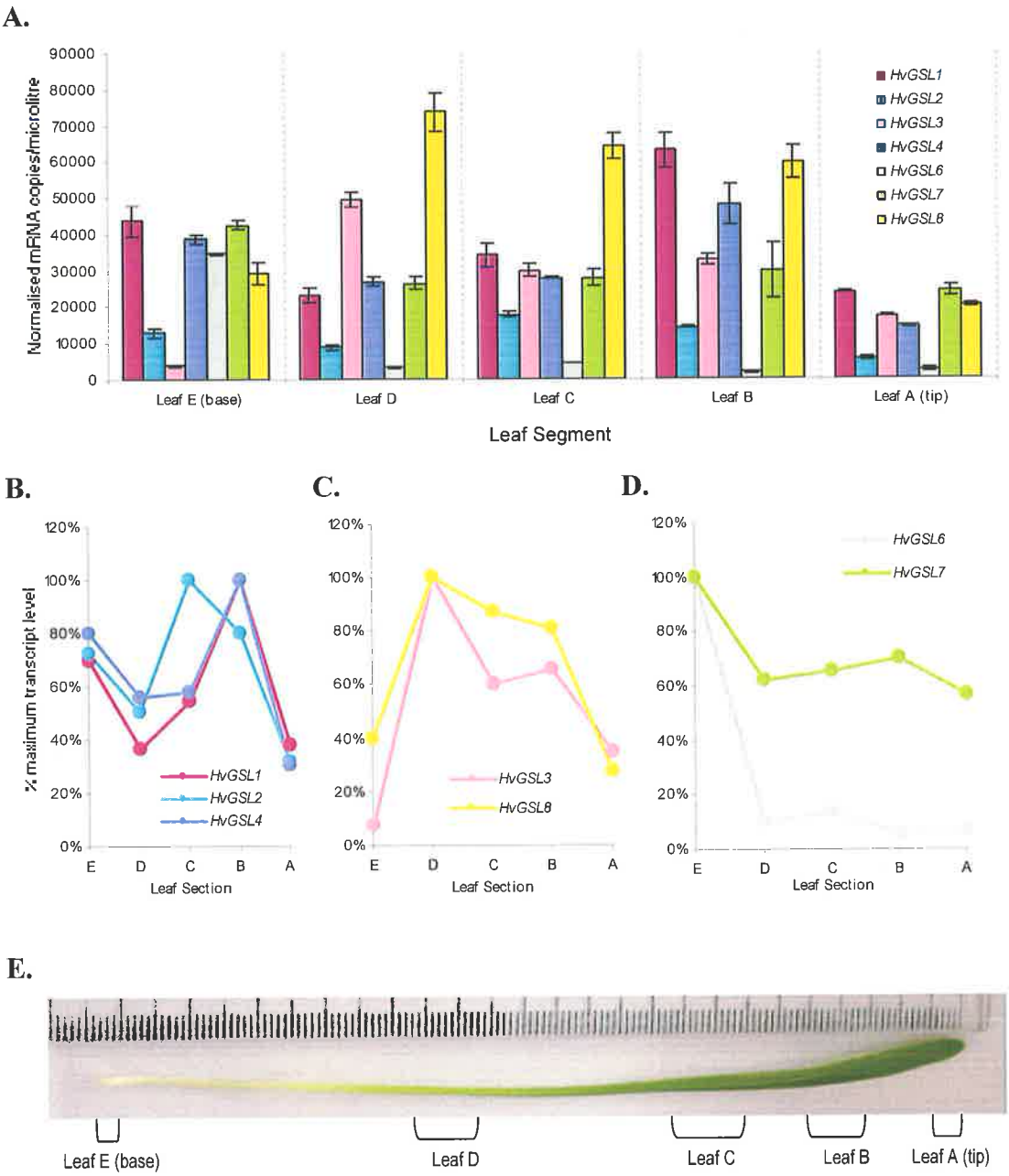

Figure 3.9: Normalised mRNA transcript levels for barley *HvGSL* genes in segments of 13 cm first leaves. A: Normalised transcription levels of mRNA are presented as number of copies per microliter of cDNA. B, C and D: Levels of *HvGSL* mRNA in leaf segments, expressed as a percent of maximum transcript levels of each gene. *HvGSL*s were grouped on the basis of gene transcription pattern. E: Regions of leaf tissue used for the isolation of mRNA for Q-PCR analysis of transcript level (Burton *et al.*, 2004).

maximum transcript abundance of both genes in the region just below the leaf tip (*Figure 3.9.B*; *Figure 3.9.E*). The level of *HvGSL2* transcript was two to three-fold lower than that of *HvGSL1* and *HvGSL4* (*Figure 3.9.A*), and it also differed by showing maximal transcription in Leaf-C (*Figure 3.9.B*; *Figure 3.9.E*). However, *HvGSL2* had similarities in the pattern of transcription to *HvGSL1* and *HvGSL4* in the Leaf-E, Leaf- D and Leaf-A regions (*Figure 3.9.B*; *Figure 3.9.E*).

It was observed that the gene transcription profile of *HvGSL3* and *HvGSL8* in the leaf sections were comparable (*Figure 3.9.C*). The abundance of transcript is below 40% of the maximal level in the Leaf-E (base) and Leaf-A (tip), with maximum transcription in the region of Leaf-D (*Figure 3.9.C*; *Figure 3.9.E*). The transcription of *HvGSL8* in the leaf segments was the highest of all *HvGSL* genes that were analysed (*Figure 3.9.A*).

The transcript profiles of *HvGSL6* and *HvGSL7* in the leaf segments were comparable, as both *HvGSL6* and *HvGSL7* are transcribed at a maximum in the Leaf-E (base) segment (*Figure 3.9.D*; *Figure 3.9.E*). The transcript levels remain relatively constant in the other segments along the leaf, at approximately 10% of maximum normalised transcript level for *HvGSL6*, and at approximately 60% of maximum transcript level *HvGSL7* (*Figure 3.9.D*).

Transcript Profiling of HvGSL *Genes in Root Tissue*

The transcription of *HvGSL* genes was analysed by Q-PCR in a variety of segments along the root of a 5 day old barley seedling. The root meristematic cells were located at the root tip in segment Root-1, while the more mature cells were located in segment Root 4 (Sharman, 1942).

As with the transcript analysis in the leaf tissue (*Figure 3.9*), there appeared to be three general patterns of *HvGSL* transcription in the root tissue series (*Figure 3.10*). There were similarities in transcription patterns between *HvGSL1* and *HvGSL2* (*Figure 3.10.B*), although the normalised levels of *HvGSL1* transcripts were much

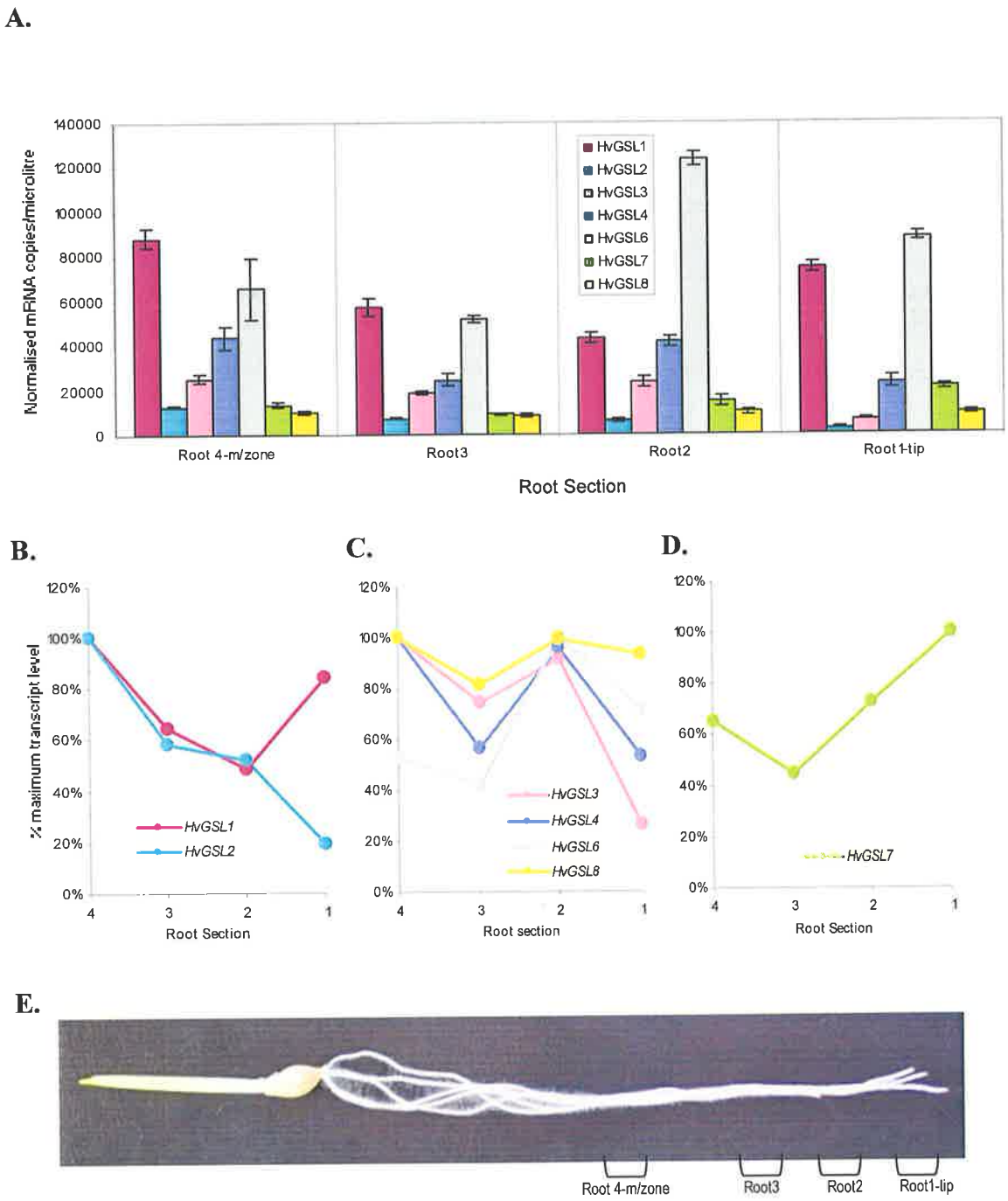

Figure 3.10: Normalised mRNA transcript levels for barley *HvGSL* genes in root segments. A: Normalised transcription levels of mRNA are presented as number of copies per microliter of cDNA. B, C, D: Levels of *HvGSL* mRNA in root segments, expressed as a percent of maximum transcript levels of each gene. E: Regions of toot tissue used for the isolation of mRNA for Q-PCR analysis of transcript level.

greater than those of *HvGSL2* (*Figure 3.10.A*). There is maximal transcription in the mature root and decreasing amounts in the regions Root-3 and Root-2 (*Figure 3.10.B*). It was observed that in the root tip, *HvGSL1* was transcribed at greater than 80% of the maximum transcript level, while *HvGSL2* was transcribed at only 20% of the maximum transcript level (*Figure 3.10.B*).

Another pattern of gene transcription was displayed by *HvGSL3*, *HvGSL4*, *HvGSL6* and *HvGSL8* in most segments (*Figure 3.10.C*). These genes were all maximally transcribed in the mature root zone, with the exception of *HvGSL6*, which was transcribed at 53% of the maximal transcription (*Figure 3.10.C*). There was decreased transcription of each of these genes in the Root-3 segment, the transcription was then at a near-maximum in the Root-2 segment and decreased transcription in the root tip (*Figure 3.10.C*). It was observed that *HvGSL6* was transcribed at the highest level in the root tip (cell division) and just below the root tip (cell elongation), where maximal transcription was observed (*Figure 3.10.A*).

The *HvGSL7* transcript profile in the root segments was clearly distinguishable from the other *HvGSL* genes (*Figure 3.10.D*).

Transcript Profiling of HvGSL *Genes in the Developing Endosperm*

The transcription of *HvGSL* genes was analysed by Q-PCR in the developing endosperm, which was collected daily from the second day after pollination. The *HvGSL* genes were maximally transcribed between the second and fourth days after pollination, but thereafter the transcription levels decreased significantly between day 5 and day 6 where levels remain relatively constant for the remainder of the tissue series (*Figure 3.11.B*; *Figure 3.11.C*). The transcription of *HvGSL6* was maximal on the fifth day after pollination at approximately 1.6 x 10^6 normalised mRNA copies per microliter, which is at least ten times higher than any other *HvGSL* in any of the tissues analysed by Q-PCR (*Figure 3.11.A*; *Figure 3.11.D*). Transcript patterns of *HvGSL1*, *HvGSL2*, *HvGSL4*, *HvGSL7* and *HvGSL8* were tightly overlapped during the first six days of endosperm development (*Figure 3.11.B*).

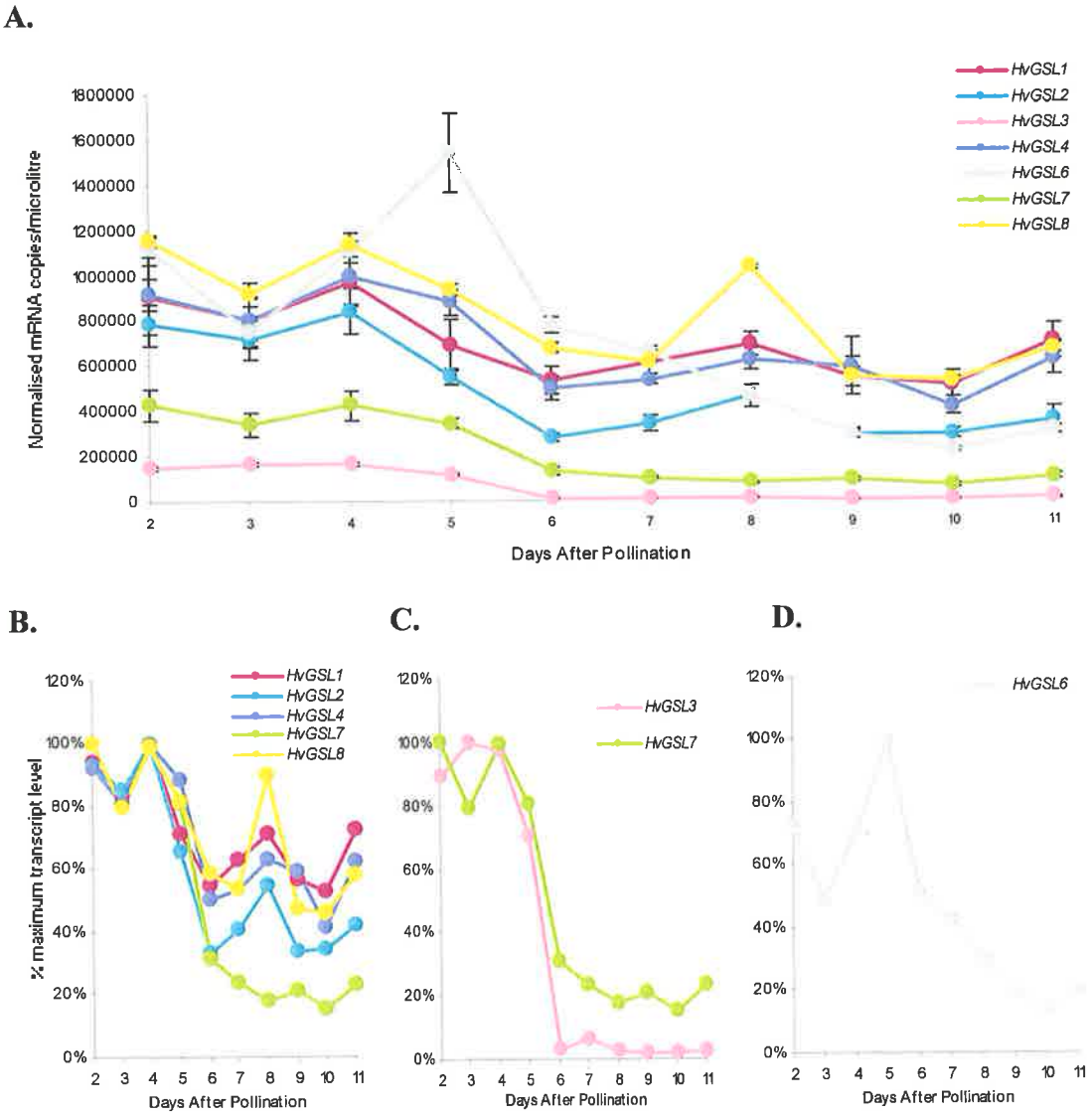

Figure 3.11: Normalised mRNA transcript level of *HvGSL* genes during the early stages of endosperm development in barley. A: Normalised transcription of *HvGSL* genes during the early stages of development, presented as number of transcript copies per microliter. B, C and D: The *HvGSL* genes were grouped based on transcription profile.

HvGSL3 had the lowest level of transcription of all *HvGSL* genes in the developing endosperm (*Figure 3.11.A*). From day six after pollination to day 11, *HvGSL3* gene transcription was below 6% of the maximal transcript level (*Figure 3.11.C*).

Transcript Profiling of HvGSL *Genes in Infected Leaf Tissue*

The transcription of *HvGSL* genes in barley epidermal tissue of uninfected leaves and *B. graminis* infected barley leaves were analysed by Q-PCR. The epidermal tissues from infected and uninfected leaves were collected every 4 hr for 24 hr. The *HvGSL* gene transcription pattern in response to *B. graminis* infection was compared to the uninfected control and subsequently placed into three groups (*Figure 3.12*; *Figure 3.13*; *Figure 3.14*).

In the first group, the observed transcription patterns of *HvGSL1*, *HvGSL4* and *HvGSL6* in *B. graminis* infected barley epidermal tissue were comparable to the uninfected control (*Figure 3.12*). The transcription profile of *HvGSL1* in infected barley epidermis is similar to the uninfected control during the first 16 hr of infection (*Figure 3.12.A*). Between 16 hr and 24 hr, *HvGSL1* gene transcription in the infected tissue decreases from 8×10^4 to 5×10^4 normalised mRNA copies per microliter, while in the uninfected control *HvGSL1* gene transcription increases from 6.5×10^4 to 9×10^4 normalised mRNA copies per microliter (*Figure 3.12.A*). The *HvGSL4* gene transcription profile in the infected tissue remained at approximately 1×10^5 normalised mRNA copies per microliter and the values were similar in the uninfected control at 4 hr, 8 hr, 12 hr and 20 hr (*Figure 3.12.B*). The transcription pattern of *HvGSL6* in the infected tissue followed a similar pattern to that observed in the uninfected control, with the transcription level in both samples consistently below 5000 normalised mRNA copies per microliter (*Figure 3.12.C*).

In the second group, transcript abundance was lower in infected leaves. Thus, between 12 hr and 24 hr, the gene transcription level of *HvGSL2*, *HvGSL3* and *HvGSL8* were lower in *B. graminis* infected barley epidermal tissue when compared with the uninfected control (*Figure 3.13*).

A.

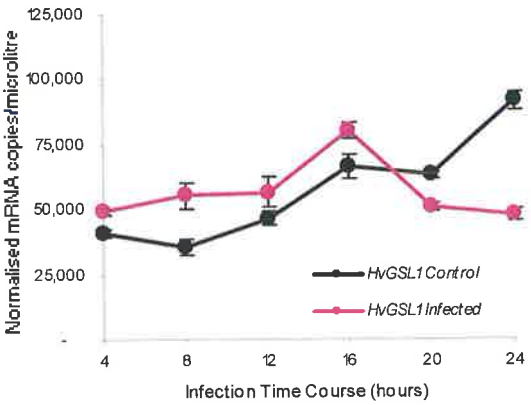

B.

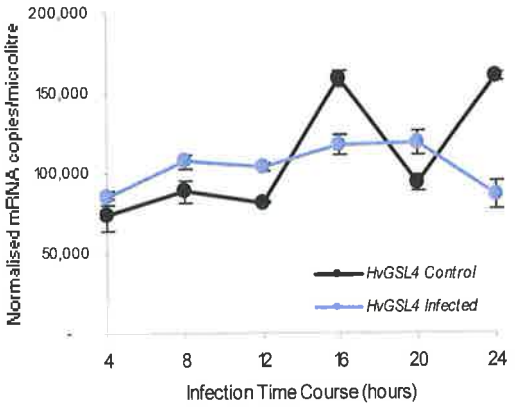

C.

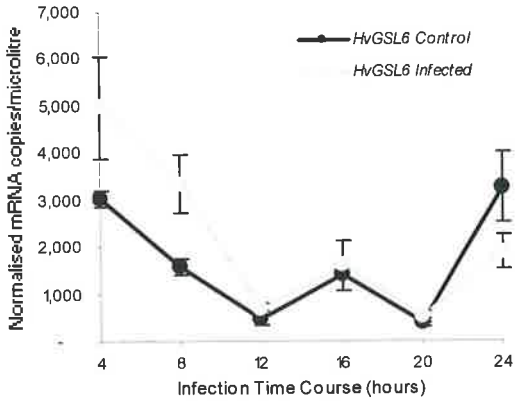

Figure 3.12: The transcription of *HvGSL1* (A), *HvGSL4* (B) and *HvGSL6* (C) in barley epidermal tissue in response to *B. graminis* infection. The transcription profiles of these genes in response to fungal attack are similar to that of the uninfected control.

A.

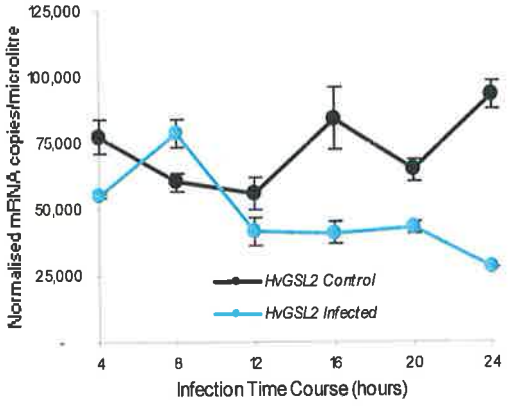

B.

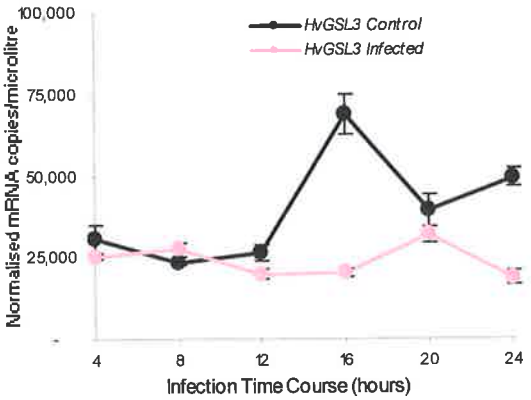

C.

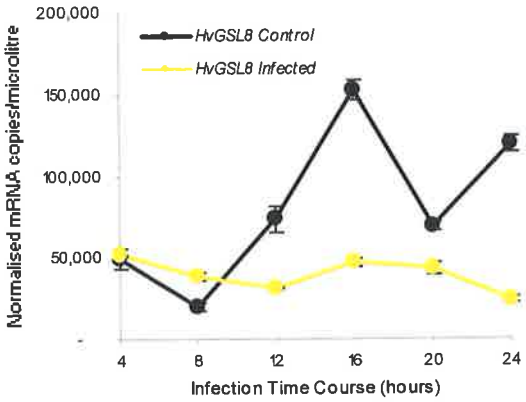

Figure 3.13: The decreased transcription level of *HvGSL2* (A), *HvGSL3* (B) and *HvGSL8* (C) in barley epidermal tissue in response to *B. graminis* infection. The transcription levels of these genes in response to fungal attack are lower than the uninfected control between 12 hr and 24 hr.

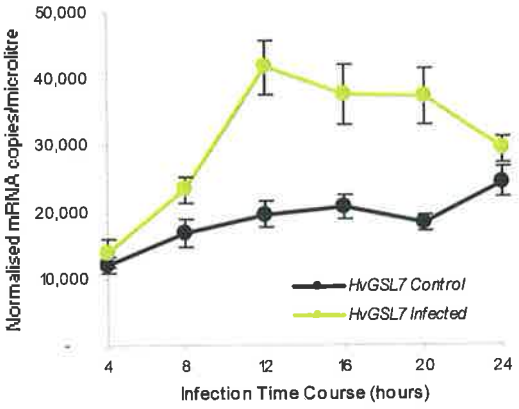

Figure 3.14: The increase of *HvGSL7* gene transcription in barley epidermal tissue in response to *B. graminis* infection.

	HvGSL1	*HvGSL2*	*HvGSL3*	*HvGSL4*	*HvGSL6*	*HvGSL7*	*HvGSL8*
HvGSL1	1.00						
HvGSL2	0.61	1.00					
HvGSL3	0.62	0.66	1.00				
HvGSL4	0.81	0.69	0.71	1.00			
HvGSL6	0.68	0.46	0.45	0.75	1.00		
HvGSL7	0.62	0.37	0.50	0.71	0.77	1.00	
HvGSL8	0.60	0.68	0.69	0.56	0.46	0.16	1.00

Table 3.9: Pearson correlation of *HvGSL* Q-PCR transcription data including all tissues analysed by Q-PCR. The correlation was performed using the percent maximum normalised transcription profiles of each tissue series.

In the third group, represented by *HvGSL7*, transcription in the *B. graminis* infected barley epidermal tissue was at consistently greater levels compared with the uninfected control (*Figure 3.14*). It was observed that the level of *HvGSL7* gene transcription increased approximately four fold between 4 hr and 12 hr in the infected tissue (*Figure 3.14*). Between 12 hr and 24 hr, the transcription of *HvGSL7* in the infected tissue was between 4.5 x 10^4 and 3 x 10^4 normalised mRNA copies per microliter, while in the uninfected control *HvGSL7* transcription levels were consistently lower between 2 x 10^4 and 2.5 x 10^4 normalised mRNA copies per microliter (*Figure 3.14*).

3.3.4 Co-ordinate Transcription of *HvGSL* Genes

All of the Q-PCR transcription analysis data was correlated with the Pearson coefficient to determine if there were co-ordinately transcribed *HvGSL* genes across all tissues in the Q-PCR experiments. As in the analysis of the microarray data (*Figure 3.2.B*), the two *HvGSL* genes that had the most similar transcription pattern in the Q-PCR data were *HvGSL1* and *HvGSL4* (0.81 correlated; *Table 3.9*). There were 14 pairs of *HvGSL* genes with transcription patterns that were correlated at greater than 0.60 and seven pairs of *HvGSL* genes with transcription patterns that were correlated at less than 0.60 (*Table 3.9*). The *HvGSL* pair with the lowest transcription pattern correlation was *HvGSL7* and *HvGSL8* (0.16; *Table 3.9*).

3.4 DISCUSSION

It is likely that specific members of the *GSL* gene family in plants are required for the specific synthesis and deposition of (1,3)-β-D-glucan at different developmental stages and in response to various biotic and abiotic stresses (*Chapter 1*). There is some evidence that regulation of (1,3)-β-D-glucan deposition in plants, at least in part, occurs *via* the activation of the (1,3)-β-D-glucan synthases with Ca^{2+} (*Section 1.4.1.2*) and signal transducers such as GTP-binding proteins (*Section 1.4.1.3*), but the extent of control of (1,3)-β-D-glucan deposition at the transcriptional level of gene expression is currently uncertain. The aim of the work described in this Chapter was to characterise individual members of the *HvGSL* gene family according to tissues in which the genes are transcribed. There was particular interest in the identification of the *AtGSL5* orthologue in barley because of its potential role in disease resistance (Jacobs *et al.*, 2003).

The analysis of *HvGSL* transcription patterns provides potentially useful information regarding gene function. For example, the correlation of *HvGSL* transcription patterns with tissues where known processes involving (1,3)-β-D-glucan are occurring, allows hypotheses to be formed on prospective functions of the individual *HvGSL* genes. The analysis of transcriptional activity may identify multiple members of the *HvGSL* gene family that could participate in a single process, through the observation of tightly coordinated transcription patterns. The correlation of transcription patterns of *HvGSL* genes with the transcription patterns of other genes also has potential to provide useful information about biological processes. For example, if a gene co-ordinately transcribed with an *HvGSL* gene is known to function in a specific cellular process, then a hypothesis on *HvGSL* gene function may be formed. Alternatively, if the gene co-ordinately transcribed with an *HvGSL* gene resembles a possible subunit of an active (1,3)-β-D-glucan synthase protein complex, then insights on the mechanism of (1,3)-β-D-glucan synthesis may be gained.

The analysis of *HvGSL* gene transcription was initially attempted by investigating the tissue origin of barley *HvGSL* ESTs. Due to the large variety of tissue sources and

the uneven distribution of ESTs among the *HvGSL* genes, it was apparent that the tissues needed to be broadly grouped (*Figure 3.1*). It was observed that ESTs corresponding to *HvGSL2* were the most abundant in the databases, particularly in leaf tissue (*Figure 3.1*), and this implies that *HvGSL2* mRNA was the most abundant *HvGSL* in the leaf tissues used to generate the EST libraries. However, this analysis was not sufficiently precise for the determination of individual *HvGSL* gene function. Thus, the transcription of *HvGSL* genes was subsequently investigated through microarray chip analysis and Q-PCR.

The analysis of microarray datasets has proven useful for the identification of genes implicated in cell wall biosynthesis (Persson *et al.*, 2005). The Barley1 Chip (Affymetrix) microarray reference data were therefore analysed to identify genes that may be co-ordinately transcribed with the *HvGSL* genes. There are many ways to analyse microarray data, including regression analysis (Persson *et al.*, 2005) and cluster analysis (Kaminski and Friedman, 2002), both of which identify genes that behave similarly across a range of conditions. Cluster analyses are based on the assumption that genes with similar transcription patterns may also have common regulatory elements or may be involved in co-regulated response pathways (Kaminski and Friedman, 2002).

It was observed that the *HvGSL* microarray transcription patterns often correlated with genes that have no known role in cellular processes requiring the synthesis or deposition of (1,3)-β-D-glucan (*Table 3.4*; *Table 3.5*; *Table 3.6*; *Table 3.7*). Furthermore, only four *HvGSL* genes out of the eight genes identified here were represented by contigs on the Barley1 Chip. Thus, it is possible that other barley genes not used in the construction of the Barley1 Chip are correlated with *HvGSL* transcription patterns, but these correlations would not be detected. The limitations to microarray analysis may be partly overcome by further investigation of *HvGSL* gene activation, using other transcript analysis platforms.

The transcription patterns of the *HvGSL1*, *HvGSL2*, *HvGSL3* and *HvGSL4* genes, as measured on the barley microarray, were further investigated by cluster analysis to

determine if any genes related to processes involving (1,3)-β-D-glucan could be identified. No genes co-ordinately transcribed with *HvGSL1* were involved in cellular processes that are known to require the deposition of (1,3)-β-D-glucan (*Table 3.4*).

Correlation of HvGSL2 *Transcription with a Barley* DMC1 *Gene*

The transcription pattern of the *HvGSL2* gene was similar to a contig that had an exact sequence match to a barley *DMC1* gene (*Table 3.5*; *Figure 3.4*). DMC1 is a meiosis specific protein that is required for recombination (Leipe *et al.*, 2000). The deposition of (1,3)-β-D-glucan is known to occur between microspores following meiotic division during microsporogenesis (Stone and Clarke, 1992). Evidence that *HvGSL2* could be responsible for (1,3)-β-D-glucan deposition in meiotic division was obtained through the analysis of the Q-PCR data, where a near-maximum normalised *HvGSL2* gene transcript level was observed in early floral tissue, which contain meiotic cells (*Figure 3.8*). However, the involvement of *HvGSL2* in the deposition of (1,3)-β-D-glucan during meiotic events will remain speculative until further experiments are conducted, including targeted silencing of the barley *HvGSL2* gene, or of the orthologous *AtGSL12* gene in Arabidopsis (*Table 2.5*), to determine if disruption of *HvGSL2* function results in meiotic arrest.

Correlation of HvGSL3 *Transcription with an Ankyrin-Like Gene*

Many of the contigs on the Barley1 Chip that had similar transcription patterns to *HvGSL* genes also had high sequence identities with genes known to be transcribed throughout the plant, including protein kinases, DNA-binding proteins, salt channels and unknown or hypothetical proteins. However, some genes that appeared to be co-ordinately transcribed with the *HvGSL3* gene. The microarray data showed that the *HvGSL3* gene is co-ordinately transcribed with a contig that has high sequence identity to a rice gene encoding an ankyrin-like protein (*Table 3.6*). The members of the ankyrin gene family are known to constitute a group of intracellular adaptor proteins that target proteins to specialised domains of the plasma membrane and endoplasmic reticulum (Bennett and Baines, 2001). It is therefore possible that

ankyrin proteins localise the subunits of the active (1,3)-β-D-glucan synthase complex, such as the UDP-glucose binding protein (*Section 1.4.1.1*), to a region of the plasma membrane adjacent to where (1,3)-β-D-glucan is to be deposited. However, the involvement of the ankyrin-like proteins in the assembly of the active (1,3)-β-D-glucan synthase complex remains speculative, and further experiments are required to test this hypothesis.

Correlation of HvGSL3 *Transcription with a Putative Glucosyltransferase Gene*

In addition to the transcription pattern correlation between the ankyrin-like gene and the *HvGSL3* gene, another contig, which had a high sequence identity to a putative glucosyltransferase, was also observed to be highly correlated with the transcription pattern of *HvGSL3* (*Table 3.6*; *Figure 3.5*). Although it is not confirmed, the HvGSL3 protein and the putative glucosyltransferase (the latter is not yet assigned to a glycosyltransferase family) might operate together in an active (1,3)-β-D-glucan synthesising complex. Experiments to further assess the interactions of plant GSLs with UDP-glucose binding proteins, may now be designed and may include yeast two hybrid analyses. Additional experiments could also assess the apparent co-ordinate transcription of the *HvGSL3* and the putative glucosyltransferase gene, which may include *in situ* hybridisation of mRNA to determine if the two genes are transcribed in the same cell types.

Correlation of HvGSL4 *Transcription with a Bio-Stress Related Gene*

The analysis of the microarray data also detected the co-ordinate transcription of the *HvGSL4* gene with a contig that encoded a deduced protein with high amino acid sequence identity to a wheat "bio-stress related" protein from the NCBI database (*Table 3.7*; *Figure 3.6*). However, the relationship of the HvGSL4 protein with the bio-stress related protein is not known and very little information is available on the wheat bio-stress related protein itself (accession number: AAM29178), except that it was identified from a cDNA library of a wheat-*Thinopyrum intermedium* translocation line HW642 with resistance to barley yellow dwarf virus (BYDV). Barley yellow dwarf virus is transmitted by aphids and the earliest symptom of

infection is leaf discoloration (Bruehl, 1961). To prevent the establishment of a systematic infection by viral particles, such as BYDV, plants respond by decreasing the size exclusion limit of the plasmodesmata, hindering cell-to-cell movement of viruses (Allison and Shalla, 1974). The change in the size limit is controlled by the deposition and removal of (1,3)-β-D-glucan (*Section 1.2.2.2*). At present the link between the transcription of *HvGSL4* and plasmodesmatal closure due to (1,3)-β-D-glucan deposition is highly tentative, and there is no published link between the transcription of any other plant *GSL* and plasmodesmatal closure. Thus, Q-PCR could be conducted to determine the level of *HvGSL* gene transcription levels in barley tissues infected with BYDV. The transcription analysis could be coupled with aniline blue fluorochrome staining of (1,3)-β-D-glucan deposits in plasmodesmatal pores of infected leaves.

Another transcript profiling procedure used here was Q-PCR. As with all transcript analyses, the abundance of a *HvGSL* transcript may be a good indicator of the extent at which the gene is transcribed, but it does not necessarily reflect the presence or levels of an active protein complex that is synthesising (1,3)-β-D-glucan. Potential methods for the regulation of *HvGSL* gene function, other than control of gene transcription, were briefly addressed in the Introduction to this Chapter (*Section 3.1*). To overcome the limitation of transcript profiling data can be further investigated through the *in situ* hybridization of fixed tissues for the detection of localised mRNA at the cellular level. Alternatively, the binding of HvGSL protein-specific antibodies to tissue sections or to membrane proteins extracted from barley tissues that are actively synthesising (1,3)-β-D-glucan, could define the specific HvGSL isoform that is responsible for the synthesis and deposition of (1,3)-β-D-glucan. Another experiment could involve the generation of GFP-HvGSL fusion proteins, which may provide information on the cellular location of HvGSL proteins. Another approach, which was successfully used to investigate the role of *HvGSL7* in the deposition of (1,3)-β-D-glucan in papillary structures (*Chapter 4*), is post-transcriptional gene silencing. By silencing individual *HvGSL* genes, and observing the associated phenotype, *HvGSL* gene function may be revealed.

Transcription of HvGSL *Genes in Meristematic Tissues*

It has been demonstrated in *Zea mays* that maturing leaves have a meristematic region and a region of cell elongation, which is localised at the leaf base (Sharman, 1942) and another meristematic region located at the root tip (Hochholdinger *et al.*, 2004). Thus, both of these meristematic regions must possess the cellular machinery required for the formation of the cell plate, which includes mRNA and proteins for the synthesis of (1,3)-β-D-glucan (*Section 1.2.2.1*). It is possible that the cellular processes during cell plate formation are fundamentally similar in the meristematic regions of the leaf base and the root tip, and that the genes and proteins involved in the synthesis and deposition of (1,3)-β-D-glucan may be the same in both tissues.

The level of individual *HvGSL* mRNAs in these meristematic regions were assessed by Q-PCR to determine if transcription patterns could provide insights into which gene is involved in the synthesis of (1,3)-β-D-glucan in the cell plate. The transcript abundance of both *HvGSL1* and *HvGSL6* in the meristematic root tip was greater than 7×10^4 normalised mRNA copies per microliter, while the transcript abundance of the other *HvGSL* genes were all below 2×10^4 normalised mRNA copies per microliter (*Figure 3.10.A*). Therefore, based on transcript abundance, *HvGSL1* and *HvGSL6* are the most likely candidates for the deposition of (1,3)-β-D-glucan at the forming cell plate of dividing cells in the root tip.

In the meristematic tissue at the leaf base, the transcript abundance of *HvGSL2* and *HvGSL3* were both below 1.2×10^4 normalised mRNA copies per microliter, while the transcript abundance of the other *HvGSL* genes were greater than 3×10^4 normalised mRNA copies per microliter (*Figure 3.9.A*). If the genes required for the synthesis of (1,3)-β-D-glucan during mitotic cell plate formation are the same in the meristematic leaf base and root tip, the most likely candidate genes are therefore *HvGSL1* and *HvGSL6*, as determined by transcript abundance. However, one cannot dismiss the possibility of subtle differences between the process of mitotic division in the meristematic leaf base and the root tip. If there are differences, then all *HvGSL* genes with the exception of *HvGSL2* and *HvGSL3* are potentially involved in the deposition of (1,3)-β-D-glucan at the forming cell plate in the meristematic tissue of

the leaf base. Of the genes that have greater than 3 x 10^4 normalised mRNA copies per microliter in the leaf tip (*Figure 3.9.A*), it was observed that the pattern of *HvGSL6* gene transcription in the leaf tissue series is almost exclusive in the meristematic tissue in the leaf base (*Figure 3.9.D*).

The amino acid sequence encoded by the *HvGSL6* gene shares 66.8% identity with the *AtGSL6* (CalS1) gene, which was shown to encode a cell plate specific protein (Hong *et al.*, 2001a). The evidence that the *AtGSL6* gene could encode a cell-plate specific protein is three-fold. Firstly, GFP-AtGSL6 fusion proteins were observed at the growing cell plate, secondly there was enhanced (1,3)-β-D-glucan deposition at the growing cell-plate in transgenic tobacco plants transcribing the *AtGSL6* gene, and thirdly, the *AtGSL6* gene product was observed to interact with phragmoplastin (Hong *et al.*, 2001a). In *Chapter 2*, it was shown that the protein encoded by the *HvGSL2* gene had the highest amino acid sequence identity to *AtGSL6* (*Table 2.4*), but the acquisition of more *HvGSL* sequence data could result in altered sequence identity scores. Thus, based on the transcript abundance in the root tip and leaf base and the pattern of transcription in the leaf series, *HvGSL6* is the most likely orthologue to *AtGSL6* and the most likely candidate to be involved in the deposition of (1,3)-β-D-glucan at the forming cell plate of dividing cells in barley meristematic tissue.

Transcription of HvGSL *Genes in the Developing Endosperm*

In barley grain approximately 3 days after fertilisation, the developing endosperm reaches a coenocyte stage (Olsen, 2004). During cellularisation of the developing endosperm, two to four days post-fertilisation, each nucleus of the coenocyte is encased within a radial microtubule system (Brown *et al.*, 1994). (1,3)-β-D-Glucan is deposited when the radial microtubule systems of adjacent nuclei meet, as detected by the aniline blue fluorochrome and specific antibodies in barley (Brown *et al.*, 1994). The process of endosperm cellularisation is completed between four and six days post-fertilisation (Olsen, 2004), whereafter the (1,3)-β-D-glucan is replaced by cellulose, arabinoxylan and (1,3-1,4)-β-D-glucan (Stone and Clarke, 1992).

The Q-PCR data reported here showed that during barley endosperm cellularisation, most *HvGSL* transcript levels were at least 80% of the normalised maximum transcript level (*Figure 3.11*). At the completion of endosperm cellularisation, there was a trend for *HvGSL* transcript abundance levels to decrease between day four and day six post-fertilisation, and these remained at lower levels after the completion of cellularisation (*Figure 3.11*). Based on the transcription patterns of *HvGSL* genes during and after cellularisation, it appears that all *HvGSL* genes are potentially involved in (1,3)-β-D-glucan deposition during the initial stages of endosperm cell wall development.

The transcription of *HvGSL3* was maximal during the stages of cellularisation when (1,3)-β-D-glucan was deposited, and the transcript abundance was decreased to less than 6% after the cellularisation process, when no further (1,3)-β-D-glucan is deposited (*Figure 3.11.C*). Thus, the *HvGSL3* transcription pattern most closely follows that expected of a gene involved in (1,3)-β-D-glucan deposition during cellularisation. However, only a maximum of 2×10^5 normalised mRNA copies per microliter of *HvGSL3* was observed during cellularisation, while most other *HvGSL* genes were at levels greater than 8×10^5 normalised mRNA copies per microliter during cellularisation (*Figure 3.11.A*). Thus, it is highly possible that *HvGSL3* has a specific role during endosperm cellularisation and that the *HvGSL3* transcript is not required following the completion of cellularisation.

The most abundant *HvGSL* mRNA in the developing endosperm was *HvGSL6*, which had approximately 1.5×10^6 normalised mRNA copies per microliter just prior to the completion of cellularisation at five days post-fertilisation (*Figure 3.11.A*; *Figure 3.11.D*). The reason for the observed increase in *HvGSL6* transcript abundance at five days post-fertilisation remains speculative, although it may be that the HvGSL6 protein is required in large quantities at the end of endosperm cellularisation possibly to assist in a final, rapid (1,3)-β-D-glucan deposition.

Transcription of HvGSL *Genes in* B. graminis *Infected Epidermal Tissue*

(1,3)-β-D-Glucan is known to be deposited within papillary structures that arise from fungal infections (*Chapter 1*). The *AtGSL5* gene was previously shown to be essential for the deposition of (1,3)-β-D-glucan in papillary structures that formed when Arabidopsis leaves were infected with the powdery mildew fungus (Jacobs *et al.*, 2003; Nishimura *et al.*, 2003). The barley genes with the highest amino acid sequence identities with the *AtGSL5* are *HvGSL7* (72.1%) and *HvGSL8* (64.1%; *Table 2.3*). The Q-PCR analysis of *B. graminis* infected epidermal tissue was performed to determine if these or other *HvGSL* genes could be involved in the deposition of (1,3)-β-D-glucan in papillary structures, through the analysis of *HvGSL* genes transcription in *B. graminis* infected barley leaf epidermal tissue in comparison to uninfected tissue.

The transcription patterns of *HvGSL* genes in response to *B. graminis* infection could be separated into three groups. The first group consisted of *HvGSL* genes for which transcription patterns were unchanged in response to *B. graminis* infection, and this group included *HvGSL1*, *HvGSL4* and *HvGSL6* (*Figure 3.12*). The second group consisted of *HvGSL* genes with lower transcript abundance in infected tissue, compared with the uninfected control, and this group included *HvGSL2*, *HvGSL3* and *HvGSL8* (*Figure 3.13*). The third type of transcription pattern was only exhibited by *HvGSL7*, which showed an increase in transcript abundance in response to *B. graminis* infection of epidermal tissue, when compared to the uninfected control (*Figure 3.14*).

Between 12 – 15 hr after leaves are inoculated with *B. graminis*, (1,3)-β-D-glucan is deposited in papillary structures (Green *et al.*, 2002; Zeyen *et al.*, 2002). The Q-PCR analysis showed that the abundance of *HvGSL7* transcripts in infected epidermal tissues was twice that of the uninfected control (*Figure 3.14*), and the level of *HvGSL7* transcript remained much higher in the infected tissue when compared with the uninfected control, until 24 hr after spore inoculation (*Figure 3.14*). Based on both amino acid sequence identity and the gene transcription patterns in response to *B. graminis* infection, the *HvGSL7* gene is the most likely orthologue of *AtGSL5*.

However, these experiments did not show a direct link between *HvGSL7* and the deposition of (1,3)-β-D-glucan in papillary structures. Transiently induced post-transcriptional gene silencing experiments were therefore designed to determine if the presence of papillary (1,3)-β-D-glucan deposition could be prevented through the down-regulation of *HvGSL7* transcripts. These experiments are described in *Chapter 4*.

It has been demonstrated that the *FKS1* and *FKS2* genes from *S. cerevisiae* have functions that are distinct and overlapping (Mazur *et al.*, 1995). It was considered possible that individual members of the *HvGSL* gene family could also have overlapping functions. Comparisons of the transcription patterns of individual *HvGSL* genes were initially grouped on the basis of graphed pattern of maximum normalised transcription levels (*Figure 3.9.B-D*; *Figure 3.10.B-D*; *Figure 3.11.B-D*; *Figure 3.12-14*). The two genes that had the most similar transcription patterns were *HvGSL1* and *HvGSL4*, which were comparable in the leaf tissue (*Figure 3.9.B*), the developing endosperm (*Figure 3.11.B*) and neither gene was up-regulated in response to *B. graminis* infection (*Figure 3.12*). The Q-PCR data showing the maximum normalised transcription patterns of *HvGSL* genes across all the tissue series were further compared using a Pearson correlation matrix. It was observed that *HvGSL1* and *HvGSL4*, both located in Clade 2 on the phylogenetic tree (*Figure 2.22*), had the strongest correlating gene transcription pattern at 81% (*Table 3.9*). Furthermore, of the four *HvGSL* genes represented on the Barley1 microarray chip, *HvGSL1* and *HvGSL4* had the strongest transcription correlation at 80% (*Figure 3.2.B*). Therefore, of the *HvGSL* genes examined here, it appears that *HvGSL1* and *HvGSL4* are most likely to have overlapping functions. However, it should be noted that the exact roles of the *HvGSL1* and *HvGSL4* genes in the synthesis of (1,3)-β-D-glucan remain uncertain.

3.4.1 Conclusions

The analysis of *HvGSL* transcription profiles was useful in linking the presence of specific transcripts to tissues where processes involving (1,3)-β-D-glucan synthesis are known to occur. A summary of the possible roles of *HvGSL* genes in (1,3)-β-D-

HvGSL Gene	Microarray Data		Q-PCR Data		Possible Gene Functions (In Relation to (1,3)-β-D-Glucan Deposition)
	Co-Transcribing Gene	Figure	Tissue	Figure	
HvGSL1	-		- Dev. Endosperm - Meristematic tissue (leaf and root)	*Figure 3.11* *Figure 3.9* *Figure 3.10*	- Endosperm cellularisation - Cell plate formation in leaf base and root tip
HvGSL2	- DMC1	*Figure 3.4*	- Dev. Endosperm	*Figure 3.11*	- (1,3)-β-D-Glucan deposition during meiotic division - Endosperm cellularisation
HvGSL3	- Ankyrin-like - Putative glucosyltransferase	*Table 3.6* *Figure 3.5*	- Dev. Endosperm	*Figure 3.11*	**- Endosperm cellularisation- not required in grain after 6 DAP**
HvGSL4	- Bio-stress related	*Figure 3.6*	- Dev. Endosperm - Meristematic tissue (leaf)	*Figure 3.11* *Figure 3.9*	- Endosperm cellularisation - Cell plate formation in leaf base - Closure of plasmodesmata
HvGSL5	-		-		-
HvGSL6	-		- Dev. Endosperm - Meristematic tissue (leaf and root)	*Figure 3.11* *Figure 3.9* *Figure 3.10*	- Endosperm cellularisation- increased transcript 5 DAP **- Most likely candidate for cell plate formation**
HvGSL7	-		- Infected Epidermins - Dev. Endosperm - Meristematic tissue (leaf)	*Figure 3.14* *Figure 3.11* *Figure 3.9*	**- Fungal induced papillary (1,3)-β-D-glucan deposition** - Endosperm cellularisation - Cell plate formation in leaf base
HvGSL8	-		- Meristematic tissue (leaf) - Dev. Endosperm	*Figure 3.9* *Figure 3.11*	- Cell plate formation in leaf base - Endosperm cellularisation

Table 3.10: The proposed functions of members of the *HvGSL* gene family, based on the transcript profiling experiments performed in this Chapter.

glucan deposition is presented in *Table 3.10*. However, it must be emphasised again that the transcript profiling methods used in this Chapter are associated with considerable interpretative constraints and that the analyses are useful primarily for the development of testable biological hypotheses.

Nevertheless, the experiments provided some evidence that the *HvGSL7* gene is the barley orthologue of the *AtGSL5* gene in Arabidopsis. The barley *HvGSL7* and the Arabidopsis *AtGSL5* genes share the highest level of sequence identity at the amino acid level (*Chapter 2*). The Arabidopsis *AtGSL5* gene was of particular interest because it is required for (1,3)-β-D-glucan deposition in response to wounding and pathogen attack, and because silencing the *AtGSL5* gene is associated with increased resistance to a range of fungal pathogens (Jacobs *et al.*, 2003; Nishimura *et al.*, 2003). For these reasons, it was considered possible that the barley orthologue of *AtGSL5* might also be involved in resistance to pathogen attack, this time in a commercially valuable cereal crop. The fact that the barley *HvGSL7* gene appeared to be the only barley *GSL* that showed an increase in transcript abundance in response to *B. graminis* infection (*Figure 3.14*) was consistent with this possibility. Since barley is subject to infection by a range of fungi, which may result in large economic losses for cereal farmers, the role of *HvGSL7* in the deposition of (1,3)-β-D-glucan in papillary structures was investigated further, through post-transcriptional gene silencing. The results of these experiments are presented in *Chapter 4*.

Chapter 4

Transient Post-Transcriptional Gene Silencing of Putative (1,3)-β-D-Glucan Synthases in Hordeum vulgare

4.1 INTRODUCTION

The overall aim of the experiments described in this Chapter was to investigate the potential role of barley *GSL* genes in barley-powdery mildew relationships. There was a particular emphasis on the identification of barley orthologous genes to the Arabidopsis *AtGSL5* gene, which has been shown to be required for wound and papillary (1,3)-β-D-glucan deposition (Jacobs *et al.*, 2003; Nishimura *et al.*, 2003). It was observed that the disruption of *AtGSL5* gene function resulted in the increased resistance to powdery mildew fungi, suggesting that the deposition of (1,3)-β-D-glucan is required to establish a successful infection (Jacobs *et al.*, 2003; Nishimura *et al.*, 2003).

Powdery mildews (*Blumeria graminis*) are biotrophic fungi that form feeding structures within epidermal cells of the host leaf, and a conidial spore that comes in contact with the plant can complete its life cycle by forming a feeding structure in a single cell (Shirasu *et al.*, 1999; Bushnell, 2002). The processes involved in the establishment of a successful powdery mildew infection are summarised in *Figure 4.1*. The loss of nutrients and a decrease in photosynthetic ability because of powdery mildew infection may result in yield decreases in plants that are important to the agricultural industry (Bushnell, 2002). Barley powdery mildew is known to cause decreases in crop yield of up to 15%, and spores may survive for over 12 months on the stubble residue of previous crops (http://www.agric.nsw.gov.au/reader/crop-sowing-guides/north-nsw-barley-update.htm). Currently the best methods of decreasing crop damage caused by powdery mildew infection include rotations, the use of resistant varieties and the use of fungicides. Understanding the ability of barley powdery mildew to infect, feed and sporulate is therefore of economical importance.

During the formation of powdery mildew feeding structures, a penetration peg emerges from beneath the appressorial lobe and may breach the epidermal layer of the barley leaf (*Figure 4.1*). The cytoplasmic membranes of the infected barley cell aggregate at the site of fungal penetration, this is the initial stage of the formation of papillary structures (*Figure 4.1*). The main polysaccharide component of papillary

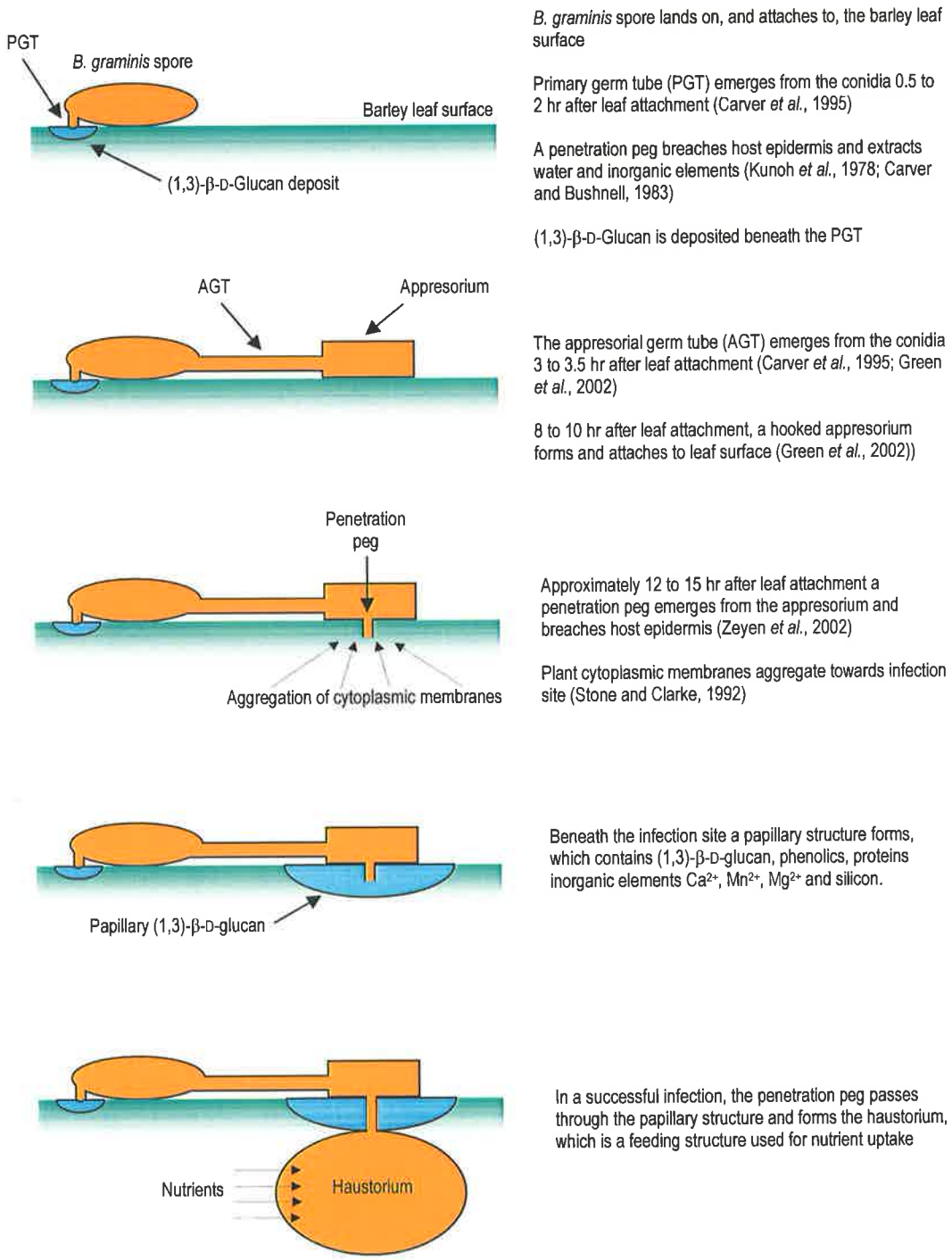

B. graminis spore lands on, and attaches to, the barley leaf surface

Primary germ tube (PGT) emerges from the conidia 0.5 to 2 hr after leaf attachment (Carver *et al.*, 1995)

A penetration peg breaches host epidermis and extracts water and inorganic elements (Kunoh *et al.*, 1978; Carver and Bushnell, 1983)

(1,3)-β-D-Glucan is deposited beneath the PGT

The appresorial germ tube (AGT) emerges from the conidia 3 to 3.5 hr after leaf attachment (Carver *et al.*, 1995; Green *et al.*, 2002)

8 to 10 hr after leaf attachment, a hooked appresorium forms and attaches to leaf surface (Green *et al.*, 2002))

Approximately 12 to 15 hr after leaf attachment a penetration peg emerges from the appresorium and breaches host epidermis (Zeyen *et al.*, 2002)

Plant cytoplasmic membranes aggregate towards infection site (Stone and Clarke, 1992)

Beneath the infection site a papillary structure forms, which contains (1,3)-β-D-glucan, phenolics, proteins inorganic elements Ca^{2+}, Mn^{2+}, Mg^{2+} and silicon.

In a successful infection, the penetration peg passes through the papillary structure and forms the haustorium, which is a feeding structure used for nutrient uptake

Figure 4.1: The major stages in the establishment of a successful fungal infection of barley by *B. graminis*.

structures is (1,3)-β-D-glucan, however papillary structures also contain traces of other polysaccharides, phenolic compounds, active oxygen species, proteins and inorganic elements including Ca^{2+}, Mn^{2+}, Mg^{2+} and silicon (Zeyen *et al.*, 2002). It was originally thought that (1,3)-β-D-glucan in papillary structures functioned as a physical barrier to the penetration of powdery mildew hyphae into epidermal cells (Stone and Clarke, 1992). It has also been suggested that papillary (1,3)-β-D-glucan might hinder the infection progress, allowing the host to release antimicrobial compounds or to respond using race-specific resistance genes (Brown *et al.*, 1998).

Recently, studies in Arabidopsis involving the functional disruption of the *GSL* genes required for (1,3)-β-D-glucan synthesis have given new insights into the role of papillary (1,3)-β-D-glucan in fungal infection (Vogel and Somerville, 2000; Jacobs *et al.*, 2003; Nishimura *et al.*, 2003). Arabidopsis transformed with double-stranded RNA interference (dsRNAi) constructs designed to silence *AtGSL5*, and an *AtGSL5* T-DNA insertion line mutant both exhibited a lack of (1,3)-β-D-glucan deposition in response to wounding (Jacobs *et al.*, 2003). These transformed Arabidopsis lines, as well as the Arabidopsis *pmr4-1* mutants that had a point mutation resulting in a truncated AtGSL5 protein, did not deposit papillary (1,3)-β-D-glucan in response to fungal infection (Jacobs *et al.*, 2003; Nishimura *et al.*, 2003). Therefore, it appears that the deposition of papillary (1,3)-β-D-glucan at fungal infection sites is a wound response and requires the presence of an active AtGSL5 protein (Jacobs *et al.*, 2003). It was further observed that the lack of (1,3)-β-D-glucan in papillary structures correlated with increased resistance against the normally virulent powdery mildew fungi; *Sphaerotheca fusca* and *Golovinomyces orontii*, as well as against infection by *Erysiphe cichoracearum* and the oomycete *Peronospora parasitica* (Vogel and Somerville, 2000; Jacobs *et al.*, 2003; Nishimura *et al.*, 2003). Thus, the presence of (1,3)-β-D-glucan in papillary structures that arise from a wound response may have been exploited for successful fungal pathogenesis (Jacobs *et al.*, 2003; Nishimura *et al.*, 2003). To explain the observation that a lack of wound-induced (1,3)-β-D-glucan deposition results in increased fungal resistance, it has been proposed that papillary (1,3)-β-D-glucan might either aid nutrient uptake by haustoria or serve as a pathogen-induced protection barrier that prevents the recognition of certain pathogen-derived

molecules by the host, which strongly activate plant defence responses (Jacobs *et al.*, 2003).

Since barley is a cereal crop that is often subject to fungal attack by powdery mildew, it was considered important to identify potential barley orthologues to the *AtGSL5* gene in Arabidopsis, and to determine whether silencing this gene would lead to resistance against fungal pathogenesis in a commercially important cereal crop species, in the same way as silencing the *AtGSL5* gene increases resistance to pathogen infection. The barley *GSL* gene family consists of at least seven members (*Chapter 2*), and to identify the potential barley orthologues of *AtGSL5*, the deduced amino acid sequence of *HvGSL* cDNA clones were compared to the amino acid sequence of the *AtGSL5* gene. It was observed that the highest amino acid sequence identity to AtGSL5 was HvGSL7 at 72.1%, while the second highest identity was with HvGSL8 at 64.1% (*Table 2.3*; *Table 2.4*). In an attempt to relate the level of gene transcription to gene function, the transcription of the *HvGSL* genes in response to *B. graminis* infection of barley leaf epidermis was subsequently analysed by Q-PCR (*Chapter 3*). It was observed that in leaf epidermal tissue, *HvGSL7* was the only *HvGSL* gene that exhibited an increase in transcription in response to *B. graminis* infection when compared to the uninfected control (*Figure 3.12*; *Figure 3.13*; *Figure 3.14*). Based on the deduced amino acid sequence identity and gene transcription profile, *HvGSL7* and *HvGSL8* were therefore considered to be possible barley orthologues to *AtGSL5*, with *HvGSL7* being the most likely homologue (*Chapter 3*).

In this Chapter, the possible role of *HvGSL7* and *HvGSL8* in the deposition of papillary (1,3)-β-D-glucan in response to fungal infection was investigated using a gene silencing approach. Transient post-transcriptional gene silencing was achieved *via* gold micro-projectile bombardment of dsRNAi *HvGSL7* and *HvGSL8* silencing vectors into excised barley leaf epidermal tissue, which was subsequently infected with *B. graminis* spores. The silencing vectors consisted of sense and anti-sense *HvGSL7* and *HvGSL8* gene-specific regions of approximately 300 bp, separated by an intron (*Figure 4.2*). When these vectors are delivered into the cell and transcribed, hairpin structures are expected to form by complementary base pairing of the sense

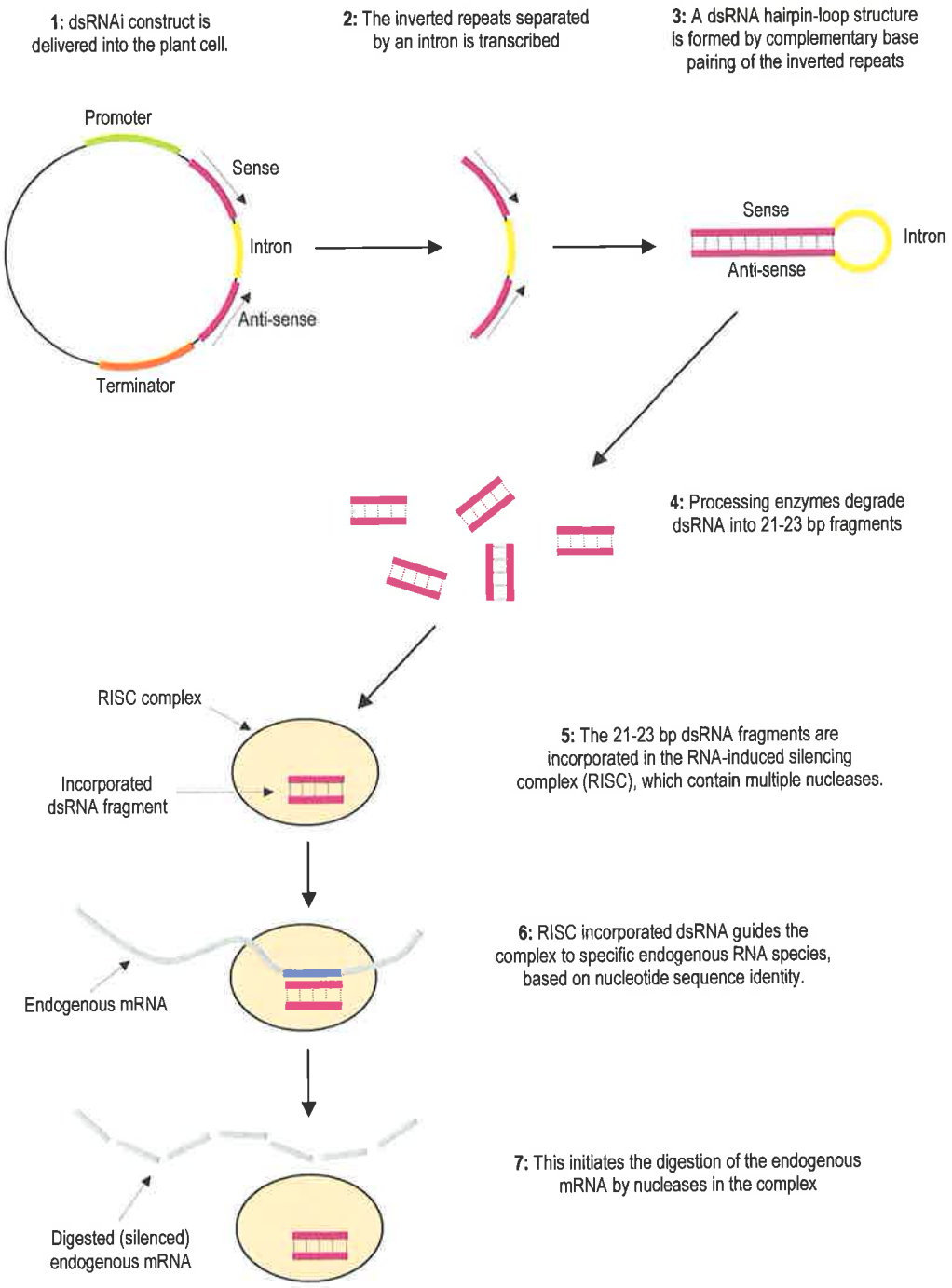

Figure 4.2: A schematic showing the post-transcriptional silencing of a gene following the delivery of gene-specific double stranded RNA interference (dsRNAi) vectors into cells. The endogenous mRNA with an identical sequence to the dsRNAi molecule is degraded by multiple nucleases located in the RNA-induced silencing complex.

and anti-sense regions (*Figure 4.2*). The detection of double stranded RNA within a plant cell results in processing enzymes degrading the dsRNA into 21 – 23 bp fragments (Hammond *et al.*, 2001). The 21 – 23 bp dsRNAi fragments become incorporated into a protein complex called the RNA-induced silencing complex (RISC), which contains multiple nucleases (Hammond *et al.*, 2001). The RISC-incorporated dsRNA guides the complex to specific mature mRNAs that have nucleotide sequence identity with the dsRNA (*Figure 4.2*). This initiates the cleavage of the mature mRNA (Waterhouse *et al.*, 1998; Hammond *et al.*, 2001). Thus, to prevent non-specific gene-silencing, it was important that the *HvGSL7* and *HvGSL8* gene-specific regions did not share identity over 21 consecutive base pairs with any other *HvGSL* gene. Post-transcriptional gene silencing can be achieved by the expression of dsRNAi molecules with 60 – 100% efficiency (Smith *et al.*, 2000). The best results occur when a splicable intron is located between the inverted repeats in the dsRNAi expression construct (Smith *et al.*, 2000). This has been attributed to the removal of the intron-loop by plant spliceosomes, which allows more efficient incorporation of the dsRNA into the RISC complex (Smith *et al.*, 2000).

Hunold *et al.* (1994) observed that bombardment with tungsten particles is more likely to result in the deposition of (1,3)-β-D-glucan at the penetration site than bombardment with gold particles (Hunold *et al.*, 1994). It was thought that the difference between the responses of leaves bombarded with tungsten *versus* gold was caused by the irregular shape of the tungsten particles compared to the smooth spherical shape of the gold particles (Hunold *et al.*, 1994). Therefore, gold particles were used to deliver the dsRNAi silencing vectors and the GUS expression vectors into the barley cells to minimise the likelihood of (1,3)-β-D-glucan deposition at the wound site.

Following bombardment, the leaf tissue was infected with *B. graminis* spores to observe the effect of silencing *HvGSL7* and *HvGSL8* on the subsequent deposition of papillary (1,3)-β-D-glucan. Excised barley leaf tissues that were both bombarded and infected were subjected to a staining protocol (*Figure 4.3*). The tissues were initially stained with a GUS staining solution for the identification of bombarded cells.

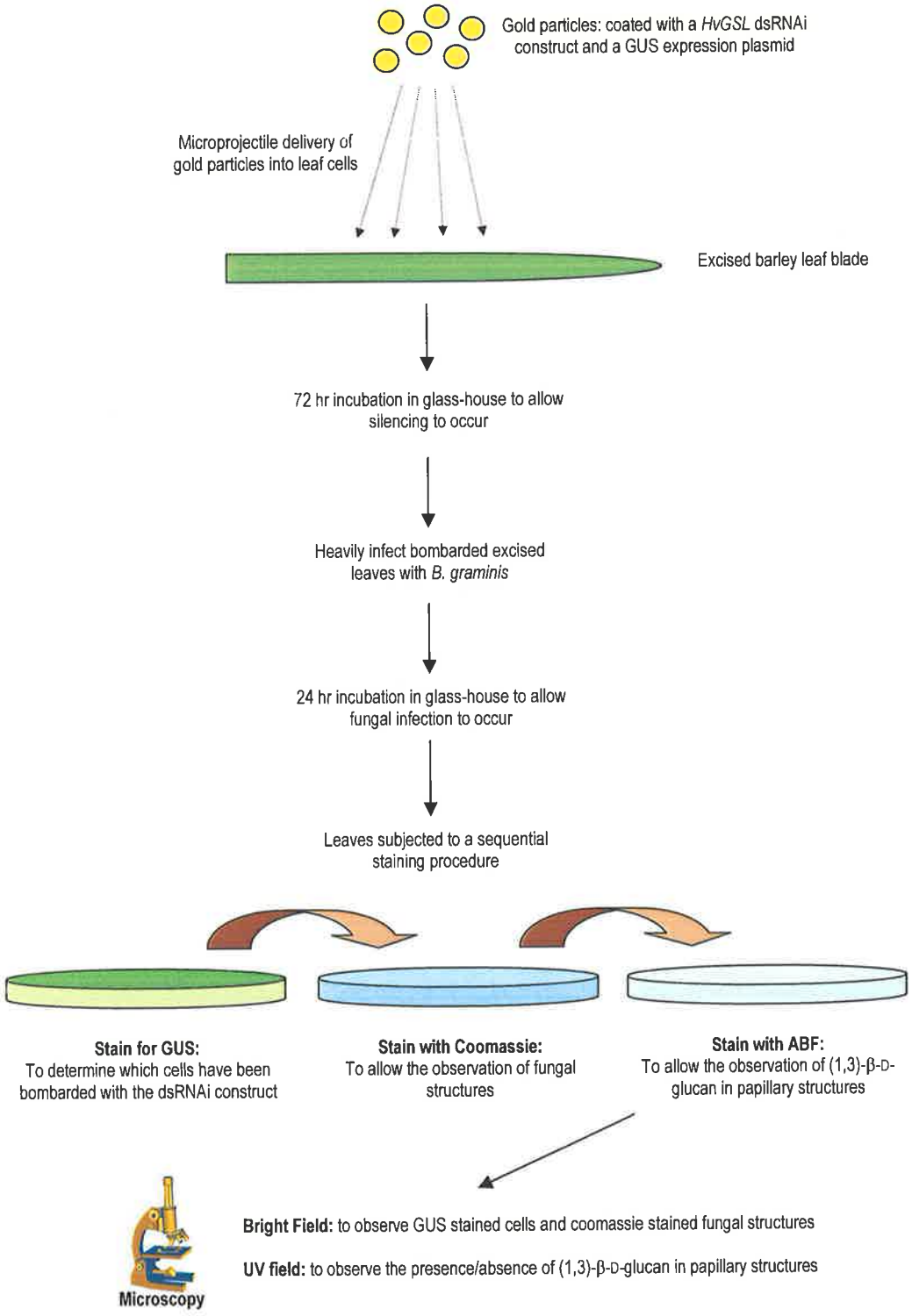

Figure 4.3: Experimental strategy to determine of the effect of transiently induced silencing of *HvGSL7* and *HvGSL8* on the deposition of papillary (1,3)-β-D-glucan. dsRNAi: double-stranded RNA inference; GUS: β-glucuronidase; ABF: aniline blue fluorochrome.

Clearly, not all individual cells in the leaf section will be struck by a gold particle. It was therefore necessary to determine which cells were bombarded, as well as being infected by powdery mildew. This was made possible by coating the gold particles with a GUS expression vector as well as the dsRNAi silencing vectors. It was assumed that positive GUS staining indicated that the cell had been struck by a gold particle, and was also likely to be transcribing the dsRNAi constructs. However, it has been reported that endogenous GUS activity can be observed in tissues from *Nicotiana tabacum* L., *Beta vulgaris* L., *Brassica napus* L., *Pisum sativum* L., *Triticum sativum* L. and *Rheum rhaponticum* L. (Hodal *et al.*, 1992). Furthermore, the leaves of *N. tabacum* exhibited endogenous GUS activity in the mesophyll, vascular bundles, trichomes and stomatal cells (Hodal *et al.*, 1992). Thus, in the experiments described here, GUS staining in the above mentioned cell types was ignored, to minimise the number of false positives. The next step of the staining protocol was to submerge the tissues in Coomassie stain, and because of the intensely low amount of protein on leaf surfaces, only the fungal structures were stained. The observation of an adhered fungal appressorium on a GUS stained epidermal cell was used as an identifiable indicator of infection (*Figure 4.1*). Finally, the presence of (1,3)-β-D-glucan in papillary structures were observed by staining the tissues with the aniline blue fluorochrome.

In setting out this Chapter, general methods including strategies used to generate the dsRNAi *HvGSL7* and *HvGSL8* silencing vectors and details of the assay are presented in the Materials and Methods (*Section 4.2*). The microscopy observations are subsequently presented in the Results (*Section 4.3*). This Chapter presents the barley *HvGSL7* gene as the most likely orthologue to the *AtGSL5* gene, which is required for wound and papillary (1,3)-β-D-glucan in Arabidopsis (Jacobs *et al.*, 2003). *HvGSL7*, but not *HvGSL8*, is required for the deposition of (1,3)-β-D-glucan in papillary structures that arise following fungal infection.

4.2 MATERIALS and METHODS

4.2.1 Materials

The materials and source companies used in general molecular biology techniques were as described in *Section 2.2.1*. The 0.6 µm gold micro-carriers (165-2262), macro-carrier discs and Biolistic® 900 psi rupture discs were purchased from BIORAD Laboratories (Hercules, CA, USA). Sucrose, $CaCl_2$, Na_2HPO_4, NaH_2PO_4, $K_4[Fe(CN)_6]$, lactic acid and methanol were obtained from Merck Pty. Ltd. (Kilsyth, Victoria, Australia). Benzimidazole, Coomassie brilliant blue R-250 and spermidine were from Sigma-Aldrich, Inc. (St. Louis, MO, USA). DIFCO™ granulated agar was from Becton, Dickinson and Company (Sparks, MD, USA). $K_3[Fe(CN)_6]$ was purchased from By-products and Chemicals Pty. Ltd. (Auburn, NSW, Australia). 5-Bromo-4-chloro-3-indolyl-beta-D-glucuronic acid (X-gluc) was obtained from Progen Industries Ltd. (Darra, Queensland, Australia). The GUS expression vector, pUbi-GUS-NOS (*Figure 4.4*), was constructed and kindly donated by Dr Andrew Jacobs and the pHannibal plasmid (*Figure 4.5*) was received from Dr Peter Waterhouse, CSIRO Plant Industry (Wesley *et al.*, 2001). Aniline blue fluorochrome was obtained from Biosupplies (Parkville, Victoria, Australia).

4.2.2 Identification of *HvGSL7* and *HvGSL8* Gene-Specific Regions

The *HvGSL7* and *HvGSL8* gene-specific regions suitable for use in gene silencing experiments were determined by multiple nucleotide sequence alignment, performed as described in *Section 2.2.2*, using the *HvGSL* gene sequences that were described in *Chapter 2*. The nucleotide sequences at the 3' ends of the cDNAs and in the 3' untranslated regions (3'UTR) of *HvGSL* genes were poorly conserved (*Figure 4.6*) and were therefore suitable for the selection of gene-specific regions for *HvGSL7* (*Figure 4.7*) and *HvGSL8* silencing by dsRNAi (*Figure 4.8*).

The *HvGSL3* and *HvGSL5* nucleotide sequences were not included in the multiple nucleotide sequence alignment (*Figure 4.6*) due of a lack of nucleotide sequence in this region (*Figure 2.17*). However, it is unlikely that the *HvGSL3* and *HvGSL5*

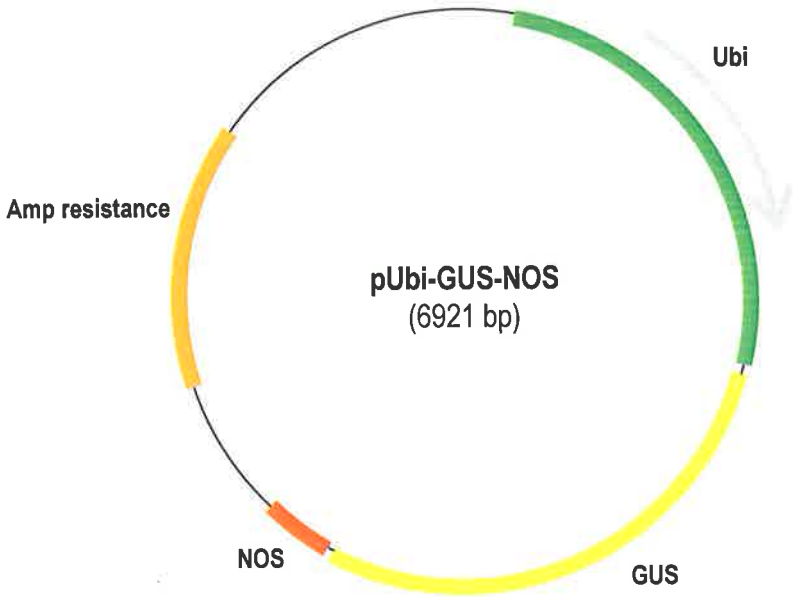

Figure 4.4: Schematic diagram of the pUbi-GUS-NOS plasmid used as a reporter plasmid for bombarded cells. The transcription of the β-glucuronidase gene (GUS) was driven by the Ubiquitin (Ubi) promoter and ended with the nopaline synthase polyadenylation (NOS) terminator. Bacterial selection was *via* the Ampicillin (Amp) antibiotic resistance gene.

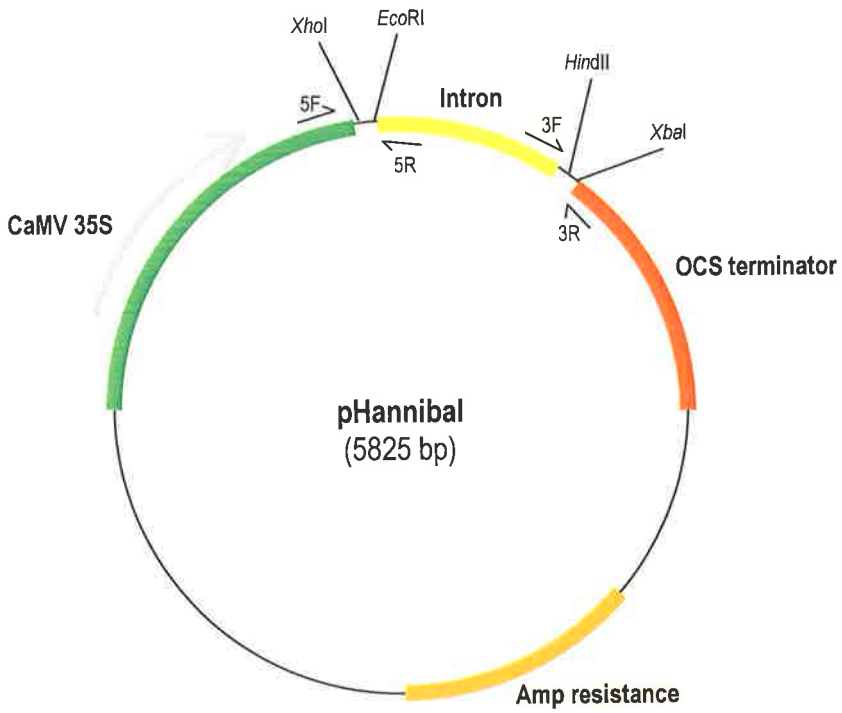

Figure 4.5: Schematic diagram of the pHannibal plasmid used in the generation of the *HvGSL7* and *HvGSL8* dsRNAi silencing constructs. The sense fragment was ligated between the *Xho*I and *Eco*RI restriction sites, while the antisense fragment was ligated into the *Hin*dIII and *Xba*I restriction sites. The transcription of the inverted repeats, which were separated by an intron (*flavaria*), was driven by the CaMV 35S promoter with a dual enhancer and ended with the octapine synthase terminator (OCS) terminator. Bacterial selection was *via* the Ampicillin (Amp) antibiotic resistance gene. The primers used for the amplification/sequencing of the sense fragment were 5F: Hannibal5F and 5R: Hannibal5R (*Table 4.1*). The primers used for the amplification/sequencing of the antisense fragment were 3F: Hannibal3F and 3R: Hannibal3R (*Table 4.1*).

Primer name	Nucleotide sequence
Hannibal_3F	CAAGGTAACATGATAGATCATGTC
Hannibal_3R	GCAAATATCATGCGATCATAGGC
Hannibal_5F	GTGACATCTCCACTGACGTAAGG
Hannibal_5R	CATACTAATTAACATCACTTAAC
f*GSL7-Eco*RI	CCGGAATTC**GAATCAAGGTAAGGATGTCGC**
f*GSL7-Xho*I	CCGCTCGAG**GGAGTGATTGTTATGACACCTG**
r*GSL7-Hin*dIII	CCCAAGCTT**GAATCAAGGTAAGGATGTCGC**
r*GSL7-Xba*I	GCTCTAGA**GGAGTGATTGTTATGACACCTG**
f*GSL8-Eco*RI	CCGGAATTC**CAAGACTCAATGCCTAAATCAC**
f*GSL8-Xho*I	CCGCTCGAG**CAAGAAATGCAGACAAGGGTA**
r*GSL8-Hin*dIII	CCCAAGCTT**CAAGACTCAATGCCTAAATCAC**
r*GSL8-Xba*I	GCTCTAGA**CAAGAAATGCAGACAAGGGTA**

Table 4.1: The nucleotide sequence of primers used to amplify gene-specific regions of *HvGSL7* and *HvGSL8* and for DNA sequencing. Underlined nucleotides indicate incorporated restriction endonuclease recognition sites. Nucleotide sequences in **bold** indicate *HvGSL7* and *HvGSL8* gene-specific regions. All sequences are written 5' to 3'.

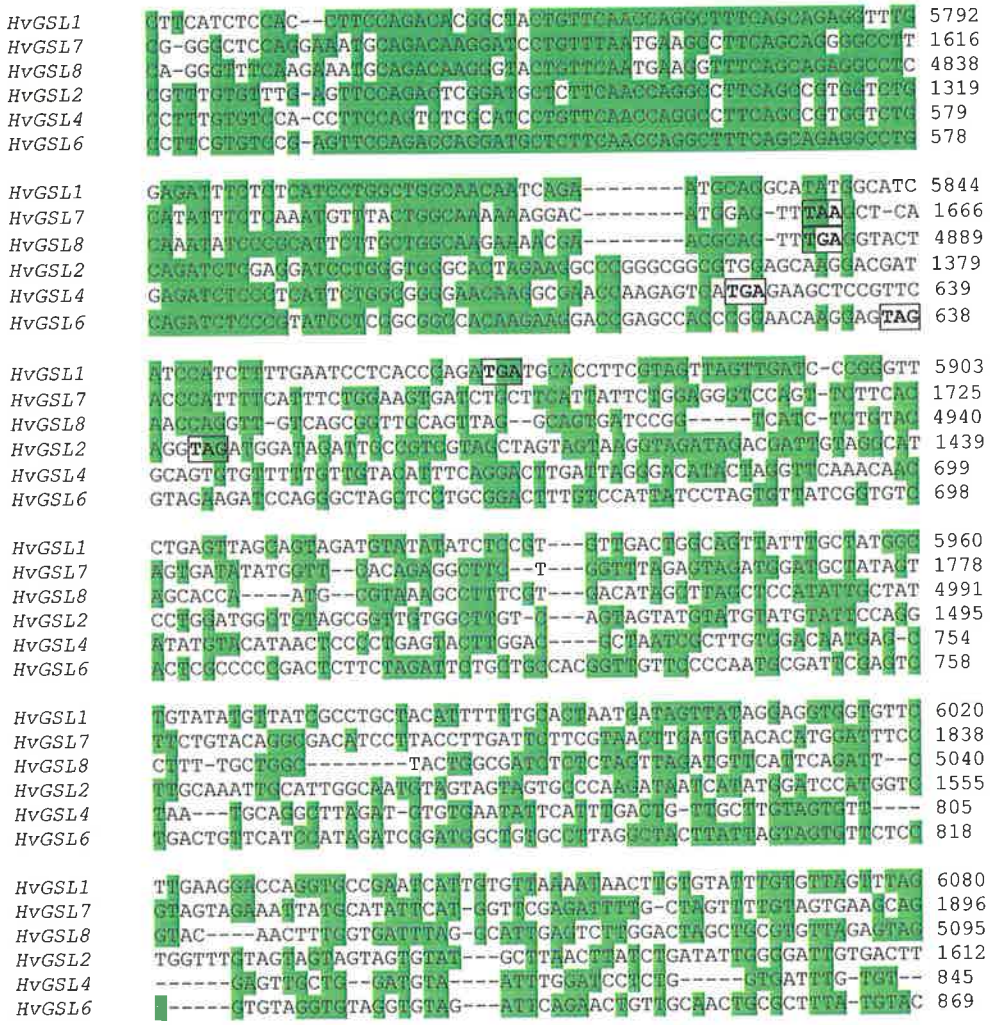

Figure 4.6: A multiple nucleotide sequence alignment of the poorly conserved 3' region and the 3' untranslated region of barley *HvGSL*s. Highlighted nucleotides are conserved in at least 50% of the available *HvGSL*s. Stop codons are in **bold** and boxed. *HvGSL3* and *HvGSL5* are omitted due to the lack of sequence data within this region. Alignments were performed with the online program ClustalW (version 1.82) (http://www.ebi.ac.uk/clustalw/).

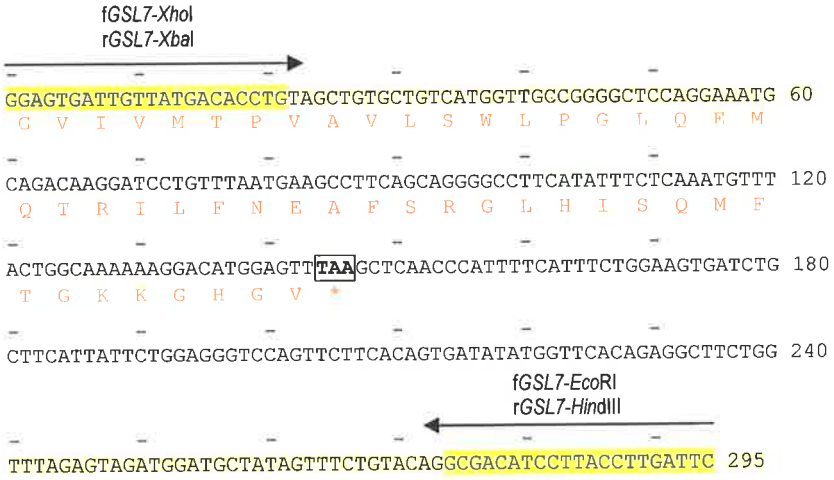

Figure 4.7: The DNA sequence and corresponding peptide sequence of the gene specific region of *HvGSL7* that was amplified by PCR and used in the dsRNAi silencing construct. Highlighted sequences are regions to which primers were designed. Arrows indicate primer direction. The stop codon is in **bold** and boxed. The restriction sites added to each primer mentioned in *Section 4.2.4* are shown in *Table 4.1*.

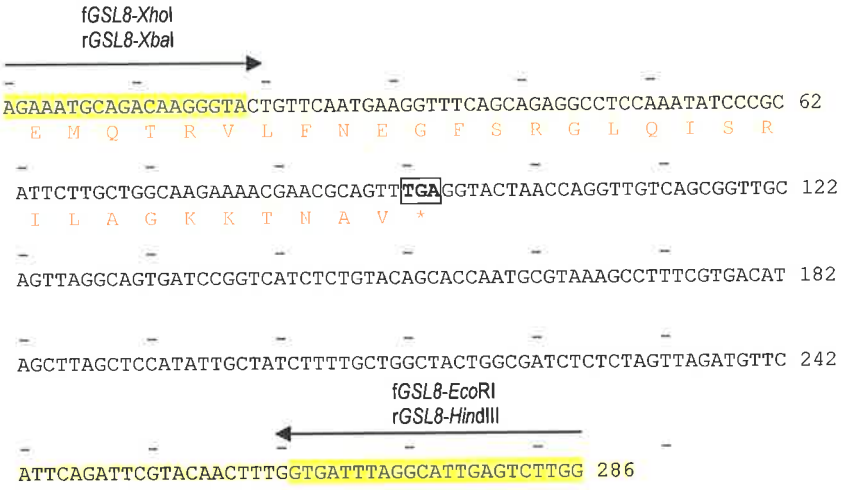

Figure 4.8: The DNA sequence and corresponding peptide sequence of the gene specific region of *HvGSL8* that was amplified by PCR and used in the dsRNAi silencing construct. Highlighted sequences are regions to which primers were designed. Arrows indicate primer direction. The stop codon is in **bold** and boxed. The restriction sites added to each primer mentioned in *Section 4.2.5* are shown in *Table 4.1*.

genes, and any additional unidentified *HvGSL* genes as mentioned in *Chapter 2*, were silenced in addition to *HvGSL7* and *HvGSL8* in these experiments due to the non-conserved nature of the 3'UTR (*Figure 4.6*).

4.2.3 General Molecular Techniques

The construction of dsRNAi *HvGSL* gene specific silencing constructs required the use of several previously described molecular biology protocols (*Section 2.2*). These protocols included PCR amplification (*Section 2.2.5*), cloning PCR amplified products into pGEM®-T Easy (*Section 2.2.6*), restriction digests (*Section 2.2.10*), cloning of restriction fragments into the corresponding restriction sites of pHannibal (*Figure 4.1*; *Section 2.2.6*), transformation of *Escherichia coli* (*Section 2.2.7*), plasmid DNA mini-preparations (*Section 2.2.9*) and DNA sequencing (*Section 2.2.11*).

4.2.4 Construction of the *HvGSL7* dsRNAi Vector

The *HvGSL7*-dsRNAi plasmid used for gene silencing was constructed by cloning inverted repeats of *HvGSL7* gene-specific region into the pHannibal vector (*Figure 4.9*). PCR was used to amplify a 295 bp gene-specific region of *HvGSL7* (*Figure 4.7*) using the previously described cloned 3'RACE fragment of *HvGSL7* (*Section 2.3.7*) as the template. The f*GSL7-Eco*RI and f*GSL7-Xho*I primers (*Table 4.1*) were used for the amplification of the *HvGSL7* sense fragment, while the r*GSL7-Hin*dIII and r*GSL7-Xba*I primers (*Table 4.1*) were used in the amplification of the *HvGSL7*-antisense fragment. These primers had restriction sites incorporated at the 5' end of the primer sequence. An additional two to three nucleotides were added at the 5' end of the restriction sites of the primer sequence to ensure the restriction endonucleases had sufficient DNA with which to bind.

The *HvGSL7*-sense PCR product was purified on agarose gels, digested with *Eco*RI and *Xho*I restriction endonucleases, and ligated into the corresponding sites of the pHannibal plasmid. Confirmation of the presence of the *HvGSL7*-sense fragment in

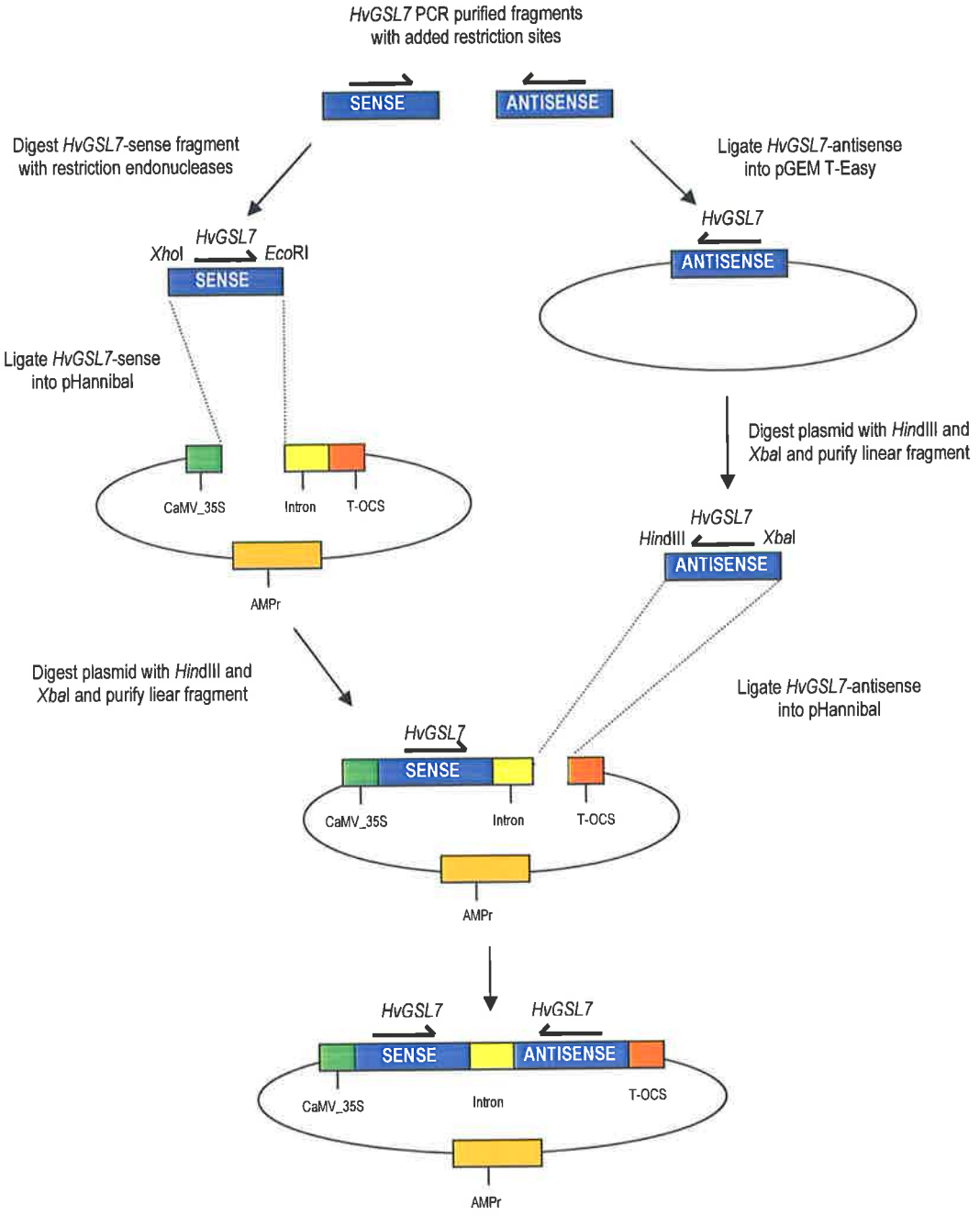

Figure 4.9: Schematic diagram of the cloning strategy used for the construction of the *HvGSL7*-dsRNAi plasmid. The pHannibal plasmid contains Ampicillin resistance for bacterial selection. Transcription of the dsRNA molecule is driven by the CaMV_35S promoter and is terminated by the OCS-terminator. The inverted repeats are separated by an 850 bp (*flavaria*) sequence.

pHannibal was *via* DNA sequencing with the Hannibal5F and Hannibal5R primers (*Figure 4.5*; *Table 4.1*).

Difficulty was experienced in cloning the restriction digested *HvGSL7*-antisense PCR fragment directly into the pHannibal-*HvGSL7*-sense plasmid, which may have been the result of incomplete restriction digestion of the *HvGSL7*-antisense PCR fragment. Thus, to ensure that the ends of the *HvGSL7*-antisense PCR product was completely digested by *Hin*dIII and *Xba*I, an additional cloning step was required. The *HvGSL7*-antisense PCR product was ligated into pGEM®-T Easy and was subsequently removed with a *Hin*dIII and *Xba*I restriction digest, gel purified and ligated into the corresponding sites of pHannibal-*HvGSL7*-sense (*Figure 4.6*). Confirmation of the *HvGSL7*-antisense fragment in the *HvGSL7*-dsRNAi construct was *via* DNA sequencing with the Hannibal3F and Hannibal3R primers (*Figure 4.1*; *Figure 4.4*).

4.2.5 Construction of the *HvGSL8* dsRNAi Vector

The construction of the *HvGSL8*-dsRNAi plasmid (*Figure 4.10*) was achieved essentially as described for the *HvGSL7*-dsRNAi plasmid (*Section 4.2.4*). A 286 bp gene-specific region of *HvGSL8* (*Figure 4.8*) was PCR amplified with two sets of primers with added restriction sites for directional cloning into pHannibal, using the cloned 3'RACE fragment of *HvGSL8* (*Section 2.3.8*) as the template. The f*GSL8-Eco*RI and f*GSL8-Xho*I primers (*Table 4.1*) were used for the amplification of the *HvGSL8* sense fragment, while the r*GSL8-Hin*dIII and r*GSL8-Xba*I primers (*Table 4.1*) were used for the amplification of the *HvGSL8*-antisense fragment.

The PCR amplified *HvGSL8*-sense fragment was purified, digested with *Eco*RI and *Xho*I restriction endonucleases, and ligated into the corresponding sites of the pHannibal plasmid vector. Confirmation of the *HvGSL8*-sense fragment in pHannibal was *via* DNA sequencing with the Hannibal5F and Hannibal5R primers. The PCR amplified *HvGSL8*-antisense fragment was cloned into pGEM®-T Easy as described for *HvGSL7* in *Section 4.2.4*. Using *Hin*dIII and *Xba*I restriction

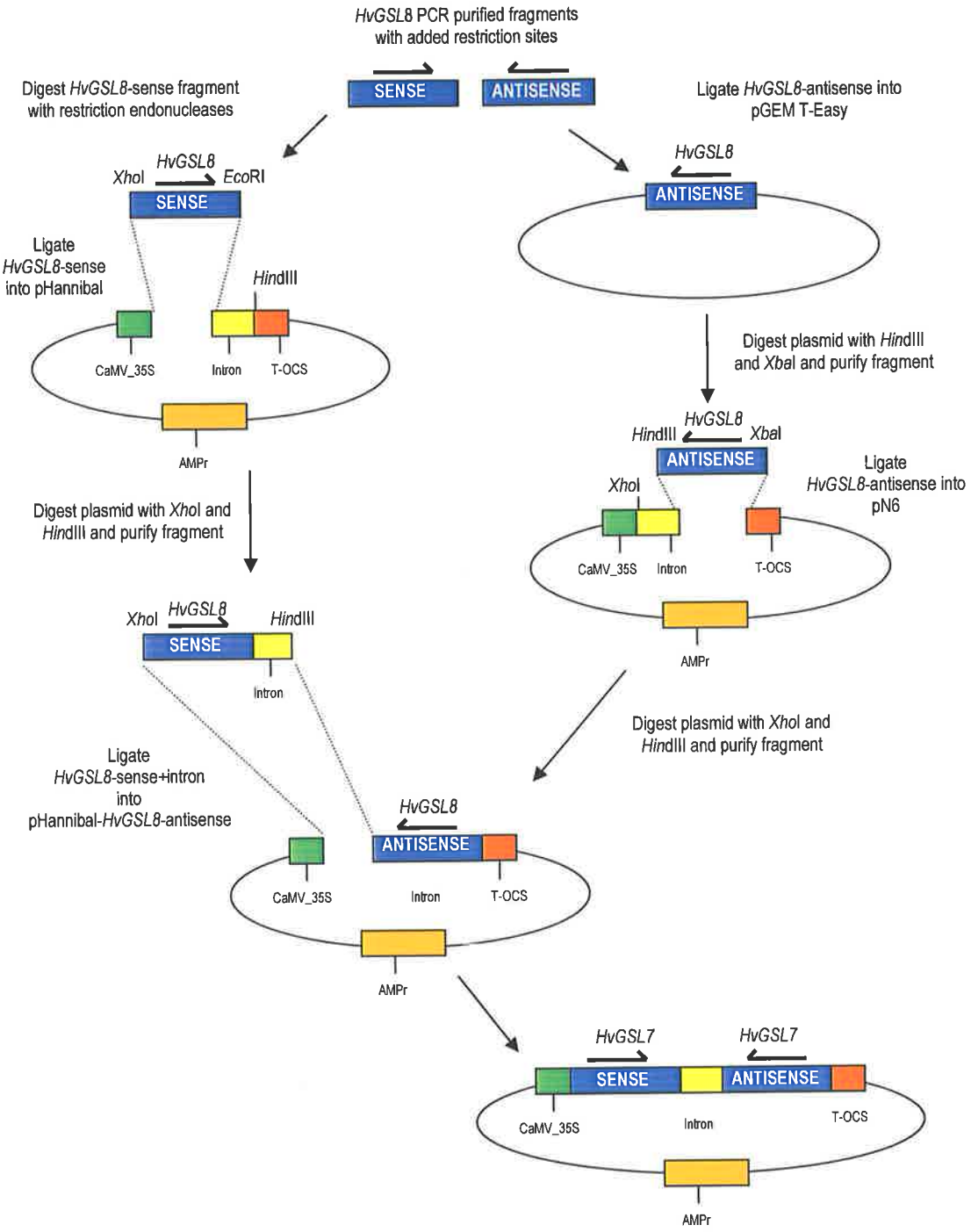

Figure 4.10: Schematic diagram of the cloning strategy use for the construction of the *HvGSL8*-dsRNAi plasmid. The pHannibal plasmid contains Ampicillin resistance for bacterial selection. Transcription of the dsRNA molecule is driven by the CaMV 35S promoter and transcription is terminated with the OCS-terminator. The inverted repeats are separated by an 850 bp intron sequence.

endonucleases, *HvGSL8*-antisense was restriction digested from the pGEM®-T Easy vector, gel purified and ligated into the corresponding restriction sites of pHannibal. Confirmation of the *HvGSL8*-antisense fragment in pHannibal was by DNA sequencing using the Hannibal3F and Hannibal3R sequencing primers (*Figure 4.5*; *Table 4.1*).

The pHannibal-*HvGSL8*-sense construct and the pHannibal-*HvGSL8*-antisense construct were digested separately with the *Xho*I and *Hin*dIII restriction endonucleases. The *HvGSL8* sense/intron fragment was ligated into the *Xho*I and *Hin*dIII restriction sites of pHannibal-*HvGSL8*-sense/minus-intron to form the *HvGSL8*-dsRNAi construct (*Figure 4.10*).

4.2.6 Transiently-Induced Post-Transcriptional Gene Silencing

Plant Material

Barley (var. Sloop) seedlings were grown in a "Keith/Horsham" soil mix in a glass house under a 25°C day and 17°C night temperature regime, with a minimum of 13 hr light. The mix contained 600 l composted pine bark, 1800 g Osmocote, 135 g ammonium nitrate, 135 g micro nutrient mix, 270 g iron sulphate and 1333 g agricultural lime, pH 6.0 – pH 6.5. The youngest emerged leaf blades were excised from 8 day old seedlings and the large vascular rib of the leaf placed face downwards onto 1.5% agar Petri dishes containing 10% sucrose. The plates were sealed with Parafilm and placed in the glasshouse for 4 hr. The leaves were transferred to 1.5% agar plates containing 85 µM benzimidazole, a senescence inhibitor, immediately prior to micro-projectile bombardment (Schweizer *et al.*, 1999; Schweizer *et al.*, 2000).

Coating the Gold Micro-Carriers with DNA

A total of 1 mg gold particle micro-carriers was added to 3.5 µg of either the *HvGSL7* dsRNAi plasmid DNA, the *HvGSL8* dsRNAi plasmid DNA or the empty pHannibal vector DNA, along with 3.5 µg pUbi-GUS-NOS DNA, 50 µl 2.5 M $CaCl_2$ and 20 µl 0.1 M spermidine. The mixture was vortexed for 3 min, and allowed to

settle for 3 min. The DNA-coated gold particles were pelleted with a brief centrifugation for 10 sec. The supernatant was discarded and the gold particles were resuspended in 250 µl 100% ethanol. The gold particles were allowed to settle for 5 min. Another brief centrifugation for 10 sec was used to pellet the gold particles, which were resuspended in 50 µl 100% ethanol. The DNA-coated gold micro-carriers were kept on ice until bombardment. The gold micro-carrier preparation was evenly distributed between four macro-carrier discs and the ethanol was allowed to evaporate.

Micro-Projectile Bombardment

Using a He Biolistic® Particle Delivery System (Model PDS-1000, BIORAD), the gold micro-carriers were fired at a pressure of 900 psi, with the stopping screen 10 cm from the excised leaves on 1.5% agar plates containing 85 µM benzimidazole. Each plate of excised leaves was bombarded twice. The plates were sealed with parafilm and returned to the glass-house for 72 hr.

Powdery Mildew Infection of Bombarded Excised Leaves

The bombarded, excised leaf material was heavily infected with *B. graminis* (Spores were initially obtained on infected plants, which were kindly supplied by Mr Mark Butt, University of Adelaide) by shaking the spores from infected barley leaves. The approximate spore density is presented in *Figure 4.11*. The Petri dishes were re-sealed with parafilm and returned to the growth room for 24 hr.

Staining Procedure

The bombarded and infected excised leaves were placed in 50 ml tubes containing GUS staining solution (0.1 M Na_2HPO_4/NaH_2PO_4 buffer, pH 7.0, containing 10 mM EDTA, 5 mM $K_4[Fe(CN)_6]$, 5 mM $K_3[Fe(CN)_6]$, 1 mg/ml X-gluc, 0.1% (v/v) Triton X-100, 20% (v/v) methanol). The staining solution was vacuum infiltrated into the leaves at a pressure of 27 inches Hg for 15 – 20 min. The tubes were incubated at 37°C for 16 hr. The GUS staining solution was decanted and discarded and the leaves were submerged in GUS destain solution (8:2:1:1 v/v ethanol: glycerol: lactic acid: water) and left at room temperature for a minimum of 48 hr. The solution was

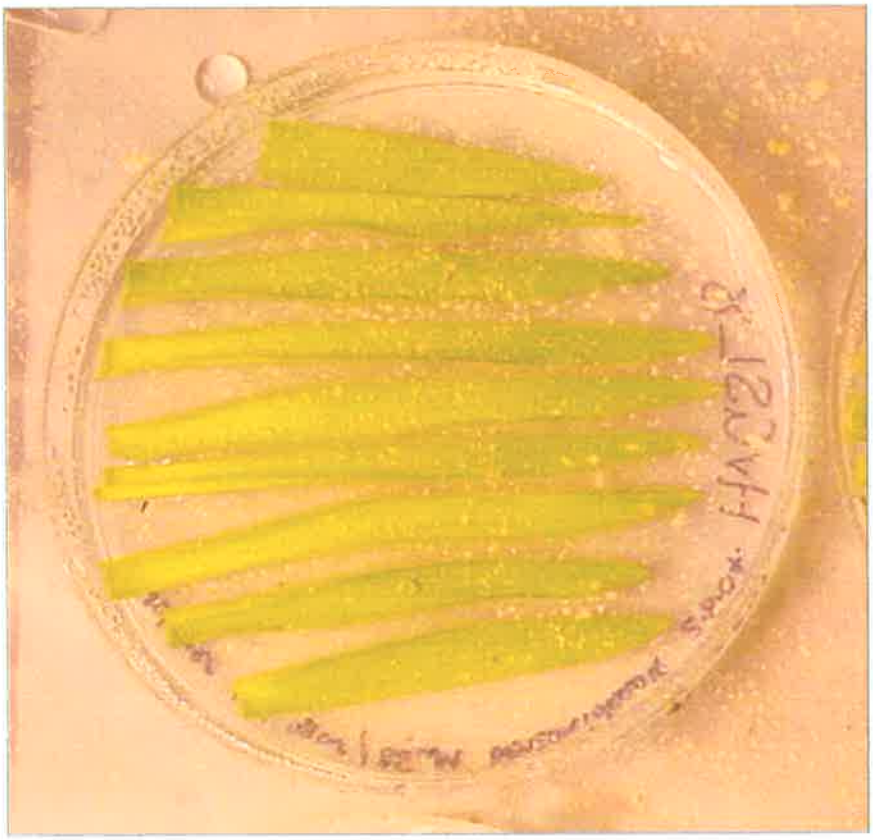

Figure 4.11: A photograph of bombarded excised barley leaves immediately following inoculation with *B. graminis*. Fungal spores were shaken from infected barley plants onto the plates.

replaced every 24 hr. The fungal structures were stained by dipping the inoculated leaves into 0.6% Coomassie brilliant blue R-250 in methanol for 10 sec. Leaves were rinsed in water to remove excess Coomassie dye. The leaves were placed into 10 mM Na_2HPO_4/NaH_2PO_4 buffer, pH 9.0, to equilibrate prior to staining with 0.02% aniline blue fluorochrome in 10 mM Na_2HPO_4/NaH_2PO_4 buffer, pH 9.0, at room temperature for 20 min.

Slide Mounting and Cell Counting

The excised leaves that had been bombarded, infected and stained were mounted on glass slides in sterile 1:1 v/v glycerol: water under glass coverslips. The leaves were viewed using a Zeiss Axioplan 20 fluorescence microscope (Carl Zeiss, Oberkochen, Germany), which was equipped with a HBO 50 W mercury vapour lamp for fluorescence observation. Observation of fluorescence in the UV field was achieved using epi-illumination with a 365 nm excitation filter and a KP620 emission filter. The images were taken with a DC300F microscope digital camera (Leica Microsystems AG, Heerbrugg, Switzerland). Digital images were saved to an IBM compatible computer using IM1000 Image Manager v1.10 software (Leica Microsystems AG, Heerbrugg, Switzerland).

The cells on the leaf surface were scored for the presence of the GUS stain, for fungal appressorial structures and for (1,3)-β-D-glucan deposits using very strict criteria. Fungal infection was only scored after the observation of an appressorial lobe at the tip of the secondary germ tube. An established fungal infection of a bombarded cell was scored by the observation of the appressorial lobe over a GUS stained cell. Scoring for the presence or absence of (1,3)-β-D-glucan in papillary structures under appressorial lobes was carried out under UV light. Guard cells were not counted because these cells have previously shown endogenous GUS expression (Bushnell, 2002). In addition, vascular tissue and long cells were not counted because they have irregular GUS staining along their length, and a reported reduction in powdery mildew infection (Bushnell, 2002).

The observations between two identical experiments were analysed using a correlation of covariance as described in *Chapter 3*.

4.3 RESULTS

4.3.1 Experimental Control for Transient Gene Silencing

In the experimental negative control, the GUS expression plasmid and the empty pHannibal plasmid were delivered into the cells of excised barley leaves by micro-projectile bombardment. It was assumed that each gold micro-carrier was coated with both the GUS expression plasmid and the empty pHannibal plasmid. The bombarded leaf tissue was infected with *B. graminis* spores and stained with a GUS staining solution, Coomassie Blue, and aniline blue fluorochrome. The treated leaves were subsequently viewed with a bright field microscope with a UV attachment. *Figure 4.12* presents the bright field view of a *B. graminis* infection of a GUS stained cell, which results in the deposition of papillary (1,3)-β-D-glucan as observed in the UV field.

The efficiency of these experiments was dependent on the percentage of individual bombarded epidermal cells, as detected by positive GUS staining, that were infected by *B. graminis* spores. It was observed that 27.0% (173/641) of epidermal cells that stained positively for GUS were also infected by *B. graminis* (*Table 4.2*). Furthermore, there were 14 out of 173 (8.1%) *B. graminis* infected bombarded cells that did not exhibit (1,3)-β-D-glucan in papillary structures (*Table 4.2*), even though the cells were bombarded with an empty pHannibal vector. Frequency variation of (1,3)-β-D-glucan in papillary structures were observed between the two experiments. The lack of (1,3)-β-D-glucan in papillary structures that resulted from the infection of GUS positive cells was observed in 7.8% (10/128) of infection events in *Experiment 1*, and in 8.9% (4/45) of infection events in *Experiment 2* (*Table 4.2*; *Figure 4.13*).

4.3.2 The Effect of Transiently Silencing *HvGSL7* on Papillary Structure

In assessing the effect of transient post-transcriptional gene silencing *HvGSL7* on papillary structure, assumptions similar to those described in *Section 4.3.1* were made. Thus, it was assumed that each gold micro-carrier was coated with both the GUS expression vector and the *HvGSL7*-dsRNAi construct, and that the observation

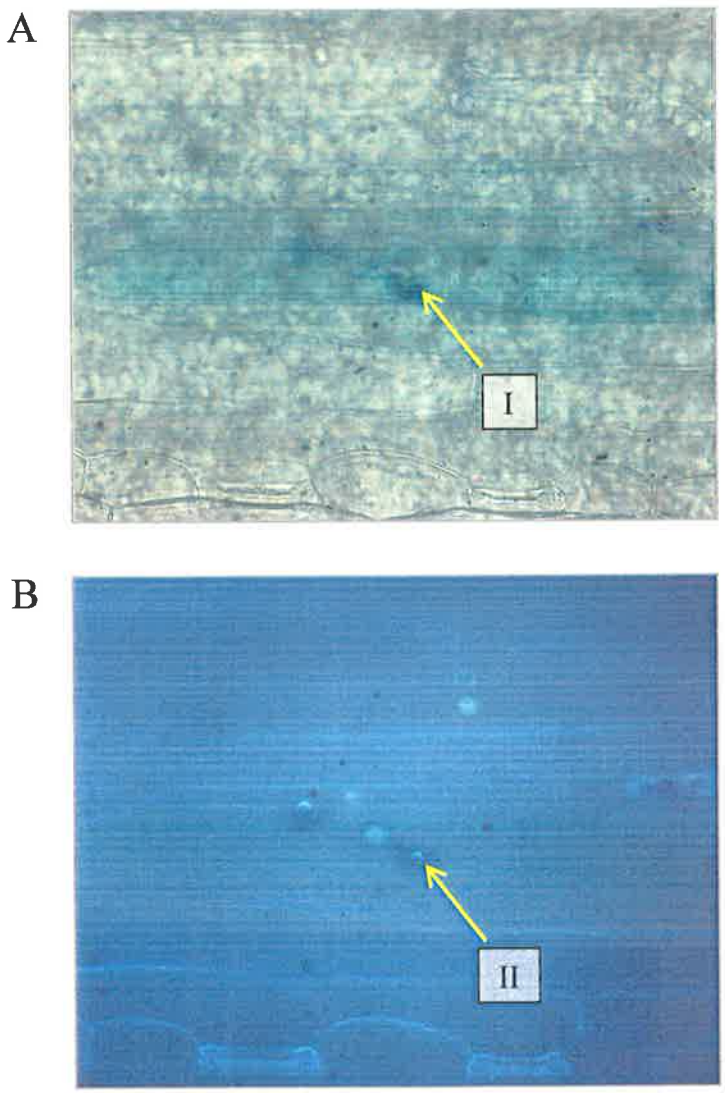

Figure 4.12: The deposition of papillary (1,3)-β-D-glucan in response to *B. graminis* infection of barley epidermal tissue bombarded with the GUS expression vector and the empty pHannibal vector. *Panel A*: Bright field of the negative control bombarded with the GUS expression vector and the empty pHannibal vector. *Arrow I* indicates a fungal hyphae infecting a GUS stained cell. *Panel B*: UV field of panel A. *Arrow II* indicates the presence of papillary (1,3)-β-D-glucan beneath the fungal appressorial lobe.

Observation	Control			*HvGSL7* dsRNAi			*HvGSL8* dsRNAi		
	Exp.1	Exp.2	Total	Exp.1	Exp.2	Total	Exp.1	Exp.2	Total
+GUS	269	372	641	214	553	767	129	247	376
+GUS +Infection	128	45	173	77	58	135	40	56	96
% GUS cells being infected	**47.6%**	**12.1%**	**27.0%**	**36.0%**	**10.5%**	**17.6%**	**31.0%**	**22.7%**	**25.5%**
+GUS +Infection +Callose	118	41	159	59	38	97	37	50	87
% with papillary callose	**92.2%**	**91.1%**	**91.9%**	**76.6%**	**65.5%**	**71.9%**	**92.5%**	**89.3%**	**90.6%**
+GUS +Infection -Callose	10	4	14	18	20	38	3	6	9
% without papillary callose	**7.8%**	**8.9%**	**8.1%**	**23.4%**	**34.5%**	**28.1%**	**7.5%**	**10.7%**	**9.4%**

Table 4.2: Observations from *HvGSL7* and *HvGSL8* gene silencing experiments. When *HvGSL8* was transiently silenced with dsRNAi, the percentage of papillary structures lacking (1,3)-β-D-glucan was comparable to the control. When *HvGSL7* was transiently silenced with dsRNAi, the percentage of papillary structures lacking (1,3)-β-D-glucan was greater than the control. Exp.1: Experiment 1. Exp.2: Experiment 2. +GUS: Cells that are stained positive for GUS. +Infection: Cells that are being infected by *B. graminis*. +/–Callose: The presence/absence of (1,3)-β-D-glucan in papillary structures.

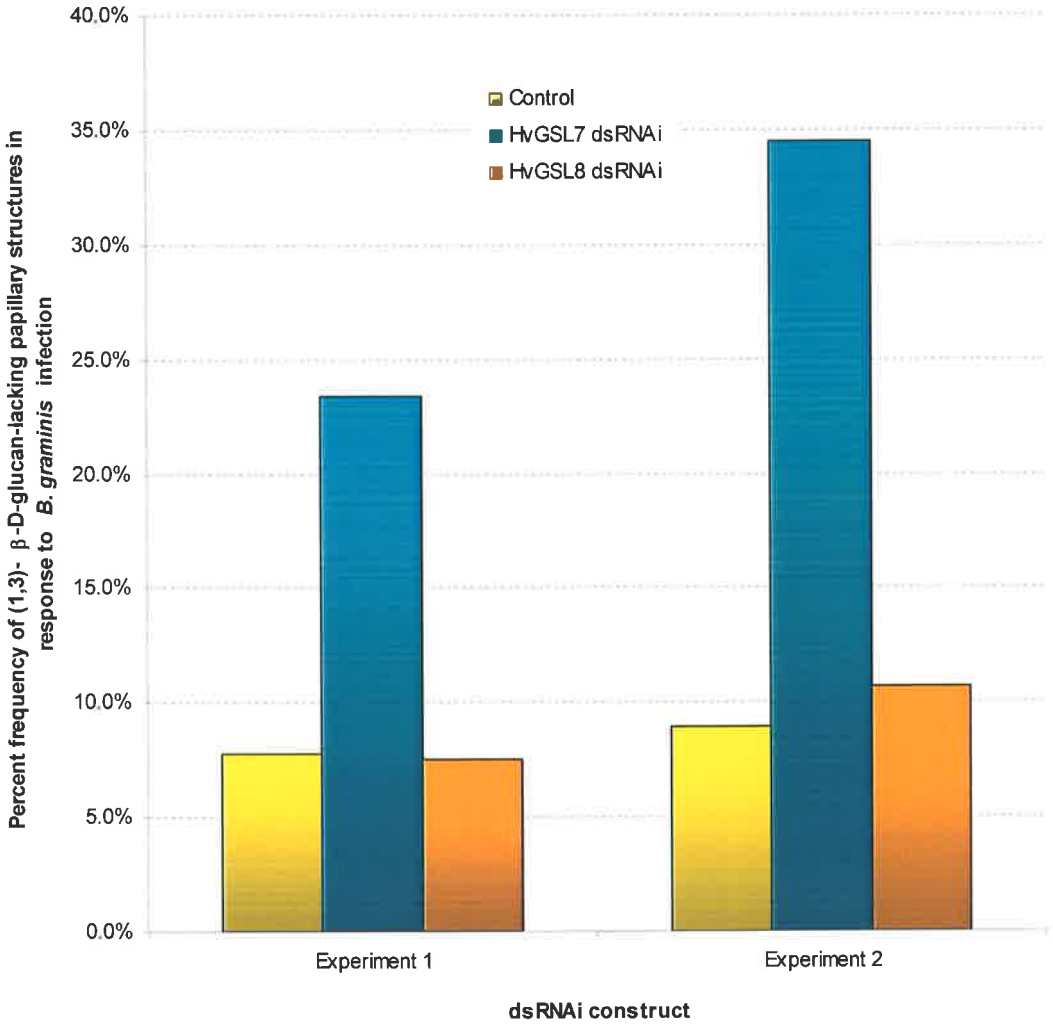

Figure 4.13: Frequency of (1,3)-β-D-glucan-lacking papillary structures in barley epidermal cells in response to *B. graminis* infection following gene silencing in two separate experiments. Pearson correlation coefficient between the two experiments: 0.997.

of a positively GUS stained cell was likely to indicate the transcription of the *HvGSL7*-dsRNAi molecule. An example of the effect of bombarding cells with the *HvGSL7*-dsRNAi construct on the deposition of (1,3)-β-D-glucan in papillary structures is illustrated by the two infection events in *Figure 4.14*. The first infection event, indicated by *Arrow I*, occurred in a cell that was not GUS-positive and presumably did not contain the high level of the *HvGSL7*-dsRNAi molecule (*Panel A*, *Figure 4.14*). When the first event was observed in the UV field, a deposit of (1,3)-β-D-glucan beneath the tip of the fungal appressorial lobe was detected by staining with the aniline blue fluorochrome (*Panel B*, *Figure 4.14*). The second infection event, indicated by *Arrow II*, occurred in a cell that was GUS-positive and presumably contained the *HvGSL7*-dsRNAi molecule (*Panel A*, *Figure 4.14*). When the second infection event was observed in the UV field, there was no (1,3)-β-D-glucan observed beneath the tip of the fungal appressorial lobe (*Arrow II*, *Panel B*, *Figure 4.14*), which suggested that the presence of the construct resulted in the prevention of (1,3)-β-D-glucan deposition.

It was observed that 17.6% (135/767) of epidermal cells that stained positively for GUS, and therefore contained the *HvGSL7*-dsRNAi molecule, were also infected by *B. graminis* (*Table 4.2*). Of the 135 infection events of GUS-positive cells that were also bombarded with the *HvGSL7*-dsRNAi molecule, it was observed that 38 (28.1%) lacked (1,3)-β-D-glucan in papillary structures (*Table 4.2*). As in the negative control, differences were observed between the two experiments. The lack of (1,3)-β-D-glucan in papillary structures that resulted from the infection of GUS positive cells was observed in 23.4% (18/77) of infection events in *Experiment 1*, and in 34.5% (20/58) of infection events in *Experiment 2* (*Table 4.2*; *Figure 4.13*). Overall, when the *HvGSL7*-dsRNAi molecule was present the percentage of papillary structures lacking (1,3)-β-D-glucan (28.1%) was higher than that observed in the negative control (8.1%; *Table 4.2*).

4.3.3 The Effect of Transiently Silencing *HvGSL8* on Papillary Structure

In assessing the effect of transient post-transcriptional gene silencing of *HvGSL8* on papillary structure, assumptions similar to those described in *Section 4.3.1* and

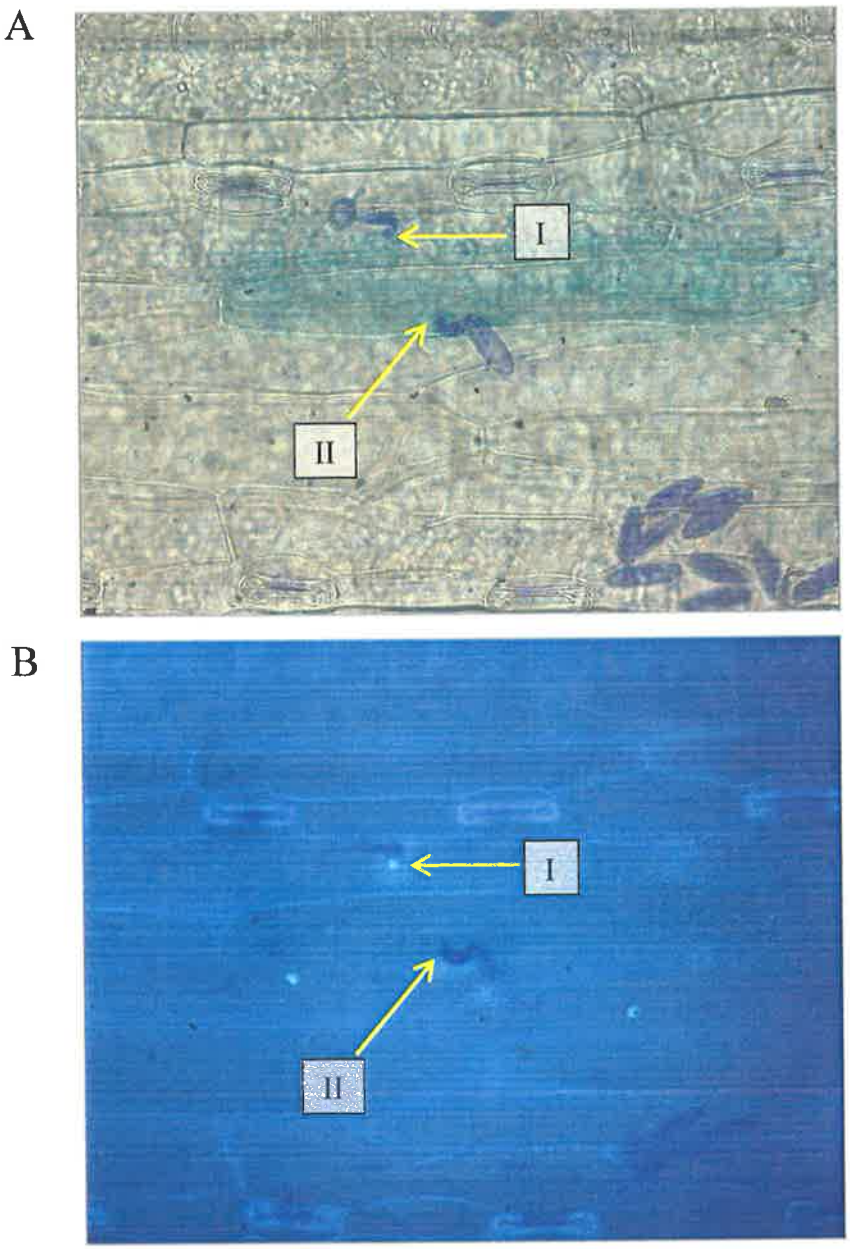

Figure 4.14: The effect of bombarding epidermal cells with the *HvGSL7* dsRNAi construct on *B. graminis* induced deposition of (1,3)-β-D-glucan in papillary structures. *Panel A*: Bright field microscopy. *Panel B*: UV field microscopy. *Arrow I*: The deposition of papillary (1,3)-β-D-glucan in a unbombarded cell. *Arrow II*: The lack of deposition of papillary (1,3)-β-D-glucan in response to the transcription of the *HvGSL7*-dsRNAi construct.

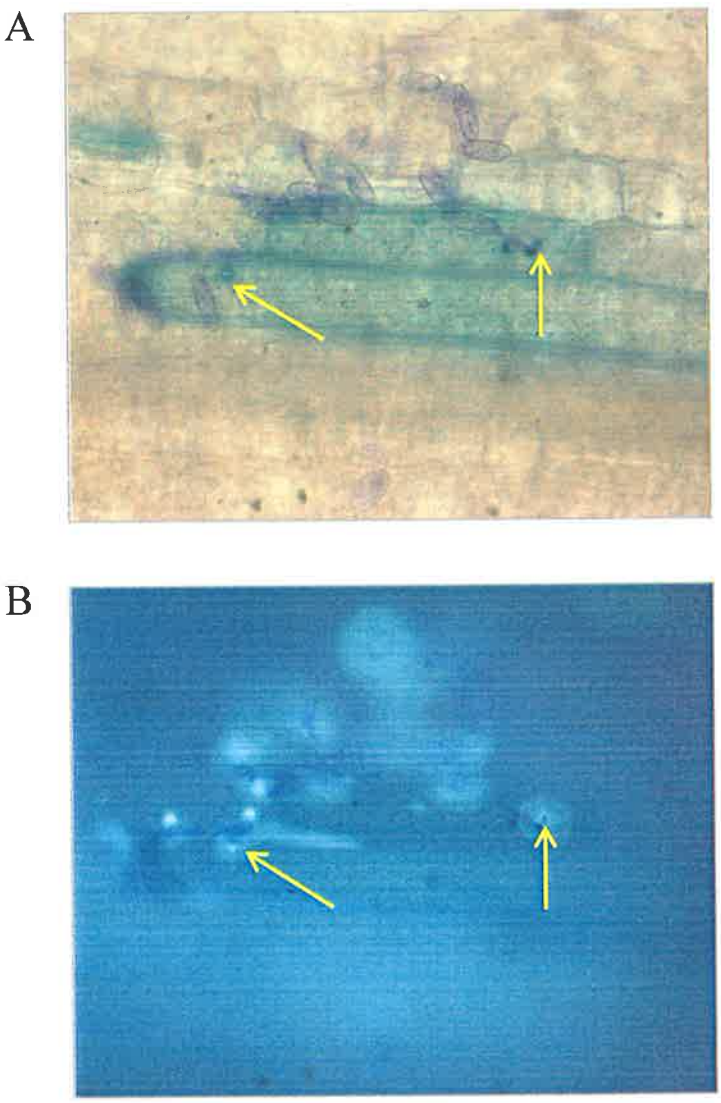

Figure 4.15: The effect of bombarding epidermal cells with the *HvGSL8* dsRNAi construct on *B. graminis* induced deposition of (1,3)-β-D-glucan in papillary structures. *Panel A*: Bright field microscopy. *Panel B*: UV field microscopy. Arrows indicate *B. graminis* structures that have induced the deposition of (1,3)-β-D-glucan in papillary of cells that are presumably transcribing the *HvGSL8* dsRNAi construct.

Section 4.3.2 were made. Thus, it was assumed that each gold micro-carrier was coated with both the GUS expression vector and the *HvGSL8*-dsRNAi construct, and that the observation of a positively GUS stained cell was likely to indicate transcription of the *HvGSL8*-dsRNAi molecule. An example of the effect of bombarding cells with the *HvGSL8*-dsRNAi construct on the deposition of (1,3)-β-D-glucan in papillary structures is illustrated by the two infection events in *Figure 4.15*. These occurred in adjacent GUS-positive cells that presumably also contained the *HvGSL8*-dsRNAi construct (*Figure 4.15*). Beneath the tip of the fungal appressorial lobes of both infection events, (1,3)-β-D-glucan was detected by staining with the aniline blue fluorochrome (*Panel B*, *Figure 4.15*).

It was observed that 96 out of 376 (25.5%) of GUS-positive epidermal cells, which presumably also contained the *HvGSL8*-dsRNAi molecule, were infected by *B. graminis* (*Table 4.2*). Of the 96 infection events, it was observed that nine papillary structures (totalling 9.4%) lacked (1,3)-β-D-glucan (*Table 4.2*). The lack of (1,3)-β-D-glucan in papillary structures that resulted from the infection of GUS-positive cells was observed in 7.5% (3/40) of infection events in *Experiment 1*, and in 10.7% (6/56) of infection events in *Experiment 2* (*Table 4.1*; *Figure 4.13*). Overall, when compared to the experimental control, the presence of the *HvGSL8*-dsRNAi molecule had no significant effect on the deposition of (1,3)-β-D-glucan in papillary structures.

4.4 DISCUSSION

The aim of the experiments described in this Chapter was to identify the *GSL* gene that is responsible for wound and papillary (1,3)-β-D-glucan deposition in barley. In Arabidopsis, *AtGSL5* is the gene that is required for wound and papillary (1,3)-β-D-glucan formation (Jacobs *et al.*, 2003; Nishimura *et al.*, 2003). When the *AtGSL5* gene function was disrupted, there was no (1,3)-β-D-glucan at wound sites or in fungal induced papillary structures (Jacobs *et al.*, 2003; Nishimura *et al.*, 2003). Thus, the penetration of fungal structures into host cells elicits a wound response (Jacobs *et al.*, 2003). It was also observed that Arabidopsis lines with disrupted *AtGSL5* gene function had increased resistance against fungal infection by various virulent powdery mildew strains (Vogel and Somerville, 2000; Jacobs *et al.*, 2003; Nishimura *et al.*, 2003), suggesting that fungi have exploited the hosts wound response for the establishment of a successful infection (*Section 4.1*).

Barley is a cereal crop that is commonly subjected to fungal infection by powdery mildew. It was anticipated that a functional orthologue of the *AtGSL5* gene in Arabidopsis would be discovered in barley. As mentioned in the *Introduction* of this Chapter (*Section 4.1*), the barley HvGSL7 and HvGSL8 enzymes had the highest deduced amino acid sequence identities to the AtGSL5 protein from Arabidopsis (*Table 2.3*). Furthermore, the analysis of transcription patterns in barley epidermal tissue in response to *B. graminis* infection showed that *HvGSL7* was the only *HvGSL* gene that exhibited an increase in transcript levels (*Figure 3.12*; *Figure 3.13*; *Figure 3.14*). Thus, at the commencement of the experiments described in this Chapter, *HvGSL7* and *HvGSL8* were considered to be likely orthologues of *AtGSL5*, with *HvGSL7* being the most likely candidate.

The experiments were designed to determine if either *HvGSL7* or *HvGSL8* were required for the deposition of papillary (1,3)-β-D-glucan in response to fungal infection of barley, and is summarised in *Figure 4.3*. Excised barley leaves were bombarded with gold particles that were coated with a GUS expression vector along with either the empty pHannibal vector, the *HvGSL7* dsRNAi vector, or the *HvGSL8* dsRNAi vector. The bombarded leaves were infected with *B. graminis* and

subsequently subjected to a staining procedure, which was used to detect GUS expression, fungal structures and the presence of (1,3)-β-D-glucan in papillary structures. The success of these experiments was dependent on the optimisation of *B. graminis* infection. One condition that had the potential to decrease the rate of *B. graminis* infection of the barley epidermal cells was the age of the leaf. It was previously reported that young 2.5 cm-long first leaf blades had a *B. graminis* infection rate of 60 – 70%, while older 14 cm-long first leaf blades had an infection rate of only 10% (Lin and Edwards, 1974; Nelson *et al.*, 1989). The initiation of germination and subsequent vigour of young barley seedlings used in the experiments described in this Chapter were variable. While some seedlings showed a first leaf of 2.5 cm-long, others had shoots that had barely emerged from the coleoptile. To ensure that the plant material was of consistent age, only seedlings with first leaf blades of 6.5 to 8 cm-long were chosen for bombardment and subsequent infection with *B. graminis*. In addition to leaf age, high fungal spore densities of over 100 spores per mm^2 may result in decreased infection rates, due to reduced germination and reduced appressorial penetration success rates (Carver and Ingerson-Morris, 1989; Bushnell, 2002). Thus, the inoculation density was adjusted until an even coverage was obtained (*Figure 4.11*), while minimising the occurrence of multiple fungal infections of a single cell. Following inoculation, the *B. graminis* spores were allowed 24 hr to establish infection (Green *et al.*, 2002). Overall, it was observed that 22.7% (404/1784) of all GUS stained cells were infected by a *B. graminis* spore (*Table 4.2*). In these infected GUS stained cells, the presence or absence of papillary (1,3)-β-D-glucan was recorded.

The detection of (1,3)-β-D-glucan in papillary structures was achieved by specific staining with the aniline blue fluorochrome. Papillary (1,3)-β-D-glucan appeared as an intense, localised, fluorescent deposit beneath the tip of the fungal appressorial lobes (*Figure 4.12*). It was observed that the aniline blue fluorochrome also detected (1,3)-β-D-glucan that was not associated with papillae. This background fluorescence was observed in trace amounts in the cell walls of guard cells and in epidermal cell walls. More importantly, (1,3)-β-D-glucan was also detected at wound sites, which resulted from leaf excision, minor damage caused whilst handling the leaves and

micro-projectile bombardment. The deposition of (1,3)-β-D-glucan is a known response to wounding (Stone and Clarke, 1992), and it has been reported that transient deposition of (1,3)-β-D-glucan is observed immediately following micro-projectile bombardment (Hunold *et al.*, 1994). The background (1,3)-β-D-glucan deposition was easily distinguishable from the papillary (1,3)-β-D-glucan, and therefore did not effect the results obtained from these experiments.

The effect of transiently silencing *HvGSL7* and *HvGSL8* genes on papillary (1,3)-β-D-glucan deposition was assessed in two separate, identical experiments to ensure reproducibility. It was observed that the two sets of experimental results had Pearson correlations of 0.997 (*Figure 4.9*). It may therefore be concluded that each experiment reflected the same result. Overall, there were fewer papillary structures that lacked (1,3)-β-D-glucan in *Experiment 1* than in *Experiment 2* (*Figure 4.9*). As stated above, there are several factors that can affect the efficiency of *B. graminis* infection, such as leaf age and the spore density. Despite taking great care to ensure consistency between the two experiments, it is possible that the leaves were slightly older and the density of spores was slightly higher in *Experiment 1* than in *Experiment 2*.

There were several assumptions that were made in the experimental duplicates. It was assumed that GUS expressing cells were also likely to be transcribing the dsRNAi silencing vectors. It was also assumed that transcription of the dsRNAi constructs resulted in the post-transcriptional gene silencing of the targeted *HvGSL*. Ideally, the transcript level of the targeted *HvGSL* in bombarded cells would be compared to a non-bombarded control to determine if the *HvGSL* was indeed down-regulated. However, detection of bombarded cells by staining for GUS involves fixing the tissue, which has an unknown effect on the RNA content of the cell. There is also considerable technical difficulty associated with the isolation of single bombarded cells from the leaf epidermis for the quantification of specific mRNAs. To overcome these difficulties, transformed barley lines stably expressing the *HvGSL7* and *HvGSL8* dsRNAi silencing molecules were constructed; these experiments are discussed in *Chapter 5*, *Section 5.2* (*Future Work*).

The combined results of both experimental controls show that most *B. graminis* infection events (91.9%) resulted (1,3)-β-D-glucan deposition in papillary structures (*Table 4.2*). It might be expected that (1,3)-β-D-glucan would be detected in all infected cells, but it is possible that some fungal spores may not have sufficiently progressed through the infection cycle to induce papillae formation and hence (1,3)-β-D-glucan may not have been deposited under the appressorial lobes. Alternatively, it has been previously reported that micro-projectile bombardment of cells may reduce the infection rate by as much as 25 – 50% (Bushnell, 2002), which may explain the lack of (1,3)-β-D-glucan in 8.1% of papillae in the experimental control.

When barley epidermal cells were bombarded with the *HvGSL8* dsRNAi silencing vector, the combined results from both experiments showed that the percentage of papillary structures lacking (1,3)-β-D-glucan (9.4%) that arose from fungal infection was comparable to the experimental control (8.1%; *Table 4.2*). Therefore, the transient silencing of *HvGSL8* did not seem to affect the deposition of (1,3)-β-D-glucan in papillary structures, and *HvGSL8* did not appear to function in the same way as the *AtGSL5* gene in Arabidopsis.

However, the combined results from both experiments showed that barley epidermal cells bombarded with the *HvGSL7* dsRNAi silencing vector had an increased number of *B. graminis* induced papillary structures that lacked (1,3)-β-D-glucan (28.1%), when compared with the experimental control (8.1%; *Table 4.2*). These results suggest that inhibition of (1,3)-β-D-glucan deposition in fungal induced papillary structures is achieved by transient transcription of the *HvGSL7*-dsRNAi construct, but not the *HvGSL8*-dsRNAi construct. It might be expected that if *HvGSL7* was required for the deposition of papillary (1,3)-β-D-glucan, then all cells that were expressing the *HvGSL7* dsRNAi silencing vector would lack (1,3)-β-D-glucan in papillary structures. However, since gene silencing by dsRNAi results in the degradation of mRNA (*Figure 4.2*), it is possible that proteins required for papillary (1,3)-β-D-glucan deposition could still have been present in the infected cells. Furthermore, it is conceivable that the efficiency of post-transcriptional gene

silencing is dependent on the number of dsRNAi constructs delivered into individual cells.

4.5 CONCLUSIONS

On the basis of amino acid sequence identity (*Chapter 2*), gene transcription patterns in response to *B. graminis* (*Chapter 3*) and other results presented in this Chapter, the barley *HvGSL7* gene is the most likely orthologue to the *AtGSL5* gene in Arabidopsis. Moreover, the data indicate that down regulation of the *HvGSL7* gene by dsRNAi is likely to reduce or abolish the deposition of wound (1,3)-β-D-glucan during penetration of fungal pathogens into barley leaves.

Chapter 5

General Discussion

5.1 SUMMARY of EXPERIMENTAL RESULTS

The central objective of the work described in this thesis was to isolate *HvGSL* cDNA fragments from barley and to characterise the functions of members of the *HvGSL* gene family. While all the genes were expected to be involved in (1,3)-β-D-glucan synthesis, the more important question related to the definition of the specific cellular processes in which (1,3)-β-D-glucan synthesis was involved, including such processes as cell plate formation, wound response and plasmodesmata (1,3)-β-D-glucan deposition. There was a particular emphasis on the identification of a barley orthologue of the Arabidopsis *AtGSL5* gene, which lacked wound (1,3)-β-D-glucan and had an increased fungal resistance in Arabidopsis lines that contained a disrupted *AtGSL5* gene (Jacobs *et al.*, 2003; Nishimura *et al.*, 2003), in the expectation that discovery of this orthologue would provide opportunities in the future for the engineering of fungal resistance into a commercially important crop.

The HvGSL *Gene Family in Barley*

To identify the barley orthologue of the *AtGSL5* gene, *HvGSL* genes were initially identified by PCR directed cloning and DNA sequencing. Prior to the commencement of this project, a former student of the Fincher laboratory, Dr Jing Li, characterised a full length *GSL* gene from barley, *HvGSL1* (Li *et al.*, 2003). During the present project, six or possibly seven additional, partial length *HvGSL* genes (denoted *HvGSL2* to *HvGSL8*) were cloned and sequenced (*Figure 2.17*). It was observed that *HvGSL5* mapped to the same chromosomal location as *HvGSL2* on the long arm of the barley chromosome 6H. Thus, it is possible that *HvGSL5* and *HvGSL2* are fragments of the same gene.

Most nucleotide sequence data was obtained for *HvGSL8* because of its high sequence identity to *AtGSL5* at the amino acid level. The deduced HvGSL8 protein was observed to have a similar predicted membrane topology, as determined by three membrane prediction programs (*Figure 2.23*), to the yeast FKS1 (Douglas *et al.*, 1994), NaGSL1 (Doblin *et al.*, 2001), cotton GhGSL1 (Cui *et al.*, 2001), barley HvGSL1 (Li *et al.*, 2003) and Arabidopsis AtGSL5 (Østergaard *et al.*, 2002) proteins. The large hydrophilic loop of the HvGSL8 protein, which is assumed to be

facing the cytoplasm (Douglas *et al.*, 1994), has approximately 700 amino acids and is flanked by two regions containing a total of 11 to 15 hydrophobic transmembrane helices. The predicted cytoplasmic domains of the putative (1,3)-β-D-glucan synthases are highly conserved throughout the plant GSL proteins and are thought to contain the amino acid residues required for enzymatic activity. However, there is no sequence identity between the conserved cytoplasmic region of the HvGSL8 protein, or other putative (1,3)-β-D-glucan synthases, with proteins such as cellulose-synthase like enzymes that are known to be involved in the attachment of a glucosyl residue to a growing glucan chain (*Section 2.3.14*). The absence of UDP-glucose binding motifs within the amino acid sequence of FKS and GSL proteins might be explained by the fact that they are active only as part of a complex with other proteins that have UDP-glucose binding capabilities (Verma and Hong, 2001). Alternatively, it is possible that a novel and previously unidentified UDP-glucose binding motif is located within the conserved cytoplasmic region of plant GSL proteins.

Determination of Orthologous Genes Based on Sequence Identity

The potential functions of cloned *HvGSL* genes were initially determined by the comparison of the barley sequences with other plant *GSL* genes for which functions have been previously defined. It was believed that *HvGSL* genes with high sequence identity with other better characterised *GSL* genes might also have functional homology with those genes. For example, the *GhGSL1* gene from cotton, which is expressed in young roots and may have a role in the development of the primary wall (Cui *et al.*, 2001), was shown to share 69.2% identity with the encoded amino acid sequence of the *HvGSL1* gene (*Table 2.4*). The *NaGSL1* gene cloned from cultured tobacco pollen tubes (Doblin *et al.*, 2001), shared a high deduced amino acid sequence identity with the *HvGSL2* gene (61.7%) and the *HvGSL3* gene (61.5%; *Table 2.4*). In Arabidopsis, the *AtGSL6* (*CalS1*) gene has been implicated in the formation of the cell plate (Hong *et al.*, 2001a) and has the highest deduced amino acid sequence identity with the *HvGSL2* gene (72.1%) and the *HvGSL6* gene (66.8%; *Table 2.4*). Also in Arabidopsis, the *AtGSL5* gene is transcribed in flowers (Østergaard *et al.*, 2002; Enns *et al.*, 2005) as well as being involved in the deposition of wound and papillary (1,3)-β-D-glucan (Jacobs *et al.*, 2003; Nishimura

et al., 2003). The most likely barley orthologue of *AtGSL5* based on amino acid sequence identity is *HvGSL7*, which had an identity of 72.1% (*Table 2.3*; *Table 2.4*).

Transcript Profiling of HvGSL *genes*

Although the *HvGSL* genes have sequence identity to other plant *GSL* genes that have been characterised functionally, it was not known for certain that they are functionally homologous. Therefore transcript profiling techniques were used in attempts to define the locations of *HvGSL* gene transcription and to identify any genes that might be co-transcribed with individual *HvGSL* genes. In this way it was expected that further clues to the specific functions of individual HvGSL genes might be revealed.

The genes that co-transcribed with barley *GSL* genes, as determined by analysis of the Affymetrix Barley1 Chip, were examined to determine if they were specifically transcribed during plant development or in tissues and processes associated with the deposition of (1,3)-β-D-glucan. Only *HvGSL1*, *HvGSL2*, *HvGSL3* and *HvGSL4* were represented by oligonucleotides on the array. No other genes that were co-ordinately transcribed with *HvGSL1* and were obviously associated with the synthesis of (1,3)-β-D-glucan were detected. However, *HvGSL2* was co-ordinately transcribed with a meiosis specific gene (*DMC1*; *Figure 3.4*), which may suggest that *HvGSL2* is required for the deposition of (1,3)-β-D-glucan during micro- or megasporogenesis (*Table 5.1*). It was also observed that *HvGSL4* was co-ordinately transcribed with a protein that was up-regulated in response to viral infection (*Figure 3.6*), which may suggest that the (1,3)-β-D-glucan deposition that is responsible for plasmodesmatal closure and limiting viral spread might be mediated by *HvGSL4* (*Table 5.1*).

The genes that were co-ordinately transcribed with *HvGSL* genes, as determined by the analysis of microarray data, were also assessed to determine if they were possible components of a proposed active (1,3)-β-D-glucan synthase complex (Verma and Hong, 2001). It was observed that *HvGSL3* had a similar transcription pattern to a putative glycosyltransferase gene (*Figure 3.5*), and it is theoretically possible that the encoded

Barley (1,3)-β-D-Glucan Synthase Genes		Orthologues	
Gene	Possible Functions in Barley	Gene and Possible Functions	References
HvGSL1	*not known*	*GhGSL1* – expressed in young roots - during the development of primary walls *AtGSL10 – not known*	(Cui *et al.*, 2001) *Table 2.5*
HvGSL2	(1,3)-β-D-Glucan deposition during meiotic division	*AtGSL6/CalS1* – possible role in cell plate formation *NaGSL1* – expressed in cultured pollen tubes *AtGSL12 – not known*	(Hong *et al.*, 2001a) (Doblin *et al.*, 2001) *Table 2.5*
HvGSL3	Endosperm cellularisation- not required in grain after 6 DAP	*NaGSL1* – expressed in cultured pollen tubes *AtGSL12 – not known*	(Doblin *et al.*, 2001) *Table 2.5*
HvGSL4	Closure of plasmodesmata	*AtGSL8 – not known*	*Table 2.5*
HvGSL5	*not known*	*AtGSL12 – not known*	*Table 2.5*
HvGSL6	Endosperm cellularisation- increased transcript 5 DAP Most likely candidate for cell plate formation	*AtGSL6/CalS1* – possible role in cell plate formation *AtGSL3 – not known*	(Hong *et al.*, 2001a) *Table 2.5*
HvGSL7	Fungal induced papillary (1,3)-β-D-glucan deposition Wound (1,3)-β-D-glucan deposition	*AtGSL5* – is expressed and has a function in flowers - Expressed in response to wounding and fungal infection	(Ostergaard *et al.*, 2002; Enns *et al.*, 2005) (Nishimura *et al.*, 2003; Jacobs *et al.*, 2003)
HvGSL8	*not known*	*AtGSL1 – not known*	*Table 2.5*

Table 5.1: Possible gene functions of barley *GSL* genes based on the results that are described in this thesis. Orthologues to the barley *GSL* genes are based on amino acid sequence identity as presented in *Table 2.5*.

protein is a component of an active enzyme complex. However, at this stage there is insufficient evidence to conclude that the putative glycosyltransferase participates with the HvGSL3 protein in a complex that synthesises (1,3)-β-D-glucan. The *HvGSL3* gene also had a similar transcription pattern with an ankyrin-like protein (*Table 3.6*), which is a protein used to target other proteins to specialised plasma membrane and endoplasmic reticulum domains (Bennett and Baines, 2001). Thus, the ankyrin-like protein might assist in the transport of protein components of the (1,3)-β-D-glucan synthase protein complex to regions that require the deposition of (1,3)-β-D-glucan. However, further experiments are required to test this hypothesis.

The transcript profiles of *HvGSL* genes were also assessed by Q-PCR analysis of various tissues, developmental stages and plant responses associated with the deposition of (1,3)-β-D-glucan. The analyses were based on the premise that *HvGSL* genes with high transcript abundance in tissues undertaking processes involving (1,3)-β-D-glucan are more likely to be synthesising the (1,3)-β-D-glucan characteristic of a particular cellular process. For example, in the developing endosperm, (1,3)-β-D-glucan is deposited during cellularisation, which occurs between two and six days post-fertilisation (*Section 1.2.2.3*). At the completion of cellularisation, (1,3)-β-D-glucan is completely replaced by other polysaccharides (*Section 1.2.2.3*). It was observed by QPCR analyses that *HvGSL3* was transcribed almost exclusively during endosperm cellularisation, and that *HvGSL6* transcript abundance was greater than other *HvGSL* genes near the completion of endosperm cellularisation (*Figure 3.11*). It therefore appears that *HvGSL3* and *HvGSL6* are the most likely candidates for (1,3)-β-D-glucan deposition during endosperm cellularisation (*Table 5.1*).

The transcript abundance of *HvGSL* genes in the meristematic leaf base (*Figure 3.9*) and the root tip (*Figure 3.10*) of barley were also determined by Q-PCR. In the meristematic tissues, the dividing cells deposit (1,3)-β-D-glucan at the forming cell plate (*Section 1.2.2.1*). It was observed that *HvGSL6* was transcribed almost exclusively in the tissue located in the leaf base, when compared with the remainder of the leaf. As mentioned above, the deduced amino acid sequence of the *HvGSL6*

gene also had the highest homology to *AtGSL6*, which has been implicated in the deposition of (1,3)-β-D-glucan at the forming cell plate of dividing cells in Arabidopsis (Hong *et al.*, 2001a). Thus, *HvGSL6* is a candidate for the deposition of (1,3)-β-D-glucan at the forming cell plate (*Table 5.1*).

To identify of the barley orthologue of the *AtGSL5* gene of Arabidopsis on the basis of transcription patterns, the *HvGSL* genes were assessed by Q-PCR in powdery mildew infected barley epidermal tissue. It was observed that *HvGSL7*, which also had the highest amino acid sequence identity to *AtGSL5* (*Table 2.4*), was the only *HvGSL* gene that exhibited an increase in transcript abundance in response to *B. graminis* infection (*Figure 3.12*; *Figure 3.13*; *Figure 3.14*). These results identified *HvGSL7* as the most likely candidate for the deposition of (1,3)-β-D-glucan in fungal induced papillary structures that arise as a result of powdery mildew infection (*Table 5.1*).

Transiently Induced Post-Transcriptional Gene Silencing of HvGSL *Genes*

As mentioned above, the deduced amino acid sequences of *HvGSL7* and *HvGSL8* have the highest identity to the deduced amino acid sequence of *AtGSL5*, and *HvGSL7* was the only *HvGSL* gene to have an increase in transcript abundance in infected epidermal tissue. Thus, the barley *HvGSL7* and *HvGSL8* genes were considered to be possible orthologues of *AtGSL5* in Arabidopsis, with *HvGSL7* being the most likely orthologue. The *AtGSL5* gene in Arabidopsis has been implicated in the deposition of (1,3)-β-D-glucan in response to wounding, and hence in papillary structures in response to fungal attack, suggesting that fungal induced papillary (1,3)-β-D-glucan deposition is a wound response (Jacobs *et al.*, 2003; Nishimura *et al.*, 2003). When *AtGSL5* was silenced with dsRNAi and T-DNA insertion (Jacobs *et al.*, 2003) or truncated (Nishimura *et al.*, 2003) such that functional AtGSL5 was reduced or absent, the Arabidopsis plants lacked (1,3)-β-D-glucan at wound sites and in papillary structures and were more resistant to a variety of virulent pathogens (Vogel and Somerville, 2000; Jacobs *et al.*, 2003).

It was not possible to investigate the effects of silencing HvGSL7 on wound (1,3)-β-D-glucan deposition without generating transgenic barley lines. Time constraints precluded this approach. However,to further investigate the possibility that *HvGSL7* and *HvGSL8* are functional orthologues of *AtGSL5*, and that they have a role in plant-pathogen interactions between barley and powdery mildew, a system was developed to transiently silence *HvGSL7* and *HvGSL8* in barley epidermal tissue such that the effects of silencing on (1,3)-β-D-glucan deposition in papillary structures following fungal attack of individual cells could be studied. It was observed that when *HvGSL7*, but not *HvGSL8*, was transiently silenced using dsRNAi in infected cells there was an increase in the number of papillary structures that lacked (1,3)-β-D-glucan. These results suggested that *HvGSL7* is the functional orthologue of *AtGSL5* and functions in the deposition of (1,3)-β-D-glucan in fungal induced papillary structures, which represent a recognised wound response (Jacobs *et al.*, 2003).

5.2 FUTURE WORK

Barley is an important crop species in the food and brewing industry. Understanding which *HvGSL* genes are involved in "yield limiting" processes such as endosperm cellularisation and fungal disease resistance may be of great commercial importance. The work described here was performed in barley and was focused on the cloning and identification of genes required for the deposition of (1,3)-β-D-glucan in various tissues at different stages of development and under fungal attack. The development of hypotheses on *HvGSL* gene function was initially achieved through the analysis of transcription patterns determined *via* Q-PCR and through the identification of co-ordinately transcribed genes *via* microarray data (*Chapter 3*). The analysis of *HvGSL* gene transcript abundance by Q-PCR was effective in determining the amount of *HvGSL* mRNA that was present in each tissue type. However, the transcript analyses do not necessarily indicate the presence of active HvGSL enzymes or the presence of (1,3)-β-D-glucan *in vivo*. Additional experiments to support the results from transcript analysis experiments may include *in situ* hybridisation to determine the specific tissue types in which transcription is occurring, and immuno-gold labelling of individual HvGSL proteins coupled with the determination of the (1,3)-β-D-glucan

content of the tissues used in the Q-PCR analysis. The results presented in *Chapter 3* also identified a putative glycosyltransferase that has a transcription profile similar to *HvGSL3*, and to determine whether a protein-protein interaction exists between these proteins it is suggested that a yeast-2-hybrid analysis is performed.

Stable Barley Transformation with HvGSL7 *and* HvGSL8 *dsRNAi*

The results described in this thesis demonstrated through sequence identity (*Chapter 2*), transcript profiling (*Chapter 3*) and post-transcriptional gene silencing (*Chapter 4*) that *HvGSL7* was required for the deposition of (1,3)-β-D-glucan in papillary structures, and was the most likely orthologue of *AtGSL5* (Jacobs *et al.*, 2003; Nishimura *et al.*, 2003). However, it is uncertain if the decreased synthesis of (1,3)-β-D-glucan in fungal induced papillary structures results in an increased level of resistance to pathogens, as was observed in the *AtGSL5* dsRNAi and T-DNA insertion lines. To further investigate this, barley lines stably transcribing the *HvGSL7* and *HvGSL8* dsRNAi molecules have now been generated. Due to time constraints these lines are yet to be analysed, but it is anticipated that analyses will provide useful insight into the infection process of barley by pathogenic fungi, as well as providing valuable information on the function of a barley *HvGSL7* gene. It is important to remember that broad spectrum resistance to fungal infection in an important crop species such as barley would carry extremely valuable social, economic and environmental benefits.

At the time of writing this thesis the T_0 *HvGSL7* dsRNAi lines, the T_0 *HvGSL8* dsRNAi lines and the T_0 control lines were being grown in the glasshouse. These lines were generated using DNA constructs described in this thesis, modifications of these constructs (*Figure 5.1*) and *Agrobacterium* mediated transformation of the barley cultivar, Golden Promise. The generated lines have been analysed by Southern hybridisation using the hygromycin antibiotic resistance gene as a probe to confirm the presence of the transgene (Dr Rohan Singh, *personal communication*). Of four plants that were putatively transformed with the pPG1 vector, two were confirmed positive by Southern hybridisation. A total of 69 putative *HvGSL7* dsRNAi transgenic plants were generated and 41 were confirmed positive by Southern

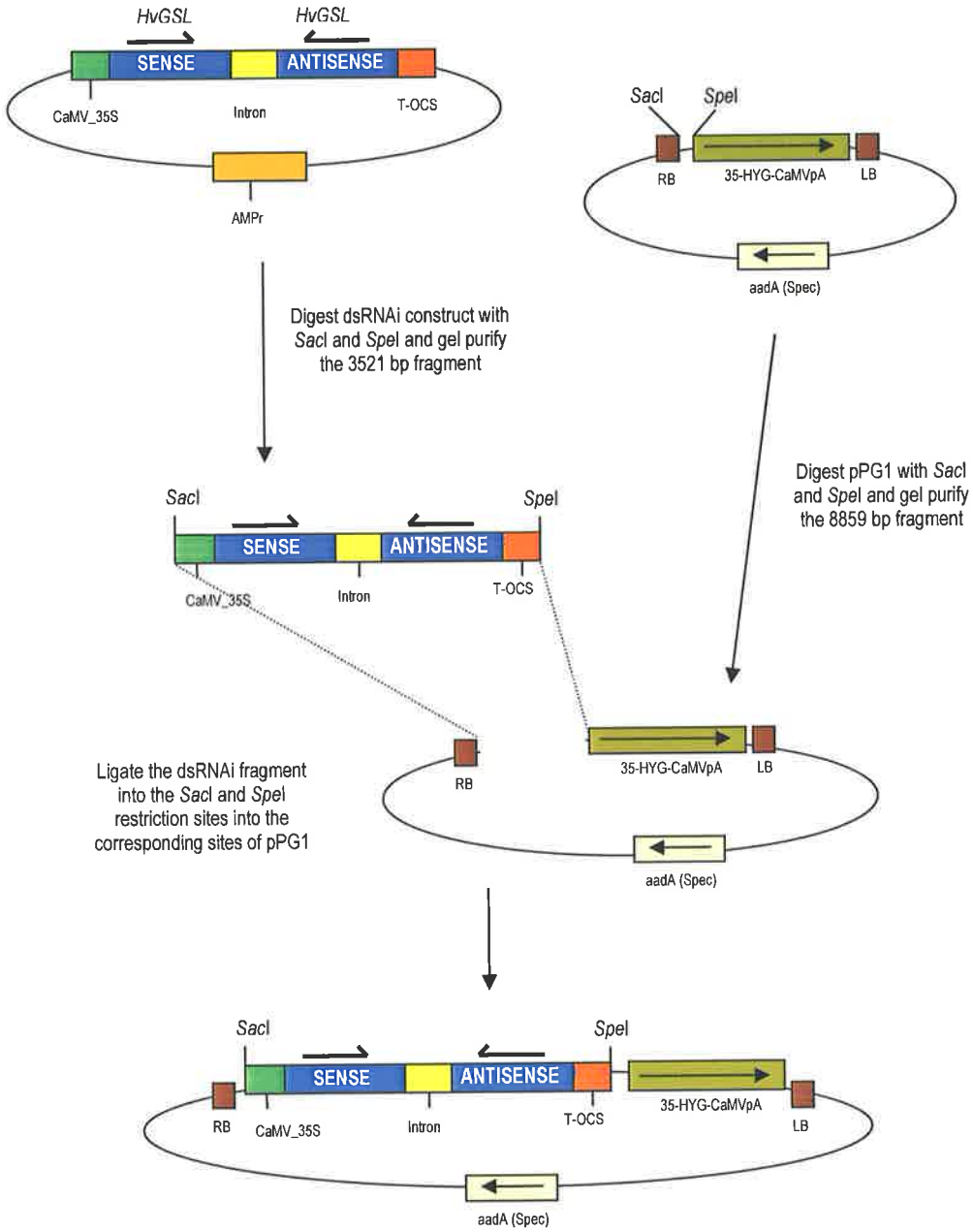

Figure 5.1: Schematic diagram of the cloning strategy used for the construction of the *HvGSL7* and *HvGSL8* dsRNAi binary plasmids for stable transformation. The hygromycin (HYG) gene in the pPG1 (*Figure 5.2*) vector is driven by the CaMV_35S promoter and is terminated by the OCS terminator. The vector also has spectinomycin bacterial selection. The right border sequence (RB) and left border sequence (LB) flank the T-DNA region, which includes the dsRNAi and hygomycin resistance gene that was inserted into the barley genome *via Agrobacterium tumefaciens*.

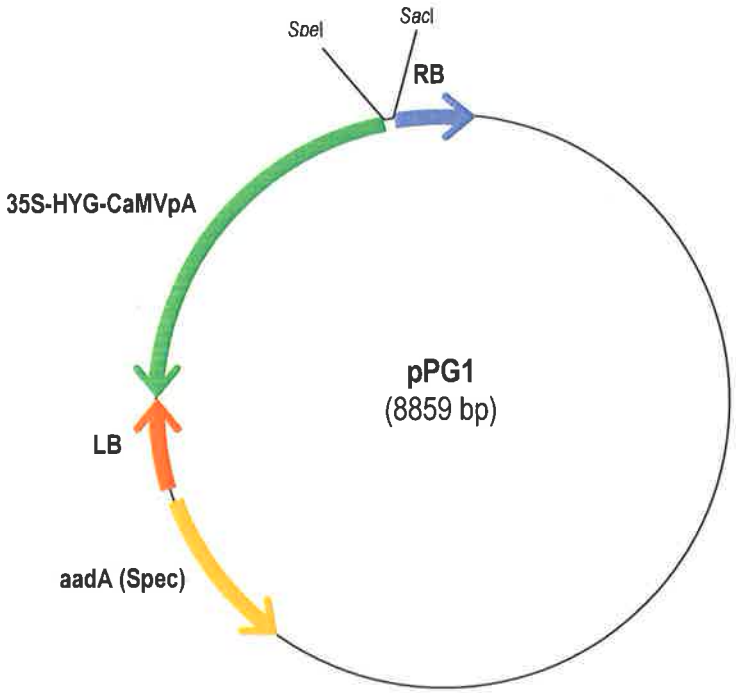

Figure 5.2: Schematic diagram of the pPG1 plasmid used in the generation of stably transformed barley lines. The binary vector was based on pPZP200 (Hajdukiewicz *et al.*, 1994) and was constructed by Dr Paul Gooding (University of Adelaide, SA, Australia). Bacterial selection was *via* the spectinomycin resistance gene (aadA). Planta selection was *via* the hygromycin resistance gene (HYG). The transcription of the HYG gene was driven by the CaMV35S promoter and stopped with the CaMV35S polyadenylation terminator. LB: left border sequence. RB: right border sequence.

hybridisation. Of 37 plants that were putatively transformed with the *HvGSL8* dsRNAi, 17 were confirmed positive by Southern hybridisation. To ensure that the presence of the dsRNAi sequences has resulted in the decrease in transcript levels, the transcript abundance of *HvGSL7* and *HvGSL8* will be assessed by Q-PCR in the transformed lines.

It was observed that when *AtGSL5* gene function was disrupted in Arabidopsis, there was an absence of wound induced (1,3)-β-D-glucan deposition (Jacobs *et al.*, 2003; Nishimura *et al.*, 2003). It is therefore of considerable interest to determine whether the dsRNAi transformed barley lines with decreased *HvGSL7* transcript abundance also lack wound induced (1,3)-β-D-glucan deposition as observed in Arabidopsis. Leaf lesions that are caused by metal toxicity (e.g. manganese and aluminium) are wound-like and result in (1,3)-β-D-glucan deposits at the lesion site (Wissemeier and Horst, 1987). To determine whether the deposition of (1,3)-β-D-glucan at these lesion sites is a wound response, it is suggested that transformed barley lines be grown in soil with toxic levels of manganese and aluminium and subsequently staining the leaves with aniline blue fluorochrome.

There are a number of foliar fungal pathogens known to infect barley, resulting in a decrease in yield from barley crops. Barley powdery mildew (*B. graminis*) potentially can cause up to 15% yield losses; stem rust (*Puccinia graminis tritici, P. secalis* and *P. tritici*) potentially causes up to 30% yield losses; leaf rust (*Puccinia hordei*) can potentially cause up to 50% yield losses (http://www.dpi.qld.gov.au/fieldcrops/7690.html); and net blotch (*Pyrenophora teres*) potentially causes yield losses of up to 50% (http://www.grdc.com.au/growers/res_upd/north/02/dubbo_barley_diseases.htm). Therefore, it would be of great commercial interest to determine the resistance of the stable *HvGSL7* dsRNAi transgenic lines against a broad spectrum of barley fungal pathogens. The transformed barley lines should be infected with the above pathogens and scored for resistance.

If the *HvGSL7* is a true homologue of *AtGSL5*, the *HvGSL7* dsRNAi lines might reasonably be expected to be resistant to a range of barley pathogens. Since cereal

fungal pathogens decrease barley crop yields by as much as 50%, these experiments are potentially of great interest to farmers and the brewing industry.

Work to be performed in Arabidopsis:

Although the work described in this thesis was performed using barley, there are several experiments that would be best performed in Arabidopsis. Arabidopsis has a small genome that has been sequenced, is readily transformed and responds to stress and disease in a similar manner to crop species. An experiment that would give insight on individual *AtGSL* gene function is the use of GFP-promoter fusions to determine when the individual genes are transcribed. Furthermore, it is suggested that tobacco plants transformed with GFP-AtGSL fusion proteins be constructed to observe the cellular location of individual AtGSL proteins. This approach has proven successful in the localisation of one AtGSL protein, namely CalS1 (AtGSL6), to the forming cell plate of dividing cells (Hong *et al.*, 2001a). It is therefore suggested that this technique is used for the remaining *AtGSL* genes.

It might also be suggested that the requirement of *AtGSL5* in the deposition of (1,3)-β-D-glucan in response to wounding and pathogen infection (Jacobs *et al.*, 2003; Nishimura *et al.*, 2003) to be used as a model system for the analysis of (1,3)-β-D-glucan synthesis. By manipulating the sequence of *AtGSL5* or other genes encoding proteins that are potentially part of the (1,3)-β-D-glucan synthase complex, and using Arabidopsis transformation techniques, the effects of these manipulations may be easily assessed by wounding the tissue and staining with aniline blue fluorochrome.

Primer	Sequence (5'-3')
T-RACE	GACTCGAGTCGACATCGATTTTTTTTTTTTTTTT
RACE3'	GACTCGAGTCGACATCG
T7	ATTATGCTGAGTGATATCCC
SP6	ATTTAGGTGACACTATAG
AP1	GGATCCTAATACGACTCACTATAGGG
AP2	AATAGGGCTCGAGCGGC
Hannibal_3F	CAAGGTAACATGATAGATCATGTC
Hannibal_3R	GCAAATATCATGCGATCATAGGC
Hannibal_5F	GTGACATCTCCACTGACGTAAGG
Hannibal_5R	CATACTAATTAACATCACTTAAC
HvGSL2	
*HvGSL2*_R2	CTCTGAGCCGTGACATCTACC (*forward primer*)
*HvGSL2*rev	CGACGGCAATCTATCCATCTACC
*GSL2*_3RACE_F1	CTCTGAGCCGTGACATCTACC
*GSL2*_3RACE_F2	CTATACTACCATTGGCTTTTAC
HvGSL3	
*HvGSL3*_F	GCCGATTACCGTCCTGTC
*HvGSL3*_R	GCCCGTTCCTTCTTCTG
*HvGSL236*_F3	GCDTGGTTYATGTCVAATCARG
HvGSL3-R3	GACAGGACGGTAATCGGC
HvGSL4	
HvGSL4-1_F3	GAGGACTTTGATGACTGGACAA
HvGSL4-1:F1	GAAAATAGTTGGGAATCT
HvGSL5	
HvGSL5-F1	CAACAGCGTAAGCTTCTCC
HvGSL5-R1	CAGCATCAACTCTCATTGG
HvGSL5-F2	CTTGCGGTTTATGCCAG
HvGSL5-R2	CATCATAGTTTCTCCTATGCG
HvGSL6	
HvGSL6-1_F1	CCGTGGAGGTATTGGTG
HvGSL6-1_F2	AATCGTGGTGGGACAAAGA
HvGSL7	
HvGSL7-F3	CAAGTTTTGTCACTCTGGGGC
HvGSL7-R2	GTTCCTGGTGATGTACTCCTCG
HvGSL7-F1	CATTATGGCCACCCAGATGT
HvGSL8	
Group1-F3	GACGA-T[C]-A[G]-TCAA-T[C]-GAGTA-T[C]-TTCTGG
HvGSL8-F3	CTGTATCTGGCTCTGAGTGG
HvGSL8-F3(r)	CCACTCAGAGCCAGATACAG
HvGSL8-F4	CCTCCAGATTAAGCCGATGGT
HvGSL8-F5	GATGAGGTCCATCACGAGATG
HvGSL8-F6	GTCGCTTGCCAGATATACG
HvGSL8-F7	GTTGGGCTTAATCAGATATCG
HvGSL8-F8	CAGTGGCAATGGTGAACAGAC
HvGSL8-R1	GCGAAACTCTTATGCTGC
HvGSL8-R2	CATCTCGTGATGGACCTCATC
HvGSL8-R3	GGATCTGGATGTCGCGGTG
HvGSL8-R4	CAATGATCATCGCTGCCTG
HvGSL8-R5	CTCAATATCGATAGAGCGG
HvGSL8-R6	GATGTAGCAGAGACATTCC

Primer	Sequence (5'-3')
Q-PCR and Mapping	
*HvGSL1*_F	TTAGTGGTTTTGGCAGGTTTG
*HvGSL1*_R	CGTGTCTGGAAGGTGGAG
*Hvgsl2*for	TGGGGCTGCTGCTCTTCAC
*Hvgsl2*rev	CGACGGCAATCTATCCATCTACC
*HvGSL3*_F	GCCGATTACCGTCCTGTC
*HvGSL3*_R	GCCCGTTCCTTCTTCTG
*HvGSL4*_F5	GAACAAGGCGAACCAAGAG
*HvGSL4*_R1	CAAGCGATTAGCGTCCAAGT
*HvGSL6*F.2	ATTCTGCTGCCACGGTTG
*HvGSL6*R.2	CCCACATCGCTACAGGTCTA
GSL7-fQPCR	GGAGTGATTGTTATGACACCTG
GSL7-rQPCR	GAATCAAGGTAAGGATGTCGC
GSL8-fQPCR	CAAGAAATGCAGACAAGGGTA
GSL8-rQPCR	CCAAGACTCAATGCCTAAATCAC
EXTRA Mapping primers	
GSL2-mapF:	CGTGGAGCAAGGACGATA
GSL2-mapR:	GTCACAATCACCAATATCAGATA
HvGSL4-R1m:	CTGTGATTACTGCTATCAGG
HvGSL6-R1m:	GATCGAACCAGACGGCTG
***HvGSL7* dsRNAi Vector Construction**	
f*GSL7-Eco*RI	CCGGAATTCGAATCAAGGTAAGGATGTCGC
f*GSL7-Xho*I	CCGCTCGAGGGAGTGATTGTTATGACACCTG
r*GSL7-Hin*dIII	CCCAAGCTTGAATCAAGGTAAGGATGTCGC
r*GSL7-Xba*I	GCTCTAGAGGAGTGATTGTTATGACACCTG
NB: restriction sites are underlined, gene specific regions are highlighted in yellow	
***HvGSL8* dsRNAi Vector Construction**	
f*GSL8-Eco*RI	CCGGAATTCCAAGACTCAATGCCTAAATCAC
fGSL8-*Xho*I	CCGCTCGAGCAAGAAATGCAGACAAGGGTA
rGSL8-*Hin*dIII	CCCAAGCTTCAAGACTCAATGCCTAAATCAC
r*GSL8-Xba*I	GCTCTAGACAAGAAATGCAGACAAGGGTA
NB: restriction sites are underlined, gene specific regions are highlighted in yellow	

HvGSL1
AJ461988; AJ467227; AJ467228; AJ467229; AJ468227; AJ468229;
AJ468228; AV836635; AV837078; BE215834; BG415664; BG417338;
BG418775; BJ474560; BU969103; CA031522

HvGSL2
AJ433457; AJ434225; AJ483959; AJ483960; AV923029; AV926707;
AV926708; AV926824; AV927733; AV931607; AV931608; AV931716;
AV932586; AV934137; AV934689; AV936387; BF265457; BF616755;
BF627189; BG369637; BG418430; BJ469639; BJ469981; BJ470174;
BJ471422; BJ472233; BJ473076; BJ473277; BJ473617; BJ474020;
BJ474554; BJ475011; BJ476230; BJ477252; BJ477461; BM374437;
BM377017; BQ661605; CA027060; CD663693; CD663695

HvGSL3
BM374568; BU972175

HvGSL4
BE559011; BU995906; CB882058; CD054711; CD057892; CD662722;
CK567361; CK567549

HvGSL5
AJ465826; AJ465827; BQ758968; BQ763060; BU994764; CB880894

HvGSL6
BU999201; CA018258

HvGSL7
BJ462458

HvGSL8
BU971000

The following is the nucleotide and deduced amino acid sequence of the *HvGSL1* open reading frame from barley as described by Li *et al.* (2003). The highlighted sequences at the 3' end of the gene are those used for the generation of mapping probes (*Chapter 2*) and for the analysis of gene transcription through Q-PCR (*Chapter 3*).

```
ATGGCGAGGGCGGAGGCCAACTGGGAGCGCCTGCTGCGGGCGGCGCTGCGCGGGGACCGGATGGGCGGCGTCTACGGGGTCCCCGCCAGC   90
 M  A  R  A  E  A  N  W  E  R  L  L  R  A  A  L  R  G  D  R  M  G  G  V  Y  G  V  P  A  S    30

GGCATCGCCGGGAACGTCCCCTCCTCGCTCGGCAACAACACCCACATCGACGAGGTGCTCCGCGCCGCCGACGAGATCCAGGACGAGGAT  180
 G  I  A  G  N  V  P  S  S  L  G  N  N  T  H  I  D  E  V  L  R  A  A  D  E  I  Q  D  E  D    60

CCCACCGTCGCCAGGATTCTGTGTGAGCACGCATATGCCCTCGCCCAAAATCTGGATCCAAATAGCGAAGGGAGAGGTGTGCTTCAGTTC  270
 P  T  V  A  R  I  L  C  E  H  A  Y  A  L  A  Q  N  L  D  P  N  S  E  G  R  G  V  L  Q  F    90

AAGACCGGTTTAATGTCAGTAATCAGGCAAAAACTAGCTAAGAGGGAAGGCGGTGCTATAGACCGAAGTCGGGATATCGCTAAACTGCAA  360
 K  T  G  L  M  S  V  I  R  Q  K  L  A  K  R  E  G  G  A  I  D  R  S  R  D  I  A  K  L  Q   120

GAATTTTATAAGCTATACAGAGAAAAACATAAAGTTGATGAGTTGTGTGAAGACGAAATGAAGCTGAGGGAATCTGGTGTGTTCAGCGGT  450
 E  F  Y  K  L  Y  R  E  K  H  K  V  D  E  L  C  E  D  E  M  K  L  R  E  S  G  V  F  S  G   150

AACCTCGGAGAGCTGGAGCGCAAAACTCTGAAGCGCAAAAAAGTACTTGCAACTCTCAAGGTCTTATGGTCAGTAATAGAGGATATAACA  540
 N  L  G  E  L  E  R  K  T  L  K  R  K  K  V  L  A  T  L  K  V  L  W  S  V  I  E  D  I  T   180

AAGGAAATTTCCCCTGAGGATGCAGCAAATTTGATTTCTGAAAAGATGAAAGAATTCATGGAAAAGGATGCGGCAAGGACAGAGGATTTT  630
 K  E  I  S  P  E  D  A  A  N  L  I  S  E  K  M  K  E  F  M  E  K  D  A  A  R  T  E  D  F   210

GTGGCGTATAATATCATTCCTCTAGATTCCTTGTCTACAACTAACCTGATTGTCACTTTTCCAGAGGTGAGGGCAGCAATATCATCTTTG  720
 V  A  Y  N  I  I  P  L  D  S  L  S  T  T  N  L  I  V  T  F  P  E  V  R  A  A  I  S  S  L   240

CAGTACCATAGGGATCTGCCCAGGCTTCCGAATACCATTTCAGTTCCTGATGCTAGGATTTCAAATATGCTGGACTTGGTGCACTGCGTG  810
 Q  Y  H  R  D  L  P  R  L  P  N  T  I  S  V  P  D  A  R  I  S  N  M  L  D  L  V  H  C  V   270

AGTGGTTATCAGAAAGACAATGTGAGCAATCAACGGGAGCACATTGTTCACCTGTTGGCAAATGAGCAGTCTCGATTAGGCAAACTATCA  900
 S  G  Y  Q  K  D  N  V  S  N  Q  R  E  H  I  V  H  L  L  A  N  E  Q  S  R  L  G  K  L  S   300

GGGAATGAACCGAAAATTGACGAGGGTGCTGTACATGTTGTGTTCTCTAAGTCCCTGGACAACTACATAAAATGGTGCAACTATTTACCA  990
 G  N  E  P  K  I  D  E  G  A  V  H  V  V  F  S  K  S  L  D  N  Y  I  K  W  C  N  Y  L  P   330

CTGCGTCCTGTCTGGAATAACATTGAATCATTGACCAAAGAAAAGAAGTTGCTATATGTTTGTTTATACTACTTGATCTGGGGAGAGGCT 1080
 L  R  P  V  W  N  N  I  E  S  L  T  K  E  K  K  L  L  Y  V  C  L  Y  Y  L  I  W  G  E  A   360

GCCAACGTACGATTTCTTCCAGAAGGCTTATGCTACATATTTCATCACGTAGCAAGAGAACTAGAGGTGATTATGCAGAAACAGACTGCC 1170
 A  N  V  R  F  L  P  E  G  L  C  Y  I  F  H  H  V  A  R  E  L  E  V  I  M  Q  K  Q  T  A   390

GAGCCAGCTGGAAGCTGCATCTCTAATGATGGCGTATCATTTCTTGACCAAGTCATTTATCCTCTATATGAAATCGTTGCAGCTGAAGCA 1260
 E  P  A  G  S  C  I  S  N  D  G  V  S  F  L  D  Q  V  I  Y  P  L  Y  E  I  V  A  A  E  A   420

GGCAACAATGACAATGGGCGGGCAGCACATTCTGCATGGAGAAACTATGATGATTTCAATGAGTTCTTCTGGTCTGAGAAATGTTTTCAG 1350
 G  N  N  D  N  G  R  A  A  H  S  A  W  R  N  Y  D  D  F  N  E  F  F  W  S  E  K  C  F  Q   450

CTGGGTTGGCCGTGGAAACTGAGCAATCCATTTTTCTCAAAGCCTAATAGGAAAGAGCAGGGCTTGATAAGTAGGAATCACCATTATGGA 1440
 L  G  W  P  W  K  L  S  N  P  F  F  S  K  P  N  R  K  E  Q  G  L  I  S  R  N  H  H  Y  G   480

AAGACATCTTTCGTTGAGCACAGAACTTTTCTGCATCTTTACCATAGCTTTCACCGCCTCTGGATGTTCCTACTTTTGATGTTTCAGGGA 1530
 K  T  S  F  V  E  H  R  T  F  L  H  L  Y  H  S  F  H  R  L  W  M  F  L  L  L  M  F  Q  G   510

CTTACTATCATTGCTTTTAACAATGGCAGTTTTGACACAAATACTGTATTGGAACTTCTTAGCCTGGGCCCAACTTATATCATAATGGAA 1620
 L  T  I  I  A  F  N  N  G  S  F  D  T  N  T  V  L  E  L  L  S  L  G  P  T  Y  I  I  M  E   540

TTTATTGAGAGTGTATTGGACATTCTAATGATGTATGGCGCCTATTCAACATCTCGTGGTTCTGCAATCACTAGAGTGATCTGGCGATTC 1710
 F  I  E  S  V  L  D  I  L  M  M  Y  G  A  Y  S  T  S  R  G  S  A  I  T  R  V  I  W  R  F   570

TGTTGGTTTACCGCAGCTTCATTGGTCATCTGTTACCTATATATCAAGGCACTTCAAGATGGGGTGCAATCTGCACCTTTTAAGATATAT 1800
 C  W  F  T  A  A  S  L  V  I  C  Y  L  Y  I  K  A  L  Q  D  G  V  Q  S  A  P  F  K  I  Y   600

GTTGTTGTCATCAGCGCGTATGCGGGTTTCCAGATAATCATCAGCCTTCTCATGAGCGTTCCCTGCTGCCGTGGTATTACCAATGCTTGC 1890
 V  V  V  I  S  A  Y  A  G  F  Q  I  I  I  S  L  L  M  S  V  P  C  C  R  G  I  T  N  A  C   630

TACAGCTGGTCTTTTGTACGCCTTGCCAAGTGGATGCATCAGGAACATAATTATGTTGGAAGAGGCTTGCATGAAAGGCCTCTAGATTAT 1980
 Y  S  W  S  F  V  R  L  A  K  W  M  H  Q  E  H  N  Y  V  G  R  G  L  H  E  R  P  L  D  Y   660
```

```
ATCAAATATGCCGCTTTCTGGCTTGTTATTTTTGCTGCGAAATTTTCATTCACCTATTTCCTCCAGATTAGACCTCTTGTAAAACCAACA 2070
 I  K  Y  A  A  F  W  L  V  I  F  A  A  K  F  S  F  T  Y  F  L  Q  I  R  P  L  V  K  P  T  690

AGACTGATAATCAGTTTCAAAGGCTTACAGTATCAATGGCATGACTTTGTTTCAAAGAATAACCATAATGCGATTACAATCCTTTCTTTA 2160
 R  L  I  I  S  F  K  G  L  Q  Y  Q  W  H  D  F  V  S  K  N  N  H  N  A  I  T  I  L  S  L  720

TGGGCTCCAGTGGCCTCAATCTATCTTTTGGACATCCATGTTTTTTACACCATCATGTCTGCTCTTGTTGGATTCCTCCTTGGTGCACGT 2250
 W  A  P  V  A  S  I  Y  L  L  D  I  H  V  F  Y  T  I  M  S  A  L  V  G  F  L  L  G  A  R  750

GATCGCCTGGGAGAGATTAGGTCTGTTGAAGCAGTTCACAGGTTCTTTGAGAAGTTCCCTGAAGTATTCATGGATAAACTTCATGTTGCT 2340
 D  R  L  G  E  I  R  S  V  E  A  V  H  R  F  F  E  K  F  P  E  V  F  M  D  K  L  H  V  A  780

GTTCCAAAAAGGAAACAACTGCTATCATCTGGTCAGCATGCAGAGTTAAACAAGCTTGATGCATCTAGATTCGCTCCTTTCTGGAATGAA 2430
 V  P  K  R  K  Q  L  L  S  S  G  Q  H  A  E  L  N  K  L  D  A  S  R  F  A  P  F  W  N  E  810

ATTGTGAAGAATTTGCGGGAAGAGGACTACATTAGCAACACTGAGCTGGATTTACTCTTGATGCCAAAGAACATAGGTGGTCTTCCAATT 2520
 I  V  K  N  L  R  E  E  D  Y  I  S  N  T  E  L  D  L  L  L  M  P  K  N  I  G  G  L  P  I  840

GTGCAGTGGCCACTTTTTTTGCTTGCTAGCAAGGTTTTCTTGGCCAAAGATATTGCCGTTGATTGCAACGACTCACAAGATGAACTATGG 2610
 V  Q  W  P  L  F  L  L  A  S  K  V  F  L  A  K  D  I  A  V  D  C  N  D  S  Q  D  E  L  W  870

CTAAGGATCTCAAAGGACGAATATATGCAATACGCTGTTGAGGAGTGCTTTCATAGCATCAAGTATATCCTGTCAAATATTCTAGATAAA 2700
 L  R  I  S  K  D  E  Y  M  Q  Y  A  V  E  E  C  F  H  S  I  K  Y  I  L  S  N  I  L  D  K  900

GAAGGCCATCTCTGGGTGCAAAGGATTTTTGATGGTATTCAAGAAAGCATTTCAAAGAACAACATCCAGAGTGATATTCATTTCAGCAAA 2790
 E  G  H  L  W  V  Q  R  I  F  D  G  I  Q  E  S  I  S  K  N  N  I  Q  S  D  I  H  F  S  K  930

TTGCCTAATGTCATTGCCAAGCTTGTTGCTGTAGCGGGAATACTGAAAGAAACGGAATCTGCTGATATGAAGAAGGGGGCAGTTAATGCT 2880
 L  P  N  V  I  A  K  L  V  A  V  A  G  I  L  K  E  T  E  S  A  D  M  K  K  G  A  V  N  A  960

ATTCAAGATCTATACGAAGTTGTTCATCACGAAGTACTTTTTGTTGATTTGAGTGGTAACATTGACGATTGGAGTCAGATAAATAGAGCA 2970
 I  Q  D  L  Y  E  V  V  H  H  E  V  L  F  V  D  L  S  G  N  I  D  D  W  S  Q  I  N  R  A  990

AGAGCCGAAGGCCGCCTCTTCAGTAATCTCAAGTGGCCAAATGAACCTGGATTGAAGGACATGATCAAACGATTGCATTCACTTCTGACC 3060
 R  A  E  G  R  L  F  S  N  L  K  W  P  N  E  P  G  L  K  D  M  I  K  R  L  H  S  L  L  T  1020

ATCAAGGAATCAGCTGCAAATGTTCCTAAAAACCTGGAAGCCAGCCGGAGACTGCAGTTCTTCACGAACTCTTTGTTCATGCGAATGCCT 3150
 I  K  E  S  A  A  N  V  P  K  N  L  E  A  S  R  R  L  Q  F  F  T  N  S  L  F  M  R  M  P  1050

GTTGCAAGGCCTGTTTCAGAAATGCTTTCCTTTAGCGTATTTACTCCATATTGCTCTGAGACAGTGCTTTATAGCATCGCCGAACTCCAA 3240
 V  A  R  P  V  S  E  M  L  S  F  S  V  F  T  P  Y  C  S  E  T  V  L  Y  S  I  A  E  L  Q  1080

AAGAAAAATGAAGATGGTATATCTACACTATTTTATCTTCAGAAGATTTATCCAGATGAATGGAAGAACTTCCTTACTCGCATCAACAGG 3330
 K  K  N  E  D  G  I  S  T  L  F  Y  L  Q  K  I  Y  P  D  E  W  K  N  F  L  T  R  I  N  R  1110

GATGAAAATGCAGCAGACAGTGAGCTTTTTAGCAGTGCGAATGACATACTAGAACTTCGGCTATGGGCATCTTACCGAGGGCAGACATTA 3420
 D  E  N  A  A  D  S  E  L  F  S  S  A  N  D  I  L  E  L  R  L  W  A  S  Y  R  G  Q  T  L  1140

GCGCGAACAGTTCGTGGGATGATGTACTACAGAAAGGCCCTTATGTTGCAAAGTTATTTGGAGAGAATGCATTCTGAAGACCTCGAATCT 3510
 A  R  T  V  R  G  M  M  Y  Y  R  K  A  L  M  L  Q  S  Y  L  E  R  M  H  S  E  D  L  E  S  1170

GCATTGGATATGGCTGGTCTGGCTGACACACATTTTGAGTACTCCCCTGAAGCACGCGCACAGGCTGATTTGAAATTTACGTATGTGGTT 3600
 A  L  D  M  A  G  L  A  D  T  H  F  E  Y  S  P  E  A  R  A  Q  A  D  L  K  F  T  Y  V  V  1200

ACCTGCCAAATCTACGGAGTGCAGAAAGGTGAAGGGAAGCCAGAAGCTGCAGATATAGCCCTTCTGATGCAAAGAAATGAAGCTCTCAGA 3690
 T  C  Q  I  Y  G  V  Q  K  G  E  G  K  P  E  A  A  D  I  A  L  L  M  Q  R  N  E  A  L  R  1230

ATTGCTTACATCGATGTTGTTGAGAGCATTAAGAATGGAAAGTCTAGCACCGAGTATTACTCAAAGCTTGTGAAAGCTGACATCCATGGA 3780
 I  A  Y  I  D  V  V  E  S  I  K  N  G  K  S  S  T  E  Y  Y  S  K  L  V  K  A  D  I  H  G  1260

AAGGACAAGGAAATTTATTCTGTTAAATTGCCTGGCAATCCAAAGCTTGGGGAGGGTAAACCCGAAAATCAAAACCATGCTGTAATATTC 3870
 K  D  K  E  I  Y  S  V  K  L  P  G  N  P  K  L  G  E  G  K  P  E  N  Q  N  H  A  V  I  F  1290

ACTCGCGGAAATGCTGTACAAACCATTGATATGAATCAGGACAACTATTTCGAGGAGGCACTCAAAATGCGAAATCTGCTTGAGGAATTC 3960
 T  R  G  N  A  V  Q  T  I  D  M  N  Q  D  N  Y  F  E  E  A  L  K  M  R  N  L  L  E  E  F  1320

TCTCAAAATCATGGCAAGTTCAAGCCTTCAATTCTTGGTGTTAGAGAACATGTCTTCACCGGAAGTGTTTCCTCCCTTGCTTCATTTATG 4050
 S  Q  N  H  G  K  F  K  P  S  I  L  G  V  R  E  H  V  F  T  G  S  V  S  S  L  A  S  F  M  1350

TCAAATCAGGAAACTAGTTTTGTGACATTAGGACAGCGTGTTCTTTCTAATCCACTGAAAGTGAGAATGCATTATGGTCACCCAGACGTG 4140
 S  N  Q  E  T  S  F  V  T  L  G  Q  R  V  L  S  N  P  L  K  V  R  M  H  Y  G  H  P  D  V  1380

TTTGATAGAATATTTCATATTACGAGGGGTGGCATCAGTAAGGCGTCCCGTATCATCAATATCAGTGAGGATATATTTGCAGGGTTTAAT 4230
 F  D  R  I  F  H  I  T  R  G  G  I  S  K  A  S  R  I  I  N  I  S  E  D  I  F  A  G  F  N  1410

TCTACTCTGCGTCAAGGGAACATAACTCACCATGAGTATATCCAGGTTGGTAAAGGAAGAGATGTTGGGCTTAATCAGATCGCACTATTT 4320
 S  T  L  R  Q  G  N  I  T  H  H  E  Y  I  Q  V  G  K  G  R  D  V  G  L  N  Q  I  A  L  F  1440

GAAGGAAAAGTTGCGGGAGGAAACGGCGAACAAGTTCTTAGCAGAGATATATACAGACTTGGGCAACTTTTTGACTTTTTCAGGATGTTA 4410
 E  G  K  V  A  G  G  N  G  E  Q  V  L  S  R  D  I  Y  R  L  G  Q  L  F  D  F  F  R  M  L  1470
```

```
TCCTTCTATGTGACTACTGTTGGGTTTTACTTCTGTACGATGCTAACTGTACTGACAGTGTACATATTTCTCTATGGTAAAACCTATCTG 4500
 S  F  Y  V  T  T  V  G  F  Y  F  C  T  M  L  T  V  L  T  V  Y  I  F  L  Y  G  K  T  Y  L  1500

GCTTTATCTGGTGTTGGAGAATCAATTCAAAATAGGGCGGATATACAGGGAAATGAAGCATTGAGCATAGCTCTGAACACCCAGTTTCTT 4590
 A  L  S  G  V  G  E  S  I  Q  N  R  A  D  I  Q  G  N  E  A  L  S  I  A  L  N  T  Q  F  L  1530

TTCCAGATTGGTGTGTTTACTGCAATTCCTATGATTCTAGGTTTCATCCTGGAAGAAGGTGTCCTGACGGCTTTTGTCAGCTTCATTACC 4680
 F  Q  I  G  V  F  T  A  I  P  M  I  L  G  F  I  L  E  E  G  V  L  T  A  F  V  S  F  I  T  1560

ATGCAGTTCCAACTATGCTCCGTATTTTTCACGTTCTCCCTTGGGACAAGGACTCACTATTTTGGTCGCACAATACTGCATGGAGGTGCA 4770
 M  Q  F  Q  L  C  S  V  F  F  T  F  S  L  G  T  R  T  H  Y  F  G  R  T  I  L  H  G  G  A  1590

AAGTATAGAGCAACTGGTAGGGGTTTTGTGGTACGGCATATTAAGTTTGCTGAGAATTACCGTCTTTATTCCCGAAGCCATTTTGTGAAA 4860
 K  Y  R  A  T  G  R  G  F  V  V  R  H  I  K  F  A  E  N  Y  R  L  Y  S  R  S  H  F  V  K  1620

GGGCTGGAGGTTGCACTTCTGTTGGTTATCTTTCTAGCTTATGGTTTTAACAACAGTGGAGCAATTGGCTATATCTTACTTTCCATAAGT 4950
 G  L  E  V  A  L  L  L  V  I  F  L  A  Y  G  F  N  N  S  G  A  I  G  Y  I  L  L  S  I  S  1650

AGCTGGTTTATGGCTCTTTCTTGGCTTTTTGCTCCATACGTATTCAACCCGTCTGGATTTGAATGGCAAAAGGTCGTCGAGGATTTCAGA 5040
 S  W  F  M  A  L  S  W  L  F  A  P  Y  V  F  N  P  S  G  F  E  W  Q  K  V  V  E  D  F  R  1680

GACTGGACAAACTGGCTTTTTTACCGAGGTGGTATTGGGGTTAAAGGAGAAGAAAGCTGGGAAGCTTGGTGGGATGAAGAACTGGCACAT 5130
 D  W  T  N  W  L  F  Y  R  G  G  I  G  V  K  G  E  E  S  W  E  A  W  W  D  E  E  L  A  H  1710

ATTCACACCTTCCGCGGGAGGATACTGGAAACTATACTTAGTTTAAGATTTTTTATTTTCCAGTATGGAGTTGTTTACCACATGAAAGCA 5220
 I  H  T  F  R  G  R  I  L  E  T  I  L  S  L  R  F  F  I  F  Q  Y  G  V  V  Y  H  M  K  A  1740

AGCAATGAAAGTACAGCATTACTGGTATATTGGGTATCATGGGCTGTGCTTGGAGGGCTTTTTGTCCTGCTAATGGTATTTAGTTTAAAC 5310
 S  N  E  S  T  A  L  L  V  Y  W  V  S  W  A  V  L  G  G  L  F  V  L  L  M  V  F  S  L  N  1770

CCCAAGGCCATGGTTCATTTCCAGTTGTTCCTGCGTCTGGTCAAAAGCATTGCACTGTTAGTGGTTTTGGCAGGTTTGGTTGTGGCAATT 5400
 P  K  A  M  V  H  F  Q  L  F  L  R  L  V  K  S  I  A  L  L  V  V  L  A  G  L  V  V  A  I  1800

GCAATTACAAGACTCGCTGTTGTAGATGTACTTGCTTCCATCCTAGCATATGTGCCTACTGGATGGGGAATTCTTTCGATTGCTGTGGCA 5490
 A  I  T  R  L  A  V  V  D  V  L  A  S  I  L  A  Y  V  P  T  G  W  G  I  L  S  I  A  V  A  1830

TGGAAACCAATTGTGAAGAGACTGGGTTTGTGGAAAACAGTGCGCTCGTTGGCTCGCCTGTATGATGCTGGCATGGGAATGATCATTTTT 5580
 W  K  P  I  V  K  R  L  G  L  W  K  T  V  R  S  L  A  R  L  Y  D  A  G  M  G  M  I  I  F  1860

GTGCCCATAGCTATCTGCTCGTGGTTTCCCTTCATCTCCACCTTCCAGACACGGCTACTGTTCAACCAGGCTTTCAGCAGAGGTTTGGAG 5670
 V  P  I  A  I  C  S  W  F  P  F  I  S  T  F  Q  T  R  L  L  F  N  Q  A  F  S  R  G  L  E  1890

ATTTCTCTCATCCTGGCTGGCAACAATCAGAATGCAGGCATATGGCATCATCCATCTTTTGAATCCTCACCCAGATGAGTGCACCTTCGTA 5760
 I  S  L  I  L  A  G  N  N  Q  N  A  G  I  W  H  H  P  S  F  E  S  S  P  R  *               1915

GTTAGTTGATCCCGGGTTCTGAGTTAGCAGTAGATGTATATATCTCCGTGTTGACTGGCAGTTATTTGCTATGGCTGTATATGTTATCGC 5850

CTGCTACATTTTTTGCACTAATGATAGTTATAGGAGGTGGTGTTCTTGAAGGACCAGGTGCCGAATCATTGTGTTAAAATAACTTGTGTA 5940

TTTGTGTTAGTTTAGATAATGGTGATTTTGGGGTAAAAGAATATGGATAAGATTGCGATATTGTGAATTACATCTGAGTTATCTCTGTTG 6030

CTACTATAAAAAAAAAAAAAAAAAAA                                                                  6055
```

The right facing arrow and highlighted sequence represents the forward *HvGSL1*-F primer, while the left facing arrow and highlighted sequence represents the reverse *HvGSL1*-R primer (*Appendix A*).

References:

Allison, AV and Shalla, TA (1974) 'The ultrastructure of local lesions induced by potato virus X: A sequence of cytological events in the course of infection' *Phytopathology* **64:** 784-793

Angra-Sharma, R and Sharma, DK (1994) 'Biochemical and histological studies on susceptible and resistant maize leaves infected by *Helminthosporium maydis*' *Plant Pathology* **43:** 972-978

Antelo, L, Cosio, EG, Hertkorn, N and Ebel, J (1998) 'Partial purification of a GTP-insensitive (1→3)-β-glucan synthase from *Phytophthora sojae*' *Federation of European Biochemical Societies Letters* **433:** 191-195

Arellano, M, Duran, A and Pérez, P (1996) 'Rho1 GTPase activates the (1-3)β-D-glucan synthase and is involved in *Schizosaccharomyces pombe* morphogenesis' *European Molecular Biology Organization Journal* **15:** 4584-4591

Bacic, A and Delmer, DP (1981) 'Stimulation of membrane-associated polysaccharide synthetases by a membrane potential in developing cotton fibers' *Planta* **152:** 346-351

Backes, G, Granner, A, Foroughi-Wehr, B, Fischbeck, G, Wenzel, G and Jahoor, A (1995) 'Localization of quantitative trait loci (QTL) for agronomic important characters by the use of a RFLP map in barley (*Hordeum vulgare* L.)' *Theoretical and Applied Genetics* **90:** 294-302

Bäumer, D, Preisfeld, A and Ruppel, HG (2001) 'Isolation and characterization of paramylon synthase from *Euglena gracilis* (Euglenophyceae)' *Journal of Phycology* **37:** 38-46

Beauvais, A, Bruneau, JM, Mol, PC, Buitrago, MJ, Legrand, R and Latgé, JP (2001) 'Glucan synthase complex of *Aspergillus fumigatus*' *Journal of Bacteriology* **183:** 2273-2279

Beauvais, A, Drake, R, Ng, K, Diaquin, M and Latgé, JP (1993) 'Characterization of the 1,3-β-glucan synthase of *Aspergillus fumigatus*' *Journal of General Microbiology* **139:** 3071-3078

Becraft, PW (2001) 'Cell fate specification in the cereal endosperm' *Cell and Developmental Biology* **12:** 387-394

Beffa, RS, Hofer, RM, Thomas, M and Meins, F, Jr (1996) 'Decreased susceptibility to viral disease of β-1,3-glucanase-deficient plants generated by antisense transformation' *Plant Cell* **8:** 1001-1011

Benhamou, N (1995) 'Ultrastructural and cytochemical aspects of the response of eggplant parenchyma cells in direct contact with *Verticillium*-infected xylem vessels' *Physiological and Molecular Plant Pathology* **46:** 321-338

Bennett, V and Baines, AJ (2001) 'Spectrin and ankyrin-based pathways: Metazoan inventions for integrating cells into tissues' *Physiological Reviews* **81:** 1353-1392

Berry, AM and McCully, ME (1990) 'Callose-containing deposits in relation to root-hair infections of *Alnus rubra* by *Frankia*' *Canadian Journal of Botany* **68:** 798-802

Bezant, J, Laurie, D, Pratchett, N, Chojecki, J and Kearsey, M (1996) 'Marker regression mapping of QTL controlling flowering time and plant height in a spring barley (*Hordeum vulgare* L.) cross' *Heredity* **77:** 64-73

Bezant, J, Laurie, D, Pratchett, N, Chojecki, J and Kearsey, M (1997) 'Mapping QTL controlling yield and yield components in a spring barley (*Hordeum vulgare* L.) cross using marker regression' *Molecular Breeding* **3:** 29-38

Bluhm, TL and Sarko, A (1977) 'The triple helical structure of lentinan, a linear β-(1,3)-D-glucan' *Canadian Journal of Chemistry* **55:** 293-299

Bonhoff, A, Rieth, B, Golecki, J and Grisebach, H (1987) 'Race cultivar-specific differences in callose deposition in soybean roots following infection with *Phytophthora Megasperma* f. sp. *Glycinea*' *Planta* **172:** 101-105

Brown, I, Trethowan, J, Kerry, M, Mansfield, J and Bolwell, GP (1998) 'Localization of components of the oxidative cross-linking of glycoproteins and of callose synthesis in papillae formed during the interaction between non-pathogenic strains of *Xanthomonas campestris* and French bean mesophyll cells' *Plant Journal* **15:** 333-343

Brown, RC, Lemmon, BE and Olsen, OA (1994) 'Endosperm development in barley: Microtubule involvement in the morphogenetic pathway' *Plant Cell* **6:** 1241-1252

Bruehl, GW (1961) 'Barley yellow dwarf' *Amercian Phytopathological Society Monographs* **1:** 1-52

Bulone, V, Fincher, GB and Stone, BA (1995) '*In vitro* synthesis of a microfibrillar (1→3)-β-glucan by a ryegrass (*Lolium multiflorum*) endosperm (1→3)-β-glucan synthase enriched by product entrapment' *Plant Journal* **8:** 213-225

Burton, RA, Shirley, NJ, King, BJ, Harvey, AJ and Fincher, GB (2004) 'The CesA gene family of barley. Quantitative analysis of transcripts reveals two groups of co-expressed genes' *Plant Physiology* **134:** 224-236

Bushnell, WR (2002) 'The role of powdery mildew research in understanding host-parasite interaction: past, present, and future' *in The powdery mildews: a comprehensive treatise* Belanger, RR, Bushnell, WR, Dik, AJ and Carver, TLW The American Phytopathology Society, St. Paul, Minnesota, USA. 1-12

Bustin, SA (2000) 'Absolute quantification of mRNA using real-time reverse transcription polymerase chain reaction assays' *Journal of Molecular Endocrinology* **25:** 169-193

Carver, TLW and Bushnell, WR (1983) 'The probable role of primary germ tubes in water uptake before infection by *Erysiphe graminis*' *Physiological Plant Pathology* **23:** 229-240

Carver, TLW and Ingerson-Morris, SM (1989) 'Effects of inoculum density on germling development by *Erysiphe graminis* f. sp. *avenae* in relation to induced resistance of oat cells to appressorial penetration' *Mycological Research* **92:** 18-24

Carver, TLW, Ingerson-Morris, SM, Thomas, BJ and Zeyen, RJ (1995) 'Early interactions during powdery mildew infection' *Canadian Journal of Botany* **73:** S632-S639

Chen, F, Prehn, D, Hayes, PM, Mulrooney, D, Corey, A and Vivar, H (1994) 'Mapping genes for resistance to barley stripe rust (*Puccinia striiformis* f. sp. *hordei*)' *Theoretical and Applied Genetics* **88:** 215-219

Clerivet, A (1993) 'Host-parasite interactions between *Solanum gilo* Raddli and *Stemphylium floridanum* Hannon and Weber: ultrastructural aspects' *Journal of Phytopathology* **138:** 257-261

Close, TJ, Wanamaker, SI, Caldo, RA, Turner, SM, Ashlock, DA, Dickerson, JA, Wing, RA, Muehlbauer, GJ, Kleinhofs, A and Wise, RP (2004) 'A new resource for cereal genomics: 22K barley GeneChip comes of age' *Plant Physiology* **134:** 960-968

Conti, GG, Bassi, M, Maffi, D and Bocci, AM (1986) 'Host-parasite relationships in a susceptible and a resistant rose cultivar inoculated with *Sphaerotheca pannosa* II. Deposition rates of callose, lignin and phenolics in infected or wounded cells and their possible role in resistance' *Journal of Phytopathology* **117:** 312-320

Cui, X, Shin, H, Song, C, Laosinchai, W, Amano, Y and Brown, RM, Jr (2001) 'A putative plant homolog of the yeast β-1,3-glucan synthase subunit *FKS1* from cotton (*Gossypium hirsutum* L.) fibers' *Planta* **213:** 223-230

Currier, HB and Shih, CY (1968) 'Sieve tubes and callose in *Elodea* leaves' *American Journal of Botany* **55:** 145-152

Cutler, SR and Ehrhardt, DW (2002) 'Polarized cytokinesis in vacuolate cells of Arabidopsis' *Proceedings of the National Academy of Sciences of the United States of America* **99:** 2812-2817

De la Pena, RC, Smith, KP, Capettini, F, Muelbauer, GJ, Gallo-Meagher, M, Dill-Macky, R, Somers, DA and Rasmuson, DC (1999) 'Quantitative trait loci associated with resistance to *Fusarium* head blight and kernel discoloration in barley' *Theoretical and Applied Genetics* **99:** 561-569

Dhugga, KS and Ray, PM (1994) 'Purification of 1,3-β-glucan synthase activity from pea tissue: Two polypeptides of 55 kDa and 70 kDa copurify with enzyme activity' *European Journal of Biochemistry* **220:** 943-953

Doblin, MS, De, ML, Newbigin, E, Bacic, A and Read, SM (2001) 'Pollen tubes of *Nicotiana alata* express two genes from different β-glucan synthase families' *Plant Physiology* **125:** 2040-2052

Douglas, CM, Foor, F, Marrinan, JA, Morin, N, Nielsen, JB, Dahl, AM, Mazur, P, Baginsky, W, Li, W, El, SM, Clemas, JA, Mandala, SM, Frommer, BR and Kurtz, MB (1994) 'The *Saccharomyces cerevisiae FKS1* (*ETG1*) gene encodes an integral membrane protein which is a subunit of 1,3-β-D-glucan synthase' *Proceedings of the National Academy of Sciences of the United States of America* **91:** 12907-12911

Drgonová, J, Drgon, T, Tanaka, K, Kollár, R, Chen, GC, Ford, RA, Chan, CSM, Takai, Y and Cabib, E (1996) 'Rho1p, a yeast protein at the interface between cell polarization and morphogenesis' *Science* **272:** 277-279

El Attari, A, Rebai, A, Hayes, PM, Barrault, G, Dechamp-Guillaume, G and Sarrafi, A (1998) 'Potential of double haploid lines and localization of quantitative trait loci (QTL) for partial resistance to bacterial leaf streak (*Xanthomonas campestris* pv. *hordei*) in barley' *Theoretical and Applied Genetics* **96:** 95-100

Endo, BY (1991) 'Ultrastructure of initial responses of susceptible and resistant soybean roots to infection by *Heterodera glycines*' *Revue Nematol.* **14:** 73-94

Enns, LC, Kanaoka, MM, Torii, KU, Comai, L, Okada, K and Cleland, RE (2005) 'Two callose synthases, GSL1 and GSL5, play an essential and redundant role in plant and pollen development and in fertility' *Plant Molecular Biology* **58:** 333-349

Esau, K and Thorsch, J (1985) 'Sieve plate pores and plasmodesmata the communication channels of the symplast: Ultrastructural aspects and developmental relations' *American Journal of Botany* **72:** 1641-1653

Evans, NA, Hoyne, PA and Stone, BA (1984) 'Characteristics and specificity of the interaction of fluorochrome from aniline blue (sirofluor) with polysaccharides' *Carbohydrate Polymers* **4:** 215-230

Evert, RF and Derr, WF (1964) 'Callose substance in sieve elements' *American Journal of Botany* **51:** 552-559

Farkas, I, Hatdy, TA, De Paoli-Roach, AA and Roach, PJ (1990) 'Isolation of the *GSY1* gene encoding yeast glycogen synthase and evidence for the existence of a second one' *Journal of Biological Chemistry* **265:** 20879-20886

Fink, L, Seeger, W, Ermert, L, Haenze, J, Stahl, U, Grimminger, F, Kummer, W and Bohle, R-M (1998) 'Real-time quantitative RT-PCR after laser-assisted cell picking' *Nature Medicine* **4:** 1329-1333

Freund, JE (2004) *Modern Elemental Statistics* Pearson Education, Inc New Jersey

Frohman, MA, Dush, MK and Martin, GR (1988) 'Rapid production of full-length cDNAs from rare transcripts: Amplification using a single gene-specific oligonucleotide primer' *Proceedings of the National Academy of Sciences of the United States of America* **85:** 8998-9002

Fulcher, RG, McCully, ME, Setterfield, G and Sutherland, J (1976) 'β-1,3-Glucans may be associated with cell plate formation during cytokinesis' *Canadian Journal of Botany* **54:** 539-542

Gheysen, G and Fenoll, C (2002) 'Gene expression in nematodes sites' *Annual Review of Phytopathology* **40:** 191-219

Gibeaut, DM and Carpita, NC (1990) 'Separation of membranes by flotation centrifugation for *in vitro* synthesis of plant cell wall polysaccharides' *Protoplasma* **156:** 82-93

Green, JR, Carver, TLW and Gurr, SJ (2002) 'The formation and function of infection and feeding structures' *in The powdery mildews: a comprehensive treatise* Belanger, RR, Bushnell, WR, Dik, AJ and Carver, TLW The American Phytopathological Society, St. Paul, Minnesota, USA. 66-82

Gregory, ACE, Smith, C, Kerry, ME, Wheatley, ER and Bolwell, GP (2002) 'Comparative subcellular immunolocation of polypeptides associated with xylan and callose synthases in French bean (*Phaseolus vulgaris*) during secondary wall formation' *Phytochemistry Oxford* **59:** 249-259

Gu, X and Verma, DPS (1996) 'Phragmosplastin, a dynamin-like protein associated with cell plate formation in plants' *European Molecular Biology Organization Journal* **15:** 695-704

Gu, X and Verma, DPS (1997) 'Dynamics of phragmoplastin in living cells during cell plate formation and uncoupling of cell elongation from the plane of cell division' *Plant Cell* **9:** 157-169

Hackett, CA, Ellis, RP, Foster, BP, McNicol, JW and Macaulay, M (1992) 'Statistical analysis of linkage experiment in barley involving quantitative trait loci for height and ear-emergence time and two genetic markers on chromosome 4' *Theoretical and Applied Genetics* **85:** 120-126

Hajdukiewicz, P, Svab, Z and Maliga, P (1994) 'The small, versatile pPZP family of *Agrobacterium* binary vectors for plant transformation' *Plant Molecular Biology* **25:** 989-994

Hammond, SM, Caudy, AA and Hannon, GJ (2001) 'Post-transciptional gene silencing by double-stranded RNA' *Nature Reviews Genetics* **2:** 110-119

Harada, T, Masada, M, Fujimori, K and Maeda (1966) 'Production of a firm, resilient gel-forming polysaccharide by a mutant of *Alcaligenes faecalis* var. *myxogenes* 10C3' *Agricultural and Biological Chemistry* **30:** 196-198

Hayes, PM, Blake, T, Chen, THH, Tragoonrung, S, Chen, F, Pan, A and Liu, B (1993) 'Quantitative trait loci on barley (*Hordeum vulgare* L.) chromosome 7 associated with components of winterhardiness' *Genome* **36:** 66-71

Hayes, PM, Prehn, D, Vivar, H, Blake, T, Comeau, A, Henry, I, Johnston, M, Jones, B and Steffenson, B (1996) 'Multiple disease resistance loci and their relationship to agronomic and quality loci in a spring barley population' *Journal of Quantitative Trait Loci* http://probe.nalusda.gov:8000/otherdocs/jqtl/index.html

Henry, RJ, Schibeci, A and Stone, BA (1983) 'Localization of β-glucan synthases on the membranes of cultured *Lolium multiflorum* (ryegrass) endosperm cells' *Biochemical Journal* **209:** 627-633

Him, JLK, Pelosi, L, Chanzy, H, Putaux, JL and Bulone, V (2001) 'Biosynthesis of (1→3)-β-D-glucan (callose) by detergent extracts of a microsomal fraction from *Arabidopsis thaliana*' *European Journal of Biochemistry* **268:** 4628-4638

Hochholdinger, F, Woll, K, Sauer, M and Dembinsky, D (2004) 'Genetic dissection of root formation in maize (*Zea mays*) reveals root-type specific developmental programmes' *Annals of Botany* **93:** 359-368

Hodal, L, Bochardt, A, Nielsen, JE, Mattsson, O and Okkels, FT (1992) 'Detection, expression and specific elimination of endogenous β-glucuronidase activity in transgenic and non-transgenic plants' *Plant Science* **87:** 115-122

Hong, Z, Delauney, AJ and Verma, DPS (2001a) 'A cell plate-specific callose synthase and its interaction with phragmoplastin' *Plant Cell* **13:** 755-768

Hong, Z, Zhang, Z, Olson, JM and Verma, DPS (2001b) 'A novel UDP-glucose transferase is part of the callose synthase complex and interacts with phragmoplastin at the forming cell plate' *Plant Cell* **13:** 769-779

Horst, WJ, Kpueschel, A and Schmohl, N (1997) 'Induction of callose formation is a sensitive marker for genotypic aluminium sensitivity in maize' *Plant and Soil* **192:** 23-30

Hrmova, M, Taft, CS and Selitrennikoff, CP (1989) '1,3-β-D-Glucan synthase of *Neurospora crassa*: Partial purification and characterization of solubilized enzyme activity' *Experimental Mycology* **13:** 129-139

Hull, R (1989) 'The movement of viruses in plants' *Annual Review of Phytopathology* **27:** 213-240

Hunold, R, Bronner, R and Hahne, G (1994) 'Early events in microprojectile bombardment: Cell viability and particle location' *Plant Journal* **5:** 593-604

Iglesias, VA and Meins, F, Jr. (2000) 'Movement of plant viruses is delayed in a β-1,3-glucanase-deficient mutant showing a reduced plasmodesmatal size exclusion limit and enhanced callose deposition' *Plant Journal* **21:** 157-166

Inoue, SB, Qadota, H, Arisawa, M, Anraku, Y, Watanabe, T and Ohya, Y (1996) 'Signaling toward yeast 1,3-β-glucan synthesis' *Cell Structure and Function* **21:** 395-402

Inoue, SB, Takewaki, N, Takasuka, T, Mio, T, Adachi, M, Fujii, Y, Miyamoto, C, Arisawa, M, Furuichi, Y and Watanabe, T (1995) 'Characterization and gene cloning of 1,3-β-D-glucan synthase from *Saccharomyces cerevisiae*' *European Journal of Biochemistry* **231:** 845-854

Ishiguro, J, Saitou, A, Duran, A and Ribas, JC (1997) '*cps1*+, a *Schizosaccharomyces pombe* gene homolog of *Saccharomyces cerevisiae FKS* genes whose mutation confers hypersensitivity to cyclosporin A and papulacandin B' *Journal of Bacteriology* **179:** 7653-7662

Islam, AKMR and Shepherd, KW (1981) 'Production of disomic wheat-barley chromosome addition lines using *Hordeum bulbosum* crosses' *Genetical Research* **37:** 215-219

Jabri, E, Quigley, DR, Alders, M, Hrmova, M, Taft, CS, Phelps, P and Selitrennikoff, CP (1989) '(1-3)-β-Glucan synthesis of *Neurospora crassa*' *Current Microbiology* **19:** 153-162

Jacobs, AK, Lipka, V, Burton, RA, Panstruga, R, Strizhov, N, Schulze, LP and Fincher, GB (2003) 'An Arabidopsis callose synthase, GSL5, is required for wound and papillary callose formation' *Plant Cell* **15:** 2503-2513

Jefferies, SP, Barr, AR, Karakousis, A, Kretschmer, JM, Maning, S, Chalmers, KJ, Nelson, JC, Islam, AKMR and Langridge, P (1999) 'Mapping of chromosome regions conferring boron toxicity tolerance in barley (*Hordeum vulgare* L.)' *Theoretical and Applied Genetics* **98:** 1293-1303

Kakimoto, T and Shibaoka, H (1992) 'Synthesis of polysaccharides in phragmoplasts isolated from tobacco BY-2 cells' *Plant and Cell Physiology* **33:** 353-361

Kaminski, N and Friedman, N (2002) 'Translational review: Practical approaches to analyzing results of microarray experiments' *American Journal of Respiratory Cell and Molecular Biology* **27:** 125-132

Kandemir, N, Kudrna, DA, Ullrich, SE and Kleinhofs, A (2000) 'Molecular marker assisted genetic analysis of head shattering in six-rowed barley' *Theoretical and Applied Genetics* **101:** 203-210

Karakousis, A, Barr, AR, Kretschmer, JM, Manning, S, Jefferies, SP, Chalmers, KJ, Islam, AKM and Langridge, P (2003) 'Mapping and QTL analysis of the barley population Clipper X Sahara' *Australian Journal of Agricultural Research* **54:** 1137-1140

Kartusch, R (2003) 'On the mechanism of callose synthesis induction by metal ions in onion epidermal cells' *Protoplasma* **220:** 219-225

Kauss, H (1987) 'Some aspects of calcium-dependent regulation in plant metabolism' *Annual Review of Plant Physiology* **38:** 47-72

Kelly, R, Register, E, Hsu, MJ, Kurtz, M and Nielsen, J (1996) 'Isolation of a gene involved in 1,3-β-glucan synthesis in *Aspergillus nidulans* and purification of the corresponding protein' *Journal of Bacteriology* **178:** 4381-4391

Kircher, S, Kozma-Bognar, L, Kim, L, Adam, E, Harter, K, Schaefer, E and Nagy, F (1999) 'Light quality-dependent nuclear import of the plant photoreceptors phytochrome A and B' *Plant Cell* **11:** 1445-1456

Kiss, JZ, Vasconcelos, AV and Triemer, RE (1987) 'Structure of the Euglenoid Storage Carbohydrate Paramylon' *American Journal of Botany* **74:** 877-882

Kondoh, O, Tachibana, Y, Ohya, Y, Arisawa, M and Watanabe, T (1997) 'Cloning of the *RHO1* gene from *Candida albicans* and its regulation of β-1,3-glucan synthesis' *Journal of Bacteriology* **179:** 7734-7741

Koreeda, A, Harada, T, Ogawa, K, Sato, S and Kasai, N (1974) 'Study of the ultrastructure of gel forming (1-3)-β-D-glucan (curdlan-type polysaccharide) by electron microscopy' *Carbohydrate Research* **33:** 396-399

Krabel, D, Eschrich, W, Wirth, S and Wolf, G (1993) 'Callase-(1,3-β-D-glucanase) activity during spring reactivation in deciduous trees' *Plant Science* **93:** 19-23

Krzeslowska, M and Wozny, A (2000) 'Wall thickenings - moss protonema apical cell reaction to lead' *Biologia Plantarum* **43:** 93-98

Kumudini, BS and Shetty, HS (2002) 'Association of lignification and callose deposition with host cultivar resistance and induced systemic resistance in pearl millet to *Sclerospora graminicola*' *Australasian Plant Pathology* **31:** 157-164

Kunoh, H, Takamatsu, S and Ishizaki, H (1978) 'Ctyological studies of powdery mildew in barley and wheat. II Distribution of residual calcium and silicon in germinated conidia of *Erysiphe graminis* hordei' *Physiological Plant Pathology* **13:** 319-325

Lairson, LL and Withers, SG (2004) 'Mechanistic analogies amongst carbohydrate modifying enzymes' *Chemical Communications* **20:** 2243-2248

Larson, SR, Habernicht, DK, Blake, TK and Adamson, AA (1997) 'Backcross gains for six-rowed grain and malt qualities with introgression of a feed barley yield QTL' *Journal of the American Society of Brewing Chemists* **55:** 52-57

Larson, SR, Kadyrzhanova, D, McDonald, M, Sorrells, M and Blake, TK (1996) 'Evaluation of barley chromosome-3 yield QTLs in a backcross F2 population using STSPCR' *Theoretical and Applied Genetics* **93:** 618-625

Laurie, DA, Pratchett, N, Bezant, JH and Snape, JW (1995) 'RFLP mapping of five major genes and eight quantitative trait loci controlling flowering time in a winter x spring barley (*Hordeum vulgare* L.) cross' *Genome* **38:** 575-585

Leipe, DD, Aravind, L, Grishin, NV and Koonin, EV (2000) 'The bacterial replicative helicase DnaB evolved from a RecA duplication' *Genome Research* **10:** 5-16

Li, H, Bacic, A and Read, SM (1997) 'Activation of pollen tube callose synthase by detergents' *Plant Physiology* **114:** 1255-1265

Li, J, Burton, RA, Harvey, AJ, Hrmova, M, Wardak, AZ, Stone, BA and Fincher, GB (2003) 'Biochemical evidence linking a putative callose synthase gene with (1→3)-β-D-glucan biosynthesis in barley' *Plant Molecular Biology* **53:** 213-225

Lin, MR and Edwards, HH (1974) 'Primary penetration process in powdery mildewed barley related to host cell age, cell type, and occurrence of basic staining material' *New Phytologist* **73:** 131-137

Lucas, WJ, Ding, B and Van Der Schoot, C (1993) 'Tansley Review No. 58: Plasmodesmata and the supracellular nature of plants' *New Phytologist* **125:** 435-476

Mahreholz, AM, Wang, Y and Roach, PJ (1989) 'Catalytic site of rabbit glycogen synthase isozymes' *Journal of Biological Chemistry* **263:** 10561-10567

Mano, Y, Takahashi, H, Sato, K and Takeda, K (1996) 'Mapping genes for callus growth and shoot regeneration in barley (*Hordeum vulgare* L.)' *Breeding Science* **46:** 137-142

Marquez-Cedillo, LA, Hayes, PM, Jones, BL, Kleinhofs, A, Legge, WG, Rossnagel, BG, Sato, K, Ullrich, SE, Wesenberg, DM and NABGMP, t (2000) 'QTL analysis of malting quality in barley based on the double haploid progeny of two elite North American varieties representing different germplasm groups' *Theoretical and Applied Genetics* **101:** 173-184

Massot, N, Llugany, M, Poschenrieder, C and Barcelo, J (1999) 'Callose production as indicator of aluminium toxicity in bean cultivars' *Journal of Plant Nutrition* **22:** 1-10

Mazur, P and Baginsky, W (1996) '*In vitro* activity of 1,3-β-D-glucan synthase requires the GTP-binding protein Rho1' *Journal of Biological Chemistry* **271:** 14604-14609

Mazur, P, Morin, N, Baginsky, W, El, SM, Clemas, JA, Neielsen, JB and Foor, F (1995) 'Differential expression and function of two homologous subunits of yeast 1,3-β-D-glucan synthase' *Molecular and Cellular Biology* **15:** 5671-5681

McCormack, BA, Gregory, ACE, Kerry, ME, Smith, C and Bolwell, GP (1997) 'Purification of an elicitor-induced glucan synthase (callose synthase) from suspension cultures of French bean (*Phaseolus vulgaris* L.): Purification and immunolocation of a probable Mr 65 000 subunit of the enzyme' *Planta* **203:** 196-203

Meikle, PJ, Ng, KF, Johnson, E, Hoogenraad, NJ and Stone, BA (1991) 'The β-glucan synthase from *Lolium multiflorum*: Detergent solubilization purification using monoclonal antibodies and photoaffinity labeling with a novel photoreactive pyrimidine analogue of uridine 5'-diphosphoglucose' *Journal of Biological Chemistry* **266:** 22569-22581

Miller, DD, Callaham, DA, Gross, DJ and Hepler, PK (1992) 'Free Calcium Gradient in Growing Pollen Tubes of *Lilium*' *Journal of Cell Science* **101:** 7-12

Mio, T, Adachi, SM, Tachibana, Y, Tabuchi, H, Inoue, SB, Yabe, T, Yamada, OT, Arisawa, M, Watanabe, T and Yamada, OH (1997) 'Cloning of the *Candida albicans* homolog of *Saccharomyces cerevisiae GSC1/FKS1* and its involvement in β-1,3-glucan synthesis' *Journal of Bacteriology* **179:** 4096-4105

Mol, PC, Park, HM, Mullins, JT and Cabib, E (1994) 'A GTP-binding protein regulates the activity of (1→3)-β-glucan synthase, an enzyme directly involved in yeast cell wall morphogenesis' *Journal of Biological Chemistry* **269:** 31267-31274

Mueller, WC, Morgham, AT and Roberts, EM (1994) 'Immunocytochemical localization of callose in the vascular tissue of tomato and cotton plants infected with *Fusarium oxysporum*' *Canadian Journal of Botany* **72:** 505-509

Nakanishi, I, Kimura, K, Kushui, S and Yamazaki, E (1974) 'Complex formation of gel-forming bacterial (1→3)-β-D-glucans (curdlan-type polysaccharides) with dyes in aqueous solution' *Carbohydrate Research* **32:** 47-52

Nelson, H, Shiraishi, T and Oku, H (1989) 'Effect of leaf age and etiolation of barley on susceptibility to powdery mildew infection' *Journal of Phytopathology* **124:** 101-106

Nishimura, MT, Stein, M, Hou, BH, Vogel, JP, Edwards, H and Somerville, SC (2003) 'Loss of a callose synthase results in salicylic acid-dependent disease resistance' *Science* **301:** 969-972

Nogueira, MA, Cardoso, EJBN and Hampp, R (2002) 'Manganese toxicity and callose deposition in leaves are attenuated in mycorrhizal soybean' *Plant and Soil* **246:** 1-10

Northcote, DH, Davey, R and Lay, J (1989) 'Use of antisera to localize callose, xylan and arabinogalactan in the cell-plate primary and secondary walls of plant cells' *Planta* **178:** 353-366

Ogawa, K and Tsurugi, J (1973) 'The dependence of the confirmation of a (1-3)-β-D-glucan on chain-length in alkaline solution' *Carbohydrate Research* **29:** 397-403

Olsen, OA (2004) 'Nuclear endosperm development in cereals and *Arabidopsis thaliana*' *Plant Cell* **16:** S214-S227

Østergaard, L, Petersen, M, Mattsson, O and Mundy, J (2002) 'An Arabidopsis callose synthase' *Plant Molecular Biology* **49:** 559-566

Otegui, MS, Mastronarde, DN, Kang, BH, Bednarek, SY and Staehelin, LA (2001) 'Three-dimensional analysis of syncytial-type cell plates during endosperm cellularization visualized by high resolution electron tomography' *Plant Cell* **13:** 2033-2051

Otegui, MS and Staehelin, LA (2004) 'Electron tomographic analysis of post-meiotic cytokinesis during pollen development in *Arabidopsis thaliana*' *Planta* **218:** 501-515

Oziel, A, Hayes, PM, Chen, FQ and Jones, B (1996) 'Application of quantitative trait locus mapping to the development of winter habit malting barley' *Plant Breeding* **115:** 43-51

Ozturk, ZN, Talame, V, Deyholos, M, Michalowski, CB, Galbraith, DW, Gozukirmizi, N, Tuberosa, R and Bohnert, HJ (2002) 'Monitoring large-scale changes in transcript abundance in drought- and salt-stressed barley' *Plant Molecular Biology* **48:** 551-573

Pedersen, LH, Jacobsen, S, Hejgaard, J and Rasmussen, SK (1993) 'Characterization and partial purification of β-1,3-D-glucan (callose) synthase from barley (*Hordeum vulgare*) leaves' *Plant Science* **91:** 127-138

Pelosi, L, Imai, T, Chanzy, H, Heux, L, Buhler, E and Bulone, V (2003) 'Structural and morphological diversity of (1→3)-β-D-glucans synthesized *in vitro* by enzymes from *Saprolegnia monoica*. Comparison with a corresponding *in vitro* product from blackberry (*Rubus fruticosus*)' *Biochemistry* **42:** 6264-6274

Pereira, M, Felipe, MSS, Brigido, MM, Soares, CM and Azevedo, MO (2000) 'Molecular cloning and characterization of a glucan synthase gene from the human pathogenic fungus *Paracoccidioides brasiliensis*' *Yeast* **16:** 451-462

Persson, S, Wei, H, Milne, J, Page, GP and Somerville, CR (2005) 'Identification of genes required for cellulose synthesis by regression analysis of public microarray data sets' *Proceedings of the National Academy of Sciences of the United States of America* **102:** 8633-8638

Powell, W, Thomas, WTB, Baird, E, Lawrence, P, Booth, A, Harrower, B, McNicol, JW and Waugh, R (1997) 'Analysis of quantitative traits in barley by the use of amplified fragment length polymorphisms' *Heredity* **79:** 48-59

Quackenbush, J (2001) 'Computational analysis of microarray data' *Nature Reviews Genetics* **2:** 418-427

Rae, AL, Harris, PJ, Bacic, A and Clarke, AE (1985) 'Composition of the cell walls of *Nicotiana alata* Link et Otto pollen tubes' *Planta* **166:** 128-133

Reddy, VS and Reddy, ASN (2004) 'Proteomics of calcium-signaling components in plants' *Phytochemistry* **65:** 1745-1776

Ride, JP and Pearce, RB (1979) 'Lignification and papilla formation at sites of attempted penetration of wheat leaves by nonpathogenic fungi' *Physiological Plant Pathology* **15:** 79-92

Ridley, AJ (2001) 'Rho family proteins: Coordinating cell responses' *Trends in Cell Biology* **11:** 471-477

Rinne, PLH and van der Schoot, C (2003) 'Plasmodesmata at the crossroads between development, dormancy, and defense' *Canadian Journal of Botany* **81:** 1182-1197

Rodriguez-Galvez, E and Mendgen, K (1995) 'Cell wall synthesis in cotton roots after infection with *Fusarium oxysporum*: The deposition of callose, arabinogalactans, xyloglucans, and pectic components into walls, wall appositions, cell plates and plasmodesmata' *Planta* **197:** 535-545

Sambrook, J, Fritsch, EF and Maniatis, T (1987) *Molecular cloning: A laboratory manual* Cold Spring Harbor Laboratory Press New York

Samuels, AL, Giddings, TH, Jr and Staehelin, LA (1995) 'Cytokinesis in tobacco BY-2 and root tip cells: A new model of cell plate formation in higher plants' *Journal of Cell Biology* **130:** 1345-1357

Schlüpmann, H, Bacic, A and Read, SM (1993) 'A novel callose synthase from pollen tubes of *Nicotiana*' *Planta* **191:** 470-481

Schlüpmann, H, Bacic, A and Read, SM (1994) 'Uridine diphosphate glucose metabolism and callose synthesis in cultured pollen tubes of *Nicotiana alata* Link et Otto' *Plant Physiology* **105:** 659-670

Schmele, I and Kauss, H (1990) 'Enhanced activity of the plasma membrane localized callose synthase in cucumber leaves with induced resistance' *Physiological and Molecular Plant Pathology* **37:** 221-228

Schreiner, KA, Hoddinott, J and Taylor, GJ (1994) 'Aluminum-induced deposition of (1,3)-β-glucans (callose) in *Triticum aestivum* L' *Plant and Soil* **162:** 273-280

Schweizer, P, Kmecl, A, Carpita, N and Dudler, R (2000) 'A soluble carbohydrate elicitor from *Blumeria graminis* f. sp. tritici is recognized by a broad range of cereals' *Physiological and Molecular Plant Pathology* **56:** 157-167

Schweizer, P, Pokorny, J, Abderhalden, O and Dudler, R (1999) 'A transient assay system for the functional assessment of defence-related genes in wheat' *Molecular Plant Microbe Interactions* **12:** 647-654

Scopes, RK (1982) *Protein Purification. Principals and Practice* Springer-Verlag New York

Sharman, BC (1942) 'Developmental anatomy of the shoot of *Zea mays* L.' *Annals of Botany* **6:** 245-282

Shirasu, K, Nielsen, K, Piffanelli, P, Oliver, R and Schulze-Lefert, P (1999) 'Cell-autonomous complementation of mlo resistance using a biolistics transient expression system' *Plant Journal* **17:** 293-299

Siebert, PD, Chenchik, A, Kellogg, DE, Lukyanov, KA and Lukyanov, SA (1995) 'An improved PCR method for walking in uncloned genomic DNA' *Nucleic Acids Research* **23:** 1087-1088

Skalamera, D and Heath, MC (1996) 'Cellular mechanisms of callose deposition in response to fungal infection or chemical damage' *Canadian Journal of Botany* **74:** 1236-1242

Slay, RM, Watada, AE, Frost, DJ and Wasserman, BP (1992) 'Characterization of the UDP-glucose: (1,3)-β-glucan (callose) synthase from plasma membranes of celery: Polypeptide profiles and photolabeling patterns on enriched fractions suggest callose synthase complexes from various sources share a common structure' *Plant Science* **86:** 125-136

Smith, H (1995) 'Physiological and ecological function within the phytochrome gene family' *Annual Review of Plant Physiology and Plant Molecular Biology* **46:** 289-315

Smith, NA, Singh, SP, Wang, MB, Stoutjesdijk, PA, Green, AG and Waterhouse, PM (2000) 'Total silencing by intron-spliced hairpin RNAs' *Nature* **407:** 319-320

Stasinopoulos, SJ, Fisher, PR, Stone, BA and Stanisich, VA (1999) 'Detection of two loci involved in (1→3)-β-glucan (curdlan) biosynthesis by *Agrobacterium* sp. ATCC31749, an comparative sequence analysis of the putative curdlan synthase gene' *Glycobiology* **9:** 31-41

Steer, MW and Steer, JM (1989) 'Tansley Review No. 16: Pollen tube tip growth' *New Phytologist* **111:** 323-358

Steffenson, BJ, Hayes, PM and Kleinhofs, A (1996) 'Genetics of seedling and adult plant resistance to net blotch (*Pyrenophora teres* f. *teres*) and spot blotch (*Cochlibus sativus*) in barley' *Theoretical and Applied Genetics* **92:** 552-558

Stone, BA and Clarke, AE (1992) *Chemistry and biology of (1,3)-β-glucans* La Trobe University Press, Victoria, Australia

Stone, BA, Evans, NA, Bonig, I and Clarke, AE (1984) 'The application of sirofluor a chemically defined fluorochrome from aniline blue for the histochemical detection of callose' *Protoplasma* **122:** 191-195

Teulat, B, This, D, Khairallah, M, Borries, C, Ragot, C, Sourdille, P, Leroy, P, Monneveux, P and Chalmers, A (1998) 'Several QTLs involved in osmotic-adjustment trait variation in barley (*Hordeum vulgare* L.)' *Theoretical and Applied Genetics* **96:** 688-698

Thomas, WTB, Powell, W, Waugh, R, Chalmers, KJ, Barua, UM, Jack, P, Lea, V, Forster, BP, Swanston, JS, Ellis, RP, Hanson, PR and Lance, RCM (1995) 'Detection of quantitative trait loci for agronomic, yield, grain and disease characters in spring barley (*Hordeum vulgare* L.)' *Theoretical and Applied Genetics* **91:** 1037-1047

Thompson, JR, Douglas, CM, Li, W, Jue, CK, Pramanik, B, Yuan, X, Rude, TH, Toffaletti, DL, Perfect, JR and Kurtz, M (1999) 'A glucan synthase *FKS1* homolog in *Cryptococcus neoformans* is single copy and encodes an essential function' *Journal of Bacteriology* **181:** 444-453

Tinker, NA, Mather, DE, Blake, TK, Briggs, KG, Choo, TM, Dahleen, L, Dofing, SM, Falk, DE, Ferguson, T, Franckowiak, JD, Graf, R, Hayes, PM, Hoffman, D, Irvine, RB, Kleinhofs, A, Legge, W, Rossnagel, BG, Saghai Maroof, MA, Scoles, GJ, Shugar, LP, Steffenson, B, Ullrich, S and Kasha, KJ (1996) 'Regions of the genome that affect agronomic performance in two-row barley' *Crop Science* **36:** 1053-1062

Turner, A, Bacic, A, Harris, PJ and Read, SM (1998) 'Membrane fractionation and enrichment of callose synthase from pollen tubes of *Nicotiana alata* Link et Otto' *Planta* **205:** 380-388

Valette, C, Nicole, M, Sarah, JL, Boisseau, M, Boher, B, Fargette, M and Geiger, JP (1997) 'Ultrastructure and cytochemistry of interactions between banana and the nematode *Radopholus similis*' *Fundamental and Applied Nematology* **20:** 65-77

van Bel, AJE, Ehlers, K and Knoblauch, M (2002) 'Sieve elements caught in the act' *Trends in Plant Science* **7:** 126-132

Vandesompele, J, De Preter, K, Pattyn, F, Poppe, B, Van Roy, N, De Paepe, A and Speleman, F (2002) 'Accurate normalization of real-time quantitative RT-PCR data by geometric averaging of multiple control genes' *Genome Biology* **3:** 1-11

Verma, DPS (2001) 'Cytokinesis and building of the cell plate in plants' *Annual Review of Plant Physiology and Plant Molecular Biology* **52:** 751-784

Verma, DPS and Hong, Z (2001) 'Plant callose synthase complexes' *Plant Molecular Biology* **47:** 693-701

Vogel, J and Somerville, S (2000) 'Isolation and characterisation of powdery mildew-resistant Arabidopsis mutants' *Proceedings of the National Academy of Sciences of the United States of America* **97:** 1897-1902

Wasserman, BP, Wu, A and Harriman, RW (1992) 'Probing the molecular architecture of (1,3)-β-glucan (callose) synthase: Polypeptide depletion studies' *Biochemical Society Transactions* **20:** 18-22

Waterhouse, PM, Graham, MW and Wang, MB (1998) 'Virus resistance and gene silencing in plants can be induced by simultaneous expression of sense and antisense RNA' *Proceedings of the National Academy of Sciences of the United States of America* **95:** 13959-13964

Wesley, SV, Helliwell, CA, Smith, NA, Wang, M, Rouse, DT, Liu, Q, Gooding, PS, Singh, SP, Abbott, D, Stoutjesdijk, PA, Robinson, SP, Gleave, AP, Green, AG and Waterhouse, PM (2001) 'Construct design for efficient, effective and high-throughput gene silencing in plants' *Plant Journal* **27:** 581-590

Williams, SJ and Davies, GJ (2001) 'Protein-carbohydrate interactions: Learning lessons from nature' *Trends in Biotechnology* **19:** 356-362

Williamson, VM and Hussey, RS (1996) 'Nematode pathogenesis and resistance in plants' *The Plant Cell* **8:** 1735-1745

Wissemeier, AH and Horst, WJ (1987) 'Callose deposition in leaves of cowpea *Vigna unguiculata* [L.] Walp. as a sensitive response to high manganese supply' *Plant and Soil* **102:** 283-286

Wong, LY, Belonogoff, V, Boyd, VL, Hunkapillar, NM, Casey, PM, Liew, SN, Lazaruk, KD and Baumhueter, S (2000) 'General method for HPLC purification and sequencing of selected dsDNA gene fragments from complex PCRs generated during gene expression profiling' *Biotechniques* **28:** 776-783

Wu, A, Harriman, RW, Frost, DJ, Read, SM and Wasserman, BP (1991) 'Rapid enrichment of CHAPS-solubilized UDP glucose 1,3-β-glucan callose synthase from *Beta vulgaris* L. by product entrapment, entrapment mechanisms and polypeptide characterization' *Plant Physiology* **97:** 684-692

Yin, X, Kropff, MJ and Stam, P (1999) 'The role of echophysiological models in QTL analysis: The example of specific leaf area in barley' *Heredity* **82:** 415-421

Zeyen, RJ, Carver, TLW and Lyngkjaer, MF (2002) 'Epidermal cell papillae' *in The powdery mildews: a comprehensive treatise* Belanger, RR, Bushnell, WR, Dik, AJ and Carver, TLW The American Phytopathological Society, St. Paul, Minnesota, USA. 107-125

Zhu, H, Bricenu, G, Dovel, R, Hayes, PM, Liu, BH, Liu, CT, Toojinda, T and Ullrich, SE (1999) 'Molecular breeding for grain yield in barley: An evaluation of QTL effects in a spring barley cross' *Theoretical and Applied Genetics* **98:** 772-779